

The Computation  
of the Localised Molecular Orbitals  
of Formaldehyde

By Janet Mary Holder

S. H. U. LIBRARY	
CLASS	TCDA
NO.	HOL
ACC. NO.	130823
DATE ACQ.	Sept 76

A thesis  
presented to the Faculty of Science  
of the University of London  
in candidature for the degree of  
Doctor of Philosophy

Chemistry Department,  
Royal Holloway College,  
(University of London),  
Egham Hill,  
Surrey,  
TW20 OEX.

November 1975

ProQuest Number: 10097396

All rights reserved

INFORMATION TO ALL USERS

The quality of this reproduction is dependent upon the quality of the copy submitted.

In the unlikely event that the author did not send a complete manuscript and there are missing pages, these will be noted. Also, if material had to be removed, a note will indicate the deletion.



ProQuest 10097396

Published by ProQuest LLC(2016). Copyright of the Dissertation is held by the Author.

All rights reserved.

This work is protected against unauthorized copying under Title 17, United States Code.  
Microform Edition © ProQuest LLC.

ProQuest LLC  
789 East Eisenhower Parkway  
P.O. Box 1346  
Ann Arbor, MI 48106-1346

ABSTRACT

The localised molecular orbitals of the formaldehyde molecule are computed using a minimum basis set of Slater atomic orbitals. The method of calculation used obtains localised molecular orbitals (l.m.o.s) directly at the Hartree-Fock level of approximation, rather than the more usual way of obtaining l.m.o.s from the canonical molecular orbitals.

The major difficulty in implementing this method is found to lie in satisfying orthogonality conditions, required by the l.m.o. theory, prior to an actual calculation. It is not found possible to satisfy these conditions completely for the formaldehyde molecule. Ways of overcoming this difficulty are discussed. L.m.o.s are calculated using Schmidt and Lowdin orthogonalisation of a suitable set of non-orthogonal starting-point functions.

The resulting l.m.o.s are found to give a unique many-electron total wavefunction, which is the same as that obtained by a canonical molecular orbital calculation. The individual l.m.o.s obtained are not unique, their forms depending on the method of orthogonalisation used and on the form of the starting-point functions.

Calculations are also made at several stages of approximation, each stage corresponding to ideas of chemical valence theory. Hence, perfectly localised molecular orbitals are computed directly. The results of calculations in which the operator is truncated to include only contributions from electrons and nuclei in the immediate environment of the l.m.o. being calculated are found to be very similar to those using the full Hartree-Fock operator.

The chemical significance of the l.m.o.s is examined by calculation of various properties including bond-energies. An examination is also made of the effect of making arbitrary changes in the polarity of one bond on some of the properties of other bonds.

Finally, a general study of the electron density given by many l.m.o.s in different molecules is made, and the use of l.m.o.s in describing the formation of a two-electron chemical bond is examined.

ACKNOWLEDGEMENTS

The author is deeply indebted to her supervisor, Dr. D. Peters, for much help and encouragement both during and after her study at Royal Holloway College.

The work described in this thesis was supported by a Science Research Council Studentship grant. The author wishes to thank Dr. M.D. Newton for making available the required integrals over atomic orbitals for formaldehyde, and also Dr. P. Melrose for his computer program to evaluate three-centre nuclear attraction integrals.

Finally, the author is also indebted to Mrs E.I. Kearsey for typing the thesis.

CONTENTS

	<u>Page</u>
List of Symbols and Abbreviations.	9
 <u>Chapter One - Introduction</u>	
1. The General Purpose of the work.	13
2. Historical Development of Localised Molecular Orbital Calculations.	16
3. Previous Calculations on the Formaldehyde Molecule.	21
4. The Scope of the Present Work.	23
 <u>Chapter Two - Basic Theory</u>	
1. Hartree-Fock Theory.	28
2. Localised Molecular Orbital Theory.	33
3. Methods of Orthogonalisation.	38
 <u>Chapter Three - Implementation of the Theory</u>	
1. Application of The Theory to Formaldehyde.	44
2. The Orthogonality Conditions.	50
3. The Search for a Suitable Starting-point.	
(a) Introduction.	58
(b) Direct Analytical Solution of Orthogonality Equations.	58
(c) Orthogonalisation of a set of Non-orthogonal Functions.	63

	<u>Page</u>
4. Description of the Various Stages of Approximation.	
(a) Introduction.	68
(b) Stage Four.	69
(c) Stage Three.	71
(d) Stages One and Two.	73
5. Details of Starting-points.	82

#### Chapter Four - Numerical Results

1. Stage Four.	
(a) Introduction.	87
(b) The Uniqueness of the Total Wavefunction.	91
(c) The Uniqueness of the Individual l.m.o.s.	96
(d) Summary of Stage 4 Results.	113
(e) Conversion of l.m.o.s to c.m.o.s.	114
2. Stage Three.	
(a) Introduction.	116
(b) Investigation of Schmidt Orthogonalisation Sequences at Stage 3.	117
(c) Results from Stage 3 Calculations.	126
3. Stages One and Two.	
(a) Introduction.	141
(b) Stage One Results.	141
(c) Stage Two Results.	143

	<u>Page</u>
<u>Chapter Five - Discussion and Chemical Interpretation of Results</u>	
1. Discussion of Results.	153
2. Ionization Potentials.	158
3. Delocalisation.	
(a) Extent of delocalisation.	162
(b) Sigmaconjugation Energies.	164
4. Hybridisation and Polarity.	167
5. Examination of Arbitrary Changes in the forms of l.m.o.s.	
(a) Introduction.	177
(b) Effect of Arbitrary Changes in the polarity of bonds on the Total Electronic Energy.	179
(c) Effect of Arbitrary Changes in the polarity of bonds on the polarity of neighbouring bonds.	184
(d) Effect of Arbitrary Changes in the polarity of bonds on the eigenvalues of other l.m.o.s.	189
6. Bond Energies.	
(a) Introduction.	211
(b) Calculation of the CH Bond Dissociation Energy.	212
(c) Calculation of the CO Bond Dissociation Energy.	215
<u>Chapter Six - Electron Densities in Two-Electron Chemical Bonds</u>	
1. Introduction.	223
2. Results.	225
3. Discussion.	247



	<u>Page</u>
<u>Chapter Seven - Computational Details</u>	
1. L.m.o. and c.m.o. Calculations.	
(a) L.m.o. Calculations.	250
(b) C.m.o. Calculations.	256
2. Solution of simultaneous Non-Linear Equations.	257
3. Electron Density Calculations.	261
References.	263

Abbreviations and Symbols Used

l.m.o.	Localised molecular orbital.
c.m.o.	Canonical molecular orbital.
a.u.	Atomic units.
$\Psi$	Total wavefunction.
$\phi$	Molecular orbital, usually an l.m.o.
$\theta$	Canonical molecular orbital.
$\chi$	Atomic orbital.
u	Free space function.
$\epsilon$	Lagrangian multiplier or eigenvalue.
$\epsilon$	Eigenvalue of a canonical molecular orbital.
$\xi$	Slater atomic orbital exponent.
n	Number of molecular orbitals ( $2n$ = number of electrons).
t	Number of atomic orbitals in the atomic orbital basis set.
s	Number of free space functions.
c	Coefficient in the expansion of a molecular orbital in terms of atomic orbitals.
k	Coefficient in the expansion of a free space function in terms of atomic orbitals.
C	Coefficient in the expansion of the orbital to be calculated in terms of the free space basis functions.
S	Overlap integral.
$\left. \begin{array}{l} S \\    \\ P \\    \\ Q \end{array} \right\}$	Overlap integral matrices.

N	Normalising constant.
$\underline{U}$	Unitary transformation.
E	Total energy.
T	Kinetic energy
V	Potential energy.
$\mu$	Dipole moment.
F	Hartree-Fock operator.
$Z_a$	Charge on nucleus a.
$J_j$	Coulomb operator, defined by equation (2.5).
$K_j$	Exchange operator, defined by equation (2.6).
$J_{ij}$	Coulomb integral, defined by equation (2.7).
$K_{ij}$	Exchange integral, defined by equation (2.8).
x	"Exchange Factor" occurring in the expression for the operator at stage 2. (equation 3.30).
$\mu$	L.m.o. describing a sigma-bond.
$\pi$	L.m.o. describing a pi-bond.
$\lambda$	L.m.o. describing a lone pair.
I	L.m.o. describing an inner shell.
$\mu^*$	Anti-bonding partner of $\mu$ .
$\nu$	Hybrid atomic orbital.
p	Polarity parameter.
$l_A$	Population of a hybrid atomic orbital on atom A.
$q_A$	Atomic charge in a hybrid atomic orbital on atom A.
$Q_A$	Total atomic charge on atom A.
IB	Ionic bond energy.
DD	Dipole-dipole interaction.

$\Delta q_c$	Change from the SCF value in the atomic charge on the carbon atom.
$\underline{\chi}$	A set of non-orthogonal functions.
$\underline{\psi}$	A set of orthogonal functions.
P	Projection operator.
$\Delta$	A measure of the orthogonality of the occupied orbitals in formaldehyde, defined by equation (3.15).
$\eta$	A measure of the overall difference between two sets of l.m.o.s., defined by equation (4.16).
M	Number of non-linear simultaneous equations given by the orthogonality conditions.
G	Jacobian matrix.
X	Electronegativity.
$\rho$	Electron density.
$\delta$	Difference density.
D	A measure of the total build-up of electron density on bond formation, defined by equation (6.7).
e	Electronic charge.
m	Electronic mass.
h	Planck's constant.
$a_0$	Bohr radius
$\delta_{ij}$	Kronecker delta. $\delta_{ij} = 1$ if $i = j$ . $\delta_{ij} = 0$ if $i \neq j$ .

A single underlining of a symbol denotes a vector, and a double underlining of a symbol denotes a matrix.

CHAPTER ONE

INTRODUCTION

## Section 1    The General Purpose of the Work

The general purpose of the work is to calculate localised molecular orbitals and to investigate their properties. The main part of the present work is concerned with the calculation of the localised molecular orbitals of the formaldehyde molecule.

The solution of Roothaan's equations<sup>1</sup> for the molecular orbitals of a molecule gives the canonical molecular orbitals which, in general, extend over the whole nuclear framework of the molecule. However, as Lennard-Jones first pointed out,<sup>2</sup> because of the invariance of the total wavefunction to a unitary transformation amongst the molecular orbitals,<sup>3</sup> orbitals may be chosen which are the most suitable for the investigation of a particular physical problem. In this way molecular orbitals may be obtained which are localised in particular regions of the molecule.

There are many reasons for preferring to calculate localised molecular orbitals (l.m.o.s) rather than the conventional canonical molecular orbitals (c.m.o.s). While the canonical molecular orbitals are convenient for describing ionization potentials and electronic spectral transitions, their inherent delocalisation does not correspond to the traditional chemical concept of a two-electron bond which was first proposed by Lewis in 1916.<sup>4</sup> As calculations of the c.m.o.s of larger molecules are reported, such as those listed by Christoffersen,<sup>5</sup> the disparity between the c.m.o.s and the chemical description of a molecule in terms of bonds, lone pairs and inner shells becomes even more apparent. When large organic and biological molecules are considered it is difficult to envisage these in terms of molecular orbitals which are completely delocalised over the entire molecule. On the other hand, molecular orbitals which are localised in specific regions of the molecule correspond more closely with intuitive chemical thinking.

The idea of a covalent local bond connecting atoms in a molecule, described by Pauling in "The Nature of the Chemical Bond",<sup>6</sup> is one of the most widespread and successful concepts in chemistry. It is one of the basic premises of the theory of organic chemistry<sup>7</sup> and stereochemistry.<sup>8</sup> It is hoped that localised molecular orbitals provide a mathematical description of the classical chemical bond and hence may be used to calculate properties of individual bonds such as bond polarities and hybridisations.

There is considerable chemical evidence, particularly from organic chemistry, that individual bonds in molecules have properties which are, to a certain extent, independent of the structure of the rest of the molecule and that a particular type of bond retains some of its properties in different molecules. This is the basis of the concept of an homologous series.<sup>7</sup> Thermodynamic data provides evidence of the additivity of certain bond properties. For example, heats of formation can be interpreted on the assumption that there is a definite amount of energy, the bond energy, associated with each type of bond.<sup>9</sup> Amongst other properties which have been found to be transferable from one molecule to another are bond moments.<sup>10</sup> Localised molecular orbitals describing chemical bonds should therefore be to some extent transferable from molecule to molecule.

The question of the transferability of l.m.o.s has been discussed by Allen and Schull<sup>11</sup> and Boys.<sup>12</sup> Rothenberg<sup>13</sup> and Peters<sup>14</sup> have shown that the l.m.o.s representing carbon-hydrogen bonds in different molecules are very similar and Schull et al.<sup>15</sup> have demonstrated actual transferability of l.m.o.s from one molecule ( $H_2O$ ) to another ( $H_2O_2$ ).

Considerable interest has been shown in this aspect of l.m.o.s in the hope that it might be possible to transfer l.m.o.s from small to large molecules.

Conventional ab initio calculations of the canonical molecular orbitals become prohibitively difficult as the size of the molecule increases, although Christoffersen has used a method for their determination based on the formation of large molecules from previously calculated molecular fragments.<sup>5</sup> The transferability of l.m.o.s indicates that it should be possible to construct wavefunctions of large molecules in terms of the appropriate l.m.o.s of smaller molecules,<sup>12,16,17</sup> and this has been investigated by Von Neissen.<sup>18</sup> This idea forms the basis of several recent calculations where wavefunctions are constructed from perfectly localised bond orbitals expressed in terms of hybridisation and polarity parameters and the total electronic energy is then minimised with respect to these parameters.<sup>19,20,21</sup>

An additional property of l.m.o.s is that they are expected to be useful in constructing wavefunctions of high accuracy which attempt to allow for electron correlation. Lennard-Jones and Pople first suggested that localised molecular orbitals should have a minimum of inter-orbital correlation.<sup>22</sup> The main correction to the wavefunction should then be given by intra-orbital correlation. L.m.o.s have been used by many workers in configuration interaction techniques,<sup>23-26</sup> although Steiner suggests that the inter-orbital correlation may not be neglected.<sup>27</sup>



Section 2 Historical Development of Localised Molecular Orbital  
Calculations

The two methods of approximation which have been developed in the quantum mechanical treatment of the electronic structure of molecules are the valence-bond method<sup>28</sup> and the molecular orbital method.<sup>29</sup> In the valence-bond method the molecule is considered as being built from its constituent atoms, a point of view which is closely related to chemical concepts. The method works well for small molecules but as the number of electrons in the molecule increases it becomes increasingly complicated.

The molecular orbital method is an extension to molecules of atomic orbital theory. Each electron is assigned to a one-electron wavefunction or molecular orbital. Electron correlation is, in the main, neglected. In the case of a closed shell system the total wavefunction is approximated by a single Slater determinant in which each occupied molecular orbital occurs twice, once with  $\alpha$  spin and once with  $\beta$  spin. The forms of the molecular orbitals are given by the Hartree-Fock equations proposed by Fock in 1930.<sup>3</sup> In his original paper Fock made the important observation that a unitary transformation among the occupied orbitals leaves the total wavefunction of the molecule unchanged. This leads to a simplification of the Hartree-Fock equations to a form which, together with the technique of expressing each molecular orbital as a linear combination of atomic orbitals,<sup>1</sup> provides a practical solution of the equations. This method gives the canonical molecular orbitals which transform as the irreducible representations of the molecular point group. A large number of ab initio calculations on molecules carried out according to the Hartree-Fock-Roothaan scheme have been reported in the literature.<sup>30</sup>

Lennard-Jones<sup>2</sup> first suggested that because of the invariance of the total wavefunction to a unitary transformation amongst the molecular orbitals, orbitals could be chosen which were localised in specific regions of a molecule and which were therefore closely allied to traditional chemical concepts. The relationship between the localised molecular orbitals and the canonical molecular orbitals has been discussed by many authors.<sup>2,31-36</sup>

Methods of calculating localised molecular orbitals have been reviewed by Weinstein, Pauncz and Cohen.<sup>35</sup> There are two possible approaches. Some workers have obtained them from the canonical molecular orbitals by applying an appropriate unitary transformation, while others have attempted to calculate localised molecular orbitals directly. The former method depends on having available the canonical orbitals, and on choosing a localising criterion. Several criteria have been proposed.

Lennard-Jones and Pople<sup>31</sup> obtained equivalent orbitals which were so defined that they transform into each other under the symmetry operations of the point group of the molecule. They observed that the equivalent orbitals gave different values for certain terms in the electronic interaction energy compared to the canonical orbitals. The electronic interaction energy is the sum of the total coulombic repulsion of all the electrons,  $\left[ \sum_{i \neq j} \sum_j 2J_{ij} + \sum_i J_{ii} \right]$ , and the total exchange attraction of all the electrons,  $\left[ \sum_{i \neq j} \sum_j K_{ij} \right]$ . Both terms are invariant under a unitary transformation. However, the sum of orbital self-interaction energies,  $\left[ \sum_i J_{ii} \right]$ , the total inter-orbital repulsions  $\left[ \sum_{i \neq j} \sum_j 2J_{ij} \right]$ , and the total self-energies of the overlap charge distributions,  $\left[ \sum_{i \neq j} \sum_j K_{ij} \right]$ , each vary with a unitary transformation of the occupied molecular orbitals. The equivalent orbitals give a larger value than the canonical orbitals for the first of these terms and smaller values for the other two terms.

Edmiston and Ruedenberg<sup>36</sup> used the criterion of maximising the sum of the orbital self-interaction energies,  $\left[ \sum_i J_{ii} \right]$ , to give a general iterative procedure for the calculation of l.m.o.s in the absence of symmetry. The resulting functions are known as energy localised orbitals and the method has been used extensively. Edmiston and Ruedenberg carried out calculations on a wide range of diatomic molecules. Pitzer<sup>37</sup> performed the first calculation on a polyatomic molecule, ethane, and Kaldor<sup>38</sup> applied the method to ammonia, ethylene and acetylene. Among more recent calculations are those on boron hydrides and on cyclic hydrocarbons by Newton, Switkes et al.<sup>39</sup> Recently a related method, known as density localisation, which minimises the sum of the charge density overlap integrals, was proposed by Von Neissen.<sup>40</sup>

Another localising criterion was proposed by Foster and Boys.<sup>23</sup> They imposed maximum separation of the centroids of the charge described by a given set of molecular orbitals, to yield a set of functions called "exclusive orbitals". Although these orbitals are localised and correspond closely to the chemical picture of valency, they were originally formulated as a step in the multiconfiguration treatment of electron correlation. Thus the exclusive orbitals were then used to define "oscillator orbitals" each of which interacts mainly with one exclusive orbital and which then enables electronic correlation to be introduced for that orbital. Later, Boys amended the definition of the exclusive orbitals slightly,<sup>41</sup> and this method has been used by Bonaccorsi, Scrocco and Tomasi to obtain l.m.o.s.<sup>42</sup> Although the criterion of Edmiston and Ruedenberg has a clearer physical significance, the method of Foster and Boys is more economical, especially for larger molecules.

Ruedenberg<sup>43</sup> classified methods of localisation based on the transformation of the canonical orbitals into "intrinsic" and "external" transformations. The methods of Edmiston and Ruedenberg and of Foster and Boys described above are based on intrinsic criteria, as they do not explicitly require localisation in a particular region of the molecule, the resulting localisation being a consequence of the condition imposed. Several external criteria have also been proposed, where physical localisation of the electron density in a particular region is imposed directly.

An early method proposed by Peters<sup>44</sup> is based on the assumption that the l.m.o.s are completely localised on the appropriate atom or atoms and have very small amplitudes outside the bond or lone pair in question. The properties of these l.m.o.s have been discussed by Peters,<sup>45-53</sup> and the electron density distribution arising from individual l.m.o.s is examined in Chapter Six of this work. Another external procedure was given by Magnasco and Perico in 1968<sup>54</sup> using a transformation based on the partition of the total electronic population according to Mulliken's method.<sup>55</sup>

The alternative approach to the calculation of localised molecular orbitals is to attempt to calculate them directly, with no reference to the canonical molecular orbitals. The possibility of obtaining l.m.o.s directly at the Hartree-Fock level of accuracy was discussed by Adams,<sup>16</sup> Gilbert<sup>17</sup> and Ruedenberg.<sup>43</sup> Adams modified the Hartree-Fock equations to obtain an eigenvalue equation, the solutions of which are the l.m.o.s by making appropriate changes in the Hartree-Fock operator. The equation is difficult to solve and Adams obtained only an approximate solution for the Lithium Hydride molecule.

Using the work of Adams, Gilbert and Ruedenberg, and also of Anderson,<sup>56</sup> Peters proposed a method<sup>57</sup> for the direct calculation of

localised molecular orbitals from the Hartree-Fock equations which retains the Hartree-Fock operator in its usual form. There is no loss of rigour from the Hartree-Fock level of approximation and the theory results in an eigenvalue equation which is easily solved by conventional methods. Each l.m.o. is calculated separately, the forms of the other occupied orbitals in the molecule remaining fixed during the calculation. This method is used in the present work to calculate the l.m.o.s of formaldehyde and details of the formal theory are given in Chapter Two. It has so far been tested with the BH molecule<sup>57</sup> and with methane<sup>58</sup> by Peters, and used recently in a slightly modified form by Wilhite and Whitten<sup>26</sup> for calculations on water, ammonia, ethylene and formaldehyde. Peters has also discussed the use of the method in Open Shell calculations.<sup>59</sup> Essentially the same idea of using orthogonalised sets of basis functions was developed at the same time by Goddard et al. for excited states.<sup>60</sup> The application of symmetry theory to the l.m.o.s is given in reference 61.

### Section 3 Previous Calculations on the Formaldehyde Molecule

There are many calculations on the ground state of the formaldehyde molecule, at various levels of approximation, reported in the literature and a brief survey of these is given below.

Formaldehyde has been the subject of a number of semi-empirical calculations. Some examples are given in reference 62. In 1960 Foster and Boys,<sup>63</sup> and Goodfriend, Birss and Duncan<sup>64</sup> carried out the first ab initio calculations. A later recalculation by Newton and Palke<sup>65</sup> indicated errors in the latter wavefunction. Formaldehyde was chosen by Foster and Boys to test their scheme for configuration interaction calculations. After solution of the Roothaan equations to give the canonical orbitals, they calculated the exclusive orbitals which they found to be localised on the bonds. The formaldehyde molecule was also used as a model by Parks and Parr<sup>66</sup> to test their theory of separated electron pairs.

More recently the Hartree-Fock-Roothaan scheme was used by Switkes, Stevens and Lipscomb<sup>67</sup> to calculate the canonical molecular orbitals of a range of molecules, which include formaldehyde, using a minimum basis set of Slater-type atomic orbitals. Calculations using basis sets of Gaussian atomic orbitals have been performed by several workers<sup>68</sup> and Whitten and Hackmeyer<sup>25</sup> have reported a configuration interaction study of the molecule. A multiconfiguration calculation using Slater atomic orbitals has been carried out by Levy.<sup>69</sup>

Localised molecular orbitals have been obtained from the canonical orbitals by Peters<sup>47</sup> and Magnasco and Perico,<sup>54</sup> using their own localising criteria, and by Newton, Switkes and Lipscomb<sup>70</sup> following the Edmiston-Ruedenberg procedure. Formaldehyde is also one of the molecules whose l.m.o.s have been calculated recently by Wilhite and Whitten<sup>26</sup> using a

method based on the l.m.o. theory which was proposed by Peters.<sup>57</sup> Wilhite and Whitten work with a basis set of Gaussian atomic orbitals and have modified the method slightly so that all the l.m.o.s. are determined together.

#### Section 4    The Scope of the Present Work

The present work provides a further test of the l.m.o. theory devised by Peters,<sup>57</sup> with the eventual aim of developing it into a working method for the direct calculation of l.m.o.s without first calculating the c.m.o.s. Prior to this work several questions remained concerning the method. It was not clear whether the orthogonality conditions, which are implicit in the theory and which must be satisfied before the calculation of an l.m.o., are not too severe for many molecules. In addition, the uniqueness of the end-point and the convergence of the method had not been fully explored, although no difficulties had been found for methane. These questions are investigated in the present work although, for reasons discussed below, no clear conclusion is reached concerning the orthogonality conditions and the uniqueness of the end-point.

It was decided to calculate the l.m.o.s of formaldehyde as this molecule gives a more searching test of the theory than the methane molecule. It is the first use of the theory for a molecule containing lone pairs of electrons and a pi-bond, and is a much more stringent test of the orthogonality conditions. There are also many experimental measurements and previous calculations reported in the literature with which to compare results. The problems arising on the application of the l.m.o. theory to formaldehyde are discussed in Chapter Three.

In addition to developing the l.m.o. theory the results of the calculations on formaldehyde are of chemical interest. Formaldehyde contains a carbonyl group ;and is the first member of the homologous series of aldehydes and ketones, which play an important part in organic chemistry.<sup>7</sup> The carbonyl group also occurs in many large biological molecules, examples being given by the peptides and proteins.



The l.m.o. theory was designed with a view to performing calculations on large molecules.<sup>57</sup> Each l.m.o. is calculated separately, while the forms of the other l.m.o.s in the molecule are kept constant, providing a possible route to the calculation of parts of a large molecule. This aspect of the theory has been investigated by Wilhite and Whitten.<sup>26</sup> The successful calculation of the l.m.o.s of formaldehyde may be regarded as a possible step towards calculating the l.m.o.s of larger molecules containing the carbonyl group, such as amides and peptides. Considerable interest has been shown recently in calculations of these molecules.<sup>71</sup>

Calculations on large molecules are further assisted by the ability to apply the l.m.o. theory at different levels of approximation, or stages. The approximations are made by neglecting the effects of distant parts of the molecule when calculating a particular l.m.o. Each stage corresponds to ideas of chemical valence theory. The first stage is the simplest approximation and corresponds most closely to chemical ideas of a two-electron bond. The final stage is the complete solution of the secular determinant given by the l.m.o. theory and corresponds to a more mathematical point of view. A detailed description of each stage is given in Chapter Three.

In the present work l.m.o.s were calculated for the formaldehyde molecule at each of the various stages to investigate how good an approximation the earlier stages give to the rigorous final stage. The results are discussed in Chapters Four and Five. These calculations differ from those of Wilhite and Whitten<sup>26</sup> who use a method which calculates all the l.m.o.s together and obtains orthogonality of the occupied orbitals by Lowdin orthogonalisation which causes a certain amount of delocalisation. This method is not applicable at the earlier stages of approximation but only at the rigorous final stage. These workers use a

basis set of Gaussian atomic orbitals whereas the present work uses a basis set of Slater atomic orbitals.

Having calculated numerical expressions for the l.m.o.s it is then necessary to interpret them in terms of their physical significance. Various properties of the individual l.m.o.s are discussed in Chapter Five. The calculated values of bond energies are of particular interest as these are quantities which may be compared with experimental values and which are of considerable chemical importance. The l.m.o.s of the methane molecule gave values which agreed unexpectedly well with the experimental values.<sup>58</sup> The formaldehyde molecule is also used as a model to investigate the effect of a variation in the polarity of a bond on some of the properties of the molecule.

Perhaps the best picture of the physical nature of the l.m.o.s would be provided by an investigation of their electron density distribution. In Chapter Six a general study is made of the electron density given by many l.m.o.s in different molecules, and the use of l.m.o.s in describing the formation of a two-electron chemical bond is examined. This work was carried out partly in preparation for the investigation of the electron density distribution given by the l.m.o.s of formaldehyde calculated by the present method, although such an investigation was not performed in this work.

The electron density distribution in the H<sub>2</sub> molecule, which contains a single bonding molecular orbital, was examined by Daudel and co-workers,<sup>72</sup> who found that the formation of the two-electron bond is accompanied by an increase of electron density in the region between the two nuclei, and a decrease of electron density outside this region. The present work examines if this is a general conclusion for all l.m.o.s describing two-electron bonds by comparing the electron density distribution of the two electrons

before and after the bond is formed. The delocalised canonical orbitals are not suitable for use in this way.<sup>73-77</sup> The electron density distribution for l.m.o.s in several molecules have been reported in the literature,<sup>39d, 42</sup> but no comparison with the situation before bonding was made.

This approach differs from that of many workers who have compared the change in the total electron density of the whole molecule on bond formation.<sup>74-82</sup> They have found an increase in electron density in the inter-nuclear region, but also an increase of electron density outside this region, which has been ascribed to the formation of lone pairs.<sup>80</sup>

CHAPTER TWO  
BASIC THEORY

## Section 1 Hartree-Fock Theory

A brief summary of the Hartree-Fock theory for a molecule with a closed shell structure is given below. More detailed treatments are given in the original literature<sup>1,3</sup> and in standard texts.<sup>83</sup>

The wavefunction of a closed shell molecule is represented by a single determinant. For a molecule with  $2n$  electrons the wavefunction is given by

$$= \frac{1}{\sqrt{2n!}} \begin{vmatrix} \phi_1 & \bar{\phi}_1 & \phi_2 & \bar{\phi}_2 & \dots & \phi_n & \bar{\phi}_n \end{vmatrix} \quad (2.1)$$

where  $\phi_1 \dots \phi_n$  are molecular orbitals (m.o.s),  $\bar{\phi}$  denoting an orbital with  $\beta$  spin. As a consequence of the determinantal form of the wavefunction, the molecular orbitals from which it is constructed are unique except for a unitary transformation among themselves. Therefore the wavefunction in equation (2.1) may be expressed in terms of a different set of m.o.s,  $\phi'_1 \dots \phi'_n$ , which are related to the first set by a unitary transformation. In matrix notation

$$\underline{\phi}' = \underline{\phi} \cdot \underline{\underline{U}} \quad (2.2)$$

where  $\underline{\phi}$  is the row vector containing the m.o.s  $\phi_1 \dots \phi_n$ ,  $\underline{\phi}'$  the row vector containing the m.o.s  $\phi'_1 \dots \phi'_n$  and  $\underline{\underline{U}}$  the  $n \times n$  matrix representing the unitary transformation. (A single underlining denotes a vector and a double underlining denotes a matrix). Hence there are infinitely many sets of m.o.s which describe the same total wavefunction  $\Psi$ .

The wavefunction for which the total energy is a minimum is given by any set of molecular orbitals satisfying the Hartree-Fock equations

$$F \phi_i = \sum_{j=1}^n \phi_j \epsilon_{ji} \quad \begin{matrix} i = 1 \dots n \\ j = 1 \dots n \end{matrix} \quad (2.3)$$

where  $F$  is the Hartree-Fock operator given by

$$F = -1/2 \nabla^2 + \sum_{a=1}^g -Z_a/r_a + \sum_{j=1}^n (2J_j - K_j) \quad (2.4)$$

The first term represents the kinetic energy of an electron in the  $i$ th m.o. The second term represents the sum over the  $g$  nuclei in the molecule of the coulombic attraction between the electron and the nuclei.  $Z_a$  is the charge on nucleus  $a$  and  $r_a$  is the distance between nucleus  $a$  and the electron. The third term represents the coulombic repulsion and exchange attraction between an electron in the  $i$ th m.o. and all the electrons in the molecule. The coulomb operator,  $J_j$ , is given by

$$J_j \phi_i(1) = \left( \int \frac{\phi_j(2) \phi_j(2)}{r_{12}} dv_2 \right) \phi_i(1) \quad (2.5)$$

where  $\phi(1)$  signifies an m.o. occupied by the first electron and  $\phi(2)$  signifies an m.o. occupied by the second electron.  $r_{12}$  is the distance between the first and second electrons and the integration is over the co-ordinates of the second electron. The exchange operator,  $K_j$ , is given by

$$K_j \phi_i(1) = \left( \int \frac{\phi_j(2) \phi_i(2)}{r_{12}} dv_2 \right) \phi_j(1) \quad (2.6)$$

It is also convenient to define coulomb integrals  $J_{ij}$  and exchange integrals  $K_{ij}$  in terms of the respective operators.

$$J_{ij} = \int \phi_i(1) J_j \phi_i(1) dv_1 \quad (2.7)$$

$$K_{ij} = \int \phi_i(1) K_j \phi_i(1) dv_1 \quad (2.8)$$

These equations may be written

$$J_{ij} = \langle \phi_i \phi_i | \phi_j \phi_j \rangle \quad (2.9)$$

$$K_{ij} = \langle \phi_i \phi_j | \phi_i \phi_j \rangle \quad (2.10)$$

adopting the convention that the left-hand side of the bracket refers to electron 1. As only real functions are used in this work complex conjugates are not indicated.

The  $\epsilon_j$  in equation (2.3) are Lagrangian multipliers arising from the auxiliary conditions that the orbitals be orthonormal. In matrix notation equation (2.3) is given by

$$F \underline{\phi} = \underline{\phi} \cdot \underline{\epsilon} \quad (2.11)$$

where  $\underline{\epsilon}$  is an  $n \times n$  matrix containing the Lagrangian multipliers.

It can be shown that when the set of m.o.s  $\underline{\phi}$  are subjected to a unitary transformation as described by equation (2.2) the set of m.o.s obtained,  $\underline{\phi}'$ , satisfy the same equation. Since the operator  $F$  is invariant under a unitary transformation, equation (2.11) may be written

$$F \underline{\phi} \cdot \underline{U} = \underline{\phi} \cdot \underline{U} ( \underline{U}^{-1} \cdot \underline{\epsilon} \cdot \underline{U} ) \quad (2.12)$$

$$\text{or} \quad F \underline{\phi}' = \underline{\phi}' \cdot \underline{\epsilon}' \quad (2.13)$$

The canonical molecular orbitals are obtained by choosing to calculate the set of m.o.s whose  $\underline{\epsilon}$  matrix is diagonal. Equation (2.3) then reduces to the simpler form

$$F \phi_i = \phi_i \epsilon_i \quad (2.14)$$

To obtain m.o.s in practice, it is necessary to express each m.o. in terms of a basis set of atomic orbitals,  $\underline{\chi}$ .

$$\phi_i = \sum_{p=1}^t \chi_p c_{pi} = \underline{\chi} \cdot \underline{c}_i \quad (2.15)$$

where  $\underline{c}_i$  is a column vector of coefficients. Assembling the columns into a rectangular matrix  $\underline{\underline{c}}$  of  $t$  rows and  $n$  columns gives the general form of (2.15)

$$\underline{\phi} = \underline{\chi} \cdot \underline{\underline{c}} \quad (2.16)$$

Substituting (2.16) into equation (2.11), premultiplying by the column of atomic orbitals and integrating gives the general form of the Hartree-Fock equations.

$$\underline{\underline{F}} \cdot \underline{\underline{c}} = \underline{\underline{S}} \cdot \underline{\underline{c}} \cdot \underline{\underline{\epsilon}} \quad (2.17)$$

where  $\underline{\underline{F}}$  is the  $t \times t$  matrix with elements

$$F_{pq} = \int \chi_p F \chi_q dV = \langle \chi_p | F | \chi_q \rangle \quad (2.18)$$

and  $\underline{\underline{S}}$  is the analogous overlap integral matrix with elements

$$S_{pq} = \int \chi_p \chi_q dV = \langle \chi_p | \chi_q \rangle \quad (2.19)$$

In the canonical case equation (2.17) reduces to

$$\left[ \underline{\underline{F}} - \epsilon_i \underline{\underline{S}} \right] \underline{c}_i = 0 \quad (2.20)$$

Solution of equation (2.20), by solving the secular equation

$$\text{Det} ( \underline{\underline{F}} - \epsilon \underline{\underline{S}} ) = 0 \quad (2.21)$$

generates  $t$  eigenvalues,  $\epsilon_i$ , and  $t$  eigenvectors,  $\underline{c}_i$ . The  $n$  eigenvectors associated with the  $n$  lowest eigenvalues correspond to the occupied m.o.s. The remaining  $(t-n)$  virtual m.o.s. have no straightforward physical significance, although they are used to build up excited states of molecules.



The canonical molecular orbitals belong to the irreducible representations of the symmetry group of the molecule, and experience shows that they are in general delocalised over all the atoms of the molecule.

## Section 2 Localised Molecular Orbital Theory

For many chemical purposes it is more helpful to work with molecular orbitals localised in particular regions of the molecule, corresponding to bonds or lone pairs. Localised molecular orbitals can be obtained from the canonical orbitals by choosing the matrix  $\underline{U}$  in equation (2.2) in such a way that this is the case.<sup>33-36</sup> If  $\underline{\Theta}$  is the set of c.m.o.s and  $\underline{\phi}$  the set of l.m.o.s then

$$\underline{\phi} = \underline{\Theta} \cdot \underline{U} \quad (2.22)$$

The following theory was developed to obtain l.m.o.s directly.<sup>57</sup>

If attention is focussed on one particular m.o., say  $\phi_i$ , the Hartree-Fock equation (2.3) may be written in the form

$$F \phi_i - \epsilon_{ii} \phi_i = \sum_{k=1(k \neq i)}^n \epsilon_{ik} \phi_k \quad (2.23)$$

The problem is then to solve this equation and determine  $\phi_i$  and  $\epsilon_{ii}$ . This may be achieved, given that the forms of all the other occupied orbitals in the molecule are known and fixed, in the following way.

As with the canonical orbitals each l.m.o. is expanded in terms of an atomic orbital basis set.

$$\phi_j = \sum_{m=1}^t \chi_m c_{mj} \quad j=1 \dots n \quad (2.24)$$

The size of the atomic orbital basis set,  $t$ , determines the size of the set of molecular orbitals. The  $t$  m.o.s span a  $t$ -dimensional function space. If the forms of  $(n-1)$  of the occupied m.o.s are fixed, this  $t$ -dimensional function space can be divided into two mutually orthogonal subspaces. One  $(n-1)$ -dimensional subspace is spanned by the fixed functions and is called the "fixed" space. The remaining subspace is of  $[t-(n-1)] = s$  dimensions and is spanned by the functions whose forms are to be determined (ie the m.o. being calculated together with the empty virtual orbitals).

This is known as the "free" space.

Each of the free space functions,  $U_1 \dots U_s$ , is expanded in terms of the atomic orbital basis set.

$$u_p = \sum_{m=1}^t \chi_m k_{mp} \quad p=1 \dots s \quad (2.25)$$

Initially the coefficients  $k_{mp}$  may be chosen arbitrarily within the restriction that each free space function,  $U_p$ , must be orthogonal to each fixed space function,  $\phi_k$ , as required by the mutual orthogonality of the fixed space and the free space.

$$\langle u_p | \phi_k \rangle = 0 \quad \begin{cases} k = 1 \dots n (k \neq i) \\ p = 1 \dots s \end{cases} \quad (2.26)$$

Equation (2.23) may be solved by expressing the  $i$ th m.o. as a linear combination of the free space functions.

$$\phi_i = \sum_{q=1}^s C_{qi} u_q \quad (2.27)$$

The free space functions therefore form a basis set for the expansion of  $\phi_i$ , termed the free space basis set to distinguish it from the atomic orbital basis set (equation 2.24)). Because of the mutual orthogonality of free and fixed spaces the right hand side of equation (2.23) may then be eliminated without loss of rigour. This can be seen by substituting (2.27) in (2.23), multiplying (2.23) from the left by  $U_p$  and integrating over the coordinates of electron 1, to give

$$\begin{aligned} & \sum_{q=1}^s C_{qi} \left\{ \langle u_p | F | u_q \rangle - \epsilon_{ii} \langle u_p | u_q \rangle \right\} \\ & = \sum_{q=1}^s C_{qi} \left\{ \sum_{\substack{k=1 \\ (k \neq i)}}^n \langle u_q | F | \phi_k \rangle \langle u_p | \phi_k \rangle \right\} \end{aligned} \quad (2.28)$$

$p=1 \dots s$

All the terms in the sum on the right hand side of the equation are zero, as all the  $\langle u_p | \phi_k \rangle$  are zero by construction of the free space functions  $U_p$  (equation 2.26). The equation then reduces to

$$\sum_{q=1}^s C_{qi} ( F_{pq} - \epsilon_{ii} S_{pq} ) = 0 \quad p=1\dots s \quad (2.29)$$

or in matrix notation

$$( \underline{\underline{F}} - \epsilon_{ii} \underline{\underline{S}} ) \underline{\underline{C}}_i = 0 \quad (2.30)$$

where  $\underline{\underline{F}}$  and  $\underline{\underline{S}}$  are  $s \times s$  matrices containing elements

$$F_{pq} = \langle u_p | F | u_q \rangle \quad (2.31)$$

and

$$S_{pq} = \langle u_p | u_q \rangle \quad (2.32)$$

respectively. The secular equation

$$\text{Det} ( \underline{\underline{F}} - \epsilon \underline{\underline{S}} ) = 0 \quad (2.33)$$

can be solved in a similar way to the Roothaan equations which give the conventional c.m.o.s. Equation (2.33) differs from equation (2.21) in that the secular determinant is of smaller dimension,  $s \times s$ , as opposed to  $\text{txt}$ . The basis functions are the free space basis functions,  $U_1 \dots U_s$ , not the atomic orbital basis set. The  $F$  operator is the conventional Hartree-Fock operator, constructed from all the occupied orbitals as in (2.4).

To calculate a set of m.o.s equation (2.30) is solved for each m.o. in turn. To show how the method works in practice the calculation of the first m.o., say  $\phi_1$ , is illustrated below. The forms of all the other occupied m.o.s.,  $\phi_2 \dots \phi_n$ , are assumed to be known. Initially these will be guesses based on physical considerations. Free space functions,  $U_1 \dots U_s$ , are constructed such that they are orthogonal to the fixed space

according to (2.26), with  $U_1$  being as close to the final form of  $\phi_1$  as possible. The F matrix, with elements given by (2.31) is then formed. Solution of (2.30) gives the eigenvalue and eigenvector of the first m.o.,  $\phi_1$ , together with those of all the virtual orbitals. The lowest and only negative eigenvalue corresponds to the occupied orbital  $\phi_1$ . The F operator is then reconstructed with the improved  $\phi_1$  and the process repeated to self-consistency. A second m.o., say  $\phi_2$ , can then be calculated in the same way, with the new form of  $\phi_1$  used in constructing the fixed space and the F operator. Further calculations are made until the forms of none of the occupied orbitals can be further improved. There are therefore two cycling processes - firstly the iteration to self-consistency within the calculation of one particular m.o., and secondly the cycling round the m.o.s until no more overall improvement can be obtained. Wilhite and Whitten<sup>26</sup> have reversed the order of these two processes so that all the molecular orbitals are improved together.

The theory set out above applies to any set of m.o.s satisfying the Hartree-Fock equations. Localised molecular orbitals are obtained by constructing the initial fixed space from localised functions thus forcing the orbital being calculated to be substantially localised, through the orthogonality conditions of equation (2.26). Hence the orthogonality conditions play an important part in forming the calculated m.o. The t atomic orbital coefficients  $c_{mi}$  describing the orbital being calculated  $\phi_i$  (equation (2.24)) are determined partly by the (n-1) or (t-s) orthogonality conditions (equation (2.26)) and partly by solution of the sxs secular determinant (equation (2.33)).

The question arises of the uniqueness of the orbitals. This is a difficult point as there is no requirement in the formal theory that the final set of orbitals be unique. A set of SCF m.o.s is uniquely determined

by making a specific choice of the off-diagonal Lagrangian multipliers  $\epsilon_{ij}$ .<sup>43</sup> The method given above is dependent on the starting-point functions to the extent that a set of SCF localised m.o.s is obtained only from a set of starting-point functions which are localised. It is hoped, however, that the detailed forms of the l.m.o.s forming the fixed space will have little influence on the form of the l.m.o. being calculated either through the operator, or through the orthogonality conditions. It has been found in previous work<sup>58</sup> that the triple criterion of firstly minimizing the total energy, secondly requiring the orbitals to be localised and thirdly requiring the orbitals to be mutually orthogonal apparently gives individual orbitals, as well as a total wavefunction, which are independent of the starting-point. This problem is investigated further in the present work, although, for reasons discussed below, it is not possible to reach a clear conclusion.

### Section 3   Methods of Orthogonalisation

In implementing the l.m.o. theory described in Section 2 it is necessary both to obtain a set of functions which are orthogonal amongst themselves and to obtain one set of functions which is orthogonal to another set. Details of the orthogonality conditions are set out in Chapter Three. Methods which may be used to attain this orthogonality have been reviewed by Lowdin<sup>84</sup> and are discussed below.

The general problem may be described in the following way. An orthogonal set of  $m$  functions,  $\underline{\Psi}$ , can be expressed in terms of a non-orthogonal set of  $m$  functions,  $\underline{\chi}$ , by a linear transformation:

$$\underline{\Psi} = \underline{\chi} \cdot \underline{A} \tag{2.34}$$

where  $\underline{A}$  is an  $m \times m$  matrix of coefficients. Given the set of non-orthogonal functions,  $\underline{\chi}$ , the problem is then to find the matrix of coefficients  $\underline{A}$  such that

$$\begin{aligned} \langle \underline{\Psi} | \underline{\Psi} \rangle &= \langle \underline{\chi} \cdot \underline{A} | \underline{\chi} \cdot \underline{A} \rangle \\ &= \underline{A}^\dagger \langle \underline{\chi} | \underline{\chi} \rangle \underline{A} \\ &= \underline{E} \end{aligned} \tag{2.35}$$

where  $\underline{E}$  is the identity matrix and  $\underline{A}^\dagger$  is the transpose of the matrix  $\underline{A}$ . There is no unique solution to equation (2.35), so that many sets of orthogonal functions can be obtained from the non-orthogonal set  $\underline{\chi}$ . Several orthogonalising procedures have been developed, each of which results in a different set of orthogonal functions.

Perhaps the most straightforward procedure to apply, and the one which has proved most useful in the present work, is the method of Schmidt orthogonalising. In its simplest form the method is as follows.

For a non-orthogonal pair of functions  $\chi_1$  and  $\chi_2$ , an orthogonal pair,  $\psi_1$  and  $\psi_2$ , are obtained by subtracting  $\chi_1$ , multiplied by the overlap integral between  $\chi_1$  and  $\chi_2$ , from  $\chi_2$ , followed by renormalisation.

$$\psi_1 = \chi_1$$

$$\psi_2 = N_{12} ( \chi_2 - \chi_1 \langle \chi_1 | \chi_2 \rangle ) \quad (2.36)$$

$N_{12}$  is a normalising constant. This procedure may be formulated in terms of a projection operator. If the form of  $\chi_1$  is kept constant the component of  $\chi_2$  orthogonal to  $\chi_1$ ,  $\psi_2$ , is selected by the operator  $(1 - P)$  where  $P$  is the projection operator

$$P = | \chi_1 \rangle \langle \chi_1 | \quad (2.37)$$

Hence

$$\begin{aligned} \psi_2 &= N_{12} ( 1 - | \chi_1 \rangle \langle \chi_1 | ) \chi_2 \\ &= N_{12} ( \chi_2 - \chi_1 \langle \chi_1 | \chi_2 \rangle ) \end{aligned} \quad (2.38)$$

The method is easily extended to obtain an orthogonal set of functions from a non-orthogonal set  $\chi_1^0 \dots \chi_m^0$ , in a step-wise process. Firstly  $\chi_2^0 \dots \chi_m^0$  are made orthogonal to  $\chi_1^0$  in a series of changes of the type given by (2.36). The superscript denotes the number of times the function has been changed.

$$\chi_i^1 = N_{1i} ( \chi_i^0 - \chi_1^0 \langle \chi_1^0 | \chi_i^0 \rangle ) \quad i=1 \dots m \quad (2.39)$$

Since  $\chi_2^1 \dots \chi_m^1$  are now all orthogonal to  $\chi_1^0$  they may be combined linearly without losing orthogonality to  $\chi_1^0$ .  $\chi_3^1 \dots \chi_m^1$  are made orthogonal to  $\chi_2^1$  in a similar series of changes

$$\chi_i^2 = N_{2i} ( \chi_i^1 - \chi_2^1 \langle \chi_2^1 | \chi_i^1 \rangle ) \quad i=1 \dots m \quad (2.40)$$



The process is repeated until all functions are orthogonal to all others. The resulting set of functions,  $\gamma_1^0, \gamma_2^1, \gamma_3^2, \dots, \gamma_m^{m-1}$  is therefore an orthogonal set. It can be seen that  $\gamma_1^0$  is left unchanged by the method,  $\gamma_2^1$  is changed once, and later functions in the set are changed increasingly. The forms of the functions in the final set therefore depend on the order in which they appear in the sequence

$$\gamma_1^0 \quad \gamma_2^0 \quad \gamma_3^0 \quad \gamma_4^0 \dots \gamma_m^0 \quad (2.41)$$

This point has proved important in the present work.

The above method corresponds to a solution of equation (2.35) in which the matrix  $\underline{\underline{A}}$  is triangular. The individual elements in  $\underline{\underline{A}}$  become rather cumbersome as the size of the set of functions increases, but the method is easy to use in a computer program.

The Schmidt orthogonalising procedure can also be used to achieve orthogonality between an orthogonal set of functions,  $\psi_1 \dots \psi_m$ , and another function  $\gamma^0$  leaving  $\psi_1 \dots \psi_m$  unchanged.  $\gamma^0$  is altered to make it orthogonal to each function in the set in a series of changes of the form

$$\gamma^k = N_k ( \gamma^{k-1} - \psi_k \langle \psi_k | \gamma^{k-1} \rangle ) \quad k=1 \dots m \quad (2.42)$$

An alternative method of orthogonalisation, symmetric orthogonalisation, which was devised by Lowdin,<sup>85</sup> makes an equal number of changes to each function in a non-orthogonal set,  $\underline{\underline{\gamma}}$ . Firstly a matrix of overlap integrals  $\underline{\underline{S}}^L$  is formed, with elements

$$S_{ij}^L = \langle \gamma_i | \gamma_j \rangle - \delta_{ij} \quad (2.43)$$

$\underline{S}^L$  differs from other overlap integral matrices in that the diagonal elements are zero. An orthogonal set of functions,  $\underline{\psi}$ , is then given by

$$\underline{\psi} = \underline{\chi} \cdot (\underline{1} + \underline{S}^L)^{-1/2} \quad (2.44)$$

The matrix  $(\underline{1} + \underline{S}^L)^{-1/2}$  can be expressed as a series

$$(\underline{1} + \underline{S}^L)^{-1/2} = \underline{1} - \frac{1}{2} \underline{S}^L + \frac{3}{8} (\underline{S}^L)^2 - \frac{5}{16} (\underline{S}^L)^3 \dots \quad (2.45)$$

and has elements

$$\begin{aligned} (\underline{1} + \underline{S}^L)^{-1/2}_{ji} &= \delta_{ij} - \frac{1}{2} S^L_{ji} + \frac{3}{8} \sum_k S^L_{jk} S^L_{ki} \\ &\quad - \frac{5}{16} \sum_k \sum_l S^L_{jk} S^L_{kl} S^L_{li} \dots \end{aligned} \quad (2.46)$$

Orthogonal functions  $\psi_i$  ( $i = 1 \dots n$ ) are therefore given by

$$\begin{aligned} \psi_i &= \chi_i - \frac{1}{2} \sum_j \chi_j S^L_{ji} - \frac{3}{8} \sum_j \sum_k \chi_j S^L_{jk} S^L_{ki} \\ &\quad - \frac{5}{16} \sum_j \sum_k \sum_l \chi_j S^L_{jk} S^L_{kl} S^L_{li} \dots \end{aligned} \quad (2.47)$$

The series given by equation (2.44) does not always converge and in this case it is necessary to evaluate  $(\underline{1} + \underline{S}^L)^{-1/2}$  in some other way.<sup>84</sup> No convergence difficulties were found, however, when this method of orthogonalising was employed for the functions occurring in this work.

It can be shown<sup>84</sup> that the method of Lowdin orthogonalising gives a set of orthogonal functions which resemble the initial non-orthogonal functions as closely as possible.

A third method of obtaining orthogonality is provided by symmetry orthogonalisation. For a pair of non-orthogonal functions  $\chi_1$  and  $\chi_2$ , an orthogonal pair,  $\psi_1$  and  $\psi_2$ , is given by the sum and difference of the two functions.

$$\begin{aligned}\psi_1 &= N_1 (\chi_1 + \chi_2) \\ \psi_2 &= N_2 (\chi_1 - \chi_2)\end{aligned}\tag{2.48}$$

Extension of the method to a larger set of non-orthogonal functions can be achieved, but becomes complicated. The functions produced are all extensively altered by orthogonalising in this way and so the method was not found suitable for use in the present work.

CHAPTER THREE

IMPLEMENTATION OF THE THEORY

Section 1 Application of The Theory to Formaldehyde

The formaldehyde molecule was chosen as a test of the l.m.o. theory partly because of the reasons mentioned in Chapter One, and partly because many of the integrals needed had been made available by Newton and Palke.<sup>65</sup> The atomic coordinates used in the calculations and shown in Table 3.1 were those employed by Newton and Palke. The positions of the axes are shown in Figure 3.1.

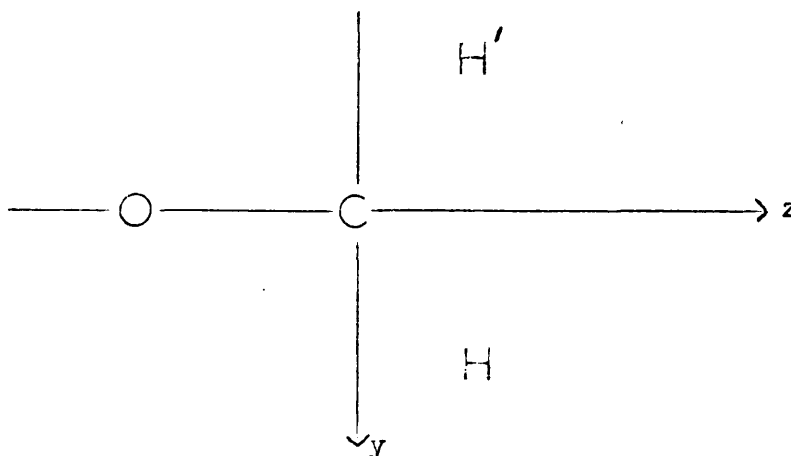


Figure 3.1 Positions of the Axes for the Formaldehyde Molecule

The calculations were performed in atomic units, defined by

$$e = m = \hbar/2\pi = 1 \quad (3.1)$$

where  $e$  is the electronic charge,  $m$  is the electronic mass and  $\hbar$  is Planck's constant. 1 a.u. of distance = 0.529 Å. 1 a.u. of energy = 27.20976 eV.

A minimum atomic orbital basis set of Slater-type orbitals was used.<sup>86</sup> The general form for these orbitals is given by

$$\chi^{nlm} = N_{nl} r^{n-1} e^{-\xi r} Y_{lm}(\theta, \phi) \quad (3.2)$$

Table 3.1 Atomic Coordinates of Formaldehyde (a.u.)

Atom	Cartesian Coordinates			Charge
	X	Y	Z	
C	0.000	0.000	0.000	6.00
O	0.000	0.000	-2.300	8.00
H	0.000	1.732	1.000	1.00
H'	0.000	-1.732	1.000	1.00

Table 3.2 Atomic Orbital Exponents

Index	Atom	Atomic Orbital	Exponent
1	C	1s	5.700
2	C	2s	1.625
3	C	2p <sub>z</sub>	1.625
4	C	2p <sub>x</sub>	1.625
5	C	2p <sub>y</sub>	1.625
6	O	1s	7.700
7	O	2s	2.275
8	O	2p <sub>z</sub>	2.275
9	O	2p <sub>x</sub>	2.275
10	O	2p <sub>y</sub>	2.275
11	H	1s	1.200
12	H'	1s	1.200

where  $Y_{lm}$  is the angular part of the function and  $N_{nl}$  is a normalising constant. The orbital exponents,  $\xi$ , used for formaldehyde are those given by Slater's Rules and are shown in Table 3.2.

The formaldehyde molecule contains 16 electrons in 8 doubly occupied molecular orbitals ( $n = 8$ ). The atomic orbital basis set used consists of 12 orbitals ( $t = 12$ ), so the Hartree-Fock function space is therefore 12 dimensional. To perform a calculation according to the l.m.o. theory<sup>57</sup> this space is divided into an ( $n - 1 = 7$ ) dimensional fixed space containing the 7 l.m.o.s whose forms are fixed, and an ( $s = t - n + 1 = 5$ ) dimensional free space containing the l.m.o. to be calculated and four virtual orbitals.

It is convenient to label the eight occupied l.m.o.s. and four empty or virtual orbitals in formaldehyde with two sets of symbols as shown in Table 3.3. One set are the general symbols which were used in describing the basic l.m.o. theory in Chapter Two. Hence  $\phi_1 \dots \phi_8$  are the eight occupied orbitals and  $U_2 \dots U_5$  are the four virtual orbitals. The l.m.o. whose form is being calculated is  $\phi_i$  or  $U_1$ . The second set of symbols is specific to the formaldehyde molecule and describes the type of l.m.o.  $\sigma$  represents a sigma-bond,  $\pi$  a pi-bond,  $\lambda$  a lone pair and I an inner shell. The forms of the four virtual orbitals are determined by the orthogonality conditions but it is convenient to envisage them initially as the anti-bonding partners  $\sigma^*$  and  $\pi^*$  of the occupied orbitals  $\sigma$  and  $\pi$ .

As discussed in Chapter Two, a final set of localised m.o.s. is obtained using the l.m.o. theory only if the starting-point functions are localised. To start the calculation a set of functions which resemble in general form the required end-point functions are therefore needed.

Table 3.3 Labelling of l.m.o.s in Formaldehyde

	<u>General</u> <u>Symbol</u>	<u>Explicit</u> <sup>1</sup> <u>Symbol</u>	<u>Description</u>
Occupied l.m.o.s	$\phi_1$	$I_C$	Inner shell on carbon atom.
	$\phi_2$	$I_O$	Inner shell on oxygen atom.
	$\phi_3$	$\lambda_O^\pi$	$\pi$ -type lone pair on oxygen atom.
	$\phi_4$	$\lambda_O^\sigma$	$\sigma$ -type lone pair on oxygen atom.
	$\phi_5$	$\mu_{CH}$	carbon-hydrogen bond.
	$\phi_6$	$\mu_{CH'}$	carbon-hydrogen bond.
	$\phi_7$	$\mu_{CO}$	carbon-oxygen $\sigma$ -bond.
	$\phi_8$	$\pi_{CO}$	carbon-oxygen $\pi$ -bond.
Virtual Orbitals	$u_2$	$\mu_{CH}^*$	anti-bonding partner of $\mu_{CH}$ .
	$u_3$	$\mu_{CH'}^*$	anti-bonding partner of $\mu_{CH'}$ .
	$u_4$	$\mu_{CO}^*$	anti-bonding partner of $\mu_{CO}$ .
	$u_5$	$\pi_{CO}^*$	anti-bonding partner of $\pi_{CO}$ .

<sup>1</sup>  $\mu$  represents a  $\sigma$ -bond,  $\pi$  a  $\pi$ -bond,  $\lambda$  a lone pair and  $I$  an inner shell. The subscript denotes the atom or atoms with which the function is associated and a superscript distinguishes between the  $\sigma$ - and  $\pi$ -type lone pairs.



In addition, the starting-point functions should be completely confined to two centres for the bonds and one centre for the lone pairs and inner shells in order to apply the theory to the formaldehyde molecule at the earlier stages of approximation, where perfectly localised molecular orbitals are calculated.  $\phi_1 \dots \phi_8$  were therefore chosen initially as completely localised functions corresponding to the bonds, lone pairs and inner shells described in Table 3.3.

The general form for a bond between atoms A and B is

$$\phi_j = N_j ( p_j^A \psi_j^A + p_j^B \psi_j^B ) \quad (3.3)$$

where  $\psi_j^A$  and  $\psi_j^B$  are normalised hybrid atomic orbitals on atoms A and B respectively.  $p_j^A$  and  $p_j^B$  are polarity parameters and  $N_j$  is the normalising constant. Perfectly localised forms for the bonds in formaldehyde,  $\phi_5 \dots \phi_8$ , are therefore given by

$$\begin{aligned} \mu_{CH} &= N_5 ( p_5^C \psi_5^C + p_5^H \psi_5^H ) \\ \mu_{CH'} &= N_6 ( p_6^C \psi_6^C + p_6^{H'} \psi_6^{H'} ) \\ \mu_{CO} &= N_7 ( p_7^C \psi_7^C + p_7^O \psi_7^O ) \\ \pi_{CO} &= N_8 ( p_8^C \psi_8^C + p_8^O \psi_8^O ) \end{aligned} \quad (3.4)$$

The perfectly localised one-centre functions  $\phi_1 \dots \phi_4$  are of the form given below, where the inner shells are chosen initially as pure 1s atomic orbitals.

$$\begin{aligned} I_c &= 1s_c \\ I_o &= 1s_o \\ \lambda_c^\pi &= \psi_3^o \\ \lambda_o^\sigma &= \psi_4^o \end{aligned} \quad (3.5)$$

The starting-point forms for the virtual orbitals should also be perfectly localised, firstly in order to apply the theory at all the various stages of approximation, and secondly to obtain localised SCF virtual orbitals for use in configuration interaction calculations.

$$\begin{aligned}
 \mu_{CH}^* &= N'_5 ( p_5^C \gamma_5^C - p_5^H \gamma_5^H ) \\
 \mu_{CH'}^* &= N'_6 ( p_6^C \gamma_6^C - p_6^{H'} \gamma_6^{H'} ) \\
 \mu_{CO}^* &= N'_7 ( p_7^C \gamma_7^C - p_7^O \gamma_7^O ) \\
 \pi_{CO}^* &= N'_8 ( p_8^C \gamma_8^C - p_8^O \gamma_8^O )
 \end{aligned}
 \tag{3.6}$$

Equations (3.4), (3.5) and (3.6) define the required starting-point functions. The exact form of the hybrid atomic orbitals,  $\gamma$ , and the values of the polarity parameters,  $p$ , then remain to be chosen subject to the restrictions imposed by the orthogonality conditions.

Section 2    The Orthogonality Conditions

It became increasingly clear as the work progressed that the orthogonality conditions are the major difficulty in the implementation of the l.m.o. theory. In discussing these conditions it is helpful first to consider the calculation of the conventional c.m.o.s. where such problems do not arise.

The Hartree-Fock equations (2.3), and in particular the construction of the Hartree-Fock operator (2.4), assume that all the occupied molecular orbitals are mutually orthogonal. This condition is easily satisfied for c.m.o.s. Given a starting-point set of non-orthogonal functions, an orthogonal set may be obtained by applying one of the orthogonalisation procedures described in Chapter Two. ~~The Hartree-Fock operator is unchanged by such a procedure as it is invariant to a linear transformation of the orbitals.~~ The alteration of the original functions is not important in the case of the c.m.o.s. as the starting-point forms of the m.o.s. affect the calculation of the improved m.o.s. only via the operator and all the m.o.s. are determined together. Moreover, the solutions of equation (2.20)

$$[\underline{F} - \epsilon_i \underline{S}] c_i = 0 \quad (2.20)$$

for the c.m.o.s. are orthogonal so that, even if the original starting-point m.o.s. are not orthogonal, orthogonal functions are produced after the first cycle of the calculation. As the operator is constructed only from the occupied orbitals, starting-point forms for the empty virtual orbitals are not required, so no orthogonality difficulties arise concerning the virtual orbitals.

Solution of equation (2.20) is often achieved by applying an orthogonalisation procedure to the basis set of atomic orbitals to give an orthogonal basis set of functions which have no physical significance.

The elements of the  $\underline{S}$  matrix are then given by

$$S_{pq} = \delta_{pq} \quad (3.7)$$

so that the secular determinant has elements

$$F_{pq} - \epsilon \delta_{pq} \quad (3.8)$$

In the case of the l.m.o. theory the situation is more complicated. Three distinct sets of orthogonality requirements may be distinguished.

(i) Firstly, as with the c.m.o.s, construction of the Hartree-Fock operator, which contains all the occupied orbitals, presupposes that these orbitals are mutually orthogonal.

$$\langle \phi_j | \phi_k \rangle = \delta_{jk} \quad \begin{array}{l} j = 1 \dots 8 \\ k = 1 \dots 8 \end{array} \quad (3.9)$$

(ii) Secondly, there is the requirement in the formal l.m.o. theory that each function in the free space, the l.m.o. being calculated and the virtual orbitals, be orthogonal to each of the orbitals in the fixed space (equation(2.26)). This condition has no parallel in the calculation of the c.m.o.s.

$$\langle u_p | \phi_k \rangle = 0 \quad \begin{array}{l} k = 1 \dots 8 \ (k \neq i) \\ p = 1 \dots 5 \end{array} \quad (3.10)$$

(iii) Thirdly, as with the c.m.o.s, the most convenient solution of the secular determinant for the l.m.o.s (equation (2.33)) is achieved by making the basis functions, in this case the free space basis functions,  $U_1 \dots U_5$ , mutually orthogonal. This requirement is convenient but not essential.

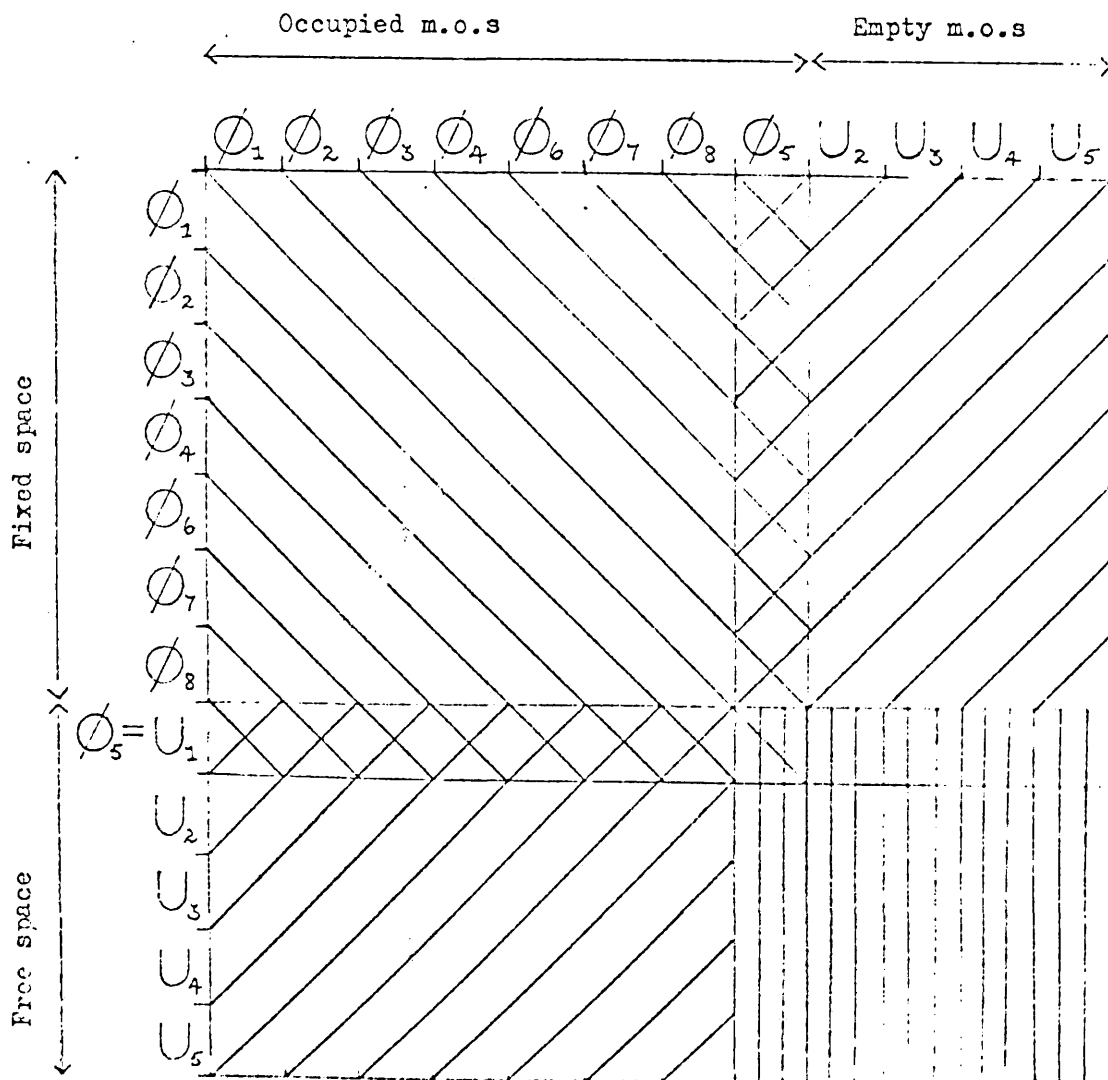
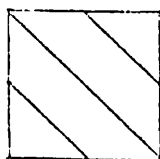
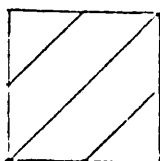


Figure 3.2 Overlap Integral Matrix for the Calculation of  $\phi_5$ , the carbon-hydrogen bond.

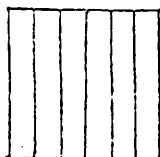
KEY



Orthogonality condition (i)



Orthogonality condition (ii)



Orthogonality condition (iii)

$$\langle u_p | u_q \rangle = \delta_{pq} \quad \begin{array}{l} p = 1 \dots 5 \\ q = 1 \dots 5 \end{array} \quad (3.11)$$

These three sets of conditions are illustrated in Figure 3.2. It can be seen that for all the orthogonality conditions described above to be obeyed all 12 l.m.o.s , filled and empty, must be mutually orthogonal.

Satisfying these conditions is made difficult by the requirement that the functions be localised (equations (3.4), (3.5) and (3.6)). This requirement is particularly important for the occupied orbitals. Orthogonality condition (i) might be satisfied by subjecting a non-orthogonal set of occupied orbitals to an orthogonalising procedure, as with the c.m.o.s. ~~This would not affect the Hartree-Fock operator which is invariant to a linear transformation of the orbitals.~~ However, in the l.m.o. theory the forms of the occupied orbitals are important and such a procedure would cause delocalisation of some or all of the functions. As well as appearing in the Hartree-Fock operator the occupied orbitals in the fixed space also affect the final form of the l.m.o. being calculated through orthogonality condition (ii), that the free space be orthogonal to the fixed space. Furthermore, as each l.m.o. is calculated in turn, the forms of the occupied orbitals in the fixed space should remain unaltered at the end of each calculation. As all the occupied orbitals appear in the fixed space at some time before the final set of l.m.o.s is obtained it would seem desirable to satisfy orthogonality condition (i) by obtaining an orthogonal set of localised occupied orbitals as a starting-point.

In previous work on methane<sup>58</sup> it was possible to construct by inspection perfectly localised occupied and virtual orbitals which satisfy all the orthogonality conditions. This was largely because of the high degree of

symmetry of the methane molecule and is not possible in formaldehyde, nor in the general case.

If the double criteria of perfect localisation and complete satisfaction of the orthogonality conditions are adhered to, for all 12 functions in formaldehyde, the problem becomes the solution of the simultaneous equations given by the orthogonality conditions (3.9), (3.10) and (3.11)

$$\langle \phi_j | \phi_k \rangle = \delta_{jk} \quad \begin{array}{l} j = 1 \dots 8 \\ k = 1 \dots 8 \end{array} \quad (3.9)$$

$$\langle u_p | \phi_k \rangle = 0 \quad \begin{array}{l} k = 1 \dots 8 \text{ (} k \neq i \text{)} \\ p = 1 \dots 5 \end{array} \quad (3.10)$$

$$\langle u_p | u_q \rangle = \delta_{pq} \quad \begin{array}{l} p = 1 \dots 5 \\ q = 1 \dots 5 \end{array} \quad (3.11)$$

for the constants  $c_{mj}$  and  $k_{mj}$  used in the expansion of the orbitals in terms of the atomic orbital basis set.

$$\phi_j = \sum_{m=1}^t \chi_m c_{mj} \quad j = 1 \dots n \quad (2.24)$$

$$u_p = \sum_{m=1}^t \chi_m k_{mp} \quad p = 1 \dots s \quad (2.25)$$

Many of these coefficients will be zero because of the localisation requirement. Thus, in terms of the atomic orbitals and their coefficients the perfectly localised molecular orbitals in formaldehyde are given below. The occupied orbitals are:

$$I_c = 1s_c$$

$$I_o = 1s_o$$

$$\lambda_o^{\pi} = 2p_{y_o}$$

$$\lambda_c^{\sigma} = c(6,4) 1s_o + c(7,4) 2s_o + c(8,4) 2p_{z_o}$$

$$\mu_{CH} = c(1,5) 1s_c + c(2,5) 2s_c + c(3,5) 2p_{z_c} + c(5,5) 2p_{y_c} + c(11,5) 1s_H$$

$$\mu_{CH'} = c(1,6) 1s_c + c(2,6) 2s_c + c(3,6) 2p_{z_c} + c(5,6) 2p_{y_c} + c(12,6) 1s_{H'} \quad (3.12)$$

$$\mu_{CO} = c(1,7) 1s_c + c(2,7) 2s_c + c(3,7) 2p_{z_c} + c(6,7) 1s_o + c(7,7) 2s_o + c(8,7) 2p_{z_o}$$

$$\pi_{CO} = c(4,8) 2p_{x_c} + c(9,8) 2p_{x_o}$$

and the virtual orbitals:

$$\mu_{CH}^* = k(1,2) 1s_c + k(2,2) 2s_c + k(3,2) 2p_{z_c} + k(5,2) 2p_{y_c} + k(11,2) 1s_H$$

$$\mu_{CH'}^* = k(1,3) 1s_c + k(2,3) 2s_c + k(3,3) 2p_{z_c} + k(5,3) 2p_{y_c} + k(12,3) 1s_{H'}$$

$$\mu_{CO}^* = k(1,4) 1s_c + k(2,4) 2s_c + k(3,4) 2p_{z_c} + k(6,4) 1s_o + k(7,4) 2s_o + k(8,4) 2p_{z_o} \quad (3.13)$$

$$\pi_{CO}^* = k(4,5) 2p_{x_c} + k(9,5) 2p_{x_o}$$

The pi orbitals are orthogonal to all other orbitals, by symmetry, and can easily be made orthogonal to each other. Disregarding the pi orbitals therefore, there are 35 disposable constants, while equations (3.9), (3.10) and (3.11) form a set of 55 simultaneous non-linear equations. The number



of equations greatly exceeds the number of disposable variables, so even if the equations were linear, straightforward solution of all the equations while keeping perfect localisation of all the functions would not therefore be possible. Ways of overcoming this difficulty had to be sought.

Two choices are available. Either the orthogonality conditions or the complete localisation requirement must be relaxed. The formal theory demands orthogonality between all functions, except for the free space within itself, but applies to any set of orthogonal orbitals whether localised or not. Moreover, non-orthogonal orbitals present difficulties in their use and linear dependencies may arise within a set of orbitals. For these reasons more importance was attached to the orthogonality conditions than to the localisation requirement.

The complete localisation of all functions imposed above can be relaxed a little in the following ways. The amount of freedom to relax the localisation requirement varies depending on the stage at which the calculation is made. More freedom is available at the final rigorous stage than at the earlier stages where a completely localised function is calculated.

Considering first the free space functions, for a rigorous final stage calculation the virtual orbitals may be allowed to delocalise extensively, although localised SCF virtual orbitals for use in configuration interaction calculations are not then obtained directly. The orbital to be calculated,  $\phi_1$ , also need not be completely localised at this stage. However, at earlier stages of approximation both  $\phi_1$  and its anti-bonding partner must be perfectly localised.

As discussed above, the localised nature of the fixed space is more important. The functions of the fixed space appear in the actual calculations only via the operator and for this purpose need not be localised,

the Hartree-Fock operator being invariant under a linear transformation.<sup>1</sup> However, the localisation condition for the fixed space cannot be relaxed completely as it is the localised nature of the fixed space which forces localisation on the orbital to be calculated via the fixed space - free space orthogonality conditions (equation (3.10)).

The best approach would therefore seem to lie in attempting to achieve orthogonality between the occupied orbitals and then to construct the virtual orbitals orthogonal both to the occupied orbitals and amongst themselves. Bearing in mind all these considerations a suitable set of starting-point functions for the calculations was sought.

### Section 3 The Search for a suitable starting-point

#### (a) Introduction

There are two main approaches to seeking a starting-point which satisfies as far as possible the double criteria of orthogonality and localisation. The first, which may be termed an "analytical" approach, is the solution of the orthogonality conditions as a set of simultaneous equations for the expansion coefficients  $c_{mj}$  and  $k_{mj}$  in equations (2.24) and (2.25). The second consists of applying an orthogonalisation procedure, such as those described in Chapter Two, to a suitable set of non-orthogonal functions. Both methods offer many possibilities and a complete investigation could not be undertaken in this work.

#### (b) Direct Analytical Solution of Orthogonality Equations

As stated above, complete satisfaction of all the orthogonality conditions whilst retaining localisation is not possible for the formaldehyde molecule. However the "analytical" method may still be used to impose as much orthogonality as possible on a set of perfectly localised orbitals. This approach was examined in the hope of obtaining an approximate solution, in which the remaining non-orthogonality was reduced to a level where the l.m.o. calculations would not be seriously affected.

As the orthogonality conditions are in general non-linear, the usual methods for the solution of linear simultaneous equations cannot be employed. Solution can be achieved by an M-dimensional generalisation of the Newton-Rapheson iterative procedure (where M is the number of equations). The method is described in detail in Chapter Seven. It involves a lengthy and complication calculation requiring a similar amount of computing time to a final stage l.m.o. calculation. Furthermore the expression for each overlap integral in

terms of the variables  $c_{mj}$  and  $k_{mj}$ , and the derivative of each expression with respect to each variable must be written explicitly into the program. In addition, it seems that the procedure does not always converge.

The method was first used to attempt to obtain orthogonality amongst the occupied orbitals (3.9). This condition consists of 36 equations, including the normalisation of each function. However  $\pi_{CC}$  is orthogonal to all other occupied l.m.o.s, and  $\lambda_C^\pi$  to all but  $\mu_{CH}$  and  $\mu_{CH}'$ , by symmetry, which reduces the number of equations to 24. The overlap integral between the inner shells was neglected as it is small (.00003) and cannot be reduced when using the forms of the functions given by (3.12). Imposing the condition that the two CH bonds should be of the same form effectively reduces the number of separate equations to 14, and the number of variables to 14. A solution of these 14 equations for the 14 variables was therefore attempted.

Estimates of the values of the coefficients are needed as a starting-point for the procedure. Values which gave non-polar bonds and conventional or Pauling<sup>28</sup> hybrids on each atom (ie  $sp^2$  hybrids on the carbon atom) were used. The calculation converges to a set of functions containing "anti-bonding" CH bonds, in which the coefficients of the atomic orbitals on the C and H atoms are of opposite sign. Indeed, it can be seen that the overlap integral between the CH bond and the  $\lambda_C^\pi$  lone pair which is given by

$$\langle \mu_{CH} | \lambda_C^\pi \rangle = c(11,5) \langle 2p_{y_O} | 1s_H \rangle + c(5,5) \langle 2p_{y_O} | 2p_{y_C} \rangle \quad (3.14)$$

cannot be set to zero if the two coefficients  $c(11,5)$  and  $c(5,5)$  are of the same sign, as the two atomic orbital overlap integrals are positive.

However, the l.m.o. theory requires as a starting-point functions which are of the same general form as the end-point functions so this solution

had to be discarded. The calculation was repeated imposing restrictions on the CH bonds, that the atomic orbital coefficients be of the sign expected on physical grounds, in an attempt to get some increase in orthogonality but none was obtained.

Attempts were then made to reduce as many of the overlap integrals between the occupied orbitals as possible to zero. The other equations were replaced with arbitrary conditions that the CH and CO bonds be non-polar and that the hybridisation on the carbon atom be the same in both the CH and CO bonds. The success of each calculation was measured by

$$\Delta = \left[ \frac{1}{56} \sum_{\substack{i=1 \\ (i \neq j)}}^8 \sum_{j=1}^8 \langle \phi_i | \phi_j \rangle^2 \right]^{1/2} \quad (3.15)$$

the root mean square value of the off-diagonal elements of the l.m.o. overlap integral matrix. An orthogonal set of l.m.o.s has a  $\Delta$  value of zero.

The overlap integrals of l.m.o.s sharing a common nucleus were first set to zero. The calculation converged to give a set of l.m.o.s shown in Table 3.4, which have a  $\Delta$  value of 0.0310, without altering greatly the general form of these functions. This is a considerable improvement on the  $\Delta$  value of the starting-point functions (0.0981) but cannot be said to be negligibly small. The overlap integrals of the CH bonds with the lone pairs are still large.

$$\begin{aligned} \langle \mu_{\text{CH}} | \lambda_o^{\sigma} \rangle &= 0.0208 \\ \langle \mu_{\text{CH}} | \lambda_o^{\pi} \rangle &= 0.1137 \end{aligned} \quad (3.16)$$

Table 3.4 Atomic Orbital Coefficients of l.m.o.s. obtained from an analytical solution of the orthogonality Equations

l.m.o.	1s <sub>c</sub>	2s <sub>c</sub>	2p <sub>z<sub>c</sub></sub>	2p <sub>x<sub>c</sub></sub>	2p <sub>y<sub>c</sub></sub>	1s <sub>o</sub>	2s <sub>o</sub>	2p <sub>z<sub>o</sub></sub>	2p <sub>x<sub>o</sub></sub>	2p <sub>y<sub>o</sub></sub>	1s <sub>H</sub>	1s <sub>H'</sub>
I <sub>c</sub>	1.0000	-	-	-	-	-	-	-	-	-	-	-
I <sub>o</sub>	-	-	-	-	-	1.0000	-	-	-	-	-	-
π <sub>o</sub>	-	-	-	-	-	-	-	-	-	1.0000	-	-
λ <sub>o</sub> <sup>+</sup>	-	-	-	-	-	-0.2221	0.9512	-0.3802	-	-	-	-
μ <sub>cl</sub>	-0.0972	0.2661	0.2219	-	0.4226	-	-	-	-	-	0.5447	-
μ <sub>cl'</sub>	-0.0972	0.2661	0.2219	-	-0.4226	-	-	-	-	-	-	0.5447
μ <sub>co</sub>	-0.0999	0.2921	-0.5239	-	-	-0.0476	0.0000	0.5955	-	-	-	-
π <sub>co</sub>	-	-	-	0.6413	-	-	-	-	0.6413	-	-	-
*μ <sub>cl</sub>	0.1168	-0.9691	-0.4948	-	-0.8484	-	-	-	-	-	1.3671	-
*μ <sub>cl'</sub>	0.1168	-0.9691	-0.4948	-	0.8484	-	-	-	-	-	-	1.3671
*μ <sub>co</sub>	0.0998	-0.8688	1.0526	-	-	-0.1227	0.9831	0.9552	-	-	-	-
*π <sub>co</sub>	-	-	-	-0.7985	-	-	-	-	0.7985	-	-	-

The arbitrary conditions were then replaced in various combinations with further l.m.o. overlap integrals set to zero. Some of these calculations did not converge to an end-point and those which did converge did not produce l.m.o.s with a  $\Delta$  value significantly less than that obtained previously.

Taking the atomic orbital coefficients for the occupied l.m.o.s shown in Table 3.4 as fixed, an "analytical" solution was also sought in constructing virtual orbitals orthogonal to the occupied orbitals, as required by orthogonality condition (ii). The CO virtual orbital is orthogonal to  $\pi_{cc}$  and  $\lambda_c^\pi$  by symmetry. As the CH bonds have the same form, there are 6 equations, including the normalisation of the orbital, to solve. There are also 6 variables  $k_{mj}$  in the orbital (equation (3.13)). Solution of the 6 equations for the 6 variables gave a CO virtual orbital orthogonal to all the occupied orbitals.

The CH virtual orbital is orthogonal to  $\pi_{cc}$  by symmetry, leaving 8 equations to solve. However, the CH virtual orbital has only five variables  $k_{mj}$ , so the 4 overlap integrals with occupied orbitals centred on the carbon atom were set to zero. The calculation reduced these four overlap integrals to zero, but the procedure leaves a large overlap integral with  $\lambda_c^\pi$ .

$$\langle \mu_{CH}^* | \lambda_c^\pi \rangle = -0.1268 \quad (3.17)$$

The coefficients of the virtual orbitals obtained in this way are also shown in Table 3.4.

It was concluded that the amount of non-orthogonality remaining in the functions resulting from these attempted "analytical" solutions was too great to be neglected. It is possible that greater mathematical expertise would yield an effective procedure along the lines followed here.

However, such a procedure would have the disadvantage of being inaccessible to the majority of chemists for whose use the l.m.o. theory is designed. Consequently, other ways of obtaining the required orthogonality were examined.

(c) Orthogonalisation of a Set of Non-orthogonal Functions

An essentially different approach in the search for a suitable starting-point is to construct, by some simple recipe, a set of non-orthogonal perfectly localised functions of the type required and then to apply an orthogonalisation procedure of some kind. This will lead to a certain amount of delocalisation of some or all of the functions. It has the advantage over an analytical solution that it is a much simpler procedure to follow and involves much less calculation. The desired non-orthogonal functions are easy to construct on physical and chemical grounds. There are several orthogonalisation procedures available and the various methods were discussed in Chapter Two. Of these, the methods of Schmidt orthogonalising and symmetric or Lowdin orthogonalising were considered.

(i) Schmidt Orthogonalising

The method of Schmidt Orthogonalising is simpler to apply than that of Lowdin orthogonalising. It is also more flexible in that the resulting functions depend on the order in which the functions appear in the original non-orthogonal set. While this has the disadvantage that the resulting set of orthogonal functions is not unique, and hence the sequence of orthogonalising must be specified, it also has advantages. Schmidt orthogonalising allows one function, the first in the sequence, to remain unchanged. This may be chosen as the orbital to be calculated, preventing



it from being delocalised by orthogonalising. The sequence of orthogonalising will therefore be different for the calculation of each l.m.o. Hence the Schmidt orthogonalising procedure provides a method which can be used for all stages of the l.m.o. calculations, both the rigorous final stage calculations, and the earlier stages which are concerned with perfectly localised orbitals. Construction of virtual orbitals orthogonal to the occupied orbitals can be achieved by placing them at the end of the sequence of orthogonalising, so that they do not affect the forms of the occupied orbitals. Satisfaction of all the orthogonality conditions can therefore be achieved before each l.m.o. calculation by successive Schmidt orthogonalisation of the occupied and virtual orbitals together in a sequence which is partly determined by the l.m.o. to be calculated and by the stage of calculation.

The Schmidt orthogonalisation procedure thus provides a simple method of meeting all the orthogonalisation requirements needed for the l.m.o. calculations, and can be applied at all the stages of approximation. Attention was therefore concentrated on this method of orthogonalisation and the use of the l.m.o. theory with Schmidt orthogonalising was examined at all the stages of approximation and for different sequences of orthogonalisation.

The only serious disadvantage of the method is that some of the occupied orbitals in the fixed space are delocalised. It was not clear before the calculations were made how this would affect the results. Thus, after the calculation of one l.m.o., say  $\phi_1$ , the next l.m.o. to be calculated, say  $\phi_2$ , may appear in the fixed space as an extensively delocalised function. This was partly overcome in the following way.

Rather than take as the starting-point for the calculation of  $\phi_2$  the form of  $\phi_2$  as it appeared in the fixed space for the previous calculation of  $\phi_1$ , the localised form of the function was taken. This was the original form it had before the orthogonalisation procedure for the calculation of  $\phi_1$  was applied. Thus for each calculation of an l.m.o. the starting-point form of the l.m.o. was localised.

The details of applying the l.m.o. theory using Schmidt orthogonalisation vary from stage to stage and are described together with the details of each stage in the next section. The main outline of the method is described below. Firstly, a set of non-orthogonal occupied and virtual orbitals of the form given by (3.4), (3.5) and (3.6) are constructed. The simplest choice is that of non-polar bonds with Pauling ( $sp^2$ ) hybrids, but other polarities and hybridisations were also used, providing different starting-points. (Details of all the starting-points used are given in Section 5). These 12 functions are arranged in the sequence appropriate to the calculation of the first l.m.o., say  $\phi_1$ , as given by (2.41) and Schmidt orthogonalised in that sequence in the way described in Chapter Two. The free space is then constructed from  $\phi_1$  and all the virtual orbitals. The fixed space consists of all the other functions, some of which will be quite extensively delocalised. An l.m.o. calculation can now be made, to give an improved form for  $\phi_1$ , and this calculation is iterated to self-consistency. Where the orbital to be calculated and the virtual orbitals do not occur together in the orthogonalising sequence it is necessary to re-orthogonalise before each iteration in order to preserve the correct form of the F operator. When self-consistency is reached the improved forms of  $\phi_1$  and the virtual orbitals are retained. These functions, together with the original, in

general non-orthogonal, forms for the other occupied orbitals, are then arranged in the sequence appropriate to the calculation of the next l.m.o., and the process repeated.

If the Schmidt orthogonalising sequence is chosen so that the l.m.o.s are not made orthogonal to the other occupied orbitals the set of energy-minimised functions obtained is non-orthogonal. An orthogonal set describing the same total wavefunction can then be obtained, if required, by Lowdin orthogonalising the 8 occupied orbitals.

(ii) Lowdin Orthogonalising

The other method of obtaining a suitable orthogonal starting-point examined was that of Lowdin orthogonalising. It has the advantage that it treats all the functions in a given set on an equal basis so that if applied to a set of localised molecular orbitals it is said to cause the smallest possible delocalisation of the orbitals.<sup>84</sup> It is also unambiguous in that the forms of the resulting functions are not dependent on the order in which the functions appear in the set. It is therefore a suitable method for a rigorous final stage l.m.o. calculation, where some delocalisation of the orbitals is allowed, but not for earlier stages where the orbital to be calculated must be perfectly localised.

Lowdin orthogonalisation is restricted in that it may only be used to orthogonalise within a set of functions and not to construct one set of functions orthogonal to another set, as the orthogonality of the fixed space to the free space requires. The 8 occupied orbitals may be Lowdin orthogonalised and then other methods used to construct virtual orbitals orthogonal to the occupied orbitals and amongst themselves. This is the method used by Wilhite and Whitten<sup>26</sup> in their l.m.o. calculations, in which all l.m.o.s are calculated together.

A starting-point set of 8 orthogonal occupied orbitals is obtained by Lowdin orthogonalising a non-orthogonal set of functions constructed on physical grounds. A different set of orthogonal free space functions is constructed for the calculation of each l.m.o. and solution of equation (2.30) for each l.m.o. then gives a new set of orbitals which in general is not orthogonal. This set of functions is again Lowdin orthogonalised and new sets of free space functions are constructed. The process is repeated until the l.m.o.s are self-consistent.

Calculations using the above method of orthogonalising were performed in this work and the results compared with those obtained by the method of Schmidt orthogonalising. A suitable set of free space functions was obtained in this case by Schmidt orthogonalising a non-orthogonal set of virtual orbitals both to the occupied orbitals and amongst themselves.

It would also be possible to use Lowdin orthogonalisation to obtain an orthogonal set of occupied orbitals and Schmidt orthogonalisation to construct the virtual orbitals, and then to calculate one l.m.o. at a time. This method is perhaps preferable as there would then be no need to re-Lowdin orthogonalise the occupied orbitals or to re-construct the virtual orbitals during the calculation, but this method was not used in the present work.

## Section 4 Description of the Various Stages of Approximation

### (a) Introduction

The l.m.o. theory described in Chapter Two can be applied to a molecule at various levels of approximation, or stages. The first stage corresponds to the simplest approximation, and the final stage is the complete solution of the secular determinant given by the l.m.o. theory. In the present work four stages are examined, the numbering of the stages differing slightly from that used previously.<sup>57</sup> The four stages are:

(i) Stage One: The calculation of a perfectly localised bond considering only the two electrons of the bond and assuming perfect shielding of the nuclei.

(ii) Stage Two: The calculation of a perfectly localised bond allowing for imperfect shielding of the nuclei and taking into account other electrons in the immediate environment of the bond.

(iii) Stage Three: The calculation of a perfectly localised bond taking into account all the other electrons and nuclei in the molecule.

(iv) Stage Four: The calculation of a slightly delocalised l.m.o. by complete solution of equation (2.30).

A localised bond is obtained by truncating the secular determinant, while effects of distant parts of the molecule are neglected by truncating the operator. The earlier stages are simpler calculations than the later stages and so involve less computing time. The theory was designed so that a stage 1 calculation is performed first, then a stage 2 calculation, and so on, until complete solution of the secular determinant is reached.<sup>57</sup>

There are several reasons for applying the l.m.o. theory at different stages. Firstly, a picture of the various factors which determine the nature of the chemical bond is built up. For example, comparison of the perfectly localised orbitals of stage 3 and the slightly delocalised orbitals of stage 4 shows the effect of delocalisation, while comparison of stages 1, 2 and 3 shows the effect of more distant parts of the molecule on a bond. Secondly, stage 3 gives functions which are perfectly localised without first making the rigorous stage 4 calculations and then truncating them. Thirdly, stages 1 and 2 are two-centre calculations requiring only two-centre electron repulsion integrals which are much easier to calculate than the three- and four-centre integrals necessary for later stages. This provides a possible route for the calculation of bonds in a large molecule where the number of electron repulsion integrals required becomes prohibitive for conventional c.m.o. all-electron calculations.

The details of the various stages are given below. Although a stage 4 calculation is lengthier than the earlier stages, and so in practice is performed last, it is conceptually the simplest of the four stages and so is described first.

(b) Stage Four

A stage 4 calculation consists of the complete solution of the secular equation (2.33), as described in Chapter Two. For formaldehyde there are 5 free space functions, and the secular determinant is 5-dimensional.

Suitable starting-point functions are constructed, as described in Section 3, and Schmidt orthogonalised. The F matrix is then formed from these functions. Each matrix element can be expressed as a sum of atomic orbital contributions

$$\langle u_p | F | u_q \rangle = \sum_{l=1}^{12} \sum_{m=1}^{12} k_{lp} k_{mq} \langle \chi_l | F | \chi_m \rangle \quad (3.18)$$

$$\begin{aligned} \text{where } u_p &= \sum_{l=1}^{12} \chi_l k_{lp} \\ u_q &= \sum_{m=1}^{12} \chi_m k_{mq} \end{aligned} \quad (3.19)$$

as in equation (2.25).

The operator is the Hartree-Fock operator (2.4) so that

$$\begin{aligned} \langle \chi_l | F | \chi_m \rangle &= \langle \chi_l | -\frac{1}{2} \nabla^2 | \chi_m \rangle + \langle \chi_l | \sum_a -\frac{Z_a}{r_a} | \chi_m \rangle \\ &+ \sum_{j=1}^8 \left[ 2 \langle \chi_l \chi_m | \phi_j \phi_j \rangle - \langle \chi_l \phi_j | \chi_m \phi_j \rangle \right] \end{aligned} \quad (3.20)$$

where  $\phi_j$  ( $j = 1 \dots 8$ ) are the occupied orbitals. These may be expressed in terms of the atomic orbitals, as in equation (2.24)

$$\begin{aligned} \langle \chi_l | F | \chi_m \rangle &= \langle \chi_l | -\frac{1}{2} \nabla^2 | \chi_m \rangle + \langle \chi_l | \sum_a -\frac{Z_a}{r_a} | \chi_m \rangle \\ &+ \sum_{j=1}^8 \sum_{k=1}^{12} \sum_{k'=1}^{12} c_{kj} c_{k'j} \left[ 2 \langle \chi_l \chi_m | \chi_k \chi_{k'} \rangle - \langle \chi_l \chi_{k'} | \chi_m \chi_k \rangle \right] \end{aligned} \quad (3.21)$$

$$\phi_j = \sum_{k=1}^{12} \chi_k c_{kj} \quad (3.22)$$

The kinetic energy integrals, nuclear attraction integrals, and electron repulsion and exchange attraction integrals shown in (3.21) for formaldehyde, using Slater atomic orbitals, were made available for this work by Newton and Palke.<sup>65</sup>

The Schmidt orthogonalising sequence used for stage 4 calculations may be represented as

$$(\chi_1 \dots \chi_8) (\chi_9 \dots \chi_{12}) \quad (3.23)$$

corresponding to (2.41), where the first eight functions are the occupied orbitals and the last four functions are the virtual orbitals. The order within the occupied orbitals does not affect the operator or total energy

as both are invariant under a linear transformation of the occupied orbitals.<sup>1</sup> However, it does affect the form of the l.m.o. used as a starting-point in a calculation. Taking the two extreme cases, if the l.m.o. to be calculated is the last occupied orbital in the sequence, i.e.  $\chi_g$ , it is altered by orthogonalisation to all the other occupied orbitals, and could become extensively delocalised. Thus the form of the orbital to be calculated is altered by being made orthogonal to the functions in the fixed space. On the other hand, if the l.m.o. to be calculated is first in the sequence, i.e.  $\chi_1$ , it is unaltered by the orthogonalising but is mixed into the other orbitals. Thus the forms of the functions in the fixed space are altered in order to make the orbital to be calculated orthogonal to them. The order within the other occupied orbitals is not important as they only appear in an actual calculation via the operator.

Calculations were made using the two extreme cases of Schmidt orthogonalising sequence and the results compared. The first sequence described above is referred to as sequence I and the second as sequence II, so that, for example, sequence I for the calculation of a CH bond might be:

$$(I_c I_o \lambda_c^\pi \lambda_o^\sigma \mu_{CH'} \mu_{CO} \pi_{CO} \mu_{CH}) (\mu_{CH}^* \mu_{CH'}^* \mu_{CO}^* \pi_{CO}^*) \quad (3.24)$$

and sequence II

$$(\mu_{CH} I_c I_o \lambda_o^\pi \lambda_o^\sigma \mu_{CH'} \mu_{CO} \pi_{CO}) (\mu_{CH}^* \mu_{CH'}^* \mu_{CO}^* \pi_{CO}^*) \quad (3.25)$$

(c) Stage Three

In a stage 3 calculation the secular determinant is truncated to a  $2 \times 2$  determinant. The free space contains two functions only, the l.m.o. to be calculated, and the virtual orbital which is its anti-bonding partner.



If both these functions are perfectly localised, the l.m.o.s resulting from the calculations are perfectly localised. Hence a stage 3 calculation provides a way of calculating directly perfectly localised occupied, and also virtual, orbitals.

Only the two-centre functions, the sigma- and pi-bonds can be calculated in this way. Attempts were made at extending the method to calculate the one-centre functions, the lone pairs and inner shells, but this did not prove successful. It was thought that one-centre functions might be calculated at stage 3 by expanding  $\phi_i$  in equation (2.27) in terms of free space functions which were all completely localised on the appropriate centre. A calculation of  $\lambda_o^\sigma$  was attempted in this way but in practice it was not found possible to construct two or more mutually orthogonal perfectly localised functions on the oxygen atom which did not have very large overlap integrals with the other occupied orbitals.

In theory, the operator used at stage 3 is the rigorous, complete Hartree-Fock operator, as at stage 4, constructed from all the nuclei, and all the electrons in the molecule. However, because of the difficulties posed in obtaining orthogonality, it is not always possible in practice to work with the Hartree-Fock operator at stage 3. In order to obtain a perfectly localised virtual orbital it is unfortunately necessary to introduce a further approximation when using Schmidt orthogonalisation.

To prevent delocalisation by the orthogonalising the virtual orbital must be placed in the orthogonalisation sequence before any function containing contributions from other atoms. Hence, first in the sequence are all the functions localised on the required atoms, including the orbital to be calculated, and the virtual orbital. Next in the sequence are all the other occupied orbitals. For example, the sequence for the calculation of a CO sigma-bond at stage 3 might be

$$(I_c I_o \lambda_o^\pi \lambda_o^\sigma \pi_{CO} \mu_{CO} \mu_{CO}^*) (\mu_{CH} \mu_{CH}') \quad (3.26)$$

The other virtual orbitals are not involved at stage 3 . Calculations with various orders of the functions within the two groups were made and the results compared.

All orbitals occurring in the sequence after the virtual orbital are altered by the mixing in of an unoccupied orbital, and hence the operator constructed from this set of orbitals is not the true Hartree-Fock operator. In practice, it was found that, provided the overlap integrals between the virtual orbital, and the occupied orbitals into which it mixed was small (i.e.  $< 0.1$ ) the effect was not too great.

The extent to which the inaccurate operator affects the calculations may be judged in two ways. Firstly a calculation which gives a final set of l.m.o.s with a higher total energy than the starting-point functions is obviously unacceptable. Secondly, the lowest eigenvalue,  $\epsilon_i$ , generated from the calculation by the inaccurate operator may be compared to a recalculated value  $\epsilon'_i$ .

$$\epsilon'_i = \langle \phi_i | F' | \phi_i \rangle \quad (3.27)$$

where  $\phi_i$  is the eigenfunction corresponding to  $\epsilon_i$  and  $F'$  is the true Hartree-Fock operator, constructed by Schmidt orthogonalisation of the occupied orbitals only, including  $\phi_i$ , without mixing in the virtual orbital, as in the computation proper. The magnitude of the quantity  $(\epsilon'_i - \epsilon_i)$  gives an indication of the error introduced by the inclusion of the virtual orbital into the F operator. A large value for this difference suggests a large error in the calculation, although a small value does not necessarily indicate that the error is small.

(d) Stages One and Two

At stages 1 and 2, as at stage 3 the secular determinant is truncated to a 2x2 determinant, and only two-centre functions may be calculated.

These will be perfectly localised if the starting-point is perfectly localised. Unlike stage 3, at stages 1 and 2 the operator is truncated. Instead of using the Hartree-Fock operator constructed from all the nuclei, and all the electrons in the molecule, a local operator containing only the nuclei of the bond is used. A different operator is therefore necessary for the calculation of each l.m.o.

(i) Stage One

At stage 1 perfect shielding of the nuclei by the electrons outside the bond is assumed, so that only the two electrons in the bond are considered, and an effective nuclear charge of +1 is assigned to each nucleus. In general, for a bond  $\phi_{AB}$  between nuclei A and B the operator  $F^{AB}$  is given by

$$F^{AB} = -\frac{1}{2}\nabla^2 - \frac{1}{r_A} - \frac{1}{r_B} + 2J_{AB} - K_{AB} \quad (3.28)$$

This operator contains expressions for the nuclear attraction associated with individual nuclei. As the integrals made available by Newton and Palke contained only the total nuclear attraction integrals, calculations of the individual nuclear attraction integrals had to be made. These integrals have the general form

$$\int \chi_i \left[ -\frac{1}{r_A} \right] \chi_j \, d\tau \quad (3.29)$$

The one- and two-centre integrals were calculated by hand, and the two-centre integrals checked by repeating the calculations using Roothaan's formulae.<sup>87</sup> The three-centre integrals were calculated using a computer program THRCEN, supplied by Melrose, which carries out Gaussian integration according to the method of Magnusson and Zauli.<sup>88</sup> The results are shown in Tables (3.5) to (3.8).

Table 3.5 Nuclear Attraction Integrals for the H nucleus over Slater Atomic Orbitals

	$1s_C$	$2s_C$	$2p_{z_C}$	$2p_{x_C}$	$2p_{y_C}$	$1s_O$	$2s_O$	$2p_{z_O}$	$2p_{x_O}$	$2p_{y_O}$	$1s_H$	$1s_{H'}$
$1s_C$	-0.500000	-0.110237	-0.008687	-	-0.015046	-0.000010	-0.016744	-0.028248	-	-0.000528	-0.038348	-0.034157
$2s_C$	-0.110237	-0.479042	-0.091925	-	-0.159219	-0.010948	-0.124903	-0.122769	-	-0.014998	-0.424583	-0.196981
$2p_{z_C}$	-0.008687	-0.091925	-0.467411	-	-0.060434	0.018700	0.138163	0.109933	-	0.012766	-0.268365	-0.108636
$2p_{x_C}$	-	-	-	-0.432520	-	-	-	-	-0.068780	-	-	-
$2p_{y_C}$	-0.015046	-0.159219	-0.060434	-	-0.537195	-0.000075	-0.018022	-0.022267	-	-0.073815	-0.464821	0.104668
$1s_O$	-0.000010	-0.010948	0.018700	-	-0.000075	-0.268320	-0.062638	-0.003445	-	-0.001808	-0.001584	-0.001568
$2s_O$	-0.016744	-0.124903	0.138163	-	-0.018022	-0.062638	-0.268316	-0.040440	-	-0.021226	-0.038288	-0.026956
$2p_{z_O}$	-0.028248	-0.122769	0.109933	-	-0.022267	-0.003445	-0.040440	-0.275885	-	-0.006907	-0.042835	-0.028019
$2p_{x_O}$	-	-	-	-0.068780	-	-	-	-	-0.262721	-	-	-
$2p_{y_O}$	-0.000528	-0.014998	0.012766	-	-0.073815	-0.001808	-0.021226	-0.006907	-	-0.266351	-0.022483	0.009075
$1s_H$	-0.038348	-0.424583	-0.268365	-	-0.464821	-0.001584	-0.038288	-0.042835	-	-0.022483	-1.200000	-0.096882
$1s_{H'}$	-0.034157	-0.196981	-0.108636	-	0.104668	-0.001568	-0.026956	-0.028019	-	0.009075	-0.096882	-0.288310

Table 3.6 Nuclear Attraction Integrals for the C nucleus over Slater Atomic Orbitals

	$1s_C$	$2s_C$	$2p_{z_C}$	$2p_{x_C}$	$2p_{y_C}$	$1s_O$	$2s_O$	$2p_{z_O}$	$2p_{x_O}$	$2p_{y_O}$	$1s_H$	$1s_{H'}$
$1s_C$	-5.700000	-0.538334	-	-	-	-0.000021	-0.097024	-0.165788	-	-	-0.200984	-0.200984
$2s_C$	-0.538334	-0.812500	-	-	-	-0.018034	-0.231551	-0.256706	-	-	-0.357523	-0.357523
$2p_{z_C}$	-	-	-0.812500	-	-	0.030798	0.256830	0.244100	-	-	-0.145069	-0.145069
$2p_{x_C}$	-	-	-	-0.812500	-	-	-	-	-0.118964	-	-	-
$2p_{y_C}$	-	-	-	-	-0.812500	-	-	-	-	-0.118964	-	-
$1s_O$	-0.000021	-0.018034	0.030798	-	-	-0.434783	-0.101499	-0.010217	-	-	-0.002593	-0.002593
$2s_O$	-0.097024	-0.231551	0.256830	-	-	-0.101499	-0.433741	-0.118094	-	-	-0.054153	-0.054153
$2p_{z_O}$	-0.165788	-0.256706	0.244100	-	-	-0.010217	-0.118094	-0.479169	-	-	-0.063137	-0.063137
$2p_{x_O}$	-	-	-	-0.118964	-	-	-	-	-0.411027	-	-	-
$2p_{y_O}$	-	-	-	-	-0.118964	-	-	-	-	-0.411027	-	-
$1s_H$	-0.200984	-0.357523	-0.145069	-	-0.251266	-0.002593	-0.054153	-0.063137	-	-	-0.020762	-0.105891
$1s_{H'}$	-0.200984	-0.357523	-0.145069	-	0.251266	-0.002593	-0.054153	-0.063137	-	0.020762	-0.105891	-0.486609

Table 3.7 Nuclear Attraction Integrals for the H<sup>+</sup> nucleus over Slater Atomic Orbitals

	$1s_C$	$2s_C$	$2p_{z_C}$	$2p_{x_C}$	$2p_{y_C}$	$1s_O$	$2s_O$	$2p_{z_O}$	$2p_{x_O}$	$2p_{y_O}$	$1s_H$	$1s_{H'}$
$1s_C$	-0.500000	-0.110237	-0.008687	-	0.015046	-0.000010	-0.016744	-0.028248	-	0.000528	-0.034157	-0.038348
$2s_C$	-0.110237	-0.479042	-0.091925	-	0.159219	-0.010948	-0.124903	-0.122769	-	0.014998	-0.196981	-0.424583
$2p_{z_C}$	-0.008687	-0.091925	-0.467411	-	0.060434	0.018700	0.138163	0.109933	-	-0.012766	-0.108636	-0.268365
$2p_{x_C}$	-	-	-	-0.432520	-	-	-	-	-0.068780	-	-	-
$2p_{y_C}$	0.015046	0.159219	0.060434	-	-0.537195	0.000075	0.018022	0.022267	-	-0.073815	-0.104668	0.464821
$1s_O$	-0.000010	-0.010948	0.018700	-	0.000075	-0.268320	-0.062638	-0.003445	-	0.001808	-0.001568	-0.001584
$2s_O$	-0.016744	-0.124903	0.138163	-	0.018022	-0.062638	-0.268316	-0.040440	-	0.021226	-0.026956	-0.038288
$2p_{z_O}$	-0.028248	-0.122769	0.109933	-	0.022267	-0.003445	-0.040440	-0.275885	-	0.006907	-0.028019	-0.042835
$2p_{x_O}$	-	-	-	-0.068780	-	-	-	-	-0.262721	-	-	-
$2p_{y_O}$	0.000528	0.014998	-0.012766	-	-0.073815	0.001808	0.021226	0.006907	-	-0.266351	-0.009075	0.022483
$1s_H$	-0.034157	-0.196981	-0.108636	-	-0.104668	-0.001568	-0.026956	-0.028019	-	-0.009075	-0.288310	-0.096882
$1s_{H'}$	-0.038348	-0.424583	-0.268365	-	0.464821	-0.001584	-0.038288	-0.042835	-	0.022483	-0.096882	-1.200000

Table 3.8 Nuclear Attraction Integrals for the O nucleus over Slater Atomic Orbitals

	$1s_C$	$2s_C$	$2p_{z_C}$	$2p_{x_C}$	$2p_{y_C}$	$1s_O$	$2s_O$	$2p_{z_O}$	$2p_{x_O}$	$2p_{y_O}$	$1s_H$	$1s_H'$
$1s_C$	-0.434783	-0.095860	0.013140	-	-	-0.000072	-0.017123	-0.028710	-	-	-0.029844	-0.029844
$2s_C$	-0.095860	-0.425419	0.151043	-	-	-0.153853	-0.307770	-0.210560	-	-	-0.179135	-0.179135
$2p_{z_C}$	0.013140	0.151043	-0.497710	-	-	0.264717	0.438365	0.259477	-	-	-0.036608	-0.036608
$2p_{x_C}$	-	-	-	-0.389273	-	-	-	-	-0.145107	-	-	-
$2p_{y_C}$	-	-	-	-	-0.389273	-	-	-	-	-0.145107	-	-
$1s_O$	-0.000072	-0.153853	0.264717	-	-	-7.700000	-0.776212	-	-	-	-0.021934	-0.021934
$2s_O$	-0.017123	-0.307770	0.438365	-	-	-0.776212	-1.137500	-	-	-	-0.059226	-0.059226
$2p_{z_O}$	-0.028710	-0.210560	0.259477	-	-	-	-	-1.137500	-	-	-0.043523	-0.043523
$2p_{x_O}$	-	-	-	-0.145107	-	-	-	-	-1.137500	-	-	-
$2p_{y_O}$	-	-	-	-	-0.145107	-	-	-	-	-1.137500	-	-
$1s_H$	-0.029844	-0.179135	-0.036608	-	-0.134723	-0.021934	-0.059226	-0.043523	-	-	-0.268128	-0.050218
$1s_H'$	-0.029844	-0.179135	-0.036608	-	0.134723	-0.021934	-0.059226	-0.043523	-	0.022844	-0.050218	-0.268128

The only starting-point functions required for each stage 1 calculation are the forms for the bond being calculated, and its anti-bonding virtual orbital, which are easily constructed to be orthogonal and so no orthogonalising difficulties arise at this stage.

(ii) Stage Two

Stage 2 provides a more realistic environment for the bond than stage 1, allowing for imperfect shielding. For a bond  $\phi_{AB}$ , between nuclei A and B, the operator is constructed from all functions centred on A or B, and the nuclei are given their true charges. The calculation is limited to a two-centre calculation by truncating to hybrids, containing one electron, bonds formed by A or B with other nuclei.

This is achieved in the following way. Firstly a set of suitable (non-orthogonal) l.m.o.s is constructed as for the other stages. Then, for each function, the coefficients of the atomic basis functions not situated on atoms A or B are set to zero, and the function is re-normalised. The result is that functions centred solely on A and B remain unchanged. These include inner shells and lone pairs on A or B, and the bonds and virtual orbitals between A and B. Functions not containing atomic basis functions on A or B, such as inner shells on other atoms, are discarded. Functions containing atomic basis functions on A or B as well as on other atoms are truncated to hybrids on A or B, with the same hybridisation as in the original l.m.o.s. These hybrids are then treated in the calculations as containing only one electron.

A stage 2 calculation may then be thought of as involving a much smaller atomic basis set than that used in stages 3 and 4, the atomic basis set being different for the calculation of each bond. For example, the calculation of a CH bond involves only the atomic orbitals of the carbon and hydrogen atoms.



The stage 2 operator has a more complicated expression than either the Hartree-Fock operator used at stages 3 and 4 or the stage 1 operator. In general it may be summarised as

$$F^{AB} = -\frac{1}{2}\nabla^2 - \frac{Z_A}{r_A} - \frac{Z_B}{r_B} + \sum_{j=1}^g (2J_j - K_j) + \sum_{k=1}^h (J_k - xK_k) \quad (3.30)$$

where the first summation is over the  $g$  doubly occupied l.m.o.s and the second summation is over the  $h$  singly occupied hybrids. The operator for the calculation of the CH bond in formaldehyde is then

$$\begin{aligned} F^{CH} = & -\frac{1}{2}\nabla^2 - \frac{1.0}{r_H} - \frac{6.0}{r_C} + (2J_{I_C} - K_{I_C}) + (2J_{\mu_{CH}} - K_{\mu_{CH}}) \\ & + (J_{\mu_{CH}^T} - xK_{\mu_{CH}^T}) + (J_{\mu_{CO}^T} - xK_{\mu_{CO}^T}) \\ & + (J_{\pi_{CO}^T} - xK_{\pi_{CO}^T}) \end{aligned} \quad (3.31)$$

where  $\mu_{CO}^T$  is the hybrid formed from the truncation of  $\mu_{CO}$ , etc.

Similarly, the operator for the calculation of the CO sigma bond is

$$\begin{aligned} F^{CO(\sigma)} = & -\frac{1}{2}\nabla^2 - \frac{6.0}{r_C} - \frac{8.0}{r_O} + (2J_{I_C} - K_{I_C}) + (2J_{I_O} - K_{I_O}) \\ & + (2J_{\lambda_O} - K_{\lambda_O}) + (2J_{\lambda_C} - K_{\lambda_C}) \\ & + (2J_{\pi_{CO}} - K_{\pi_{CO}}) + (2J_{\mu_{CO}} - K_{\mu_{CO}}) \\ & + (J_{\mu_{CH}^T} - xK_{\mu_{CH}^T}) + (J_{\mu_{CH}^T} - xK_{\mu_{CH}^T}) \end{aligned} \quad (3.32)$$

Although the expressions for stage 2 operators appear complicated they are straightforward to construct on physical grounds, apart from the question of the weight of inclusion of the exchange integrals, represented by the unknown,  $x$ . There is no difficulty with the doubly occupied orbitals. Each exchange integral occurs once as in the Hartree-Fock

operator, as one electron from the pair must have a spin parallel to that of the electron considered. However, the spin of the electron in the singly occupied hybrid atomic orbitals is not known. If it is parallel to that of the electron considered, the exchange integral for the hybrid should occur in the operator ( $x=1$ ). If the spins are paired no exchange integral should occur ( $x=0$ ). This situation is shown by including an "exchange factor",  $x$ , in the expression for the operator. Calculations with various values of  $x$  varying from one to zero were made, and the results compared to determine firstly how much the value of  $x$  affected the result of the calculation, and secondly which value of  $x$  gave the lowest total energy. This value was then used in subsequent calculations.

After the truncation procedure described above, the resulting functions were Schmidt orthogonalised before each calculation. As all the functions contain contributions only from atomic orbitals on the two-nuclei of the bond being calculated, orthogonalisation produces no delocalisation. The virtual orbital may therefore be placed at the end of the orthogonalising sequence, so that the mixing of the virtual orbital into the occupied orbitals which occurs at stage 3, does not occur at stage 2.

### Section 5   Details of Starting-Points

The results of the l.m.o. calculations using the orthogonalisation procedures described in Section 3 were found to be affected by the choice of the set of non-orthogonal functions used as a starting-point. Consequently details of all the various starting-points are given below. These are all sets of perfectly localised non-orthogonal functions of the form given by (3.4), (3.5) and (3.6). They are numbered (a) to (h).

Starting-point (a) is a set of non-polar bonds with  $sp^2$  hybrid atomic orbitals on the carbon atom directed along the internuclear axes. In this case all the polarity parameters in equations (3.4) are 1.0. and the normalised hybrid atomic orbitals are:

$$\begin{aligned}
 \psi_5^C &= 0.5773 \, 2s_C + 0.4083 \, 2p_{z_C} + 0.7071 \, 2p_{y_C} \\
 \psi_5^H &= 1s_H \\
 \psi_6^C &= 0.5773 \, 2s_C + 0.4083 \, 2p_{z_C} - 0.7071 \, 2p_{y_C} \\
 \psi_6^{H'} &= 1s_{H'} \\
 \psi_7^C &= 0.5773 \, 2s_C - 0.8165 \, 2p_{z_C} \\
 \psi_7^O &= 2p_{z_O} \\
 \psi_8^C &= 2p_{x_C} \\
 \psi_8^O &= 2p_{x_O}
 \end{aligned} \tag{3.33}$$

The sigma-type lone pair is approximated by the single  $2s_O$  atomic orbital and the pi-type lone pair by the  $2p_{y_O}$  atomic orbital.

$$\begin{aligned}
 \lambda_O^\pi &= 2p_{y_O} \\
 \lambda_C^\sigma &= 2s_O
 \end{aligned} \tag{3.34}$$

Starting-point (b) is the same as starting-point (a) except for the sigma-type lone pair which is constructed orthogonal to the CO sigma-bond and to the inner shell on the oxygen atom.

$$\lambda_o^{\epsilon} = 0.9505 2s_o - 0.3817 2p_{z_o} - 0.2219 1s_o \quad (3.35)$$

Another starting-point, (bb), was used in which the sigma-type lone pair was only constructed orthogonal to the CO sigma-bond.

$$\lambda_o^{\epsilon} = 0.9238 2p_{z_o} - 0.3829 2p_{z_o} \quad (3.36)$$

Starting-point (c) has non-polar bonds with sp hybridisation on the carbon atom. Hence all the polarity parameters in equations (3.4) are 1.0. The normalised hybrid atomic orbitals on the carbon atom are

$$\begin{aligned} \psi_5^C &= 0.7071 2s_c + 0.3536 2p_{z_c} + 0.6124 2p_{y_c} \\ \psi_6^C &= 0.7071 2s_c + 0.3536 2p_{z_c} - 0.6124 2p_{y_c} \\ \psi_7^C &= 0.7071 2s_c - 0.7071 2p_{z_c} \\ \psi_8^C &= 2p_{x_c} \end{aligned} \quad (3.37)$$

and the normalised hybrid atomic orbitals on the other atoms are the same as for starting-point (a). The sigma-type lone pair is constructed orthogonal to the CO sigma-bond and to the inner shell on the oxygen atom.

$$\lambda_c^{\epsilon} = 0.9514 2s_o - 0.3796 2p_{z_o} - 0.2221 1s_o \quad (3.38)$$

Starting-point (d) is the best result obtained by the attempted analytical solution of the orthogonality equations. The atomic orbital coefficients are given in Table 3.4. These functions were treated as a

non-orthogonal set and orthogonalised in the same way as the other starting-points.

Starting-point (e), used at stage 4, is the result of a stage 3 calculation using starting-point (bb) and Schmidt orthogonalising in sequence III (defined in Chapter Four).

Starting-point (f) has highly polar bonds. The hybridisation on the carbon atom is  $sp^2$  and the sigma-type lone pair is the single  $2s_o$  atomic orbital, as in starting-point (a). The polarity parameters of each bond are in the ratio 2/1 with all the bonds polarised towards the positive z direction.

$$\begin{aligned} p_5^C &= p_6^C = p_7^O = p_8^O = 1.0 \\ p_5^H &= p_6^{H'} = p_7^C = p_8^C = 2.0 \end{aligned} \quad (3.39)$$

Starting-point (g) is the same as starting-point (f) except for the sigma-type lone pair which is constructed orthogonal to the CO sigma-bond and to the inner shell on the oxygen atom.

$$\lambda_c^{\sigma} = 0.8651 2s_o - 0.5408 2p_{z_o} - 0.2020 1s_o \quad (3.40)$$

Starting-point (h), used at stage 3, is the result of a stage 2 calculation using starting-point (bb) and a value of the exchange factor, x, of 0.5.

The total electronic energies and orbital energies of starting-points (a) to (h) are given in Table 3.9.

Table 3.9 Total Electronic Energies and Orbital Energies of Starting-points (a.u.)

	(a)	(b)	(c)	(d)	(e)	(f)	(g)	(h)
Total Electronic Energy	-144.7572	-144.7650	-144.7808	-144.7458	-144.7857	-144.3456	-144.3301	-144.7859
Orbital Energy								
$I_C$	-11.374	-11.405	-11.432	-11.400	-11.332	-11.255	-11.350	-11.350
$I_O$	-20.550	-20.603	-20.591	-20.601	-20.555	-21.219	-21.257	-20.513
$\lambda_0^\pi$	-0.458	-0.473	-0.472	-0.472	-0.452	-0.834	-0.832	-0.428
$\lambda_0^\sigma$	-2.450	-2.028	-1.029	-1.030	-2.011	-2.796	-1.236	-1.987
$\mu_{CH}$	-0.877	-0.891	-0.969	-0.735	-0.740	-0.707	-0.746	-0.891
$\mu_{CH}'$	-0.877	-0.891	-0.969	-0.735	-0.740	-0.707	-0.746	-0.891
$\mu_{CO}$	-1.091	-1.135	-1.212	-0.898	-0.910	-1.329	-1.410	-1.103
$\pi_{CO}$	-0.471	-0.493	-0.498	-0.490	-0.459	-0.506	-0.554	-0.454

CHAPTER FOUR  
NUMERICAL RESULTS

Section 1   Stage 4(a) Introduction

A typical stage four l.m.o. calculation for formaldehyde using Schmidt orthogonalisation is shown in Table 4.1. The starting-point used here was a set of l.m.o.s with non-polar bonds, Pauling hybrids, and the sigma-type lone pair as the 2s atomic orbital on the oxygen atom. This is starting point (a), as described in Chapter Three, which has a total electronic energy of  $-144.7572$  a.u. The order in which the functions were orthogonalised in this calculation was sequence I, where the l.m.o. to be calculated is made orthogonal to the rest of the occupied orbitals.

Newton and Palke claim an accuracy of six or more decimal places in the integrals used in the calculations and an accuracy of four decimal places in the resulting value of the total energy.<sup>65</sup> The l.m.o. calculations were therefore cycled until the value of the total electronic energy differed by no more than 0.0005 a.u. from the value of the previous cycle. Generally, the starting-points used, which were chosen to be as near to the end-point functions as possible, required only 3 cycles of the l.m.o.s. The only more extreme starting-point used at stage 4, the "polar" starting-point (f), required more cycles. No convergence problems were encountered in any stage 4 calculation.

For comparison with the l.m.o. calculations a conventional canonical calculation of formaldehyde was performed. The results are shown in Table 4.2. The resulting total energy differs by 0.05 a.u. from the value reported by Newton and Palke.

Direct comparison of the computing times taken by l.m.o. and c.m.o. calculations is not straightforward, largely because the choice of the initial starting-point is different in the two cases. Each cycle within



Table 4.1 A Typical Stage 4 Calculation for Formaldehyde

Cycle	l.m.o. calculated	Number of iterations	Resulting total electronic energy (a.u.)	Energy Decrease (a.u.)
1	$\mu_{CH}$	5	-144.7686	0.0114
	$\mu_{CH'}$	4	-144.7795	0.0109
	$\mu_{CO}$	4	-144.7927	0.0132
	$\lambda_0^{\sigma}$	5	-144.8133	0.0206
	$\lambda_0^{\pi}$	6	-144.8160	0.0327
	$I_c$	4	-144.8483	0.0022
	$I_o$	4	-144.8500	0.0018
	$\pi_{CO}$	3	-144.8500	0.0000
2	$\mu_{CH}$	3	-144.8505	0.0005
	$\mu_{CH'}$	2	-144.8507	0.0002
	$\mu_{CO}$	5	-144.8531	0.0024
	$\lambda_0^{\sigma}$	4	-144.8532	0.0001
	$\lambda_0^{\pi}$	4	-144.8533	0.0001
	$I_c$	2	-144.8531	-0.0002
	$I_o$	2	-144.8531	0.0000
	$\pi_{CO}$	3	-144.8535	0.0004
3	$\mu_{CH}$	2	-144.8535	0.0000
	$\mu_{CH'}$	2	-144.8536	0.0001
	$\mu_{CO}$	4	-144.8538	0.0002
	$\lambda_0^{\sigma}$	2	-144.8538	0.0000
	$\lambda_0^{\pi}$	3	-144.8538	0.0000
	$I_c$	2	-144.8538	0.0000
	$I_o$	2	-144.8538	0.0000
	$\pi_{CO}$	3	-144.8538	0.0000

Table 4.2 The Canonical Molecular Orbitals of Formaldehyde

Orbital Energy (a.u.)	1s <sub>C</sub>	2s <sub>C</sub>	2p <sub>z<sub>C</sub></sub>	2p <sub>x<sub>C</sub></sub>	2p <sub>y<sub>C</sub></sub>	1s <sub>O</sub>	2s <sub>O</sub>	2p <sub>z<sub>O</sub></sub>	2p <sub>x<sub>O</sub></sub>	2p <sub>y<sub>O</sub></sub>	1s <sub>H</sub>	1s <sub>H'</sub>	
a <sub>1</sub>	-20.5815	0.0004	-0.0058	0.0052	0.0000	0.0000	0.9961	0.0186	0.0000	0.0000	0.0000	0.0002	0.0002
a <sub>1</sub>	-11.3180	0.9960	0.0157	0.0077	0.0000	0.0000	-0.0008	0.0024	0.0162	0.0000	0.0000	-0.0053	-0.0053
a <sub>1</sub>	-1.3608	-0.1125	0.2826	-0.1567	0.0000	0.0000	-0.2129	0.7656	0.1548	0.0000	0.0000	0.0265	0.0265
a <sub>1</sub>	-0.8297	-0.1706	0.5950	0.2308	0.0000	0.0000	0.0939	-0.4294	0.1143	0.0000	0.0000	0.2533	0.2533
b <sub>2</sub>	-0.6747	0.0000	0.0000	0.0000	0.0000	0.5600	0.0000	0.0000	0.0000	0.0000	0.4066	0.2818	-0.2818
a <sub>1</sub>	-0.5581	0.0419	-0.1078	0.4319	0.0000	0.0000	-0.0866	0.4952	-0.7124	0.0000	0.0000	0.1289	0.1289
b <sub>1</sub>	-0.4684	0.0000	0.0000	0.0000	0.6622	0.0000	0.0000	0.0000	0.6200	0.0000	0.0000	0.0000	0.0000
b <sub>2</sub>	-0.3772	0.0000	0.0000	0.0000	0.0000	-0.1650	0.0000	0.0000	0.0000	0.8875	-0.3475	0.3475	0.3475
b <sub>1</sub>	0.2481	0.0000	0.0000	0.0000	-0.7813	0.0000	0.0000	0.0000	0.8152	0.0000	0.0000	0.0000	0.0000
a <sub>1</sub>	0.6056	0.1726	-1.5146	-0.3086	0.0000	0.0000	-0.0416	0.2918	0.3393	0.0000	0.0000	0.9598	0.9598
b <sub>2</sub>	0.7416	0.0000	0.0000	0.0000	0.0000	1.2557	0.0000	0.0000	0.0000	-0.3300	-0.9523	0.9523	0.9523
a <sub>1</sub>	0.8461	0.0415	-0.4289	1.2491	0.0000	0.0000	-0.1053	0.8787	0.8676	0.0000	0.0000	-0.2663	-0.2663

Total Electronic Energy = -144.8539 a.u.    Nuclear Repulsion = 31.4514 a.u.    Total Energy = -113.4026 a.u.

Virial Theorem:  $-\pi/E = 1.0069$     Dipole Moment = 2.42 D ( $c^+o^-$ )

an individual stage 4 l.m.o. calculation is generally slightly faster than each cycle of a canonical calculation. However, the l.m.o. theory is designed so that the complete cycle of all the l.m.o.s, comprising the calculation to self-consistency of each l.m.o. at stage 4, is expected to be much slower than a single cycle of a canonical calculation,<sup>58</sup> although fewer cycles of the l.m.o. calculations should be needed to reach overall self-consistency. For the formaldehyde molecule a single complete cycle of l.m.o.s took approximately 20 times the computing time of one canonical calculation cycle. The computing time taken by l.m.o. calculations made following Wilhite and Whitten's method<sup>26</sup> using Lowdin orthogonalising was similar to that taken by the corresponding l.m.o. calculations using Schmidt orthogonalisation.

Fourteen stage 4 calculations were made to test whether the l.m.o. theory used resulted in a unique end-point which was independent firstly of the starting-point l.m.o.s, secondly of the details of the orthogonalising, and thirdly of the order in which the l.m.o.s were computed. Three different orders of calculating the l.m.o.s were used.

They are:

- (i) The order shown in Table 4.1, which was the order normally used.

$$\mu_{CH} \mu_{CH'} \mu_{CO} \lambda_c^{\sigma} \lambda_o^{\pi} I_c I_o \pi_{CO} \quad (4.1)$$

- (ii) The reverse of the order shown in Table 4.1, except for the pi bond.

$$I_o I_c \lambda_o^{\pi} \lambda_c^{\sigma} \mu_{CO} \mu_{CH'} \mu_{CH} \pi_{CO} \quad (4.2)$$

- (iii) A third order which calculates  $\lambda_o^{\sigma}$  first

$$\lambda_c^{\sigma} \lambda_o^{\pi} \mu_{CO} \mu_{CH'} \mu_{CH} I_c I_o \pi_{CO} \quad (4.3)$$

The formal theory does not make it clear whether the results of the method are dependent on the starting-point, as discussed in Chapter Two, and so calculations were performed using starting-points which were different, but of a similar form, to examine how far this is so in practice.

There are two ways in which the end-points of l.m.o. calculations may differ. Firstly, as for the calculation of the canonical m.o.s, different calculations could result in a different total wavefunction, which would give different values for properties dependent on the total wavefunction such as the total electronic energy and the electric dipole moment. Secondly, different calculations could give the same total wavefunction, but result in different l.m.o.s, one set of l.m.o.s being related to the other by a linear transformation. In this case, only properties associated with the individual l.m.o.s would differ, the eigenvalues, and bond properties such as atomic charges and bond moments. These two possibilities are examined separately below.

(b) The Uniqueness of the Total Wavefunction

The results of the various stage 4 calculations were first examined to see if they gave the same total wavefunction. Table 4.3 shows values of the total electronic energy and dipole moment, as well as a test of how well the results obey the virial theorem, which states that

$$E = -T = V/2 \quad (4.4)$$

where E is the total energy, T the kinetic energy and V the potential energy.

The dipole moment is given by the expectation value of the dipole moment operator  $\hat{\mu}$ .

$$\langle \Psi | \hat{\mu} | \Psi \rangle \quad (4.5)$$

$$\hat{\mu} = \sum_i q_i \mathbf{r}_i \quad (4.6)$$

Table 4.3 Properties Dependent on the Total Wavefunction

Method of Orthogonalisation	Orthogonalising sequence. <sup>1</sup>	Starting-point. <sup>2</sup>	Order of calculating l.m.o.s. <sup>2</sup>	Total Electronic Energy (a.u.)	Virial Theorem test -T/E	Dipole Moment <sup>3</sup> (D)
Schmidt orthogonalising	I	(a)	(i)	-144.8538	1.0069	2.44
		(a)	(ii)	-144.8537	1.0074	2.47
		(a)	(iii)	-144.8540	1.0072	2.46
		(d)	(i)	-144.8538	1.0072	2.46
		(d)	(ii)	-144.8539	1.0069	2.44
		(f)	(i)	-144.8538	1.0071	-
	II	(a)	(i)	-144.8539	1.0072	2.53
		(a)	(ii)	-144.8537	1.0073	-
		(b)	(i)	-144.8539	1.0070	2.44
		(c)	(i)	-144.8538	1.0072	2.46
		(d)	(i)	-144.8539	1.0070	2.44
		(e)	(i)	-144.8538	1.0070	2.44
	Lowdin orthogonalising	-	(a)	-	-144.8539	1.0070
-		(d)	-	-144.8539	1.0070	-

- 1) Orthogonalising sequences I and II, and starting-points (a) to (f) are defined in Chapter 3.
- 2) Orders (i), (ii) and (iii) of calculating the l.m.o.s are defined in this Chapter, by (4.1), (4.2) and (4.3).
- 3) All the dipole moments given are in the sense  $C^+O^-$ , and are in Debye (1 a.u. = 2.5413 Debye).

where  $q_i$  is the  $i$ th element of charge, and  $\mathbf{r}_i$  is the vector from an arbitrary origin to the element of charge  $q_i$ . For the formaldehyde molecule, only the dipole moment along the  $z$ -axis need be considered

$$\hat{\mu}_z = \sum_i q_i z_i \quad (4.7)$$

The electronic part of the dipole moment,  $\mu_z^e$ , may be expressed in terms of atomic orbitals using equation (2.24)

$$\mu_z^e = -2 \sum_{j=1} \sum_{m=1} \sum_{m'=1} c_{mj} c_{m'j} \langle \chi_m | z | \chi_{m'} \rangle \quad (4.8)$$

The integrals over atomic orbitals

$$\langle \chi_m | z | \chi_{m'} \rangle \quad (4.9)$$

were evaluated by hand. The nuclear part of the dipole moment,  $\mu_z^N$ , is given by

$$\mu_z^N = \sum_{i=1}^4 q_i^N z_i \quad (4.10)$$

where  $q_i^N$  is the charge on the  $i$ th nucleus. The total dipole moment is then given by

$$\mu_z = \mu_z^e + \mu_z^N \quad (4.11)$$

The total electronic energies shown in Table 4.3 differ by only 0.0003 a.u., which is well within the expected error, and these values agree with the total electronic energy obtained for the canonical m.o.s (-144.8539 a.u.). The virial theorem test,  $-T/E$ , is consistent at a value of  $1.0071 \pm 0.0002$ , as near to unity as may be expected from a minimum basis set calculation.<sup>67</sup> This again agrees with the result of the canonical calculation (1.0069). The values of the dipole moment also agree fairly well at 2.45 D  $\pm$  0.02, with one exception (2.53D). The value for the

canonical m.o.s is 2.42 D. These values agree reasonably well with the experimental value of 2.33 D.<sup>89</sup> These results therefore suggest that the various calculations shown in Table 4.3 lead to the same total wavefunction, and that this total wavefunction is the same as that obtained by the canonical calculation.

Confirmation that two different calculations give the same total wavefunction may be obtained by finding the overlap integral between the two wavefunctions. Let  $\bar{\Psi}_a$  and  $\bar{\Psi}_b$  represent wavefunctions obtained from calculations (a) and (b) respectively, and be made up of doubly occupied l.m.o.s  $\phi_i^a$  and  $\phi_i^b$  ( $i = 1 \dots 8$ ). The overlap integral between  $\bar{\Psi}_a$  and  $\bar{\Psi}_b$  is given by

$$\langle \bar{\Psi}_a | \bar{\Psi}_b \rangle = [\det(\underline{\underline{S}}^{ab})]^2 / \sqrt{[\det(\underline{\underline{S}}^{aa})]^2 \cdot [\det(\underline{\underline{S}}^{bb})]^2} \quad (4.12)$$

where  $\underline{\underline{S}}^{ab}$ ,  $\underline{\underline{S}}^{aa}$  and  $\underline{\underline{S}}^{bb}$  are 8x8 matrices of l.m.o. overlap integrals, with elements

$$\begin{aligned} S_{ij}^{ab} &= \langle \phi_i^a | \phi_j^b \rangle \\ S_{ij}^{aa} &= \langle \phi_i^a | \phi_j^a \rangle \\ S_{ij}^{bb} &= \langle \phi_i^b | \phi_j^b \rangle \end{aligned} \quad (4.13)$$

If the l.m.o.s of  $\bar{\Psi}_a$  and  $\bar{\Psi}_b$  are mutually orthogonal, then  $\det(\underline{\underline{S}}^{aa})$  and  $\det(\underline{\underline{S}}^{bb})$  are unity, and (4.12) is simplified to

$$\langle \bar{\Psi}_a | \bar{\Psi}_b \rangle = [\det(\underline{\underline{S}}^{ab})]^2 \quad (4.14)$$

Table 4.4 shows the overlap integrals between the results of various stage 4 l.m.o. calculations using the Schmidt orthogonalising procedure.

Table 4.4 Overlap Integrals of Stage Four Wavefunctions

Ortho- gonalising sequence <sup>1</sup>	Starting- point <sup>1</sup>	I				II				
		(a)	(a)	(a)	(d)	(a)	(b)	(c)	(d)	(e)
		(i)	(ii)	(iii)	(i)	(d)	(i)	(i)	(i)	(i)
	Order of calculation <sup>1</sup>	(i)	(ii)	(iii)	(i)	(ii)	(i)	(i)	(i)	(i)
I	(a)	1.0000	0.9999	0.9999	-	-	-	-	0.9999	-
	(a)	0.9999	1.0000	-	-	-	-	-	-	-
	(a)	0.9999	-	1.0000	1.0000	-	-	-	0.9999	-
	(d)	-	-	1.0000	1.0000	0.9999	-	-	-	-
	(d)	-	-	-	0.9999	1.0000	-	-	-	-
II	(a)	0.9999	-	-	-	-	-	0.9999	0.9999	0.9999
	(b)	-	-	0.9999	-	-	-	0.9999	1.0000	1.0000
	(c)	-	-	-	-	-	-	0.9999	0.9999	0.9999
	(d)	-	-	-	-	-	-	0.9999	1.0000	1.0000
	(e)	-	-	-	-	-	-	0.9999	1.0000	1.0000

<sup>1</sup> See footnotes to Table 4.3



The closeness of all the off-diagonal values to unity confirms that these calculations all lead to the same total wavefunction.

It may therefore be concluded that the total wavefunction obtained at the end of the stage 4 l.m.o. calculations of formaldehyde is independent of the starting-point, of the order of calculating the l.m.o.s, of the method of orthogonalisation used, and (with Schmidt orthogonalising) of the sequence of orthogonalisation. Furthermore, this total wavefunction is the same as that obtained by a canonical calculation.

(c) The Uniqueness of the Individual l.m.o.s.

It has been established that the stage 4 l.m.o. calculations all lead to the same many-electron total wavefunction. There remains the possibility that the sets of occupied l.m.o.s obtained from the calculations are rotated with respect to each other. Accordingly, the individual l.m.o.s were examined to see whether or not the method resulted in a unique set of l.m.o.s. For convenience the calculations which use Schmidt orthogonalisation are numbered 1 to 12, as in Table 4.5.

The question arises of how to determine whether two sets of l.m.o.s are the same. The most direct way is to compare the atomic orbital coefficients but this is cumbersome since each l.m.o. is described by up to 12 coefficients. Two l.m.o.s can also be shown to be the same if they have the same eigenvalue. Since the total wavefunction is the same in both cases, and the operator is invariant under a linear transformation, any differences in corresponding eigenvalues are due to differences in the individual l.m.o.s. The eigenvalues of l.m.o.s obtained by Schmidt orthogonalising using sequences I and II are shown in Tables 4.6 and 4.8 respectively. The values for the pi bond, which is unchanged by a linear

Table 4.5    Description of Stage 4 l.m.o. Calculations  
Using Schmidt Orthogonalisation

Calculation Number	Schmidt Orthogonalising sequence <sup>1</sup>	Starting-point <sup>1</sup>	Order of calculating l.m.o.s. <sup>2</sup>
1	I	a	(i)
2		a	(ii)
3		a	(iii)
4		d	(i)
5		d	(ii)
6		f	(i)
7	II	a	(i)
8		a	(ii)
9		b	(i)
10		c	(i)
11		d	(i)
12		e	(i)

<sup>1</sup> Orthogonalising sequences I and II, and Starting-points (a) to (f) are defined in Chapter 3.

<sup>2</sup> Orders (i), (ii) and (iii) of calculating the l.m.o.s. are defined in this Chapter, by (4.1), (4.2) and (4.3).

transformation amongst the l.m.o.s by reason of its symmetry, agree to within an accuracy of  $\pm 0.001$  a.u., both amongst themselves and with the value obtained by the canonical calculation ( $-0.468$  a.u.). However the eigenvalues of the other l.m.o.s are very sensitive to small changes in the total energy, a change of  $0.0005$  a.u. in the total energy producing changes of up to  $0.01$  a.u. in the eigenvalues. Two l.m.o.s were therefore judged to be significantly different if their eigenvalues differed by more than  $0.01$  a.u.

Two l.m.o.s may also be compared by evaluating the overlap integral between them. If two different calculations, a and b, give two sets of l.m.o.s  $\phi_1^a, \phi_2^a, \dots, \phi_8^a$  and  $\phi_1^b, \phi_2^b, \dots, \phi_8^b$ , the overlap integrals

$$\langle \phi_i^a | \phi_i^b \rangle \quad i = 1 \dots 8 \quad (4.15)$$

appear in Tables 4.7 and 4.9 for Schmidt orthogonalising in sequences I and II respectively. The last entry in these tables,  $\eta$ , is a measure of the over-all difference of the l.m.o.s in the two sets.

$$\eta = \sum_{i=1}^8 [\langle \phi_i^a | \phi_i^b \rangle - 1]^2 \quad (4.16)$$

Two l.m.o.s may be judged to be the same if their overlap integral is greater than  $0.998$ . If each of the eight overlap integrals between two sets of l.m.o.s is  $0.998$  then  $\eta$  is  $4.0 \times 10^{-5}$ .

The individual l.m.o.s obtained from stage 4 l.m.o. calculations using Schmidt orthogonalising sequences I and II and using Lowdin orthogonalising are examined in detail below.

(i) Schmidt Orthogonalising in Sequence I

The first six calculations described in Table 4.5 use Schmidt orthogonalising sequence I, where the l.m.o. being calculated is made orthogonal to all the other occupied orbitals, and hence the final set of

l.m.o.s obtained is an orthogonal one. The first three calculations have the same starting-point, (a), and differ in the order in which the l.m.o.s are calculated. Calculations 4 and 5 have another starting-point, (d), using different orders of calculating the l.m.o.s, and the last calculation has a third starting-point, (f). The eigenvalues associated with the l.m.o.s obtained by these calculations are given in Table 4.6 and their overlap integrals in Table 4.7.

Considering first calculations 1, 2 and 3, the eigenvalues of all the l.m.o.s, except the pi-bonds, differ by more than 0.01 a.u., in some cases by 1.0 a.u. The overlap integrals between these functions are much less than 0.998, with the exception of the inner shells in one case. Calculations 1, 2 and 3 therefore produce different individual l.m.o.s. The l.m.o.s given by calculations 4 and 5 have eigenvalues which agree to within 0.01 a.u. except those of the CH bonds and pi-type lone pair which differ by 0.02 a.u. and 0.04 a.u. respectively. The overlap integrals for these functions are both less than 0.998. Calculations 4 and 5 therefore also produce different individual l.m.o.s, though the differences are less than between calculations 1, 2 and 3. The form of the l.m.o.s obtained by Schmidt orthogonalising in sequence I therefore depends on the order in which the l.m.o.s are calculated, the dependence being less for starting-point (d) than for starting-point (a).

This dependence on the order in which the l.m.o.s are calculated can be seen to be a consequence of Schmidt orthogonalising the l.m.o. to be calculated to all the remaining occupied orbitals, as in sequence I. For a set of l.m.o.s  $\phi_1 \dots \phi_8$ , if  $\phi_1$  is calculated first, its form is changed so that it is then orthogonal to the other l.m.o.s  $\phi_2 \dots \phi_8$ . When next  $\phi_2$  is calculated it is already orthogonal to  $\phi_1$ , so that its form is altered to make it orthogonal to  $\phi_3 \dots \phi_8$ , but not to  $\phi_1$ .

Table 4.6 Eigenvalues of l.m.o.s Calculated using Schmidt  
Orthogonalising Sequence I. (a.u.).

$\phi_i$	Calculation					
	1	2	3	4	5	6
$I_O$	-20.586	-19.370	-20.583	-20.583	-20.585	-20.580
$I_C$	-11.341	-10.972	-11.337	-11.337	-11.340	-11.341
$\lambda_O^{\sigma}$	-1.272	-2.202	-1.043	-1.043	-1.042	-1.272
$\mu_{CO}$	-0.673	-1.044	-0.871	-0.881	-0.885	-0.670
$\mu_{CH}$	-0.687	-0.879	-0.742	-0.726	-0.706	-0.684
$\mu_{CH'}$	-0.710	-0.829	-0.721	-0.728	-0.706	-0.712
$\lambda_O^{\pi}$	-0.471	-0.430	-0.431	-0.430	-0.471	-0.471
$\mu_{CO}$	-0.470	-0.468	-0.468	-0.468	-0.469	-0.468

Table 4.7 Overlap Integrals between l.m.o.s Calculated using  
Schmidt Orthogonalising Sequence I.

$\phi_i$	Calculations			
	1 and 2	1 and 3	4 and 5	3 and 4
$I_C$	0.9851	1.0000	1.0000	1.0000
$I_O$	0.9715	1.0000	1.0000	1.0000
$\lambda_C^\pi$	0.9877	0.9877	0.9868	1.0000
$\lambda_C^\sigma$	0.9068	0.9355	0.9994	0.9999
$\mu_{CH}$	0.9809	0.9866	0.9931	0.9983
$\mu_{CH'}$	0.9908	0.9865	0.9931	0.9984
$\mu_{CO}$	0.9291	0.9348	1.0000	0.9996
$\pi_{CO}$	1.0000	1.0000	1.0000	1.0000
$\eta^1$	$1.6 \times 10^{-2}$	$8.9 \times 10^{-3}$	$3.0 \times 10^{-4}$	$6.0 \times 10^{-6}$

1.  $\eta$  is defined by equation (4.16).

If, however,  $\phi_2$  is calculated first it is changed so that it is orthogonal to the other l.m.o.s  $\phi_3 \dots \phi_8$  and  $\phi_1$ . When  $\phi_1$  is calculated it is then already orthogonal to  $\phi_2$  and only changed by orthogonalising to  $\phi_3 \dots \phi_8$ , not to  $\phi_2$ . Hence the order in which they are calculated determines whether  $\phi_1$  is constructed orthogonal to  $\phi_2$  or  $\phi_2$  is constructed orthogonal to  $\phi_1$ . This applies to all other pairs of functions in  $\phi_1 \dots \phi_8$ . The dependence of the calculations on the order in which the l.m.o.s are calculated is therefore a feature of Schmidt orthogonalising in sequence I, and a totally orthogonal starting-point would not be affected in this way. A set of starting-point functions which is close to orthogonal, such as (d), will be affected less by the order in which the l.m.o.s are calculated, than a set of functions such as (a), where there are much larger overlap integrals between the l.m.o.s. In particular the orthogonality of  $\lambda_c^r$  to  $\mu_{c0}$  and  $I_0$  seems to play an important part. In starting-point (d) the three functions are orthogonal. In calculation 3, which has starting-point (a),  $\lambda_c^r$  is calculated first and constructed orthogonal to  $\mu_{c0}$  and  $I_0$ , giving it a similar form to  $\lambda_c^r$  in (d). Comparison of calculations 3 and 4 in Tables 4.6 and 4.7 shows them to have similar end-points.

The dependence of Schmidt orthogonalising in sequence I on the order in which the l.m.o.s are calculated confuses the examination of the dependence of the method on the starting-point. Only three calculations were made which used different starting-points, (a), (d) and (f), calculating the l.m.o.s in the same order, (i). These are calculations 1, 4 and 6. Comparison of the eigenvalues in Table 4.6 shows that calculations 1 and 4 give different forms for the l.m.o.s, their eigenvalues, except those of the inner shells, all differing by more than 0.01 a.u. The eigenvalues given by calculations 1 and 6, however, agree

to well within 0.01 a.u., and so starting-points (a) and (f) give the same form for the l.m.o.s, when the l.m.o.s are calculated in the same order. These two starting-points differ only in the polarity of the bonds, and have the same form for the inner shells and lone pairs, and the same hybridisation on the carbon and oxygen atoms.

In conclusion, stage 4 calculations which use Schmidt orthogonalising sequence I produce end-point l.m.o.s which are mutually orthogonal but which are arbitrarily rotated. In particular the forms of the l.m.o.s obtained depend on the order in which they are calculated.

(ii) Schmidt Orthogonalising in Sequence II

Calculations 7 to 12 described in Table 4.5 use Schmidt orthogonalising sequence II, where the other occupied orbitals are made orthogonal to the l.m.o. to be calculated, and hence orthogonality of the l.m.o. to the other orbitals is not imposed. The resulting set of energy-minimised orbitals are therefore not mutually orthogonal, and so two end-points may differ from one another in the amount of non-orthogonality. The eigenvalues obtained for calculations 7 to 12 are given in Table 4.8, and the l.m.o. overlap integrals between the results of various calculations are given in Table 4.9.

Calculations 7 and 8 have the same starting-point, (a), and differ in the order of calculation of the l.m.o.s. Their end-points have eigenvalues which agree to within 0.01 a.u. The atomic orbital coefficients agree to within 0.001 and the overlap integrals between the l.m.o.s are all unity (to 4 decimal places). Hence calculations 7 and 8 have the same, non-orthogonal, end-point and Schmidt orthogonalising in sequence II is therefore independent of the order in which the l.m.o.s are calculated.



Table 4.8 Eigenvalues of l.m.o.s. Calculated using Schmidt  
Orthogonalising Sequence II. (a.u.)

$\phi_i$	Calculation					
	7	8	9	10	11	12
$I_0$	-20.570	-20.582	-20.582	-20.584	-20.584	-20.581
$I_C$	-11.349	-11.337	-11.342	-11.338	-11.341	-11.342
$\lambda_0^E$	-2.447	-2.455	-1.040	-1.045	-1.042	-1.031
$\pi_{CO}$	-1.105	-1.109	-1.118	-1.180	-0.886	-0.912
$\pi_{CH}$	-0.887	-0.878	-0.883	-0.948	-0.729	-0.743
$\pi_{CH'}$	-0.885	-0.880	-0.881	-0.949	-0.727	-0.743
$\lambda_0^\pi$	-0.462	-0.470	-0.470	-0.472	-0.471	-0.469
$\pi_{CO}$	-0.469	-0.468	-0.469	-0.468	-0.469	-0.468

Table 4.9 Overlap Integrals between l.m.o.s Calculated using Schmidt Orthogonalising Sequence II

$\phi_i$	Calculations												
	7 and 8	7 and 9	7 and 10	7 and 11	7 and 12	9 and 10	9 and 11	9 and 12	11 and 12	11 and 11	11 and 10	11 and 9	
$I_C$	1.0000	1.0000	1.0000	1.0000	1.0000	1.0000	1.0000	1.0000	1.0000	1.0000	1.0000	1.0000	1.0000
$I_O$	1.0000	1.0000	1.0000	1.0000	1.0000	1.0000	1.0000	1.0000	1.0000	1.0000	1.0000	1.0000	1.0000
$\lambda_0^{\pi}$	1.0000	1.0000	1.0000	1.0000	1.0000	1.0000	1.0000	1.0000	1.0000	1.0000	1.0000	1.0000	1.0000
$\lambda_0^{\sigma}$	1.0000	0.9087	0.9105	0.9094	0.9048	1.0000	1.0000	1.0000	1.0000	1.0000	1.0000	1.0000	0.9999
$\mu_{CH}$	1.0000	1.0000	0.9969	0.9927	0.9942	0.9968	0.9928	0.9990	0.9990	0.9990	0.9990	0.9990	0.9990
$\mu_{CH}'$	1.0000	1.0000	0.9962	0.9927	0.9942	0.9961	0.9927	0.9987	0.9987	0.9987	0.9987	0.9987	0.9987
$\mu_{CO}$	0.9999	1.0000	0.9952	0.9910	0.9926	0.9951	0.9910	0.9978	0.9978	0.9978	0.9978	0.9978	0.9978
$\pi_{CO}$	1.0000	0.9999	1.0000	0.9999	0.9999	1.0000	1.0000	1.0000	1.0000	1.0000	1.0000	1.0000	1.0000
$\eta^1$	$< 10^{-6}$	$8.3 \times 10^{-3}$	$8.1 \times 10^{-3}$	$8.4 \times 10^{-3}$	$9.2 \times 10^{-3}$	$5.0 \times 10^{-5}$	$2.0 \times 10^{-4}$	$8.0 \times 10^{-6}$	$8.0 \times 10^{-6}$	$8.0 \times 10^{-6}$	$8.0 \times 10^{-6}$	$8.0 \times 10^{-6}$	$8.0 \times 10^{-6}$

1.  $\eta$  is defined by equation (4.16).

Calculations 9 to 12 have different starting-points. Table 4.8 shows that, in general, the eigenvalues obtained by calculations 7 and 9 to 12 do not agree to within 0.01 a.u., and in Table 4.9 no pair of these calculations have overlap integrals for all the l.m.o.s greater than 0.998. The resulting forms of the l.m.o.s therefore do differ with the starting-point used.

Comparison of the values in Table 4.8 with the eigenvalues of the starting-point functions (Table 3.9) shows that the eigenvalues obtained by Schmidt orthogonalising in sequence II are quite close to the starting-point values. The stage 4 calculations only change the eigenvalues of the four bonds in formaldehyde by between 0.002 a.u. and 0.032 a.u., although the values for the other functions are changed by up to 1.0 a.u.

Where the eigenvalues of l.m.o.s obtained from different calculations agree to within 0.01 a.u. and the overlap integral between the l.m.o.s is greater than 0.998, the starting-point forms for the function are the same, or very similar, in the two cases. For example, all the starting-points have the same form for the inner shells and the pi-type lone pair. The eigenvalues obtained for these functions all agree to within 0.01 a.u., and the corresponding l.m.o. overlap integrals are all 1.0000.

Starting-points (a) and (b) differ only in the form of the sigma-type lone pair, the forms of the CH and CO bonds being the same. The resulting CH and CO bonds (calculations 7 and 9) have overlap integrals of 1.0000 and their eigenvalues agree to within 0.01 a.u. The eigenvalues obtained for the sigma-type lone pair, however, differ by 1.4 a.u., and the corresponding overlap integral is low (0.909). Calculations 7 and 9 therefore give the same form for the CH and CO bonds, but a different form for the sigma-type lone pair.

The starting-point forms for  $\lambda_o^{\epsilon}$  in calculations 9 to 12 are all constructed orthogonal to  $\mu_{cc}$  and  $I_o$ , which gives them a similar form. In calculation 7 the starting-point form of  $\lambda_o^{\epsilon}$  is the  $2s_o$  atomic orbital. The eigenvalues of  $\lambda_o^{\epsilon}$  obtained by calculations 9 to 12 agree at  $1.040 \pm .01$  a.u., which differs from the value obtained by calculation 7, 2.447 a.u. The overlap integrals for  $\lambda_o^{\epsilon}$  are unity between calculations 9 and 10, 9 and 11, and 11 and 12, but very low ( $\sim 0.91$ ) between calculation 7 and calculations 9 to 12. The resulting form of the sigma-type lone pair is therefore very similar for calculations 9 to 12 and different to that obtained by calculation 7.

In conclusion, a stage 4 calculation which Schmidt orthogonalises in sequence II results in a set of energy-minimised individual l.m.o.s which are not mutually orthogonal. The forms of these l.m.o.s depend on the starting-point used, but not on the order in which the l.m.o.s are calculated. Moreover, the l.m.o.s obtained have a form closely resembling the starting-point used so that the choice of different starting-points rotates the end-point functions.

Figure 4.1 shows how two such sets of l.m.o.s A and B, comprising l.m.o.s  $\phi_1^A, \phi_2^A \dots \phi_8^A$  and  $\phi_1^B, \phi_2^B \dots \phi_8^B$  respectively, are related, as both sets give the same total wavefunction.

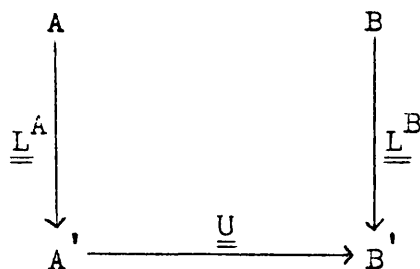


Figure 4.1 Representation of the relationship between sets of l.m.o.s  
obtained using Schmidt orthogonalising sequence II.

$\underline{\underline{L}}^A$  and  $\underline{\underline{L}}^B$  are linear transformations converting the non-orthogonal sets of l.m.o.s  $\underline{A}$  and  $\underline{B}$  into orthogonal ones  $\underline{A}'$  and  $\underline{B}'$ . This is equivalent to applying on orthogonalising procedure, as in equation (2.34)

$$\begin{aligned}\underline{A}' &= \underline{A} \cdot \underline{\underline{L}}^A \\ \underline{B}' &= \underline{B} \cdot \underline{\underline{L}}^B\end{aligned}\quad (4.17)$$

$\underline{A}'$  and  $\underline{B}'$  are then related by a unitary transformation  $\underline{U}$ .

$$\underline{B}' = \underline{A}' \cdot \underline{U} \quad (4.18)$$

The connection between  $\underline{A}$  and  $\underline{B}$  is given by

$$\underline{B} \cdot \underline{\underline{L}}^B = \underline{A} \cdot \underline{\underline{L}}^A \cdot \underline{U} \quad (4.19)$$

Providing  $\underline{\underline{L}}^B$  has an inverse,

$$\underline{B} = \underline{A} \cdot \underline{\underline{L}}^A \cdot \underline{U} \cdot \underline{\underline{L}}^B^{-1} \quad (4.20)$$

A measure of the non-orthogonality of a set of functions is given by  $\Delta$ , defined in Chapter Three.

$$\Delta = \left[ \frac{1}{56} \sum_{\substack{i=1 \\ i \neq j}}^8 \sum_{j=1}^8 \langle \phi_i | \phi_j \rangle^2 \right]^{\frac{1}{2}} \quad (3.15)$$

Values of  $\Delta$  for various starting-points and for the sets of functions obtained by calculations using Schmidt orthogonalising sequence II from these starting-points are shown in Table 4.10.

Table 4.10 Values of  $\Delta$ 

Starting-Point	$\Delta$ at Starting-Point	$\Delta$ after calculation using Schmidt orthogonalising sequence II
(a)	0.0981	0.0979
(b)	0.0553	0.0550
(c)	0.0871	0.0869
(d)	0.0310	0.0307
(e)	0.0391	0.0390

It can be seen that the values of  $\Delta$  after the calculations are the same as those before the calculations. The amount of non-orthogonality in the l.m.o.s obtained by calculations using Schmidt orthogonalising in sequence II is therefore the same as the amount of non-orthogonality in the starting-point. The two starting-points which have low  $\Delta$  values, (d) and (e) give l.m.o.s which differ the least.

To determine whether the differences between the sets of l.m.o.s obtained by using Schmidt orthogonalising sequence II were due to differences in the amount of non-orthogonality, each set was converted to an orthogonal set set of l.m.o.s, as described by (4.17). The method of Lowdin orthogonalisation was chosen so as to alter as little as possible the localised nature of the functions. The eigenvalues of the orthogonal l.m.o.s were then re-calculated, and their values are shown in Table 4.11. The overlap integrals between the orthogonal l.m.o.s are shown in Table 4.12. Lowdin orthogonalising produces greater changes in the less orthogonal sets of l.m.o.s, so that the eigenvalues obtained from calculation 7 are changed by up to 1.0 a.u., and those from calculations 9 and 10 by about 0.1 a.u., while the largest change in the results from calculations 11 and 12 is 0.03 a.u..

Table 4.11 Eigenvalues of l.m.o.s. Calculated using Schmidt

Orthogonalising Sequence II

(re-calculated after Lowdin Orthogonalisation)<sup>1</sup> (a.u.)

$\phi_i$	Calculation				
	7	9	10	11	12
$I_O$	-20.246	-20.569	-20.571	-20.584	-20.581
$I_C$	-11.231	-11.224	-11.206	-11.342	-11.342
$\lambda_C^{\sigma}$	-1.492	-1.039	-1.044	-1.040	-1.030
$\mu_{CO}$	-0.813	-0.953	-0.955	-0.886	-0.900
$\mu_{CH}$	-0.754	-0.752	-0.752	-0.719	-0.717
$\mu_{CH^*}$	-0.752	-0.750	-0.753	-0.719	-0.716
$\lambda_O^{\pi}$	-0.445	-0.451	-0.453	-0.449	-0.448
$\pi_{CO}$	-0.469	-0.469	-0.468	-0.469	-0.468

1. The values shown are those re-calculated after Lowdin orthogonalisation of the final set of l.m.o.s. The eigenvalues of the (non-orthogonal) l.m.o.s. obtained directly from the calculations are shown in Table 4.8.

Table 4.12 Overlap Integrals between l.m.o.s Calculated using Schmidt Orthogonalising Sequence II, after the final set of l.m.o.s has been Lowdin Orthogonalised

$\phi_i$	Calculations												
	7 and 9	7 and 10	7 and 11	7 and 12	9 and 10	9 and 11	9 and 12	10 and 11	10 and 12	11 and 12	11 and 12	11 and 12	
$I_C$	1.0000	0.9959	0.9959	0.9959	1.0000	0.9959	0.9959	0.9959	0.9953	0.9953	0.9953	0.9953	1.0000
$I_O$	0.9936	0.9973	0.9930	0.9930	1.0000	0.9997	0.9997	0.9997	0.9998	0.9998	0.9998	0.9998	1.0000
$\lambda_O^\pi$	1.0000	0.9969	1.0000	0.9999	0.9999	1.0000	0.9999	0.9999	0.9998	0.9998	0.9998	0.9998	1.0000
$\lambda_C^E$	0.9765	0.9996	0.9766	0.9744	0.9998	1.0000	0.9999	0.9999	0.9996	0.9996	0.9996	0.9996	0.9999
$\mu_{CH}$	1.0000	0.9956	0.9986	0.9986	0.9998	0.9986	0.9987	0.9980	0.9982	0.9982	0.9982	0.9982	0.9999
$\mu_{CH}^\pi$	1.0000	0.9956	0.9986	0.9986	0.9998	0.9986	0.9986	0.9980	0.9983	0.9983	0.9983	0.9983	0.9999
$\mu_{CO}$	0.9833	0.9976	0.9818	0.9796	0.9999	0.9982	0.9982	0.9976	0.9978	0.9978	0.9978	0.9978	0.9997
$\pi_{CO}$	1.0000	1.0000	0.9999	0.9999	1.0000	1.0000	1.0000	1.0000	1.0000	1.0000	1.0000	1.0000	1.0000
$\eta^1$	$9.0 \times 10^{-4}$	$7.0 \times 10^{-5}$	$9.0 \times 10^{-5}$	$1.1 \times 10^{-3}$	$< 10^{-6}$	$2.0 \times 10^{-5}$	$2.0 \times 10^{-5}$	$1.0 \times 10^{-5}$	$3.0 \times 10^{-5}$	$3.0 \times 10^{-5}$	$3.0 \times 10^{-5}$	$3.0 \times 10^{-5}$	$< 10^{-6}$

1.  $\eta$  is defined by equation (4.16).



The effect of Lowdin orthogonalising on the eigenvalues is, in general, to increase the differences between the values for the inner shells, but to decrease the differences between the values for the other l.m.o.s. The spread of these values, however, remains greater than 0.01 a.u. The overlap integrals between the inner shells after Lowdin orthogonalisation are in many cases smaller than before, indicating that the differences between their forms are increased, but the over-all differences between different sets of l.m.o.s, measured by  $\eta$  are in each case decreased. The values of  $\eta$  between calculations 9 to 12, which all have starting-points in which  $\lambda_c^F$  is constructed orthogonal to  $\mu_{c0}$  and  $I_0$ , are all below  $4.0 \times 10^{-5}$ . In particular calculations 9 and 10, and 11 and 12 both have  $\eta$  values of less than  $10^{-6}$ . The re-calculated eigenvalues of calculations 9 and 10 agree to within 0.01 a.u., with the exception of the values for  $I_c$ , which differ by 0.018 a.u. The re-calculated eigenvalues of calculations 11 and 12 agree to within 0.01 a.u., with the exception of the values for  $\mu_{c0}$ , which differ by 0.014 a.u. The l.m.o.s resulting from these two pairs of calculations are therefore of a very similar form after Lowdin orthogonalisation.

Lowdin orthogonalisation of the results of a stage 4 l.m.o. calculation using Schmidt orthogonalising sequence II therefore eliminates some of the differences between the various end-points, but does not result in a unique end-point.

(iii) Lowdin Orthogonalising

Only two calculations were made using this method of obtaining an orthogonal starting-point. The eigenvalues, given in Table 4.13, differ by more than 0.01 a.u., and so it appears that use of this method of orthogonalisation is also dependent on the starting-point, although more calculations are needed for a fuller examination. From the limited results

available the eigenvalues seem to be similar to those obtained by Schmidt orthogonalising in sequence II followed by Lowdin orthogonalisation of the resulting l.m.o.s. (Table 4.11).

Table 4.13 Eigenvalues of l.m.o.s obtained using Lowdin orthogonalisation (a.u.)

$\phi_i$	Starting-Point	
	(a)	(d)
$I_0$	-20.254	-20.584
$I_c$	-11.224	-11.341
$\lambda_c^{\sigma}$	-1.494	-1.042
$\mu_{cc}$	-0.816	-0.884
$\mu_{cn}$	-0.749	-0.718
$\mu_{cn'}$	-0.749	-0.718
$\lambda_c^{\pi}$	-0.151	-0.149
$\pi_{cn}$	-0.169	-0.169

(d) Summary of Stage 4 Results

The results of the stage 4 l.m.o. calculations on the formaldehyde molecule are summarised below. The calculations give a unique many-electron total wavefunction which is the same as that obtained by a canonical molecular orbital calculation. The forms of the individual l.m.o.s, however, are not unique. They depend on the method of orthogonalisation employed.

When Schmidt orthogonalisation is used the result depends on the sequence in which the l.m.o.s are orthogonalised. Furthermore, when using sequence I, where the l.m.o. to be calculated is made orthogonal to all the other occupied orbitals, the result depends on the order in

which the l.m.o.s are calculated. If sequence II is used, where the remaining occupied orbitals are made orthogonal to the l.m.o. to be calculated, the result does not depend on the order in which the l.m.o.s are calculated, but a non-orthogonal end-point results. Orthogonalisation of this end-point does not produce a unique set of l.m.o.s.

In all the methods of obtaining orthogonality used the forms of the individual l.m.o.s. obtained depend on the form of the initial starting-point, despite the fact that the total wavefunction obtained is independent of the starting-point. When Schmidt orthogonalisation in sequence II is used the forms of the end-point l.m.o.s. closely resemble the forms of the starting-point l.m.o.s. These results are discussed further in Chapter Five.

(e) Conversion of l.m.o.s to c.m.o.s.

The above results show that each stage 4 l.m.o. calculation produced the same total wavefunction, but different individual l.m.o.s. Each of these sets of l.m.o.s.  $\underline{\phi}$  is related to the canonical m.o.s.  $\underline{\theta}$  by a unitary transformation  $\underline{U}$ , which is slightly different in each case. As in equation (2.22):

$$\underline{\phi} = \underline{\theta} \cdot \underline{U} \quad (4.21)$$

To demonstrate this, some of the sets of l.m.o.s from stage 4 calculations were converted to the canonical m.o.s.

The  $8 \times 8$   $\underline{\epsilon}$  matrix was formed, with elements

$$\epsilon_{ij} = \langle \phi_i | F | \phi_j \rangle \quad (4.22)$$

The canonical m.o.s. have eigenvalues given by the diagonalised form of this matrix, denoted by  $\underline{\xi}$ . The canonical m.o.s. and their eigenvalues may therefore be found by solution of the eigenvalue equation

$$(\underline{\underline{\epsilon}} - \epsilon_i \underline{\underline{S}}) \underline{c}_i = 0 \quad (4.23)$$

where (4.24)

$$\theta_i = \underline{\phi} \cdot \underline{c}_i$$

and (4.25)

$$S_{kj} = \langle \phi_k | \phi_j \rangle$$

The eigenvalues of the canonical m.o.s obtained in this way from l.m.o. calculations 1, 7 and 12 are shown in Table 4.14. The values agree within themselves and with the eigenvalues of the canonical m.o.s calculated directly, to within 0.01 a.u.

Table 4.14 Eigenvalues of the canonical m.o.s obtained from  
l.m.o.s (a.u.)

l.m.o. Calculation		
1	7	12
-20.589	-20.583	-20.581
-11.345	-11.353	-11.345
-1.363	-1.362	-1.360
-0.829	-0.830	-0.829
-0.675	-0.675	-0.674
-0.560	-0.554	-0.558
-0.470	-0.469	-0.467
-0.379	-0.375	-0.380

Section 2    Stage Three

(a) Introduction

The basic aim of a stage 3 calculation is to compute the best set of perfectly localised molecular orbitals. The only available orthogonalisation procedure which preserves the perfectly localised nature of the l.m.o. being calculated is Schmidt orthogonalisation. The method, discussed in Chapter Three, involves the division of the l.m.o.s into two groups. The first group contains all the functions centred on the two atoms of the bond to be calculated and the second group contains all the other occupied orbitals. Table 4.15 shows which l.m.o.s occur in which group for the four bonds in formaldehyde calculated at stage 3.

Table 4.15    Groups of l.m.o.s in stage 3 Schmidt Orthogonalising sequences

l.m.o. to be calculated	l.m.o.s in group 1	l.m.o.s in group 2
$\mu_{CH}$	$I_c \mu_{CH} \mu_{CH}^*$	$I_o \lambda_c^{\sigma} \lambda_c^{\pi} \mu_{CH'} \mu_{CO} \pi_{CO}$
$\mu_{CH'}$	$I_c \mu_{CH'} \mu_{CH'}^*$	$I_o \lambda_c^{\sigma} \lambda_c^{\pi} \mu_{CH} \mu_{CO} \pi_{CO}$
$\mu_{CO}$	$I_c I_o \lambda_c^{\sigma} \lambda_c^{\pi} \pi_{CO} \mu_{CO} \mu_{CO}^*$	$\mu_{CH} \mu_{CH'}$
$\pi_{CO}$	$I_c I_o \lambda_c^{\sigma} \lambda_c^{\pi} \mu_{CO} \pi_{CO} \pi_{CO}^*$	$\mu_{CH} \mu_{CH'}$

Use of this method introduces inaccuracies into the operator by allowing one of the virtual orbitals to mix into some of the occupied orbitals. Preliminary calculations were therefore made to investigate whether these inaccuracies would prove to be a serious difficulty and, if this was not the case, which sequence of l.m.o.s would give the best results.

(b) Investigation of Schmidt Orthogonalising Sequences at Stage 3

The preliminary calculations were carried out in the following way. From starting-point (a) or (bb), which differ only in the form of the sigma-type lone pair, a single calculation was performed of a CH or a CO sigma bond using various sequences of the l.m.o.s within the two groups. The success of the calculation was judged firstly by whether it resulted in a decrease in the total energy and secondly by the quantity  $(\epsilon'_i - \epsilon_i)$ , defined in Chapter Three.

The results of calculating a single CH bond from starting-point (bb) are shown in Table 4.16. The values of the total electronic energy given are re-calculated after the calculation. These are formed from the l.m.o. given by the calculation and the other occupied orbitals so that they do not include contributions from the virtual orbital. The first three entries in Table 4.16 show that the order of the functions in the second group does not affect the resulting total energy or the eigenvalue of the CH bond, so that it may be concluded that the order of the functions within the second group is unimportant.

The results of calculating a single CO sigma bond from starting points (a) and (bb) are shown in Tables 4.17 and 4.18 respectively. These results together with the last entry in Table 4.16 show that different orders within the first group of functions give different values for the total electronic energy and for the eigenvalue of the l.m.o. calculated. Changes within the fixed space functions in this group lead to the same results, so that it may be concluded that the different values obtained are determined by the position in the orthogonalising sequence of the l.m.o. to be calculated, and the virtual orbital.

The position of the virtual orbital determines into which occupied orbitals it is mixed by the orthogonalising and hence the extent of the

Table 4.16 Results of Calculating a single CH bond from  
Starting-point (bb) at Stage 3.

Schmidt Orthogonalising Sequence		Total Electronic Energy (a.u.)	Eigenvalues <sup>1</sup>		$\epsilon'_{\mu_{CH}} - \epsilon_{\mu_{CH}}$ (a.u.)
group 1	group 2		$\epsilon_{\mu_{CH}}$ (a.u.)	$\epsilon'_{\mu_{CH}}$ (a.u.)	
$I_C \mu_{CH} \mu_{CH}^*$	$I_O \lambda_O^\pi \lambda_O^\sigma \mu_{CH} \mu_{CO} \pi_{CO}$	-144.7811	-0.719	-0.750	-0.032
$I_C \mu_{CH} \mu_{CH}^*$	$\pi_{CO} \mu_{CH} \mu_{CO} \lambda_O^\pi \lambda_O^\sigma I_O$	-144.7812	-0.719	-0.750	-0.032
$I_C \mu_{CH} \mu_{CH}^*$	$I_O \mu_{CH} \lambda_O^\pi \mu_{CO} \lambda_O^\sigma \pi_{CO}$	-144.7812	-0.719	-0.750	-0.032
$\mu_{CH} \mu_{CH}^* I_C$	$I_O \lambda_O^\pi \lambda_O^\sigma \mu_{CH} \mu_{CO} \pi_{CO}$	-144.7664	-0.872	-0.901	-0.029

1.  $\epsilon_{\mu_{CH}}$  is the eigenvalue given by the stage 3 calculation,  $\epsilon'_{\mu_{CH}}$  the eigenvalue re-computed after the calculation.

Table 4.17 Results of Calculating a single CO sigma-bond  
from Starting-point (a) at Stage 3.

Schmidt Orthogonalising Sequence		Total Electronic Energy (a.u.)	Eigenvalues <sup>1</sup>		$\epsilon'_{\mu\sigma} - \epsilon_{\mu\sigma}$ (a.u.)
group 1	group 2		$\epsilon_{\mu\sigma}$ (a.u.)	$\epsilon'_{\mu\sigma}$ (a.u.)	
$I_c I_c \lambda_0^\sigma \lambda_0^\pi \pi_{CO} \mu_{CO} \mu_{CO}^*$	$\mu_{CH} \mu_{CH}'$	-144.7637	-0.629	-0.640	-0.011
$\mu_{CO} I_c I_c \lambda_0^\sigma \lambda_0^\pi \pi_{CO} \mu_{CO}^*$	$\mu_{CH} \mu_{CH}'$	-144.7623	-1.079	-1.091	-0.012
$\mu_{CO} \lambda_0^\sigma \lambda_0^\pi I_0 I_c \pi_{CO} \mu_{CO}^*$	$\mu_{CH} \mu_{CH}'$	-144.7623	-1.079	-1.091	-0.012
$I_c I_0 \mu_{CO} \lambda_0^\sigma \lambda_0^\pi \pi_{CO} \mu_{CO}^*$	$\mu_{CH} \mu_{CH}'$	-144.7606	-0.864	-0.876	-0.011
$\mu_{CO} \mu_{CO}^* I_c I_0 \lambda_0^\sigma \lambda_0^\pi \pi_{CO}$	$\mu_{CH} \mu_{CH}'$	-144.4191	-1.020	-1.206	-0.186

1.  $\epsilon_{\mu\sigma}$  is the eigenvalue given by the stage 3 calculation,  $\epsilon'_{\mu\sigma}$  the eigenvalue re-computed after the calculation.



Table 4.18 Results of Calculating a single CO sigma-bond  
 from Starting-point (bb) at Stage 3.

Schmidt Orthogonalising Sequence		Total Electronic Energy (a.u.)	Eigenvalues <sup>1</sup>		$\epsilon_{\mu\sigma}^i - \epsilon_{\mu\sigma}$ (a.u.)
group 1	group 2		$\epsilon_{\mu\sigma}$ (a.u.)	$\epsilon_{\mu\sigma}^i$ (a.u.)	
$I_c I_o \lambda_o^E \lambda_o^\pi \pi_{co} \mu_{co} \mu_{co}^*$	$\mu_{CH} \mu_{CH}^i$	-144.7726	-0.911	-0.923	-0.013
$\lambda_o^E \lambda_o^\pi I_c I_o \pi_{co} \mu_{co} \mu_{co}^*$	$\mu_{CH} \mu_{CH}^i$	-144.7726	-0.911	-0.923	-0.013
$\mu_{co} I_o I_c \lambda_o^E \lambda_o^\pi \pi_{co} \mu_{co}^*$	$\mu_{CH} \mu_{CH}^i$	-144.7726	-1.118	-1.131	-0.012
$\lambda_c^E \lambda_o^\pi \mu_{co} \mu_{co}^* I_c I_o \pi_{co}$	$\mu_{CH} \mu_{CH}^i$	-144.7718	-1.122	-1.129	-0.008
$I_c I_o \mu_{co} \mu_{co}^* \lambda_o^E \lambda_o^\pi \pi_{co}$	$\mu_{CH} \mu_{CH}^i$	-144.6974	-0.738	-0.977	-0.239
$\mu_{co} \mu_{co}^* I_c I_o \lambda_c^E \lambda_o^\pi \pi_{co}$	$\mu_{CH} \mu_{CH}^i$	-144.5066	-1.020	-1.287	-0.267

1.  $\epsilon_{\mu\sigma}$  is the eigenvalue given by the stage 3 calculation,  $\epsilon_{\mu\sigma}^i$  the eigenvalue re-computed after the calculation.

inaccuracies in the operator. These inaccuracies will be minimised, at stage 3, by placing the virtual orbital at the end of the functions in the first group, the furthest along the orthogonalising sequence possible whilst preserving localisation, so that it mixes only into the l.m.o.s in the second group. Where this is done the total electronic energy in each case shows a decrease on the starting-point value, and values of  $(\epsilon'_i - \epsilon_i)$  of approximately  $-0.01$  a.u. for the CO sigma bond and  $-0.03$  a.u. for the CH bond occur.

The extent to which the virtual orbital mixes into an occupied orbital which is placed after it in the Schmidt orthogonalising sequence is determined by its overlap integral with the occupied orbital. Values of these overlap integrals are given in Table 4.19. For the calculation of  $\mu_{CO}$ , the only l.m.o.s in the second group of functions are  $\mu_{CH}$  and  $\mu_{CH'}$ , with which the virtual orbital has a low overlap integral of 0.01. For the calculation of  $\mu_{CH}$ , there are six l.m.o.s in the second group of functions, but the virtual orbital has a fairly low overlap integral with each of them, the largest being  $-0.15$  for the overlap integral with the pi-type lone pair.

These results may be compared with those orthogonalising sequences where the virtual orbital is not placed at the end of the first group of functions. The virtual orbital is then mixed into more occupied orbitals, and the inaccuracy of the operator is increased. In each case the resulting total electronic energy is much less of an improvement on the starting point value. In particular where  $\mu_{CO}^*$  is placed before  $\lambda_O^F$ , with which it has a very large overlap integral, the resulting total electronic energy is higher than that of the starting-point functions, and the value of  $(\epsilon'_i - \epsilon_i)$  is greater than  $-0.20$  a.u. The effect of placing the virtual orbital before the inner shell functions in the first group is less.

Table 4.19 Overlap Integrals of Virtual Orbitals with Occupied  
Orbitals, for Starting-Points (a) and (bb).

Occupied l.m.o.	Overlap Integral with $\psi_{CH}^*$	Overlap Integral with $\psi_{CO}^*$
$I_C$	-0.0750	-0.0632
$I_O$	0.0141	-0.0738
$\lambda_o^\pi$	-0.1480	0.0000
$\lambda_o^\sigma$	0.0778, 0.0589 <sup>1</sup>	-0.5527, -0.7155 <sup>1</sup>
$\psi_{CH}$	0.0000	0.0126
$\psi_{CH}'$	0.1225	0.0126
$\psi_{CO}$	0.1039	0.0000
$\pi_{CO}$	0.0000	0.0000

<sup>1</sup> The first value is for starting-point (a), the second for starting-point (bb).

For the calculation of both  $\mu_{CH}$  and  $\mu_{CO}$  the value of  $(\epsilon'_i - \epsilon_i)$  is not altered significantly, but the resulting total electronic energy is in each case higher than when the virtual orbital is placed after these functions. The overlap integrals of the virtual orbitals with the inner shells are low ( $< 0.10$  a.u.).

The above results suggest that the inaccuracies incurred in the operator by Schmidt orthogonalising as described for stage 3 in Chapter Three will not seriously disrupt the calculations if the virtual orbital is placed at the end of the first group of functions. This has the effect of only allowing the virtual orbital to mix into functions with which it is likely to have a small overlap integral. The orthogonalising sequence used for a stage 3 calculation of a bond  $\mu_{AB}$  may therefore be re-written

$$(\phi_1 \phi_2 \dots) \mu_{AB}^* (\phi'_1 \phi'_2 \dots) \quad (4.26)$$

where  $\phi_1, \phi_2 \dots$  are l.m.o.s centred on atoms A and/or B, and  $\phi'_1, \phi'_2 \dots$  are the remaining occupied l.m.o.s.

Tables 4.17 and 4.18 show that different results are also obtained by orthogonalising sequences with different positions of the l.m.o. to be calculated. As at stage 4, if the l.m.o. to be calculated occurs before all the other functions it is unaltered by the orthogonalising. If it occurs after the other functions in the first group it is altered by being made orthogonal to them. After the calculation of  $\mu_{CO}$ , different values for the eigenvalue of  $\mu_{CO}$  result.

The effect of the position of the l.m.o. to be calculated and of the virtual orbital on the results may be further illustrated by examination of the total electronic energy after orthogonalisation and after the calculation of  $\mu_{CO}$ . The values are shown in Table 4.20. An orthogonalising sequence where the virtual orbital is mixed into none of the occupied orbitals

Table 4.20 Total Electronic Energy after Orthogonalisation and after Calculation of the CO sigma-bond, at Stage 3.

Orthogonalising Sequence within group 1	Total Electronic Energy (a.u.)		
	Starting-point <sup>1</sup>	After Orthogonalisation	After Calculation of $r_{CO}$
$\mu_{CO} \mu_{CO}^* (I_C I_O \lambda_O^{\sigma} \lambda_O^{\pi} \pi_{CO})$	-144.7572	-143.1262	-144.4191
$\mu_{CO} (I_C I_O \lambda_O^{\sigma} \lambda_O^{\pi} \pi_{CO}) \mu_{CO}^*$	-144.7572	-144.7588	-144.7623
$(I_C I_O \lambda_O^{\sigma} \lambda_O^{\pi} \pi_{CO}) \mu_{CO} \mu_{CO}^*$	-144.7572	-144.7588	-144.7637

<sup>1</sup> Starting-point (a).

will have the same energy after orthogonalisation as before. Comparison of the first and second entries in Table 4.20 shows that placing the virtual orbital before all the fixed space l.m.o.s leads to a large rise in the total electronic energy after orthogonalisation (1.6 a.u.), whereas placing it at the end of the first group of functions raises the total electronic energy by only 0.001 a.u. The value of the total electronic energy after the subsequent calculation of the CO sigma bond is therefore different. The second and third entries in Table 4.20, which differ in the position of  $\mu_{CO}$  but have the same position for  $\mu_{CO}^*$ , have the same total electronic energy after orthogonalisation. They vary in the total electronic energy after the calculation of  $\mu_{CO}$ .

Stage 3 calculations were therefore made using two sequences of Schmidt orthogonalisation. The first, denoted as sequence III to avoid confusion with the sequences used at stage 4, places the l.m.o. to be calculated next to its virtual orbital and after all the other functions in the first group. For example, sequence III for  $\mu_{CO}$  is

$$\left( I_c \ I_0 \ \lambda_0^e \ \lambda_0^\pi \ \pi_{CO} \ \underline{\mu_{CO}} \right) \mu_{CO}^* \left( \mu_{CH} \ \mu_{CH'} \right) \quad (4.27)$$

and for  $\mu_{CH}$

$$\left( I_c \ \underline{\mu_{CH}} \right) \mu_{CH}^* \left( I_0 \ \lambda_0^e \ \lambda_0^\pi \ \mu_{CO} \ \mu_{CH'} \ \pi_{CO} \right) \quad (4.28)$$

The second sequence, sequence IV, places the l.m.o. to be calculated at the beginning. For example, sequence IV for  $\mu_{CO}$  is

$$\left( \underline{\mu_{CO}} \ I_c \ I_0 \ \lambda_0^e \ \lambda_0^\pi \ \pi_{CO} \right) \mu_{CO}^* \left( \mu_{CH} \ \mu_{CH'} \right) \quad (4.29)$$

and for  $\mu_{CH}$

$$\left( \underline{\mu_{CH}} \ I_c \right) \mu_{CH}^* \left( I_0 \ \lambda_0^e \ \lambda_0^\pi \ \mu_{CO} \ \mu_{CH'} \ \pi_{CO} \right) \quad (4.30)$$

(c) Results from Stage 3 Calculations

A typical stage 3 l.m.o. calculation for formaldehyde is shown in Table 4.21. The starting-point used was (a) and the l.m.o.s were Schmidt orthogonalised in sequence III. As at stage 4, the stage 3 calculations were cycled until the value of the total electronic energy differed by no more than 0.0005 a.u. from the value of the previous cycle. Generally only 3 cycles of the bonds were required, although the "polar" starting-points required more cycles. A stage 3 calculation was found to take approximately between 5 and 10 times less computing time per l.m.o. than the corresponding stage 4 calculation.

Twelve stage 3 calculations were performed using starting-points (a) to (h) and Schmidt orthogonalising sequences III and IV. The resulting total electronic energies and eigenvalues are shown in Tables 4.23, 4.24 and 4.25. The results were examined to see if they depended on the order in which the bonds were calculated, the sequence of Schmidt orthogonalising, and the starting-point used. At stage 3 the one-centre functions, the inner shells and lone pairs, remain fixed and only the bonds are calculated. The values of the total electronic energy and the eigenvalues obtained will therefore depend on the form of the one-centre functions used in the starting-point. However, when comparing two calculations using the same starting-point the form of these functions is the same in both cases so that if the calculation leads to the same form for the four bonds the total electronic energy, and also the eigenvalues, should be the same in each case. The eigenvalues quoted at stage 3 are the values  $\epsilon'_i$  re-calculated after the calculation has reached self-consistency, with the operator constructed from the l.m.o.s given by the calculation, and not the values  $\epsilon_i$  which occur during the

Table 4.21 A Typical Stage 3 Calculation for Formaldehyde

Cycle	l.m.o. calculated	Number of iterations	Resulting Total Electronic Energy (a.u.)	Energy Decrease (a.u.)
1	$\mu_{\text{CH}}$	3	-144.7603	0.0031
	$\mu_{\text{CH}'}$	3	-144.7628	0.0025
	$\mu_{\text{CO}}$	5	-144.7707	0.0079
	$\pi_{\text{CO}}$	4	-144.7736	0.0029
2	$\mu_{\text{CH}}$	2	-144.7737	0.0001
	$\mu_{\text{CH}'}$	2	-144.7737	0.0000
	$\mu_{\text{CO}}$	4	-144.7744	0.0007
	$\pi_{\text{CO}}$	3	-144.7746	0.0002
3	$\mu_{\text{CH}}$	2	-144.7746	0.0000
	$\mu_{\text{CH}'}$	2	-144.7745	0.0001
	$\mu_{\text{CO}}$	4	-144.7746	-0.0001
	$\pi_{\text{CO}}$	3	-144.7746	0.0000



Table 4.22 Two Stage 3 Calculations with Different Orders of  
Calculating the l.m.o.s.<sup>1</sup>

Order of l.m.o. Calculation	From $\mu_{CH}$ to $\pi_{CO}$	From $\pi_{CO}$ to $\mu_{CH}$
Total Electronic Energy (a.u.)	-144.7856	-144.7857
Re-calculated Eigenvalue, $\epsilon'_i$ (a.u.)		
$\phi_i = \mu_{CH}$	-0.739	-0.740
$\phi_i = \mu_{CO}$	-0.906	-0.909
$\phi_i = \pi_{CO}$	-0.459	-0.460

<sup>1</sup> Using starting-point (bb) and Schmidt orthogonalising sequence III.

calculation when the operator includes contributions from the virtual orbital.

In sequence IV, like sequence II at stage 4, the l.m.o. to be calculated is not made orthogonal to the other occupied orbitals. The stage 4 results suggest that calculations using sequence IV will not be dependent on the order in which the l.m.o.s are calculated, although no results were obtained at stage 3.

Sequence III orthogonalises the l.m.o. to be calculated to some of the occupied orbitals, and is therefore similar to sequence I at stage 4 where the l.m.o. to be calculated is made orthogonal to all of the other occupied orbitals. The results of Schmidt orthogonalising in sequence I were found to be dependent on the order in which the bonds were calculated. However, in sequence III the l.m.o. to be calculated is only made orthogonal to the one-centre functions which are not calculated at stage 3, and not to the other l.m.o.s calculated at this stage. In order to test the dependence of sequence III on the order in which the l.m.o.s are calculated, two calculations were performed using sequence III and the same starting point (bb). The first calculated the l.m.o.s in the order shown in Table 4.21, the second in the reverse order. The resulting values of the total electronic energy and eigenvalues, both re-calculated after the calculation are shown in Table 4.22. The atomic orbital coefficients obtained from the two calculations agree to within  $\pm 0.001$ , and the overlap integrals between the corresponding l.m.o.s are all 1.0000. It may therefore be concluded that calculations using sequence III are not dependent on the order in which the l.m.o.s are calculated.

The total electronic energies after the various stage 3 calculations performed using sequences III and IV are given in Table 4.23, and the

Table 4.23 Total Electronic Energies given by Stage 3  
Calculations. (a.u.)

Schmidt Orthogonalising Sequence.	Starting -point.	Total Electronic Energy.
III	a	-144.7746
	b	-144.7868
	bb	-144.7856
	c	-144.8013
	d	-144.7695
	f	-144.7745
	g	-144.7636
	h	-144.7844
IV	a	-144.7722
	b	-144.7872
	f	-144.7714

Table 4.24 Eigenvalues<sup>1</sup> of l.m.o.s Calculated using Schmidt  
Orthogonalising Sequence III (a.u.)

$\phi_i$	Starting-point						
	a	b	c	d	f	g	h
$I_O$	-20.514	-20.555	-20.550	-20.538	-20.511	-20.551	-20.541
$I_C$	-11.316	-11.332	-11.294	-11.301	-11.317	-11.341	-11.296
$\lambda_c^\sigma$	-2.439	-1.012	-1.007	-1.002	-2.428	-0.867	-2.000
$\mu_{CO}$	-0.636	-0.901	-0.904	-0.865	-0.637	-1.038	-0.891
$\mu_{CH}$	-0.731	-0.740	-0.771	-0.721	-0.731	-0.742	-0.738
$\mu_{CH'}$	-0.731	-0.740	-0.771	-0.721	-0.731	-0.742	-0.738
$\lambda_c^\pi$	-0.440	-0.452	-0.443	-0.438	-0.439	-0.450	-0.439
$\pi_{CO}$	-0.444	-0.459	-0.449	-0.446	-0.444	-0.460	-0.446

1. Re-computed after the l.m.o. calculations.

Table 4.25 Eigenvalues<sup>1</sup> of l.m.o.s Calculated using Schmidt  
Orthogonalising Sequence IV. (a.u.).

$\phi_i$	Starting-point		
	a	b	c
$I_0$	-20.522	-20.551	-20.524
$I_C$	-11.302	-11.326	-11.300
$\lambda_c^{\epsilon}$	-2.430	-1.016	-2.430
$\mu_{CO}$	-1.070	-1.109	-1.203
$\mu_{CH}$	-0.865	-0.876	-0.838
$\mu_{CH'}$	-0.865	-0.876	-0.838
$\lambda_c^{\pi}$	-0.440	-0.449	-0.440
$\pi_{CO}$	-0.444	-0.456	-0.444

1. Re-computed after the l.m.o. calculations.

recalculated eigenvalues in Tables 4.24 and 4.25 respectively. Comparison of calculations with the same starting-point, but different sequences of Schmidt orthogonalisation shows that the resulting values of the total electronic energy are generally not the same, but vary by only a small amount (0.002 a.u., 0.0004 a.u., and 0.003 a.u. for starting-points (a), (b) and (f) respectively). For starting-point (b), where the sigma-type lone pair is constructed orthogonal to the CO sigma-bond and the oxygen atom inner shell, the difference is within the expected error in the value of the total electronic energy. For the other two starting-points the value obtained by sequence III is lower than that obtained by sequence IV. Sequence III might be expected to lead to a lower total electronic energy as it imposes some orthogonality of the bonds to the inner shells.

The eigenvalues obtained by sequences III and IV, however, differ considerably so that although the two sequences give similar values for the total electronic energy they give different forms for the individual l.m.o.s. This confirms the preliminary results of the previous section and agrees with the stage 4 results. The eigenvalues obtained by sequence IV, in which the bond is not altered by orthogonalisation, are similar to the eigenvalues of the starting-point functions, as is the case with sequence II at stage 4.

The different starting-points used with both sequences III and IV lead to different values of the total electronic energy. These values range from 0.0526 a.u. to 0.0903 a.u. above the stage 4 value. However, in each case the value is lower than the starting-point value.

The different starting-points also lead to different eigenvalues for the bonds. The quantities  $(\epsilon'_i - \epsilon_i)$  for all the stage 3 calculations performed are given in Table 4.26 for the CH and CO sigma bonds. Values of

Table 4.26 Values of  $\epsilon'_i - \epsilon_i$  for Stage 3 Calculations (a.u.)

Schmidt Orthogonalising sequence	Starting -point	$\epsilon'_i - \epsilon_i$	
		$\Gamma^{\text{CH}}$	$\Gamma^{\text{CO}}$
III	a	-0.031	-0.012
	b	-0.032	-0.014
	c	-0.001	-0.017
	d	-0.004	-0.001
	f	-0.031	-0.012
	g	-0.032	-0.014
	h	-0.002	0.005
	IV	a	-0.032
b		-0.032	-0.014
c		-0.032	-0.013

Table 4.27 Virial Theorem Test after Stage 3 Calculations

Schmidt Orthogonalising Sequence	Starting- point	-T/E
III	a	1.0124
	b	1.0077
	c	1.0087
	d	1.0085
	f	1.0124
	g	1.0071
	h	1.0085
	IV	a
b		1.0080
f		1.0125



up to  $-0.017$  for  $\mu_{CO}$  and up to  $-0.032$  for  $\mu_{CH}$  occur. These are of the order of magnitude predicted by the preliminary calculations in the previous section. It may therefore be concluded that the inaccuracies incurred by including the virtual orbitals in the operator at stage 3 are not seriously affecting the calculations.

A check was also made to see how nearly the virial theorem was obeyed at stage 3. The results are shown in Table 4.27. For starting-points where the sigma-type lone pair is made orthogonal to the CO sigma bond and the oxygen atom inner shell the values of  $-T/E$  range from 1.0071 to 1.0087, a difference of from zero to 0.0016 from the stage 4 results. For starting-points (a) and (f), where the form of the sigma-type lone pair is  $2s_o$ ,  $-T/E$  differs from the stage 4 results by 0.0053.

Part, at least, of the differences found in the values of the total electronic energy and the eigenvalues is due to the different forms for the sigma-type lone pair used in different starting-points and not altered at stage 3. It is the only one-centre function which has different forms in starting-points (a) to (h). The simplest form for this function is  $2s_o$  as in starting-point (a). The importance of the form of the sigma-type lone pair can be seen by comparing the total electronic energy obtained with starting point (a) ( $-144.7746$  a.u. and  $-144.7722$  a.u. for sequences III and IV respectively) with that obtained from starting point (b) where  $\lambda_o^r$  is constructed orthogonal to  $\mu_{CO}$  and  $I_o$  ( $-144.7868$  a.u. and  $-144.7872$  a.u. for sequences III and IV respectively).

In order to investigate further the best form for this function to use at stage 3, a stage 4 calculation of  $\lambda_o^r$  was made using as a starting-point the results of the stage 3 calculation made with starting-point (b) and sequence III, (i.e. starting-point (e)), and Schmidt orthogonalising in sequence II. The form of  $\lambda_o^r$  obtained was then

truncated to give

$$\lambda_c^f = 0.9697 \ 2s_o - 0.3332 \ 2p_{z_o} - 0.2206 \ 1s_o \quad (4.31)$$

which is fairly similar to the form used in starting-point (b)

$$\lambda_c^g = 0.9506 \ 2s_o - 0.3817 \ 2p_{z_o} - 0.2219 \ 1s_o \quad (4.32)$$

Use of this form (4.31) in a further stage 3 calculation (using sequence III) resulted in a total electronic energy of  $-144.7910$  a.u., only  $0.0042$  a.u. lower than that obtained by the starting-point (b) form (4.32). The method used in starting-point (b) of constructing the sigma-type lone pair orthogonal to the CO sigma-bond and the oxygen atom inner shell would therefore seem to give a good approximate form for the function. This method, however, depends heavily on the starting-point form for the CO sigma-bond, so that a very different form for the sigma-type lone pair is obtained by constructing it orthogonal to the polar CO sigma-bond, as in starting-point (g).

$$\lambda_c^h = 0.8651 \ 2s_o - 0.5408 \ 2p_{z_o} - 0.2020 \ 1s_o \quad (4.33)$$

The total electronic energy obtained by using starting-point (g) is higher than that obtained by starting-point (f) which has the simple  $2s_o$  form for  $\lambda_c^f$ . One solution might be to construct  $\lambda_c^f$  orthogonal to the hybrid atomic orbital on the oxygen atom making up the CO sigma-bond, which would at least discount the affect of differences in polarity, but this was not done in this work.

The only starting-points used above which have the same form for  $\lambda_c^f$  are (a) and (f). Sequence III leads to the same value for the total electronic energy and for the eigenvalues for the two calculations while sequence IV does not. The atomic orbital coefficients of all the l.m.o.s

obtained by the two calculations using sequence III agree to within  $\pm 0.001$ , so that it may be concluded that in this case the two starting-points (a) and (f) give the same end-point. The l.m.o.s obtained by the two calculations using sequence IV have overlap integrals of 0.9999 for the CH bonds, but only 0.9942 for the CO sigma bond, giving a  $\eta$  value of  $3.4 \times 10^{-5}$ . Use of sequence IV therefore gives different end-points for starting-points (a) and (f).

These starting-points, however, differ only in the polarity of the bonds. To investigate further the effect of the form of the sigma-type lone pair several more calculations were made, using Schmidt orthogonalising sequence III, with different forms for the bonds but with the same form for the sigma-type lone pair. The form chosen was that of starting-point (bb)

$$\lambda_o^{\sigma} = 0.9238 \ 2s_o - 0.3829 \ 2p_{z_o} \quad (4.34)$$

The results of these calculations are given in Table 4.28, and show that in general the different starting-points still give different values for the total electronic energy when the form of  $\lambda_o^{\sigma}$  is the same in each case, so that the form of this function is not entirely responsible for the differences in the values of the total electronic energy shown in Table 4.23. The eigenvalues in Table 4.28 are also different for different starting-points but differ less than the values in Table 4.24. Apart from the effect of the sigma-type lone pair, the stage 3 calculations therefore, in general, give bonds whose forms are dependent on the form of the starting-point bonds.

Table 4.28 Results of Stage 3 Calculations<sup>1</sup> with the same form for the sigma-type Lone pair.<sup>2</sup>

Starting-point form for bonds.	(a) or (b)	(c)	(d)	(f) or (g)
Total Electronic Energy (a.u.)	-144.7857	-144.8000	-144.7676	-144.7857
Re-calculated Eigenvalues, $\epsilon'_i$ (a.u.)				
$\phi_i = I_O$	-20.557	-20.550	-20.550	-20.553
$\phi_i = I_C$	-11.332	-11.294	-11.336	-11.335
$\phi_i = \lambda_C^\sigma$	-2.011	-2.003	-2.009	-2.010
$\phi_i = \mu_{CO}$	-0.909	-0.915	-0.892	-0.910
$\phi_i = \mu_{CH}$	-0.740	-0.771	-0.723	-0.740
$\phi_i = \mu_{CH}'$	-0.740	-0.771	-0.723	-0.740
$\phi_i = \lambda_O^\pi$	-0.452	-0.443	-0.449	-0.451
$\phi_i = \pi_{CO}$	-0.459	-0.449	-0.458	-0.459

1. Using Schmidt orthogonalising sequence III.
2. The form of the sigma-type lone pair used is that occurring in starting-point (bb).

The exception to this general conclusion occurs when a bond and its anti-bonding virtual orbital have the same hybridisation on each atom, as with starting-points (a) and (f), which, as shown in Table 4.2<sup>8</sup> and above, give the same end-point for calculations using Schmidt orthogonalising sequence III. Solution of the truncated  $2 \times 2$  secular determinant then determines only the polarity of the bond calculated. This was used to examine the effect of changes in the polarity of bonds and the results are given in Chapter Five.

In theory the Schmidt orthogonalising will alter the hybridisation before a calculation is made. In sequence III, which places the l.m.o. to be calculated next to the virtual orbital, both functions are made orthogonal to the one-centre functions and the hybridisation is kept effectively the same in each case. In sequence IV the virtual orbital is made orthogonal to the one-centre functions, while the l.m.o. to be calculated is not, so the hybridisation is altered by the orthogonalising in one case and not in the other. The calculations made to examine the effect of changes in the polarity of bonds were therefore carried out using sequence III.

In conclusion, the inaccuracies introduced into the operator at stage 3 by the Schmidt orthogonalising sequences used did not prove too serious a difficulty, and the resulting sets of perfectly localised molecular orbitals had total electronic energies ranging from 0.0526 a.u. to 0.0903 a.u. above the stage 4 value. The different values obtained for the total electronic energy were shown to be due firstly to different forms for the bonds calculated at stage 3 and secondly due to different forms for the one-centre functions which remain unaltered, the form of the sigma-type lone pair being particularly important. The forms of the bonds were found to depend both on the starting-point used and on the sequence of Schmidt orthogonalisation as at stage 4. The results of the stage 3 calculations are discussed further in Chapter Five.

### Section 3    Stages One and Two

#### (a) Introduction

At stages 1 and 2 a set of perfectly localised molecular orbitals is computed using a truncated operator. The success of this approximation may be judged by comparing the results of stage 1 and stage 2 calculations on the formaldehyde molecule with the results of stage 3 calculations where the full Hartree-Fock operator is used. The stage 1 results are discussed first.

#### (b) Stage One Results

The ability of the stage 1 model of an isolated two-electron bond to give reasonable forms for the bonds was tested by performing a single stage 1 calculation of each of the four bonds in formaldehyde. The starting-point forms used for the bonds and their anti-bonding partners were those of starting-point (a), non-polar bonds with  $sp^2$  hybridisation on the carbon atom, and with the virtual orbitals constructed orthogonal to the corresponding bonds. As described in Chapter Three, a charge of +1 was assigned to each nucleus. The computing time taken by the stage 1 calculations was approximately the same as that taken by a stage 3 calculation of a single bond, the number of cycles needed to reach self-consistency being greater.

The success of a stage 1 calculation was judged by the form of the function produced and by the eigenvalue given by the calculation. A further test would be given by the values of the total electronic energy and the eigenvalue produced when the function replaced its starting-point form in the set of starting-point functions, but these results were not obtained in this work.

The form given by a stage 1 calculation for the CH bond was

$$\mu_{\text{CH}} = 0.1320 2s_{\text{C}} + 0.0976 2p_{z_{\text{C}}} + 0.1691 2p_{y_{\text{C}}} + 0.8225 1s_{\text{H}} \quad (4.35)$$

which is heavily polarised towards the hydrogen atom. The eigenvalue given by the calculation was  $-0.2776$  a.u. The forms obtained for the sigma and pi CO bonds were

$$\mu_{\text{CO}} = 0.5693 2s_{\text{C}} - 0.8052 2p_{z_{\text{C}}} + 0.0315 2p_{z_{\text{O}}} \quad (4.36)$$

$$\pi_{\text{CO}} = 0.9241 2p_{x_{\text{C}}} + 0.2316 2p_{x_{\text{O}}} \quad (4.37)$$

which are both heavily polarised towards the carbon atom. The eigenvalues given by the calculations were  $0.3271$  a.u. and  $0.6778$  a.u. for the sigma- and pi-bond respectively.

These results bear no relation to those of the detailed computations. The operator used at stage 1 is therefore too simple an approximation to be useful. The bonds given by the calculations are all heavily polarised away from the larger of the two atoms making up the bond and all three of the eigenvalues obtained are far too high when compared to the results obtained at stages 3 and 4, those associated with the CO bond being both positive.

It would be possible to vary the values of the nuclear charges in some systematic manner while retaining the simple formulation of the stage 1 operator. In this way l.m.o.s which resembled the stage 3 and stage 4 l.m.o.s might be obtained. However, no exploration along these lines was attempted in this work, and it was concluded, for the present, that the stage 1 operator does not provide a satisfactory method of approximation for the calculation of the l.m.o.s of formaldehyde.

(c) Stage Two Results

A number of calculations were made with the stage 2 form of the truncated operator (3.30) and with several different Schmidt orthogonalising sequences. Starting-points (a) and (bb) were used, together with a value of the exchange factor,  $x$ , of 0.5. This work is therefore not a complete analysis of the problems of satisfying the orthogonality conditions for the formaldehyde molecule at this level of approximation. The results proved to be sensitive to the orthogonalising sequence.

Where the l.m.o. to be calculated was placed after all the other occupied orbitals in the orthogonalising sequence the cycling of the bonds did not converge satisfactorily to an end-point, but rather oscillated, the calculation of some l.m.o.s resulting in an increase rather than a decrease in the total energy. This is the only occasion in the whole of this work on which convergence did not occur. Such a sequence for the calculation of a CH bond might be

$$I_C \mu_{CH}^T \mu_{CO}^T \pi_{CO}^T \underline{\mu_{CH}} \mu_{CH}^* \quad (4.38)$$

and for the calculation of a CO sigma bond

$$I_O I_C \lambda_O^\pi \lambda_O^\sigma \mu_{CH}^T \mu_{CH}^T \pi_{CO} \underline{\mu_{CO}} \mu_{CO}^* \quad (4.39)$$

so that the singly occupied hybrids  $\mu_{CH}^T$ ,  $\mu_{CO}^T$  etc. are mixed by the orthogonalising into a doubly occupied orbital. The reason for the oscillating behaviour may be that the orthogonalisation raises the total energy, while the solution of the secular determinant lowers the total energy.

On the other hand, when the l.m.o. to be calculated was placed first in the sequence the calculations did converge satisfactorily as in stages



3 and 4. In this case the orthogonalising sequence used for a CH bond was

$$\underline{\mu_{CH}} \quad I_C \quad \mu_{CH}^{\tau} \quad \mu_{CO}^{\tau} \quad \pi_{CO}^{\tau} \quad \mu_{CH}^* \quad (4.40)$$

and for a CO sigma bond

$$\underline{\mu_{CO}} \quad I_O I_C \quad \lambda_O^{\pi} \quad \lambda_O^{\sigma} \quad \pi_{CO}^{\tau} \quad \mu_{CH}^{\tau} \quad \mu_{CH'}^{\tau} \quad \mu_{CO}^* \quad (4.41)$$

No singly occupied orbitals were then mixed into doubly occupied orbitals. This latter method was therefore used in all the subsequent calculations at this stage.

A typical stage 2 calculation using this Schmidt orthogonalising sequence with starting-point (a) and a value of x of 0.5 is shown in Table 4.29. As at stages 3 and 4 the stage 2 calculations were cycled

Table 4.29    A Typical Stage 2 Calculation for Formaldehyde

Cycle	l.m.o. calculated	Number of iterations	Resulting Total Electronic Energy (a.u.)	Energy Decrease (a.u.)
1	$\mu_{CH}$	3	-144.7612	0.0040
	$\mu_{CH'}$	3	-144.7642	0.0030
	$\mu_{CO}$	4	-144.7707	0.0065
	$\pi_{CO}$	2	-144.7707	0.0000
2	$\mu_{CH}$	2	-144.7707	0.0000
	$\mu_{CH'}$	2	-144.7706	0.0001
	$\mu_{CO}$	2	-144.7707	-0.0001
	$\pi_{CO}$	2	-144.7707	0.0000

until the value of the total electronic energy differed by no more than 0.0005 a.u. from the value of the previous cycle. In general, only 2 or 3

cycles of the bonds were required. The computing time taken by a stage 2 calculation was found to be approximately the same as that taken by a stage 3 calculation.

As at stage 3, only the bonds are calculated at stage 2, the one-centre functions, the inner shells and lone pairs, remaining fixed. It follows that the values of the total electronic energy and the eigenvalues obtained will again depend on the form of the one-centre functions used in the starting-point.

Before a stage 2 calculation is made some of the l.m.o.s are truncated to give the truncated operator. The eigenvalues obtained during a calculation are formed with the truncated operator. Similarly, values of the total electronic energy computed with the forms of the l.m.o.s as they appear in an individual calculation refer to the particular fragment of the molecule concerned with the bond being calculated. After a stage 2 calculation had reached self-consistency, therefore, a new set of l.m.o.s was formed comprising the l.m.o. which had been calculated together with the original untruncated forms for the other occupied orbitals. This set of l.m.o.s was then used to evaluate both the eigenvalues, using the full Hartree-Fock operator, and the total electronic energy so that a comparison could be made with the values of these quantities given by other stages.

Several stage 2 calculations were made with values of the exchange factor  $x$  varying from 0 to 1 and using the same starting-point, (a). Table 4.30 shows the variation in the eigenvalues given by the calculations with the value of  $x$ . They all decrease with increasing  $x$  value and all vary over a range of about 0.10 a.u. The variation in the total energy is shown in Figure 4.2. The value of  $x$  was found to affect the value of the total electronic energy by about 0.01 a.u. (about 0.25 eV). The lowest

Table 4.30 Eigenvalues given by Calculations<sup>1</sup> with different values for the Exchange Factor,  $x$ .

$\phi_i$	$x$				
	1.00	0.75	0.50	0.25	0.00
$\mu_{CH}$	-0.880	-0.852	-0.825	-0.798	-0.772
$\mu_{CH'}$	-0.880	-0.852	-0.825	-0.798	-0.772
$\mu_{CO}$	-1.085	-1.069	-1.053	-1.037	-1.022
$\pi_{CO}$	-0.465	-0.447	-0.429	-0.412	-0.395

1. Using Starting-point (a).

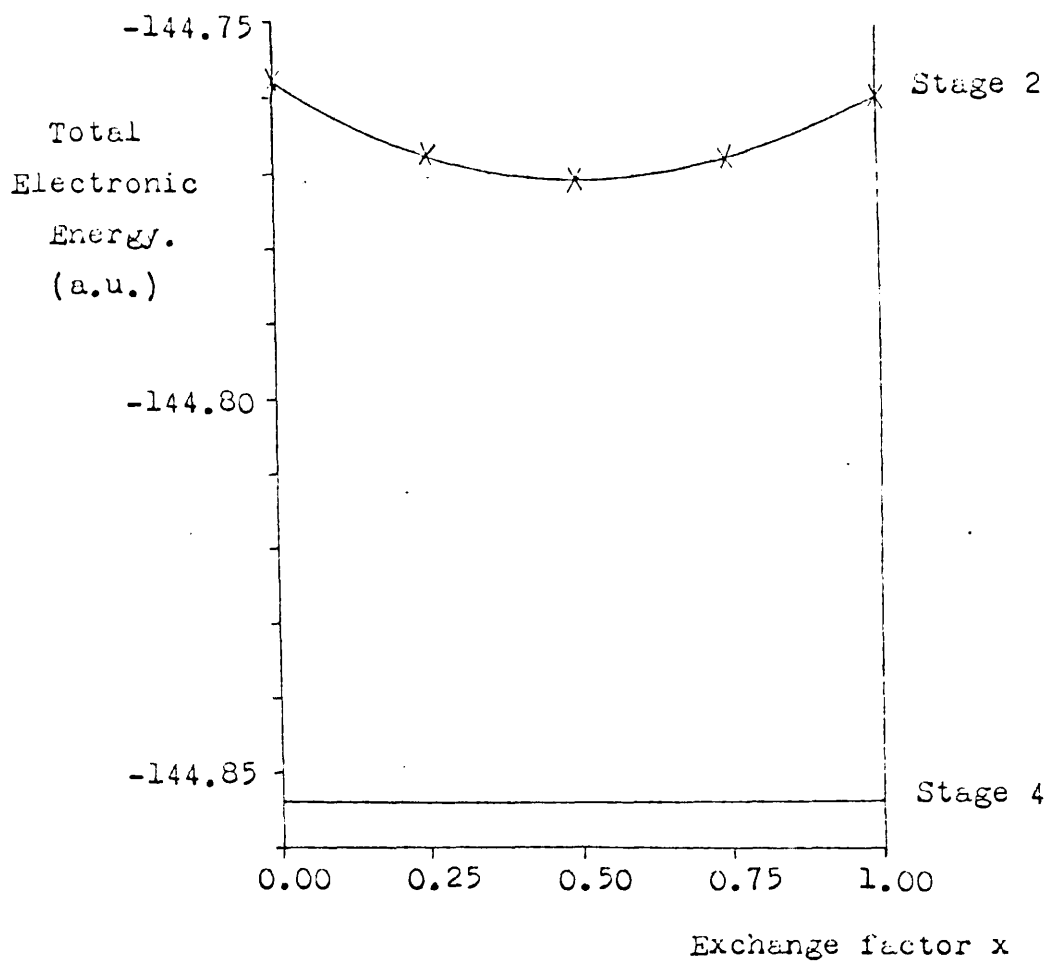


Figure 4.2 Variation of the Total Electronic Energy with the exchange factor  $x$ .

value of the total electronic energy ( $-144.7706$  a.u.) was given when  $x$  was  $0.5$ . Moreover this agrees well with the values obtained for starting-point (a) at stage 3 ( $-144.7746$  a.u. using sequence III and  $-144.7722$  a.u. using sequence IV). This value of  $x$  was therefore used in subsequent calculations.

Table 4.31 shows the values of the total electronic energy resulting from stage 2 calculations with various starting-points, all using a value for  $x$  of  $0.5$ . As at stage 3 different values are obtained for different starting-points. These results were compared with the values obtained by the corresponding calculations performed at stage 3. They should strictly be compared with stage 3 calculations using Schmidt orthogonalising sequence IV, where the l.m.o. to be calculated is also not made orthogonal to the other occupied orbitals. However, as only a few calculations were performed using sequence IV, and these were shown to give total electronic energies near to those obtained by sequence III (within  $0.005$  a.u.) the results of the stage 2 calculations were compared with those of stage 3 using sequence III. Table 4.31 shows that the values of the total electronic energy given by stage 2 calculations with the truncated operator are very close (also within  $0.005$  a.u.) to the values given by the stage 3 calculations with the complete Hartree-Fock operator.

The eigenvalues obtained from the calculations are given in Table 4.32, and the values re-calculated after the calculation are given in Table 4.33. Comparison of the values in the two tables shows that the eigenvalues obtained with the truncated operator in Table 4.32 are in each case slightly higher than the eigenvalues obtained with the full Hartree-Fock operator in Table 4.33. The differences between the values for the CO sigma and pi bonds range from  $0.001$  a.u. to  $0.013$  a.u. The differences between the values for the CH bonds are greater, ranging from  $0.053$  to  $0.078$  a.u.

Table 4.31 Total Electronic Energies given by Stage 2 Calculations.<sup>1</sup> (a.u.)

Starting -point.	Total Electronic Energy.	Difference from Stage 3 values. <sup>2</sup>	
		Sequence III	Sequence IV
a	-144.7707	0.0040	0.0015
bb	-144.7859	-0.0003	-
c	-144.8030	-0.0020	-
d	-144.7699	-0.0004	-
f	-144.7736	0.0010	-0.0022

1. Exchange factor  $x=0.5$ .
2. Stage 2 result minus stage 3 result. Values are given for stage 3 results obtained by Schmidt orthogonalising in sequence III and in sequence IV.

Table 4.32 Eigenvalues obtained directly from stage 2 Calculations  
(a.u.).

$\phi_i$	Starting-point				
	a	bb	c	d	f
$\mu_{CO}$	-1.053	-1.091	-1.165	-0.867	-1.185
$\mu_{CH}$	-0.825	-0.825	-0.889	-0.677	-0.807
$\mu_{CH'}$	-0.825	-0.825	-0.889	-0.676	-0.806
$\pi_{CO}$	-0.429	-0.444	-0.443	-0.444	-0.429

Table 4.33 Eigenvalues re-computed after stage 2 Calculations (a.u.)

$\phi_i$	Starting-point				
	a	bb	c	d	f
$I_0$	-20.482	-20.519	-20.504	-20.517	-20.482
$I_C$	-11.316	-11.349	-11.362	-11.350	-11.315
$\lambda_0^E$	-2.409	-1.988	-0.987	-0.992	-2.409
$\mu_{CO}$	-1.056	-1.104	-1.173	-0.868	-1.184
$\mu_{CH}$	-0.878	-0.890	-0.967	-0.735	-0.860
$\mu_{CH'}$	-0.878	-0.890	-0.967	-0.735	-0.859
$\lambda_0^\pi$	-0.417	-0.430	-0.423	-0.429	-0.416
$\pi_{CO}$	-0.438	-0.456	-0.456	-0.454	-0.438

Unfortunately the eigenvalues obtained at stage 2 may not be compared with the stage 3 results using sequence III, which were found to differ from those obtained using sequence IV. Only two stage 3 calculations, those using sequence IV and starting-points (a) and (f) are therefore available for comparison. The corresponding entries in Table 4.25 and Table 4.33 all differ by about 0.02 a.u., except the values for  $I_0$  which differ by 0.04 a.u., and  $\pi_{CO}$  which differ by 0.002 a.u. No conclusion was therefore drawn from the limited results available. More stage 2 and stage 3 calculations with the same starting-point are required to ascertain whether the truncated stage 2 operator gives a good approximation to the form of the l.m.o. given by a stage 3 calculation.

Finally, the success of the stage 2 calculations which require only one- and two-centre electron repulsion integrals may be compared to a stage 3 type calculation where all the three- and four-centre integrals are simply put to zero. A calculation of this kind was made using starting-point (a) and Schmidt orthogonalising in sequence III. The resulting l.m.o.s have a total electronic energy of -144.6084 a.u., higher than the starting-point value, whereas the corresponding stage 2 calculation gives l.m.o.s with a total electronic energy of -144.7707 a.u.

In conclusion, stage 2 calculations which placed the l.m.o. to be calculated first in the Schmidt orthogonalising sequence so that it was unaltered by the orthogonalising proved successful. As at stages 3 and 4 the forms of the individual l.m.o.s depend on the starting-point used. A value of the exchange factor,  $x$ , of  $\frac{1}{2}$  was found to give l.m.o.s with the lowest total electronic energy and providing this value is used the stage 2 calculations give results which are in good agreement with those obtained at stage 3. The success of the stage 2 calculations is discussed further in Chapter Five.



CHAPTER FIVE  
DISCUSSION  
AND  
CHEMICAL INTERPRETATION  
OF RESULTS

## Section 1   Discussion of Results

The greatest difficulty encountered in using the l.m.o. theory to compute l.m.o.s of formaldehyde is that the original orthogonality conditions cannot be satisfied in a straightforward way for this molecule prior to the actual calculations. The method of Schmidt orthogonalising before each individual l.m.o. calculation which was used to overcome this difficulty is successful in giving a unique many-electron total wavefunction which is the same as that obtained by a conventional canonical molecular orbital calculation. Unfortunately, the individual l.m.o.s obtained are not unique, their forms depending on the sequence in which the functions are orthogonalised. The most successful sequence at the rigorous stage 4 level of approximation is perhaps that which leaves the l.m.o. to be calculated unchanged by orthogonalisation, sequence II. L.m.o.s obtained using this sequence depend only on the starting-point, and not on the order in which the l.m.o.s are calculated, although there is the disadvantage that the final l.m.o.s are not mutually orthogonal.

Both Schmidt and Lowdin orthogonalising appear to produce l.m.o.s whose forms depend on the form of the starting-point functions. The question arises of whether this dependence on the starting-point is a consequence of the basic theory as discussed in Chapter Two, or whether it is a result of the methods used to overcome the difficulty of not being able to obtain a localised orthogonal starting-point. The results for formaldehyde indicate that starting-points which are closer to orthogonal have similar end-points so it may be the case that unique l.m.o.s would be obtained from an orthogonal starting-point, as they were in the simpler example of the methane molecule.<sup>58</sup> No final conclusions may be drawn from the results obtained in the present work and further calculations on other molecules are needed to decide this question.

If a localised starting-point could be obtained for formaldehyde, the form of an l.m.o. would be partly determined by its orthogonality to the other occupied orbitals forming the fixed space before a calculation is made. When Schmidt orthogonalisation in sequence II is performed it is chosen to alter the other occupied orbitals forming the fixed space, so that the l.m.o. to be calculated is retained in its original arbitrary form. The form of the final l.m.o. is therefore determined only by the solution of the secular determinant so that it is to a certain extent dependent on its initial starting-point form. Use of sequence I, and of Lowdin orthogonalisation, however, also give l.m.o.s which appear to be dependent on the starting-point. Here the l.m.o. to be calculated is altered by being made orthogonal to all the other occupied orbitals before a calculation is made, but the situation is not clear since the orthogonalising necessarily delocalises the function.

The results show that l.m.o.s obtained by Schmidt orthogonalising in sequence II have forms very similar to their starting-point forms. While in many ways this is a disadvantage, it could be in one sense an advantage. It may be that this method produces l.m.o.s which, while energy-minimized, differ as little as possible from the starting-point functions, though this is not demonstrated conclusively in this work. In this way the required forms of l.m.o.s may be chosen by choosing a particular set of starting-point functions, in the same way as it is chosen to calculate localised rather than canonical molecular orbitals. This may be of use in extending the method to calculations of parts of large molecules.

An additional point on the question of the dependence of the l.m.o.s on the starting-point is that the l.m.o. theory is expected to give the same l.m.o.s only from qualitatively similar starting-points. It may be that the starting-points used in this work differed too extensively, particularly

in the form used for the sigma-type lone pair. The results obtained indicate that starting-points which have similar forms for this function have similar end-points. Further stage 4 l.m.o. calculations are required to reveal how similar the starting-point functions must be to give effectively the same end-point set of l.m.o.s.

The calculation of properties of the l.m.o.s proved difficult because a unique set of l.m.o.s was not obtained in this work. In some cases calculations on all the different sets of l.m.o.s obtained were performed and the results compared, but in other cases the set of l.m.o.s obtained from calculation 12 (see Table 4.5) was taken arbitrarily as a typical example. The results of these calculations are discussed in the remaining sections of this Chapter.

The Schmidt orthogonalising procedure also enables calculations on the formaldehyde molecule to be carried out successfully at the earlier levels of approximation, stages 2 and 3, so that a set of perfectly localised functions, which are not mutually orthogonal, may be calculated despite the fact that a perfectly localised orthogonal starting-point cannot be found. A disadvantage associated with this method at stage 3 is that in order to obtain a perfectly localised virtual orbital, the virtual orbital must be mixed by the orthogonalising into some of the occupied orbitals, introducing inaccuracies into the operator. This did not prove to be too serious a difficulty in practice.

The main aim of a stage 3 calculation is to calculate directly the best set of perfectly localised molecular orbitals. It is conjectured that these may be of the same, or possibly even lower total electronic energy than those obtained by truncating the stage 4 functions. The stage 3 l.m.o.s obtained in the present work have total electronic energies which are typically only 0.5 to 1.0 a.u. higher than those of the truncated

stage 4 functions. The latter are discussed below in Section 3.

It is a feature of the stage 2 and stage 3 calculations that the one-centre functions cannot be calculated at this level of approximation, so the values of the total electronic energy will be expected to vary with the form of these functions, particularly the sigma-type lone pair. No way of calculating this function while keeping it localised was found in this work. It was demonstrated in Chapter Four, however, that for the stage 3 l.m.o.s differences in the form of this function did not account solely for the differences in the values of the total electronic energy.

The forms of the end-point l.m.o.s obtained for formaldehyde at stage 3 depend on the form of the starting-point functions used, as at stage 4. In order to preserve the localised nature of the l.m.o. being calculated a Schmidt orthogonalising sequence is chosen at stage 3 so that the l.m.o. is not altered by being made orthogonal to all of the other occupied orbitals. With sequence IV, where the l.m.o. is unaltered by the orthogonalising as with sequence II at stage 4, the form of the l.m.o. is determined only by solution of the secular determinant, and a certain dependence on the starting-point is therefore introduced. Here also the forms of the l.m.o.s obtained are close to their starting-point forms. The situation is less clear with sequence III, where the l.m.o. to be calculated is made orthogonal to the one-centre functions, but not to the other bonds.

Stage 2 calculations of formaldehyde proved to be feasible provided a Schmidt orthogonalising sequence was chosen which placed the l.m.o. to be calculated before the truncated orbitals. The individual l.m.o.s obtained at stage 2 again depend on the starting-point used. As the l.m.o. to be calculated is unaltered by the orthogonalising procedure, its form is determined only by solution of the secular determinant.

Stage 2 calculations using a value of the exchange factor,  $x$ , of  $\frac{1}{2}$  give results which are in good agreement with those obtained at stage 3. Values of the total electronic energy obtained by the two stages, using the same starting-point were found to differ by less than 0.005 a.u. The truncated stage 2 operator therefore provides a very good approximation to the complete Hartree-Fock operator used at stage 3, indicating that the l.m.o. being calculated is not influenced greatly by distant parts of the molecule, a result which is consistent with the conventional chemical picture of a classical two-electron chemical bond. This is confirmed by the good agreement between the eigenvalues given by stage 2 calculations, using the truncated operator, and those re-calculated afterwards using the full Hartree-Fock operator. This result suggests that it may well be possible to extend the l.m.o. theory to the calculation of parts of large molecules. It is an important result which confirms that some of the basic ideas behind this approach are essentially correct, at least for this example.

Finally, in contrast to the good results obtained with the stage 2 truncated operator, the stage 1 truncated operator proved to be too simple an approximation to be useful.

## Section 2 Ionization Potentials

According to Koopmans' theorem<sup>90</sup> the molecular orbitals of an ion may be approximated by those of the neutral molecule. The difference in energy between the ion and the neutral molecule is then given by the appropriate eigenvalue from the Hartree-Fock equation (2.5). It is further thought that the observable ionization potential of an electron is given by the eigenvalue of the canonical molecular orbital which the electron occupies.<sup>91</sup> It follows that the eigenvalues of the c.m.o.s are observable quantities whereas the eigenvalues of the l.m.o.s are, in general, not observable quantities. This is demonstrated in Figure 5.1 where the eigenvalues of the c.m.o.s and l.m.o.s of formaldehyde are compared with the experimental ionization potentials. As discussed above many different sets of l.m.o.s were obtained at stage 4, depending on the method of orthogonalisation and the starting-point used. In Figure 5.1 the values obtained by calculation 12 are shown. Much the same result occurs with the other sets of l.m.o.s.

The first four ionization potentials of formaldehyde have been found experimentally by high resolution photoelectron spectroscopy.<sup>92</sup> No experimental values are available in the literature for the remaining ionization potentials of the formaldehyde molecule in the gas phase. However, the ionization potentials of the carbon and oxygen inner shell electrons have been estimated<sup>93</sup> to be approximately 294.0 eV and 537.5 eV respectively from ESCA studies of the closely related molecules acetaldehyde and acetone.

Koopmans' theorem neglects the reorganisation of the remaining electrons after ionization, which causes the magnitude of the experimental ionization potential to be less than the corresponding eigenvalue, as well as differences in the correlation energy and relativistic effects between

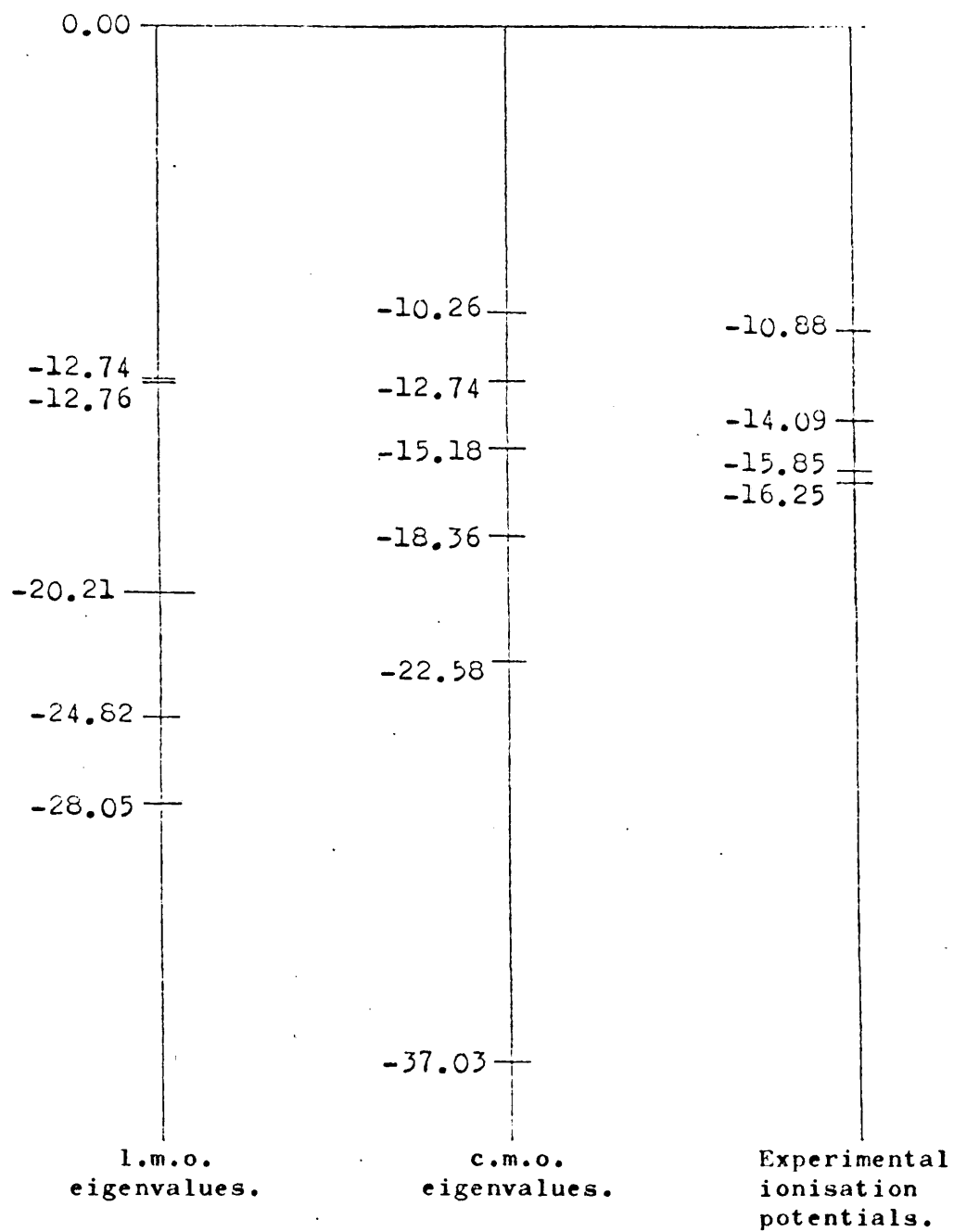


Figure 5.1 Eigenvalues of l.m.o.s and c.m.o.s and Experimental Ionisation Potentials.(eV)



the ion and the molecule. Newton estimates the error using Koopmans' theorem to be between 1 and 10%. Bearing this in mind, it can be seen from Figure 5.1 that the eigenvalues of the c.m.o.s of the valence orbitals correspond to the experimental ionization potentials, whereas the eigenvalues of the l.m.o.s in general do not. The canonical molecular orbitals, and not the localised molecular orbitals, are therefore useful in describing processes concerned with ionization.

In some cases the l.m.o.s give the same value for an eigenvalue as the c.m.o.s. In these cases the l.m.o.s become observable quantities and should correspond to the experimental ionization potential. This occurs when an l.m.o. is prevented from mixing with the other l.m.o.s. One example is the pi-bond in formaldehyde which is prevented from mixing with the other orbitals by symmetry requirements. The eigenvalue for the pi-bond from the c.m.o. and l.m.o. calculations is the same, and differs from the experimental value of an ionization potential by only 1.34 eV.

Another example is given by the inner shells. Orbitals of the same energy interact most strongly,<sup>95</sup> so that the inner shells, which have energies well separated from those of other orbitals, do not interact greatly with the other l.m.o.s. Table 5.1 shows that the eigenvalues for the inner shells from l.m.o. and c.m.o. calculations do not differ greatly, indicating that the eigenvalues of the inner shell l.m.o.s should correspond well with the experimental ionization potential. However, the calculated values are lower than the estimated experimental values by about 14 eV for the carbon inner shell and 21 eV for the oxygen inner shell. This is consistent with the anticipated 1 to 10% error in Koopmans' theorem.<sup>94</sup> Siegbahn and co-workers<sup>96</sup> have found that the ionization potentials obtained by calculations on neutral molecules by Koopmans' theorem for inner shells of light elements are systematically 10 - 20 eV lower than those found experimentally.

Table 5.1 Eigenvalues of l.m.o.s and c.m.o.s and Experimental Ionisation Potentials for the inner shells (eV).

	$I_0$	$I_C$
l.m.o. Eigenvalues <sup>1</sup>	-559.70	-308.81
	-560.03	-308.61
	-560.08	-308.50
	-560.08	-308.59
	-560.01	-308.60
c.m.o. Eigenvalues	-560.02	-308.77
Experimental Ionisation Potentials <sup>2</sup>	-537.5	-294.0

1. The five values shown are from stage 4 calculations using Schmidt orthogonalising sequence II and starting-points (a) to (e).
2. Estimated values (see text).

### Section 3 Delocalisation

#### (a) Extent of Delocalisation

The l.m.o.s obtained at stage 4 are localised mainly on one or two atoms with small contributions from atomic orbitals on the other atoms in the molecule. A perfectly localised orbital can be obtained by deleting these contributions from other atoms and re-normalising to give a truncated orbital. The overlap integral between a stage 4 l.m.o.  $\phi$  and the normalised truncated orbital  $\phi^T$  gives a measure of how well localised the l.m.o.  $\phi$  is. The results are usually expressed in terms of a delocalisation parameter  $d$ ,<sup>70</sup> with a range 0 to 100, given by

$$d = 100 \times [1 - \langle \phi | \phi^T \rangle]^{\frac{1}{2}} \quad (5.1)$$

A function may be considered localised if the overlap integral  $\langle \phi | \phi^T \rangle$  is greater than 0.99 or the value of  $d$  is less than 10. Values of  $d$  for the l.m.o.s obtained at stage 4 are given in Table 5.2. The last column shows the average  $d$  value for all the eight occupied orbitals, providing a measure of how well localised the set of l.m.o.s is.

It can be seen from Table 5.2 that the majority of  $d$  values are below 10, although calculations using Schmidt orthogonalising sequence I give some values as high as 15.

Schmidt orthogonalising in sequence II gives l.m.o.s with  $d$  values which are all below 10. The values for  $I_c$  and  $I_o$  are consistent at 0.8 and 0.6 respectively, giving inner shells which are well localised on the appropriate atom. The values for  $\lambda_o^\pi$  are also fairly consistent at about 9.7 indicating that the pi-type lone pair is more extensively delocalised than the other l.m.o.s. The values for the remaining functions vary with the starting-point, and are all intermediate between these two extremes.

Table 5.2 Delocalisation Parameters<sup>1</sup>

Calculation <sup>2</sup>	$I_c$	$I_o$	$\lambda_c^\pi$	$\lambda_c^\sigma$	$\mu_{en}$	$\mu_{cc}$	$\pi_{cc}$	Average Inner Shell d Value	Average Valence Shell d Value	Average d Value
(Schmidt Orthogonalising in sequence I)										
1	0.88	0.64	10.04	7.10	13.99	11.86	4.65	0.76	7.94	6.15
2	6.00	1.38	14.77	6.68	6.35	9.22	7.62	3.69	7.44	6.50
3	0.84	0.59	14.72	6.40	6.34	8.95	7.27	0.72	7.28	5.64
4	0.83	0.56	15.05	5.93	8.22	8.06	6.36	0.70	7.27	5.63
5	1.06	0.57	9.84	4.66	12.06	12.03	6.41	0.82	7.50	5.83
average	1.92	0.75	12.88	6.15	9.39	10.02	6.46	1.34	7.49	5.95
(Schmidt Orthogonalising in sequence II)										
7	0.87	0.62	9.89	6.23	6.01	6.18	4.78	0.75	5.52	4.32
9	0.88	0.66	9.74	4.68	6.18	6.35	4.65	0.74	5.27	4.14
10	0.87	0.61	9.65	4.99	3.36	3.31	1.79	0.74	3.85	3.07
11	0.83	0.60	9.76	4.63	8.05	8.28	6.40	0.72	6.19	4.82
12	0.88	0.66	9.56	5.00	6.50	6.49	4.06	0.77	5.27	4.14
average	0.87	0.63	9.72	5.11	6.02	6.12	4.34	0.74	5.22	4.10
7*	3.23	1.27	11.34	2.41	9.63	9.83	6.05	2.25	6.54	5.47
9*	3.23	1.44	11.24	5.14	9.63	9.83	6.05	2.34	6.98	5.82
10*	3.37	1.43	10.76	5.96	9.99	9.97	5.75	2.40	7.07	5.90
11*	0.87	0.63	11.41	4.91	9.39	9.65	6.40	0.75	6.96	5.41
12*	0.89	0.60	11.40	5.41	9.54	9.55	5.43	0.75	6.89	5.35
average	2.32	1.27	11.23	4.77	9.64	9.77	5.94	1.70	6.80	5.59
Localisation of c.m.o.s.	4.5	0.8	-	-	9.1	9.1	6.2	2.65	8.23	6.84

1) Defined by equation (5.1). 2) See Table 4.5. \* refers to the l.m.o.s. obtained by Lowdin orthogonalising the set of l.m.o.s. given by the calculation.

3) Reference 70.

The average  $d$  values for calculations Schmidt orthogonalising in sequence II are all less than those obtained by Schmidt orthogonalising in sequence I suggesting that the former method results in a more localised set of functions. However, these functions are not mutually orthogonal. Lowdin orthogonalisation leads, with only a few exceptions, to an increase in the value of  $d$  for each of these functions, and hence to an increase in the average  $d$  values. The resulting average  $d$  values are comparable with those obtained by calculations Schmidt orthogonalising in sequence I, although when comparing calculations with the same starting-point, the former remain slightly smaller. All the average  $d$  values obtained in the present work compare favourably with the average of the  $d$  values obtained by localisation of the canonical molecular orbitals.<sup>70</sup>

(b) Sigmaconjugation Energies

The total electronic energies of three of the sets of truncated l.m.o.s are given in Table 5.3. The values differ by only 0.01 a.u., although as values for the remaining sets of l.m.o.s were not obtained in this work it is not clear if this is fortuitous. The difference between the energy of the stage 4 l.m.o.s and that of the truncated l.m.o.s gives the energy gained by the l.m.o.s from delocalisation, the sigmaconjugation energy. An upper limit to the value of this quantity is given by the difference between the stage 3 and stage 4 total electronic energies. The results range between 1.43 eV and 2.46 eV. The truncated stage 4 l.m.o.s in table 5.3 give a value of the hyperconjugation energy of between 1.23 eV and 1.50 eV. This compares well with the value obtained by Wilhite and Whitten<sup>26</sup> for their formaldehyde l.m.o. calculation, 1.40 eV, and is smaller than the value obtained by localisation of the c.m.o.s,<sup>70</sup> 2.25 eV.

Table 5.3 Total Electronic Energies of Truncated l.m.o.s and Sigmaconjugation Energies

Calculation <sup>1</sup>	Total Electronic Energy of Truncated l.m.o. (a.u.)	Sigmaconjugation Energy	
		(a.u.)	(eV)
1	-144.7988	0.0551	1.499
7	-144.8033	0.0506	1.377
12	-144.8087	0.0452	1.229

1. See Table 4.5.

Table 5.4 Contributions to the Sigmaconjugation Energy<sup>1</sup> by individual l.m.o.s

l.m.o.	Energy Decrease on Delocalisation	
	(a.u.)	(eV)
$I_C$	0.0006	0.016
$I_O$	0.0007	0.019
$\lambda_c^\pi$	0.0344	0.936
$\lambda_o^\epsilon$	0.0034	0.093
$\mu_{CH}$	0.0020	0.054
$\mu_{CH^*}$	0.0025	0.068
$\mu_{CO}$	0.0014	0.038

1. Results from calculation 12.

The total sigmaconjugation energy may be broken down into contributions from each of the eight l.m.o.s. This was carried out for the results of calculation 12. Taking the truncated stage 4 l.m.o.s as a starting-point a further stage 4 calculation was performed. The energy decrease after the calculation of each l.m.o. then gives the energy gained by the l.m.o. on delocalisation. Two calculations were performed calculating the l.m.o.s in two different orders, (i) and (ii) as defined in Chapter Four. The value of the total electronic energy after the first cycle of the l.m.o.s was within 0.0005 a.u. of the stage 4 SCF value, so further cycling of the l.m.o.s was not needed. The values of the energy decrease obtained for each l.m.o. in the two cases agreed to within 0.0005 a.u. and the average value is shown in Table 5.4. It can be seen that the delocalisation of the pi-type lone pair accounts for nearly 1 eV of the total sigmaconjugation energy of 1.23 eV. This agrees with an early conclusion reached by Mulliken<sup>97</sup> that the pi-type lone pair in formaldehyde is extensively delocalised.

#### Section 4 Hybridisation and Polarity

The most direct chemical information which may be derived from l.m.o.s describing bonds and lone pairs is the hybridisation, direction and, in the case of the two-centre functions, the polarity. A perfectly localised orbital, such as the truncated stage 4 l.m.o.s. discussed in the last section, or a stage 2 or stage 3 l.m.o., may be expressed in the following way. A sigma bond between atoms A and B is given by

$$\begin{aligned} \psi_{AB} = & c_{A_1} 1s_A + c_{A_2} 2s_A + c_{A_3} 2p_{\sigma_A} \\ & + c_{B_1} 1s_B + c_{B_2} 2s_B + c_{B_3} 2p_{\sigma_B} \end{aligned} \quad (5.2)$$

a pi-bond between atoms A and B by

$$\pi_{AB} = c_A 2p_{\pi_A} + c_B 2p_{\pi_B} \quad (5.3)$$

and a sigma-type lone pair on atom A by

$$\lambda_A^{\sigma} = c_{A_1} 1s_A + c_{A_2} 2s_A + c_{A_3} 2p_{\sigma_A} \quad (5.4)$$

A bond  $\phi_{AB}$  may be expressed as a sum of two normalised hybrids,  $\psi_A$  and  $\psi_B$ , one on each atom, as in equation (3.3).

$$\phi_{AB} = p_A \psi_A + p_B \psi_B \quad (5.5)$$

where  $p_A$  and  $p_B$  are the polarity parameters. For a sigma bond

$$\psi_A = N_A (c_{A_1} 1s_A + c_{A_2} 2s_A + c_{A_3} 2p_{\sigma_A}) \quad (5.6)$$

and similarly for  $\psi_B$ , where  $N_A$  and  $N_B$  are normalising constants.

The polarity parameter  $p_A$  is then given by

$$p_A = 1/N_A \quad (5.7)$$

For a pi bond

$$\psi_A = 2p_{\pi_A} \quad (5.8)$$

and

$$p_A = c_A \quad (5.9)$$

and similarly for atom B.



The hybridisation in the hybrid  $\psi_A$  or in the lone pair  $\lambda_A^-$  is given by the ratio of the squares of the coefficients of the  $2p_\sigma$  and  $2s$  atomic orbitals.

$$\text{Hybridisation parameter} = c_{A_3}^2 / c_{A_2}^2 \quad (5.10)$$

This quantity corresponds to the value of  $x$  in the expression  $sp^x$ .

The angle the two CH bonds in formaldehyde make with the  $z$ -axis is given by the ratio of the  $2p_y$  and  $2p_z$  atomic orbital coefficients.

The charge on atom A resulting from the polarity of the bond  $\phi_{AB}$  between the atoms A and B may be obtained using Mulliken's population analysis.<sup>98</sup> The population of the hybrid atomic orbital on atom A,  $\psi_A$ , is given by

$$l_A(\phi_{AB}) = p_A^2 + p_A p_B S_{AB} \quad (5.11)$$

where  $S_{AB}$  is the overlap integral between the hybrid atomic orbitals  $\psi_A$  and  $\psi_B$  which form the bond  $\phi_{AB}$ . The charge in the hybrid atomic orbital  $\psi_A$  is defined as the difference between the population of the hybrid atomic orbital in the molecule and that of the neutral free atom suitably hybridised. It is given by

$$q_A(\phi_{AB}) = 1 - 2 l_A(\phi_{AB}) \quad (5.12)$$

and has a negative sign if charge accumulates in the hybrid atomic orbital as compared with the free atom. The total charge on atom A arising from the polarity of all the bonds in the molecule is given by

$$Q_A = \sum_{i=1}^m q_A(\phi_i) \quad (5.13)$$

where  $m$  is the number of bonds centred on atom A.

The polarity parameters of the l.m.o.s obtained by the various stage 4 calculations of the formaldehyde molecule are shown in Table 5.5. The values for the pi-bond are constant as all the calculations gave the same form for this function. The polarity parameters of the CO sigma-bond and the CH bonds are also fairly consistent, despite the fact that the over-all form of the l.m.o.s vary between the different calculations, as shown by their eigenvalues and overlap integrals in Chapter Four. All the l.m.o.s describing the CH bonds are polarised towards the carbon atom which is the more electronegative of the two atoms. Similarly all the l.m.o.s describing the CO sigma-bond are polarised towards the oxygen atom. The pi-bond, however, is seen to be polarised slightly towards the carbon atom rather than the more electronegative oxygen atom as might have been expected, suggesting that the sigma-electron accumulation on the oxygen atom is sufficient to cancel the effect of the electronegativity of this atom. A similar result was obtained for formaldehyde by Peters<sup>46</sup> from localisation of the canonical molecular orbitals, although Newton's result,<sup>70</sup> based on the localisation criterion of Edmiston and Ruedenberg, gives both a pi-bond and a sigma-bond polarised towards the oxygen atom.

The polarity parameters of both the CO sigma-bond and the CH bonds obtained using Schmidt orthogonalising sequence II agree particularly well (within 0.02). Lowdin orthogonalisation of these sets of functions does not affect greatly the polarity parameters of the l.m.o.s describing the CH bond, or those describing the CO sigma-bond with one exception, the form of  $\mu_{CO}$  obtained with starting-point (a). This becomes much more heavily polarised towards the oxygen atom on orthogonalisation. The values for l.m.o.s obtained using Schmidt orthogonalising sequence I agree well with those of l.m.o.s obtained using sequence II, again with one exception, one of the forms of  $\mu_{CO}$  obtained with starting-point (a). The polarity

Table 5.5 Polarity Parameters<sup>1</sup> of Stage 4 l.m.o.s

Calculation <sup>2</sup>	$\rho_{CH}$		$\rho_{CO}$		$\pi_{CO}$		
	$P_C$	$P_H$	$P_C$	$P_O$	$P_C$	$P_O$	
(Schmidt Orthogonalising in Sequence I)	1	0.59	0.49	0.51	0.78	0.66	0.62
	2	0.61	0.47	0.51	0.65	0.66	0.62
	3	0.61	0.47	0.52	0.65	0.66	0.62
	4	0.61	0.47	0.52	0.65	0.66	0.62
	5	0.59	0.49	0.51	0.65	0.66	0.62
(Schmidt Orthogonalising in Sequence II)	7	0.61	0.46	0.52	0.64	0.65	0.63
	9	0.61	0.46	0.51	0.64	0.66	0.62
	10	0.62	0.45	0.54	0.63	0.66	0.62
	11	0.60	0.47	0.51	0.65	0.66	0.62
	12	0.61	0.47	0.51	0.65	0.66	0.62
	7*	0.59	0.48	0.52	0.70	0.65	0.63
	9*	0.59	0.48	0.51	0.65	0.66	0.62
	10*	0.59	0.48	0.52	0.65	0.66	0.62
	11*	0.60	0.48	0.51	0.65	0.66	0.62
	12*	0.60	0.48	0.51	0.65	0.66	0.62
	Localisation of c.m.o.s <sup>3</sup>	0.56	0.54	0.48	0.62	0.61	0.68

1. Defined by equation (5.5)

2. See Table 4.5. \* refers to the l.m.o.s. obtained by Lowdin orthogonalising the set of l.m.o.s. given by the calculation.

3. Reference 70.

parameters therefore seem to be insensitive to the precise form of the l.m.o.s obtained at stage 4.

In contrast, the hybridisation in each l.m.o., and the angle between the two CH bonds vary considerably between the various calculations. The values are shown in Table 5.6. The hybrid atomic orbital on the oxygen atom in the CO sigma-bond is mainly the  $2p_{z_o}$  atomic orbital. Where the hybridisation parameter, as defined by equation (5.10) is greater than 10 it is denoted by the symbol p in the table. The hybridisation on the carbon atom is, with only a few exceptions, nearer to  $sp$  than  $sp^2$ . A hybridisation of  $sp$  would imply that the carbon atom in formaldehyde is about  $s^{1.5} p^{1.5}$ , intermediate between the unpromoted  $s^2 p^2$  state and the promoted  $sp^2$  stage. A similar result was obtained for the methane molecule<sup>58</sup> where the hybridisation was found to be closer to  $sp^2$  than  $sp^3$ .

The atomic charge on the carbon atom from  $\mu_{CH}$ ,  $\mu_{CO}$  and  $\pi_{CO}$  is shown in Table 5.7. The values differ in magnitude between the various calculations, but do not differ in sign. There is seen to be an accumulation on the carbon atom in the CH bonds of between 0.11 and 0.18 of an electron and in the CO pi-bond of between 0.02 and 0.06 of an electron. There is a decrease on the carbon atom in the CO sigma-bond of between 0.10 and 0.34 of an electron. As the polarity parameters have been shown not to vary greatly the differences in the values of the atomic charges may be presumed to occur through differences in the values of the overlap integral between the hybrid atomic orbitals forming the bond arising through the differences in hybridisation. The total charge on each of the four atoms in formaldehyde is given in Table 5.8. These values are seen to vary considerably.

Table 5.6 Hybridisation<sup>1</sup> in Stage 4 l.m.o.s

Calculation <sup>2</sup>	$\lambda_0^\sigma$	$\rho_{CO}$		$\rho_{CH}$	Angle $\angle HCH^\circ$	
		C Atom	O Atom	C Atom		
(Schmidt Orthogonalising in Sequence I)	1	0.01	1.23	5.79	1.34	119°
	2	0.10	2.04	P	1.25	125°
	3	0.10	1.89	P	1.23	125°
	4	0.10	1.62	P	1.28	124°
	5	0.11	1.69	P	1.19	123°
(Schmidt Orthogonalising in Sequence II)	7	0.01	1.22	P	1.04	120°
	9	0.11	1.24	P	1.03	121°
	10	0.10	0.77	P	0.78	118°
	11	0.11	1.69	P	1.26	124°
	12	0.12	1.26	P	1.07	122°
	7*	0.04	1.48	P	1.28	121°
	9*	0.11	1.58	P	1.27	122°
	10*	0.10	0.46	P	1.30	121°
	11*	0.11	1.67	P	1.22	124°
	12*	0.12	1.58	P	1.28	122°
	Localisation of c.m.o.s <sup>3</sup>	-	1.56	5.87	1.63	112.96°

1. Defined by equation (5.10). Where the hybridisation parameter is greater than 10 it is denoted by the symbol p in the table.
2. See Table 4.5. \* refers to the l.m.o.s obtained by Lowdin orthogonalising the set of l.m.o.s given by the calculation.
3. Reference 70.

Table 5.7 Atomic Charge on the Carbon Atom<sup>1</sup> in Stage 4 l.m.o.s

Calculation <sup>2</sup>		$q_C(\mu_{CH})$	$q_C(\mu_{CO})$	$q_C(\pi_{CO})$
(Schmidt Orthogonalising in Sequence I)	1	-0.11	+0.34	-0.04
	2	-0.13	+0.17	-0.05
	3	-0.15	+0.16	-0.04
	4	-0.14	+0.15	-0.04
	5	-0.11	+0.16	-0.05
(Schmidt Orthogonalising in Sequence II)	7	-0.15	+0.13	-0.02
	9	-0.16	+0.15	-0.05
	10	-0.18	+0.10	-0.04
	11	-0.14	+0.17	-0.05
	12	-0.15	+0.16	-0.06
	7*	-0.12	+0.22	-0.02
	9*	-0.12	+0.16	-0.05
	10*	-0.12	+0.15	-0.04
	11*	-0.13	+0.17	-0.05
	12*	-0.12	+0.17	-0.06

1. Defined by equation (5.12).

2. See Table 4.5. \* refers to the l.m.o.s obtained by Lowdin orthogonalising the set of l.m.o.s given by the calculation.

Table 5.8 Total Atomic Charge<sup>1</sup> on each atom given by Stage 4 l.m.o.s

Calculation <sup>2</sup>	Atom				
	O	C	H	H'	
(Schmidt Orthogonalising in Sequence I)	1	-0.30	+0.09	+0.11	+0.11
	2	-0.12	-0.14	+0.13	+0.13
	3	-0.12	-0.17	+0.15	+0.15
	4	-0.13	-0.17	+0.14	+0.14
	5	-0.11	-0.11	+0.11	+0.11
(Schmidt Orthogonalising in Sequence II)	7	-0.11	-0.19	+0.15	+0.15
	9	-0.10	-0.22	+0.16	+0.16
	10	-0.06	-0.30	+0.18	+0.18
	11	-0.12	-0.16	+0.14	+0.14
	12	-0.10	-0.20	+0.15	+0.15
	7*	-0.20	-0.04	+0.12	+0.12
	9*	-0.11	-0.13	+0.12	+0.12
	10*	-0.11	-0.13	+0.12	+0.12
	11*	-0.12	-0.13	+0.13	+0.13
	12*	-0.11	-0.13	+0.12	+0.12

1. Defined by equation (5.13).

2. See Table 4.5. \* refers to the l.m.o.s. obtained by Lowdin orthogonalising the set of l.m.o.s given by the calculation.

The polarity parameters of the stage 2 and stage 3 l.m.o.s are given in Table 5.9. The values for the CH bond at both stage 3 and stage 2 are fairly consistent and agree well with the stage 4 polarity parameters. The stage 3 and stage 2 values for the CO sigma-bond differ amongst themselves a little more, but not greatly, and also agree with the stage 4 result obtained with the same starting-point and similar Schmidt orthogonalising sequence. The stage 3 pi-bond polarity parameters are consistent and show that the stage 3 form of this function is slightly more polarised towards the carbon atom than the stage 4 l.m.o. The stage 2 pi-bond polarity parameters vary a little more, between a non-polar bond and one which is slightly polarised towards the carbon atom. In general, then, the polarity parameters of the stage 2 l.m.o.s agree fairly well with those of the stage 3 l.m.o.s. The polarity parameters of the stage 3 l.m.o.s are reasonably consistent and give a good approximation to those obtained at stage 4. This is in agreement with the results obtained for the methane molecule<sup>58</sup> where it was demonstrated that the polarity of the CH bond did not change as it became delocalised.



Table 5.9 Polarity Parameters<sup>1</sup> of Stage 2 and Stage 3 l.m.o.s

	Starting-point used	$\Gamma_{CH}$		$\Gamma_{CO}$		$\Pi_{CO}$	
		$P_C$	$P_H$	$P_C$	$P_O$	$P_C$	$P_O$
Stage 3 Schmidt Orthogonalising Sequence III	a	0.60	0.48	0.53	0.78	0.69	0.59
	b	0.60	0.48	0.49	0.67	0.69	0.59
	bb	0.60	0.48	0.49	0.67	0.69	0.59
	c	0.64	0.44	0.53	0.65	0.68	0.60
	d	0.63	0.46	0.50	0.68	0.69	0.60
	g	0.61	0.48	0.45	0.67	0.70	0.58
	h	0.62	0.46	0.49	0.67	0.68	0.60
	Schmidt Orthogonalising Sequence IV	a	0.61	0.48	0.54	0.63	0.67
b		0.60	0.48	0.48	0.67	0.69	0.59
f		0.60	0.48	0.52	0.62	0.67	0.62
Stage 2	a	0.60	0.48	0.55	0.62	0.64	0.64
	bb	0.60	0.48	0.48	0.67	0.67	0.61
	c	0.61	0.47	0.50	0.66	0.67	0.61
	d	0.61	0.49	0.50	0.67	0.67	0.62
	f	0.60	0.47	0.53	0.61	0.64	0.64

1. Defined by equation (5.5).

## Section 5 Examination of Arbitrary Changes in the Forms of l.m.o.s.

### (a) Introduction

The l.m.o. theory was set up so that it is possible to examine the effects of making arbitrary changes in one l.m.o. on both its own properties and also on the forms and properties of other l.m.o.s in the molecule. In this way, the formaldehyde molecule may be used as a model for higher members of the homologous series of aldehydes and ketones with a view to possibly being able to predict some of the properties of these molecules. This information may be obtained using the present l.m.o. theory as one l.m.o. is calculated at a time the other l.m.o.s remaining fixed. Hence, the l.m.o. theory enables effects from different l.m.o.s to be distinguished. An analysis of this kind cannot be carried out with methods which calculate all functions simultaneously as with the canonical molecular orbital calculations.

The three parameters of an l.m.o. which may be changed are its polarity, the hybridisation and the extent of delocalisation. For an l.m.o. describing a bond all three parameters may be changed, while for an l.m.o. describing a lone pair, or an inner shell, the hybridisation and delocalisation may be changed. A complete analysis would examine the effect of changes in all the possible parameters for all the l.m.o.s in formaldehyde. Changes in the total energy of the molecule on delocalisation of all the l.m.o.s were discussed briefly in Section 3. The detailed analysis given below is confined to an examination of changes of properties resulting from changes in the polarity of the bonds. This provides an investigation of whether it is possible to think of a chemical bond in terms of simple electrostatics and regard it as a dipole with a positive and negative end. The polarity of a bond was demonstrated

in Section 4 to be insensitive to the different end-points obtained from different l.m.o. calculations.

The analysis was carried out in the following way. An SCF set of l.m.o.s was taken and one, or more, of the bonds was constructed at a particular polarity without altering the hybridisation or delocalisation and the eigenvalues of all the l.m.o.s and the total electronic energy were computed. The polarities chosen were those which gave polarity parameters in the ratios 2/1, 1/1 and 1/2. An individual l.m.o. calculation was then made of each of the remaining bonds in turn and the resulting polarities of these bonds, the eigenvalues of all the l.m.o.s and the total electronic energy were again computed.

These calculations were made at the stage 3 level of approximation and with stage 3 functions as a stage 3 calculation is much less time consuming than a rigorous stage 4 calculation. The results of the stage 3 calculations were demonstrated in the last section to reproduce well the polarities of the stage 4 l.m.o.s. In addition, the stage 3 functions are perfectly localised and, if Schmidt orthogonalising sequence III is used, only the polarity of the bond changes during a calculation. In this way the hybridisation and extent of delocalisation is easily kept constant, so that any changes in properties are due to changes in the polarity of the bonds. The SCF set of l.m.o.s used was that obtained by a stage 3 calculation using starting-point (b).

The effect of changing the polarity of the four bonds in formaldehyde on the total energy, on the polarity of the other bonds, and on the eigenvalues of the other l.m.o.s are discussed in turn below.

(b) Effect of Arbitrary Changes in the polarity of bonds on the Total Electronic Energy

The difference between the total electronic energy of a polar molecule and that of a molecule with all its bonds non-polar may be considered to be composed of two terms.<sup>52</sup> The first is the sum of the ionic bond energies, the internal stabilisation resulting from the bond being polar rather than non-polar. Each ionic bond energy is expected to be negative, indicating that the polar bond leads to a lowering of the total electronic energy of the molecule, although only the sum of the ionic bond energies need be negative. The second term consists of the electrostatic interactions between the polar bonds. These may be initially considered to be dipole-dipole interactions, neglecting any contributions from interactions between higher multipoles. The dipole-dipole interactions will presumably be positive or negative according to the orientation of the two polar bonds in the molecule. In the following work  $IB(\phi_i)$  denotes the ionic bond energy of the bond  $\phi_i$  and  $DD(\phi_i, \phi_j)$  denotes the dipole-dipole interaction between the bonds  $\phi_i$  and  $\phi_j$ .

The difference between the total electronic energy of the polar SCF l.m.o.s of formaldehyde and the total electronic energy when all four of the bonds in the molecule are constructed to be non-polar is 0.0218 a.u. and is made up of the following contributions.

$$\begin{aligned}
 & IB(\mu_{CH}) + IB(\mu_{CH'}) + IB(\mu_{CO}) + IB(\pi_{CO}) \\
 & + DD(\mu_{CH}, \mu_{CH'}) + DD(\mu_{CH}, \mu_{CO}) + DD(\mu_{CH'}, \mu_{CO}) \\
 & + DD(\mu_{CH}, \pi_{CO}) + DD(\mu_{CH'}, \pi_{CO}) + DD(\mu_{CO}, \pi_{CO}) = -0.0218 \quad (5.14)
 \end{aligned}$$

Since the two CH bonds in formaldehyde have the same form, their ionic bond energies and the dipole-dipole interactions with the other bonds

Table 5.10 Total Electronic Energy after one or more Bonds is constructed to be Non-polar

Bond(s) constructed non-polar	Total Electronic Energy (a.u.)	Difference from SCF l.m.o.s (a.u.)
None (SCF l.m.o.s )	-144.7868	-
$\mu_{\text{CH}}$	-144.7838	-0.0030
$\mu_{\text{CO}}$	-144.7683	-0.0185
$\pi_{\text{CO}}$	-144.7812	-0.0056
$\mu_{\text{CO}}, \pi_{\text{CO}}$	-144.7720	-0.0148
$\mu_{\text{CH}}, \mu_{\text{CH}}^*$	-144.7799	-0.0069
$\mu_{\text{CH}}, \pi_{\text{CO}}$	-144.7772	-0.0096
$\mu_{\text{CH}}, \mu_{\text{CH}}^*, \mu_{\text{CO}}, \pi_{\text{CO}}$	-144.7650	-0.0218

will have the same value, so equation (5.14) may be written

$$\begin{aligned}
 & 2 \times \text{IB}(\mu_{\text{CH}}) + \text{IB}(\mu_{\text{CO}}) + \text{IB}(\pi_{\text{CC}}) \\
 & + 2 \times \text{DD}(\mu_{\text{CH}}, \mu_{\text{CO}}) + 2 \times \text{DD}(\mu_{\text{CH}}, \pi_{\text{CC}}) + \text{DD}(\mu_{\text{CO}}, \pi_{\text{CC}}) \\
 & + \text{DD}(\mu_{\text{CH}}, \mu_{\text{CH}}') = -0.0218 \qquad (5.15)
 \end{aligned}$$

The values of the individual ionic bond energies and dipole-dipole interactions may be found from the rise in the total electronic energy after each of the bonds, and various combinations of the bonds, have been constructed to be non-polar. For example, the rise in the total electronic energy when one CH bond is constructed non-polar is 0.0030 a.u. This rise is due to a loss of the ionic bond energy of the CH bond as well as the dipole-dipole interactions of the CH bond with the other bonds in the molecule.

$$\begin{aligned}
 & \text{IB}(\mu_{\text{CH}}) + \text{DD}(\mu_{\text{CH}}, \mu_{\text{CH}}') + \text{DD}(\mu_{\text{CH}}, \mu_{\text{CO}}) \\
 & + \text{DD}(\mu_{\text{CH}}, \pi_{\text{CC}}) = -0.0030 \qquad (5.16)
 \end{aligned}$$

Six equations of this type were obtained and the values of the total electronic energies are given in Table 5.10. These equations, together with equation (5.15) were then solved for the seven individual values of the ionic bond energies and dipole-dipole interactions. The results are shown in Table 5.11. The ionic bond energies of the CH and CO sigma-bonds are negative, as expected, but that of the pi-bond is positive indicating a slight destabilisation of the bond on becoming polar. The value for the CH bond in formaldehyde is of the same order as that obtained for the CH bond in methane<sup>58</sup> (0.0065 a.u.). The signs of the dipole-dipole interactions are consistent with the atomic charges of the SCF l.m.o.s. The values of the atomic charges for the actual stage 3 l.m.o.s used in this section are shown in Figure 5.2.

Table 5.11 Ionic Bond Energies and Dipole-Dipole Interactions

	a.u.	eV
<u>Ionic Bond Energies</u>		
IB ( $\mu_{\text{CH}}$ )	-0.0040	-0.11
IB ( $\mu_{\text{CO}}$ )	-0.0073	-0.20
IB ( $\pi_{\text{CO}}$ )	+0.0017	+0.05
<u>Dipole-Dipole Interactions</u>		
DD ( $\mu_{\text{CH}}, \mu_{\text{CH}'}$ )	+0.0009	+0.02
DD ( $\mu_{\text{CH}}, \mu_{\text{CO}}$ )	-0.0010	-0.03
DD ( $\mu_{\text{CH}}, \pi_{\text{CO}}$ )	+0.0010	+0.03
DD ( $\mu_{\text{CO}}, \pi_{\text{CO}}$ )	-0.0093	-0.25

Table 5.12 Predicted Total Electronic Energies when Bonds are constructed to be non-polar

Bonds constructed non-polar	Total Electronic Energy (a.u.)	
	Predicted	Obtained
$\mu_{\text{CH}}, \mu_{\text{CO}}$	-144.7663	-144.7662
$\mu_{\text{CH}}, \mu_{\text{CH}'}, \mu_{\text{CO}}$	-144.7633	-144.7632
$\mu_{\text{CH}}, \mu_{\text{CH}'}, \pi_{\text{CO}}$	-144.7723	-144.7724

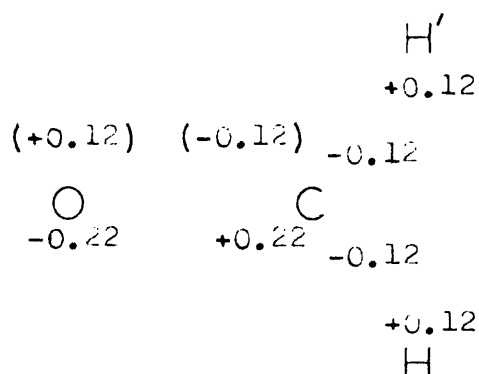


Figure 5.2 Atomic charges of l.m.o.s obtained by the stage 3 calculation using Starting-Point (b) and Schmidt Orthogonalising Sequence III

1) Values for the pi-bond are shown in brackets.

The dipole-dipole interactions are in general an order of magnitude smaller than the ionic bond energies, as has been found in previous work.<sup>52</sup> The exception is that between the CO sigma- and pi-bonds which is very large. This may be expected because of the close proximity of these bonds, and perhaps compensates for the positive value of the pi-bond's ionic bond energy.

The values of the ionic bond energies and dipole-dipole interactions shown in Table 5.11 may be used to predict the rise in total electronic energy when other combinations of bonds are made non-polar. These predictions, together with the actual value of the total electronic energy obtained when this is done are shown in Table 5.12. The two values agree to well within the expected error, showing the values in Table 5.11 to be consistent.



(c) Effect of Arbitrary Changes in the Polarity of bonds on the polarity of neighbouring bonds

The variation in the polarity of a neighbouring bond when the polarity of a bond is altered gives an indication of the extent to which the bonds polarise one another. Accordingly, each of the bonds in formaldehyde was taken in turn and its polarity altered to a fixed value as described above. A separate calculation made on each of the remaining three bonds then enabled the polarity of that bond to alter in response to the polarity of the fixed bond. Hence the polarity of the bond which was calculated altered from its SCF value to a value which would help to minimise the total energy of a molecule which contained the bond whose polarity was fixed.

All the four bonds in the formaldehyde molecule have the carbon atom in common. The change in the atomic charge on the carbon atom was therefore chosen as a measure of the change in the polarity of a bond, in order to enable the different bonds to be compared. If the bond whose polarity is fixed is  $\phi_i$  the change in the SCF value of the atomic charge on the carbon atom is denoted by  $\Delta q_C^F(\phi_i)$ . Similarly, if the bond whose resultant change in polarity is measured is  $\phi_j$  the change from the SCF value of the atomic charge on the carbon atom is denoted by  $\Delta q_C^R(\phi_j)$ .

$\Delta q_C^R(\phi_j)$  was plotted against  $\Delta q_C^F(\phi_i)$ . The results for  $\phi_i = \nu_{CH}$  are shown in Figure 5.3, for  $\phi_i = \nu_{CO}$  in Figure 5.4 and for  $\phi_i = \pi_{CO}$  in Figure 5.5. Although only four points, including the origin which represents the SCF set of l.m.o.s, are shown for each plot these points lie on definite straight lines, indicating a linear relationship between the polarity of the fixed bond and that of its neighbouring bonds. The gradients of these lines are shown in Table 5.13.

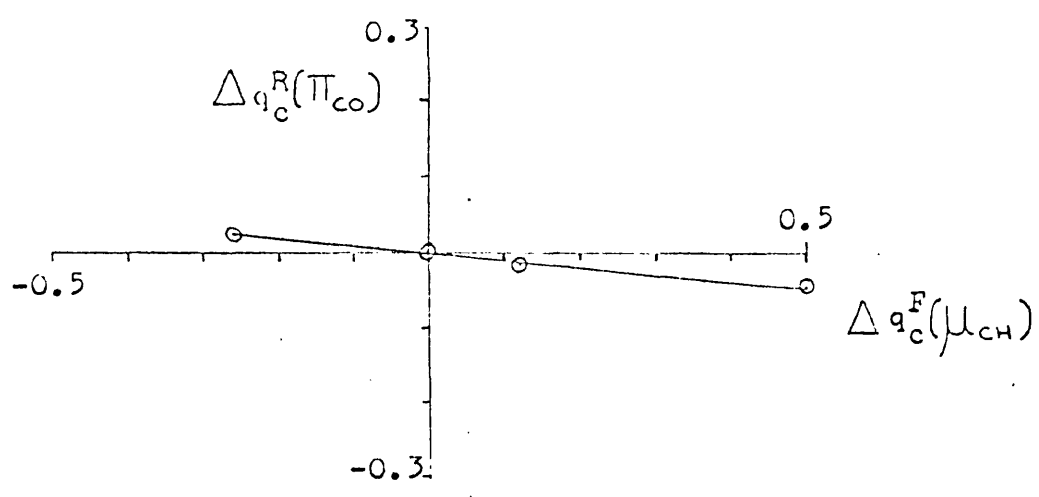
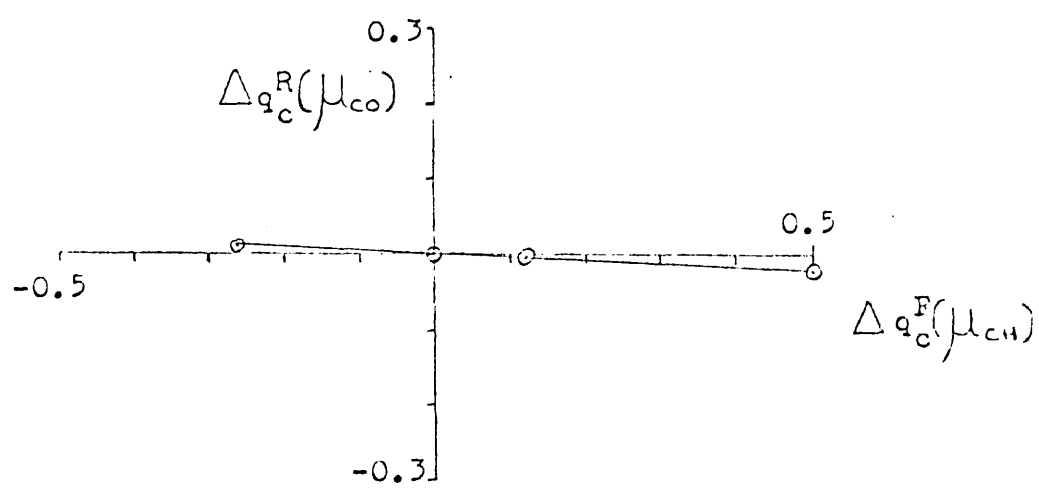
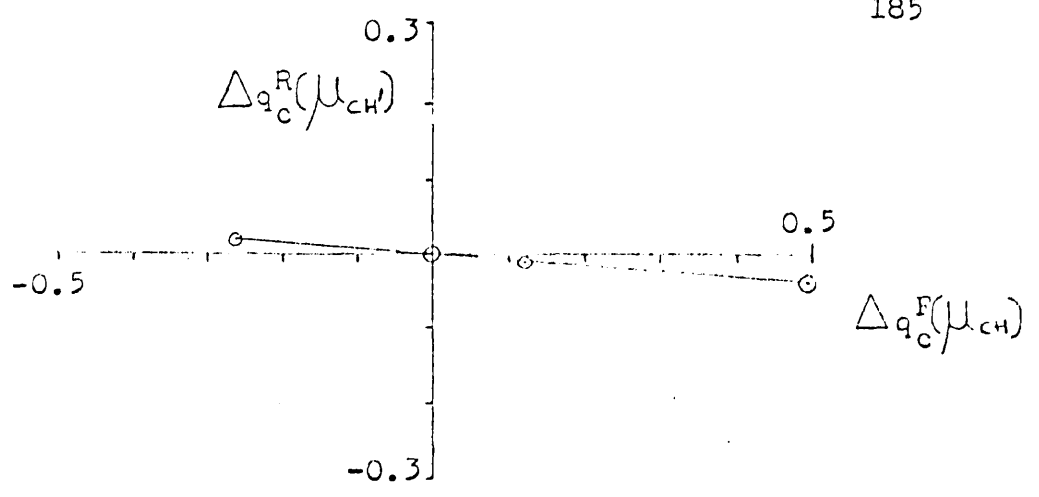


Figure 5.3 Changes in the Polarity of Neighbouring Bonds due to Changes in the Polarity of  $\mu_{CH}$

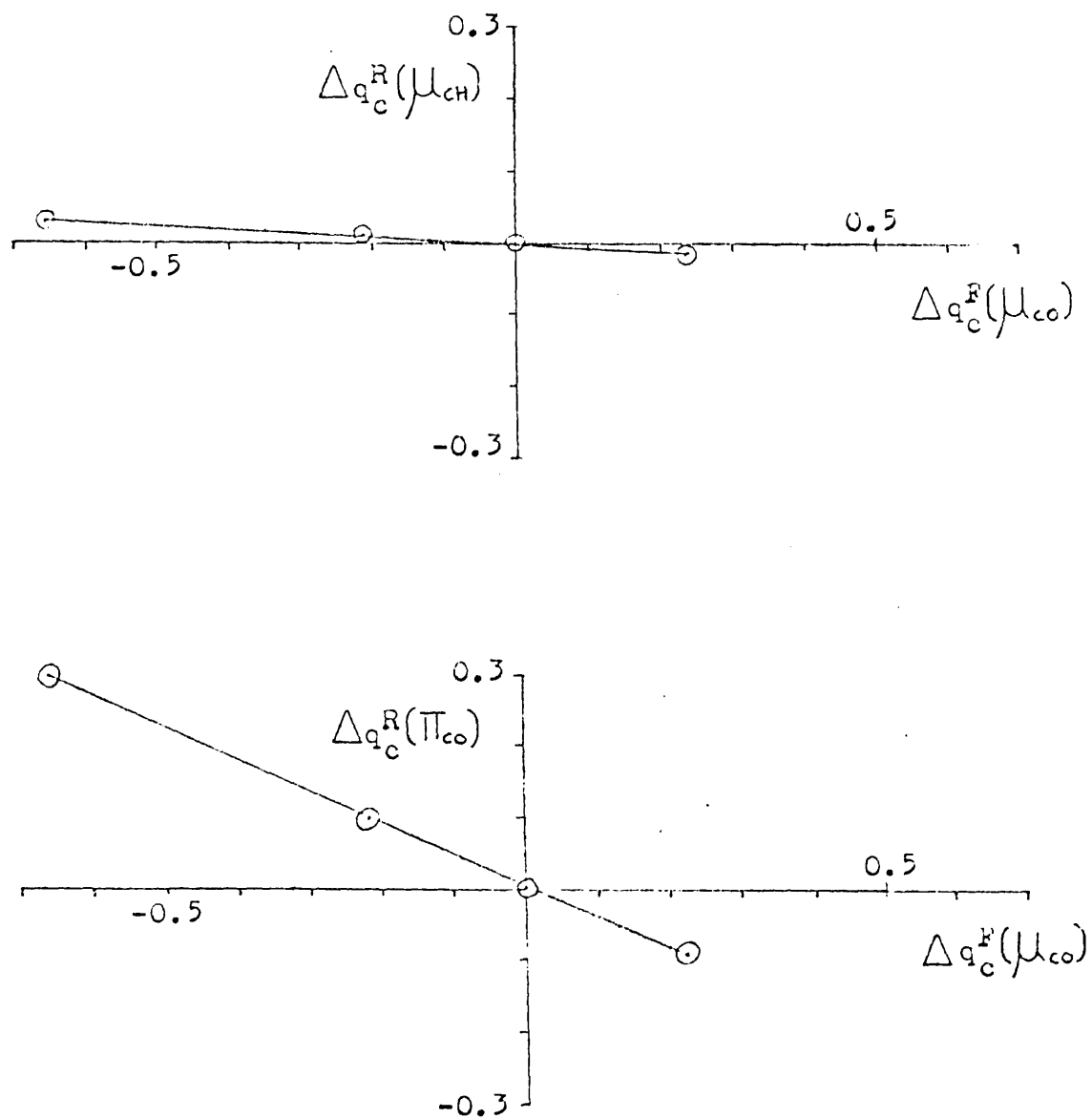


Figure 5.4 Changes in the Polarity of Neighbouring Bonds due to Changes in the Polarity of  $\mu_{CO}$

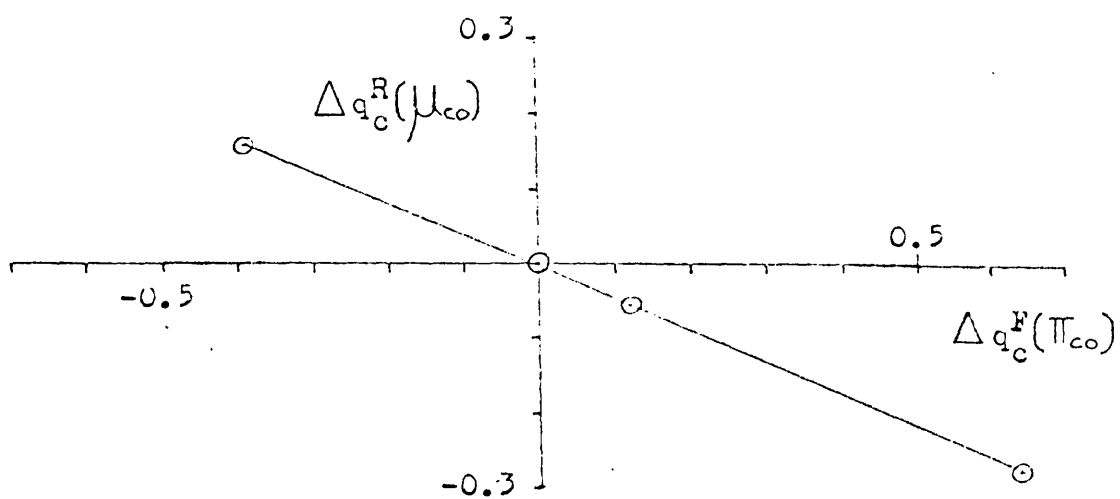
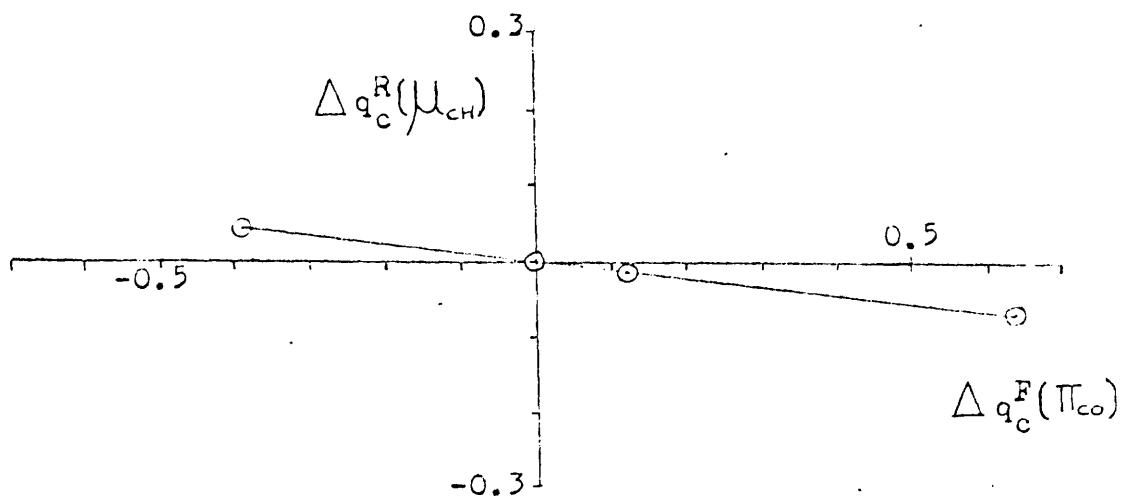


Figure 5.5 Changes in the Polarity of Neighbouring Bonds due to Changes in the Polarity of  $\pi_{CO}$

Table 5.13 Gradients of Figures 5.3, 5.4 and 5.5

Bond whose polarity is fixed, $\phi_i$	Bond whose change in polarity is measured, $\phi_j$	Gradient $\Delta q_C^R(\phi_j)/\Delta q_C^F(\phi_i)$
$\mu_{CH}$	$\mu_{CH}$	-0.089
	$\mu_{CO}$	-0.042
	$\pi_{CO}$	-0.083
$\mu_{CO}$	$\mu_{CH}$	-0.053
	$\pi_{CO}$	-0.431
$\pi_{CO}$	$\mu_{CH}$	-0.107
	$\mu_{CO}$	-0.424

In each case the polarity of the neighbouring bonds alters in the direction expected from electrostatic considerations. Hence if the CH bond, for example, is heavily polarised towards the hydrogen atom the atomic charge on the carbon atom increases so  $\Delta q_C^F (\mu_{CH})$  is positive. The polarity of a neighbouring bond, for example the CO sigma-bond, then alters in the direction of the carbon atom, decreasing the atomic charge on the carbon atom so  $\Delta q_C^R (\mu_{CO})$  is negative. The gradient of the graph of  $\Delta q_C^R (\mu_{CO})$  against  $\Delta q_C^F (\mu_{CH})$  is therefore negative, as is each of the gradients shown in Table 5.13.

A large absolute value of these gradients indicates a large polarisation of one bond by the other and conversely a small absolute value indicates a small amount of polarisation. The results show that there is a definite polarisation of one bond by another, but that in general it is small (5 - 10%). The CH bonds show little polarisation by the other bonds. A similar result was obtained in work on the methane molecule<sup>58</sup> where it was concluded that the CH bonds in methane do not polarise one another to any great extent. The CO sigma- and pi-bonds show little polarisation by the CH bonds, but do show a large polarisation of one by the other. As would be expected these two bonds are closely linked, a change in the polarity of one causing a change of polarity in the opposite sense of the other. The sigma-bond appears to be polarised by the pi-bond to the same extent as the pi-bond is polarised by the sigma-bond.

(d) Effect of Arbitrary changes in the polarity of bonds on the eigenvalues of other l.m.o.s

The eigenvalue of a function is determined firstly by the form of the function itself and secondly by the form of all the other functions in the molecule, from which the operator is constructed. The following work

examines the effect on the eigenvalue of one function of changes in the polarity of other functions. The form of the function whose eigenvalue is studied is kept constant, so that any changes in its eigenvalue are due to changes in the operator.

(i) Eigenvalues of Inner Shells

The eigenvalues of the inner shells are examined first. These are observable quantities, as discussed in Section 2. The variation of the ionization potentials, or binding energies, of the inner shells with the polarity of the bonds is of interest from the point of view of ESCA studies. Siegbahn and co-workers<sup>99,100</sup> have found that the experimental core-electron binding energies shift measurably with their chemical environment, and that there is a well established linear relationship between the shift and the degree of bond polarity in different molecules as estimated from electronegativity considerations.

As described above, each of the four bonds in formaldehyde was fixed at various polarities and the eigenvalues of the carbon and oxygen inner shells re-calculated. Figure 5.6 shows the resulting eigenvalue of the carbon atom inner shell at different polarities of  $\mu_{CH}$ ,  $\mu_{CO}$  and  $\pi_{CO}$ , as measured by the changes in the atomic charge on the carbon atom  $\Delta q_c^F(\mu_{CH})$ ,  $\Delta q_c^F(\mu_{CO})$  and  $\Delta q_c^F(\pi_{CO})$ . Although only four points are again shown for each plot, there is seen to be a definite linear relationship between the eigenvalue and the polarity of the bonds. This relationship is different for each bond. The gradients are given in Table 5.14. The results are those which would be expected from electrostatic considerations, an increase, for example, in the charge on the carbon atom producing a decrease in the eigenvalue, or an increase in the binding energy.

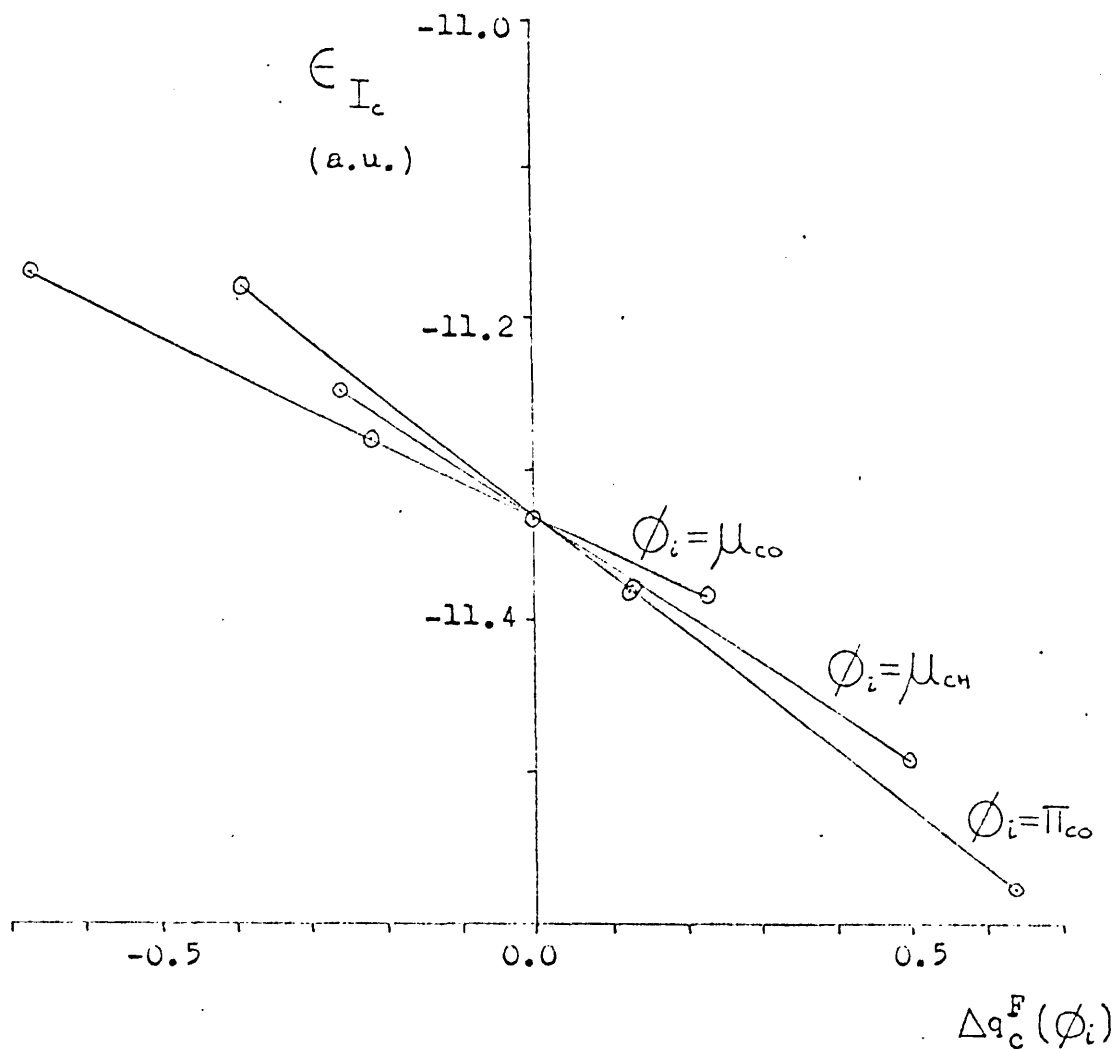


Figure 5.6 Variation of the  $I_C$  Eigenvalue with Changes in the Atomic Charge on the Carbon Atom.



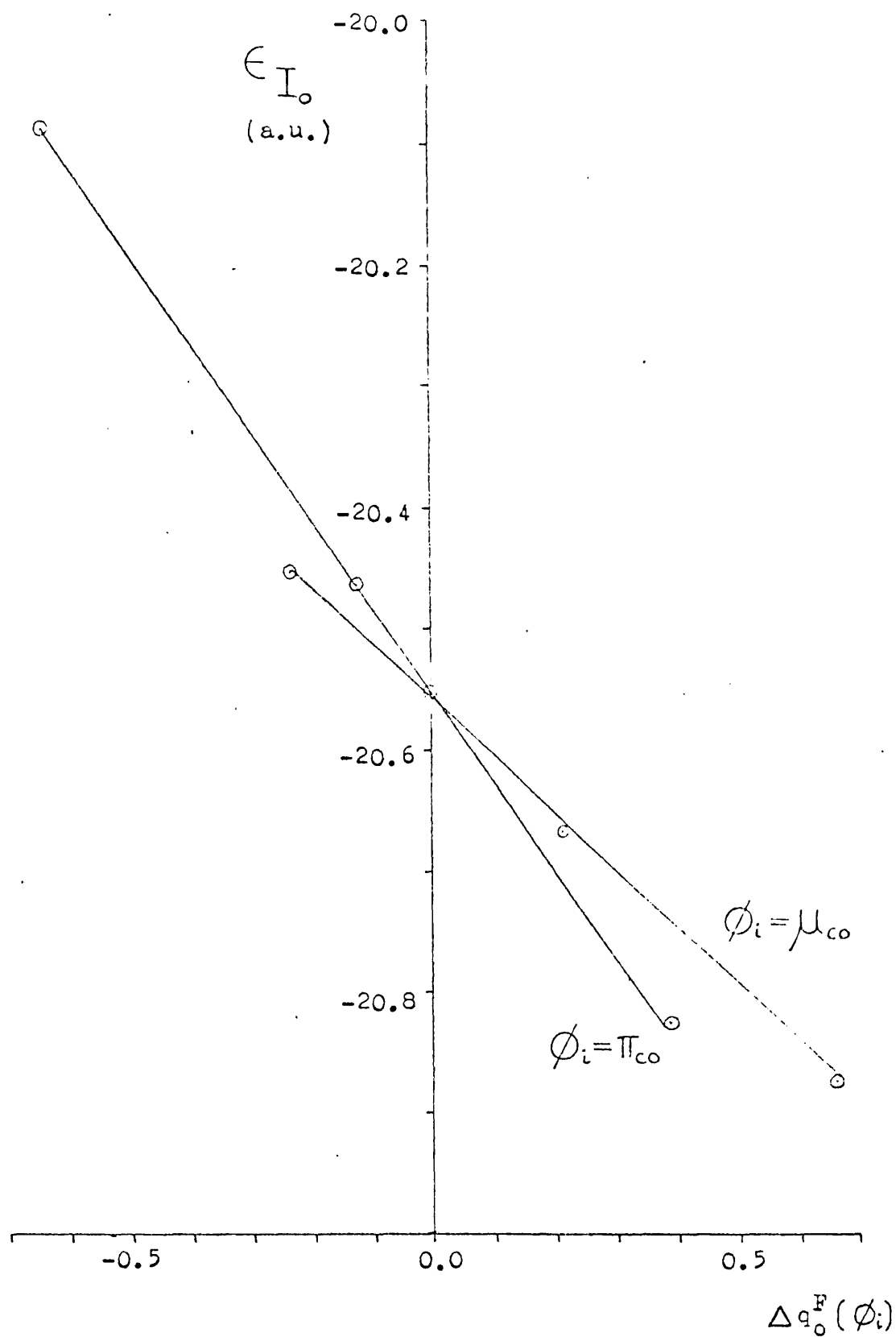


Figure 5.7 Variation of the  $I_0$  Eigenvalue with Changes in the Atomic Charge on the Oxygen Atom.

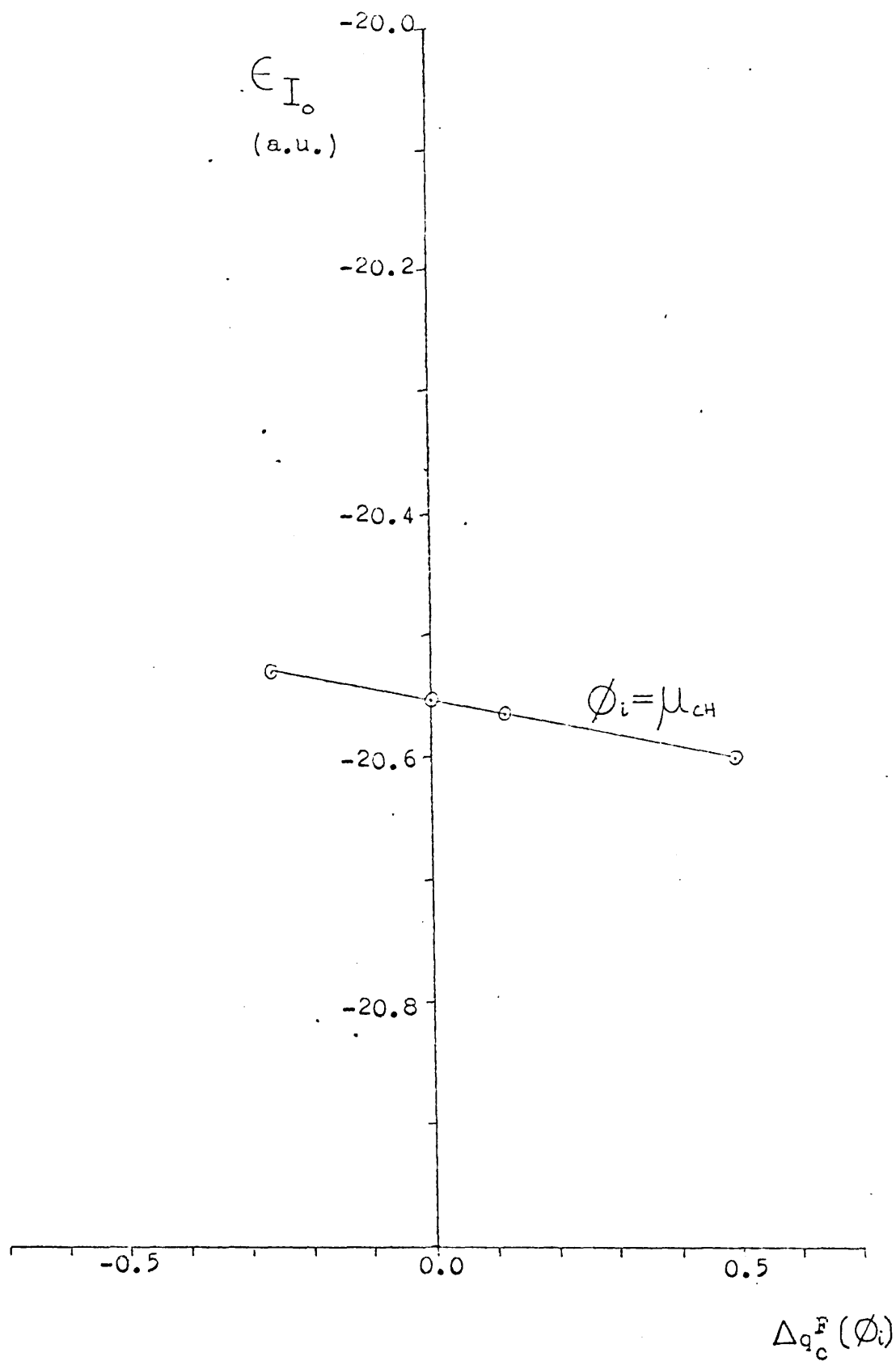


Figure 5.8 Variation of the  $I_0$  Eigenvalue with Changes in the Atomic Charge on the Carbon Atom.

Table 5.14 Gradients of Figures 5.6, 5.7 and 5.8

Bond whose polarity is fixed, $\phi_i$	Gradients		
	$\epsilon_{I_C}$ vs. $\Delta q_C^F(\phi_i)$	$\epsilon_{I_O}$ vs. $\Delta q_O^F(\phi_i)$	$\epsilon_{I_O}$ vs. $\Delta q_C^F(\phi_i)$
$\mu_{CH}$	-0.325	-	-0.087
$\mu_{CO}$	-0.242	-0.471	-
$\pi_{CO}$	-0.388	-0.727	-

Table 5.15 Values of the Gradients in Figures 5.6, 5.7 and 5.8  
predicted from Equation (5.25)

Bond whose polarity is fixed, $\phi_i$	Gradients		
	$\epsilon_{I_C}$ vs. $\Delta q_C^F(\phi_i)$	$\epsilon_{I_O}$ vs. $\Delta q_O^F$	$\epsilon_{I_O}$ vs. $\Delta q_C^F(\phi_i)$
$\mu_{CH}$	-0.353	-	-0.089
$\mu_{CO}$	-0.358	-0.536	-
$\pi_{CO}$	-0.396	-0.740	-

Figure 5.7 shows the variation of the eigenvalue of the oxygen atom inner shell with the polarities of the CO sigma- and pi-bonds as measured by the changes in the atomic charge on the oxygen atom  $\Delta q_{\text{O}}^{\text{F}}(\mu_{\text{CO}})$  and  $\Delta q_{\text{O}}^{\text{F}}(\pi_{\text{CO}})$ . Again there is a linear relationship which is different for the two bonds, changes in the polarity of the pi-bond giving a much greater change in the eigenvalue than changes in the polarity of the sigma-bond. An increase in the charge on the oxygen atom produces a decrease in the eigenvalue and vice versa.

The eigenvalue of the oxygen atom inner shell was also found to be effected by changes in the polarity of the CH bond. Figure 5.8 shows the variation of the eigenvalue with changes in the atomic charge on the carbon atom caused by changes in the polarity of the CH bond,  $\Delta q_{\text{C}}^{\text{F}}(\mu_{\text{CH}})$ . The effect is therefore not confined to bonds centred on the same atom as the inner shell. The variation of the eigenvalue of the oxygen inner shell with the polarity of the CH bond is a longer range effect, and is smaller than those shown in Figure 5.7. It is, however, linear and is in the direction expected from electrostatics. The gradients of the plots in Figures 5.7 and 5.8 are shown in Table 5.14.

In conclusion, the present analysis shows the eigenvalues of the inner shells to be linearly dependent on the polarity of the bonds in the formaldehyde molecule. This is in agreement with the findings of Siegbahn and others<sup>96,99,100,101</sup> that the experimental binding energies of the inner shells in different molecules vary linearly with the polarity of the bonds. These workers find a linear relationship between the binding energy of an inner shell and the calculated total charge on the atom concerned. The present work uses the formaldehyde molecule as a model to examine the separate effect from each bond. The results suggest that the variation in the eigenvalues of the inner shells may be explained in terms of simple electrostatics. If this is the case, it should be possible to predict the

values of the gradients in Table 5.14 from an electrostatic model of the molecule.

The eigenvalue of the inner shell on atom A is given by

$$\epsilon_{I_A} = \langle I_A | F | I_A \rangle \quad (5.17)$$

A change in the polarity of a bond between atoms B and C,  $\phi_{BC}$ , produces a change in the eigenvalue through the operator. If  $\phi'_{BC}$  and  $\phi''_{BC}$  represent the bond  $\phi_{BC}$  at two different polarities and  $\epsilon'_{I_A}$  and  $\epsilon''_{I_A}$  are the eigenvalues of  $I_A$  at these polarities, the only difference between  $\epsilon'_{I_A}$  and  $\epsilon''_{I_A}$  will be in terms in the operator involving  $\phi_{BC}$ , all the other terms in the operator being the same in the two cases. Considering only coulombic terms and neglecting the exchange terms the change in the eigenvalue is given by

$$\left[ \epsilon'_{I_A} - \epsilon''_{I_A} \right] = 2 \langle I_A^2 | \phi'^2_{BC} \rangle - 2 \langle I_A^2 | \phi''^2_{BC} \rangle \quad (5.18)$$

Expressing  $\phi'_{BC}$  and  $\phi''_{BC}$  in terms of polarity parameters and normalised hybrid atomic orbitals,  $\nu_B$  and  $\nu_C$ , as in equation (5.5)

$$\phi'_{BC} = p'_B \nu_B + p'_C \nu_C \quad (5.5)$$

gives

$$\begin{aligned} \left[ \epsilon'_{I_A} - \epsilon''_{I_A} \right] &= 2(p_B'^2 - p_B''^2) \langle I_A^2 | \nu_B^2 \rangle + \\ &2(p_C'^2 - p_C''^2) \langle I_A^2 | \nu_C^2 \rangle + 4(p'_B p'_C - p''_B p''_C) \langle I_A^2 | \nu_B \nu_C \rangle \end{aligned} \quad (5.19)$$

After substitution of Mulliken's Approximation<sup>102</sup>

$$\langle I_A^2 | \nu_B \nu_C \rangle = \frac{1}{2} \langle \nu_B | \nu_C \rangle (\langle I_A^2 | \nu_B^2 \rangle - \langle I_A^2 | \nu_C^2 \rangle) \quad (5.20)$$

equation (5.19) may be expressed in terms of the atomic charges given by equation(5.12)

$$\left[ \epsilon'_{I_A} - \epsilon''_{I_A} \right] = - \left\{ (q_B(\phi'_{BC}) - q_B(\phi''_{BC})) \langle I_A^2 | \nu_B^2 \rangle + (q_C(\phi'_{BC}) - q_C(\phi''_{BC})) \langle I_A^2 | \nu_C^2 \rangle \right\} \quad (5.21)$$

The atomic charge on atom B, for example, due to the polarity of  $\phi_{BC}$  is equal to minus the atomic charge on atom C due to the polarity of  $\phi_{BC}$

$$q_B(\phi_{BC}) = -q_C(\phi_{BC}) \quad (5.22)$$

Therefore

$$\left[ \epsilon'_{I_A} - \epsilon''_{I_A} \right] = - (q_B(\phi'_{BC}) - q_B(\phi''_{BC})) \left\{ \langle I_A^2 | \nu_B^2 \rangle - \langle I_A^2 | \nu_C^2 \rangle \right\} \quad (5.23)$$

Expressing equation (5.23) in terms of the changes from the SCF

values in the atomic charges as shown in Figures 5.6, 5.7 and 5.8 gives

$$\left[ \epsilon'_{I_A} - \epsilon''_{I_A} \right] = - (\Delta q_B^F(\phi'_{BC}) - \Delta q_B^F(\phi''_{BC})) \left\{ \langle I_A^2 | \nu_B^2 \rangle - \langle I_A^2 | \nu_C^2 \rangle \right\} \quad (5.24)$$

A plot of the eigenvalue  $\epsilon_{I_A}$  against the change in the atomic charge on atom B caused by a change in the polarity of  $\phi_{BC}$  should therefore have a gradient given by:

$$\text{gradient} = - \left\{ \langle I_A^2 | \nu_B^2 \rangle - \langle I_A^2 | \nu_C^2 \rangle \right\} \quad (5.25)$$

This quantity was evaluated for each of the plots in Figures 5.6 to 5.8, and the values are shown in Table 5.15. They are in fairly good agreement with the gradients obtained from the graphs.

Equation (5.24) is derived by assuming that the contributions from other parts of the molecule are constant, as they are in the present work which considers changes in the polarity of one of the bonds of a single molecule. Siegbahn and co-workers<sup>96</sup> have used an electrostatic potential model for the calculation of changes in the inner shell binding energies due to different polarities of bonds in different molecules, with good results.

From the information in Table 5.14 an attempt was made to predict the binding energies of the carbon and oxygen inner shells of acetaldehyde and acetone, by assuming the carbon-carbon bonds in these molecules to be approximated by the non-polar CH bonds of the present work. The absolute value of the eigenvalue of inner shells is expected to be approximately 10 to 20 eV larger than the experimental ionization energy, as discussed in section 2. However, several workers<sup>96,101,103</sup> have found that it is possible to predict successfully the difference in the binding energy between one molecule and another by the difference in the eigenvalues of the inner shells in the two molecules, although good results have not been obtained with a small atomic orbital basis set such as is used in the present work.

The experimental shifts in the binding energy,<sup>93</sup> together with the shifts predicted by the results in Table 5.14 are shown in Table 5.16. The experimental shifts are based on estimated experimental values for the ionization energies in formaldehyde, as discussed in section 2. A positive value of a shift as shown in Table 5.16 indicates a decrease in the eigenvalue or an increase in the binding energy in the larger molecule. The predicted values are seen not to reflect very successfully the experimental values. The experimental error for the ESCA measurements is estimated to be about 0.2 eV so the binding energy of the carbon inner shell does not

Table 5.16 Predicted and Experimental Shifts in Binding  
Energies of Inner Shells (eV)

	$I_C$		$I_O$	
	Predicted value	Experimental value	Predicted value	Experimental value
Formaldehyde to Acetaldehyde	+1.09	$[-0.1]^1$	+0.29	$[+0.6]^1$
Acetaldehyde to Acetone	+1.09	-0.1	+0.29	+1.4

1. Estimated values (see text).



change significantly in the three molecules considered, whereas a rise of approximately 1 eV is predicted in each case. The experimental binding energy of the oxygen inner shell rises from formaldehyde to acetone. The predicted values do show a rise in the binding energy, but by too small an amount.

(ii) Eigenvalues of Valence Shell l.m.o.s

The eigenvalues of the remaining l.m.o.s are not observable quantities, with the exception of the pi-bond. It is, however, still of interest to investigate how these quantities change with the polarity of the bonds. As with the inner shells, the eigenvalues of all the other l.m.o.s in the molecule were found to vary linearly with changes in the atomic charge on the appropriate atom.

The variation of the eigenvalues of the lone pairs resulting from changes in the polarity of the CO sigma- and pi-bonds, as measured by the change in the atomic charge on the oxygen atom are shown in Figures 5.9 and 5.10. It can be seen that the pi-bond affects the eigenvalues of the lone pairs to a greater extent than the sigma-bond, and that the effect of each bond on both lone pairs is the same. As with the inner shell on the oxygen atom, the lone pairs were also found to vary with the polarity of the CH bond, as measured by the change in the atomic charge on the carbon atom. This is shown in Figures 5.11 and 5.12. Again the effect is less than that of the CO bonds, the pi-type lone pair being affected to a slightly greater extent than the sigma-type lone pair. The gradients for Figures 5.9 to 5.12 are shown in Table 5.17. The variation of both the lone pairs with the polarity of the bonds is in the direction expected from electrostatic considerations. The experimental ionization energies of lone pairs in different molecules (which correspond to the eigenvalues of the c.m.o.s not the l.m.o.s) have been observed to vary with the polarity of the bonds.<sup>104</sup>

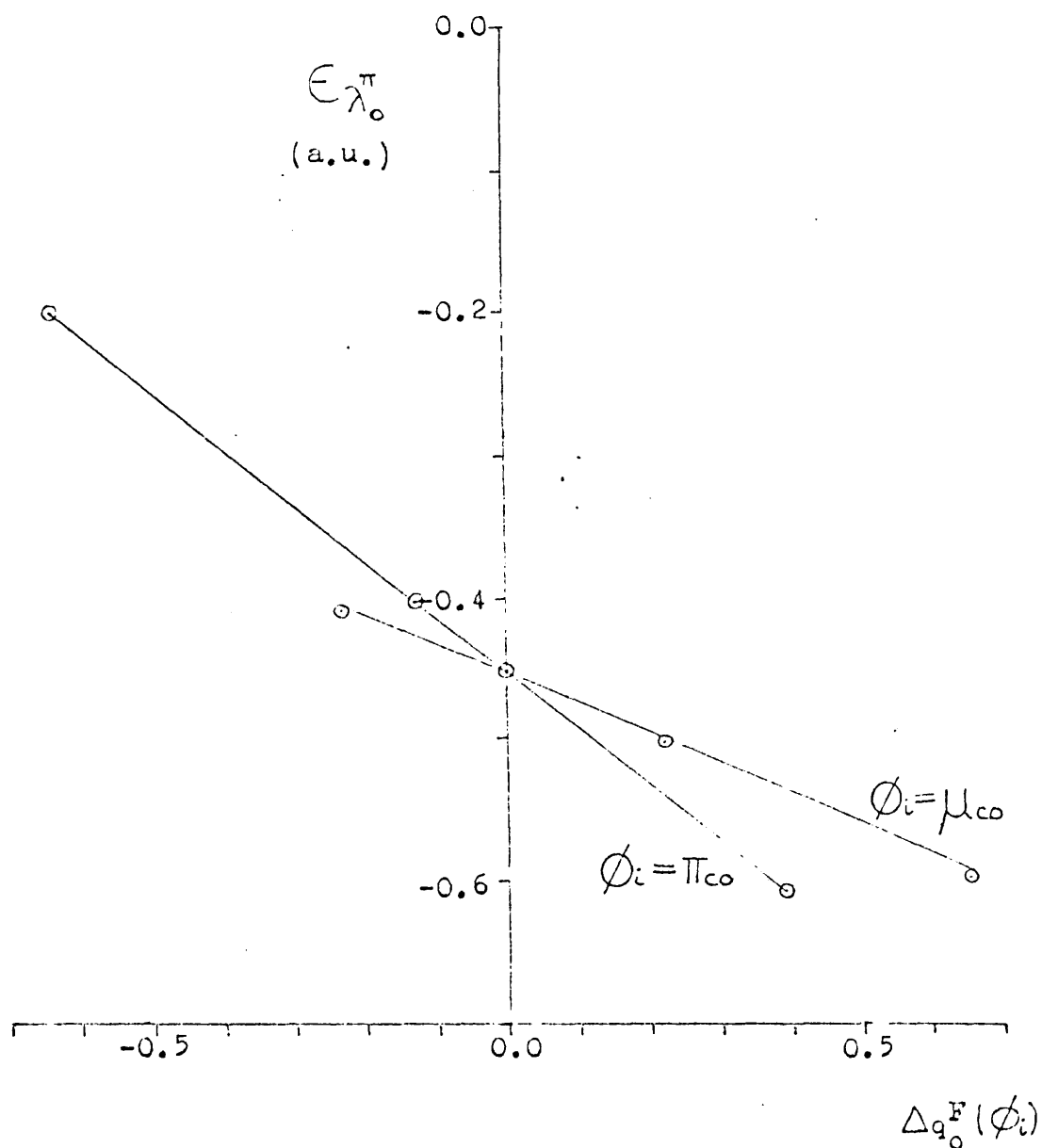


Figure 5.9 Variation of the  $\lambda_0^{\pi}$  Eigenvalue with Changes in the Atomic Charge on the Oxygen Atom.

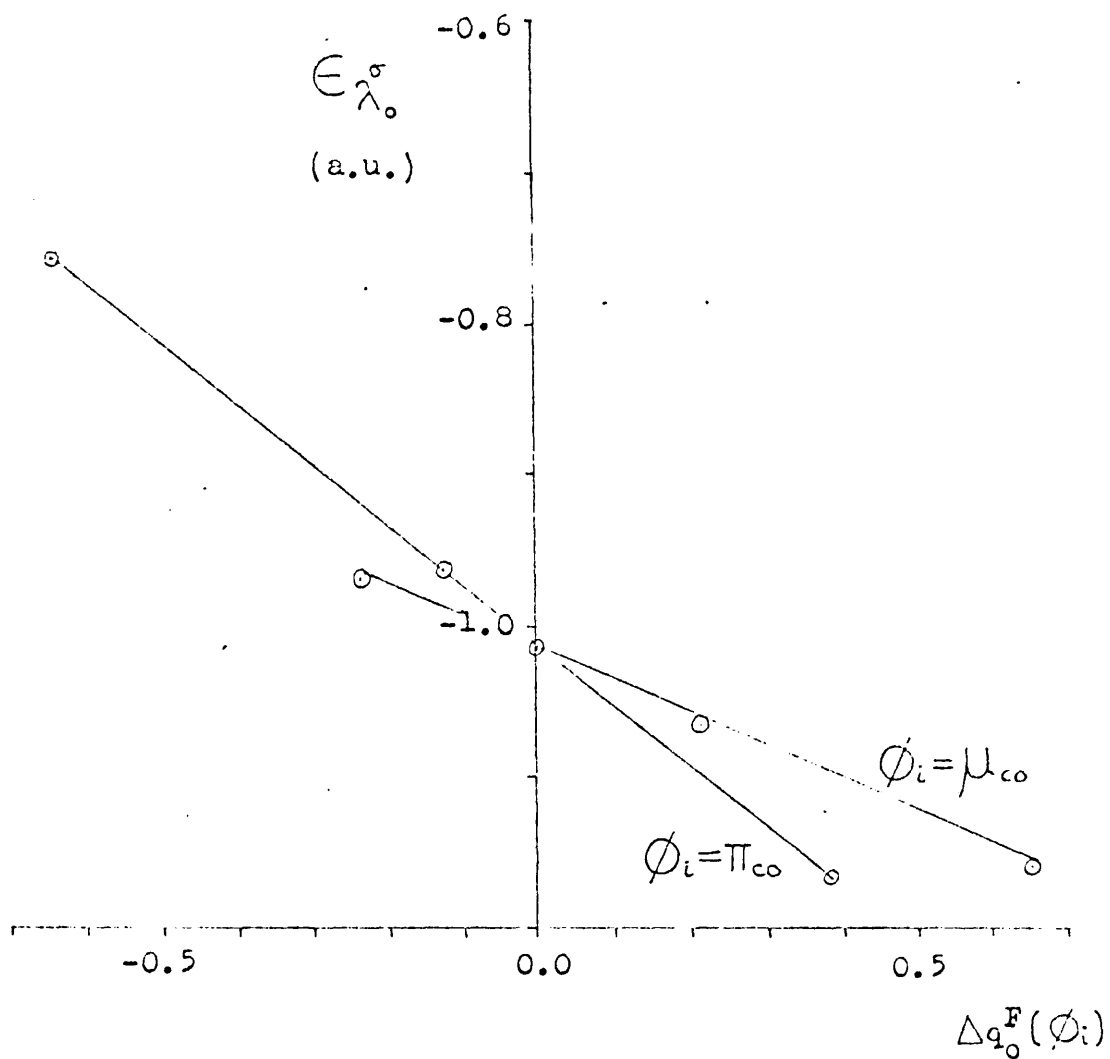


Figure 5.10 Variation of the  $\lambda_0^{\sigma}$  Eigenvalue with Changes in the Atomic Charge on the Oxygen Atom.

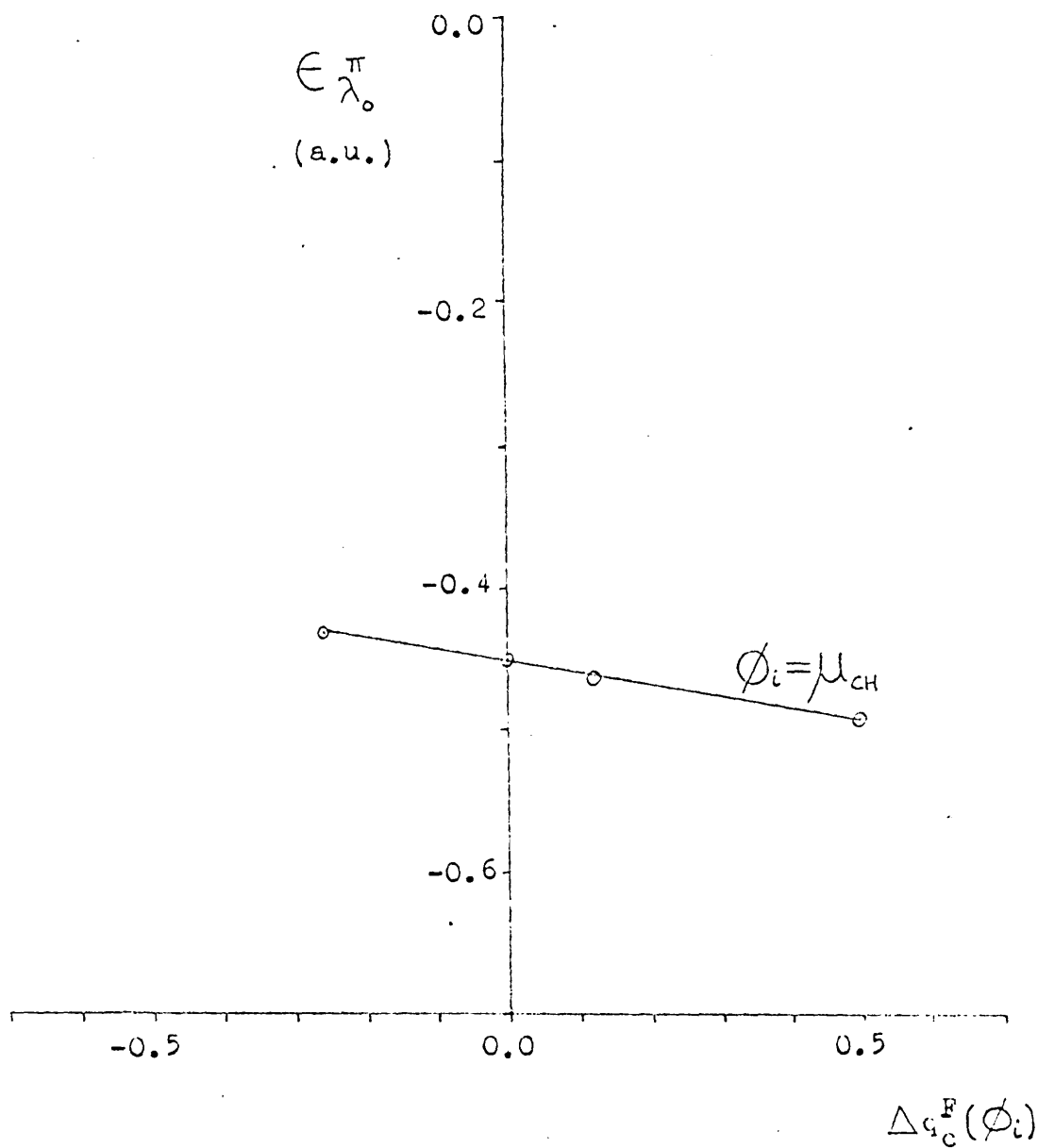


Figure 5.11 Variation of the  $\lambda_0^{\pi}$  Eigenvalue with Changes in the Atomic Charge on the Carbon Atom.

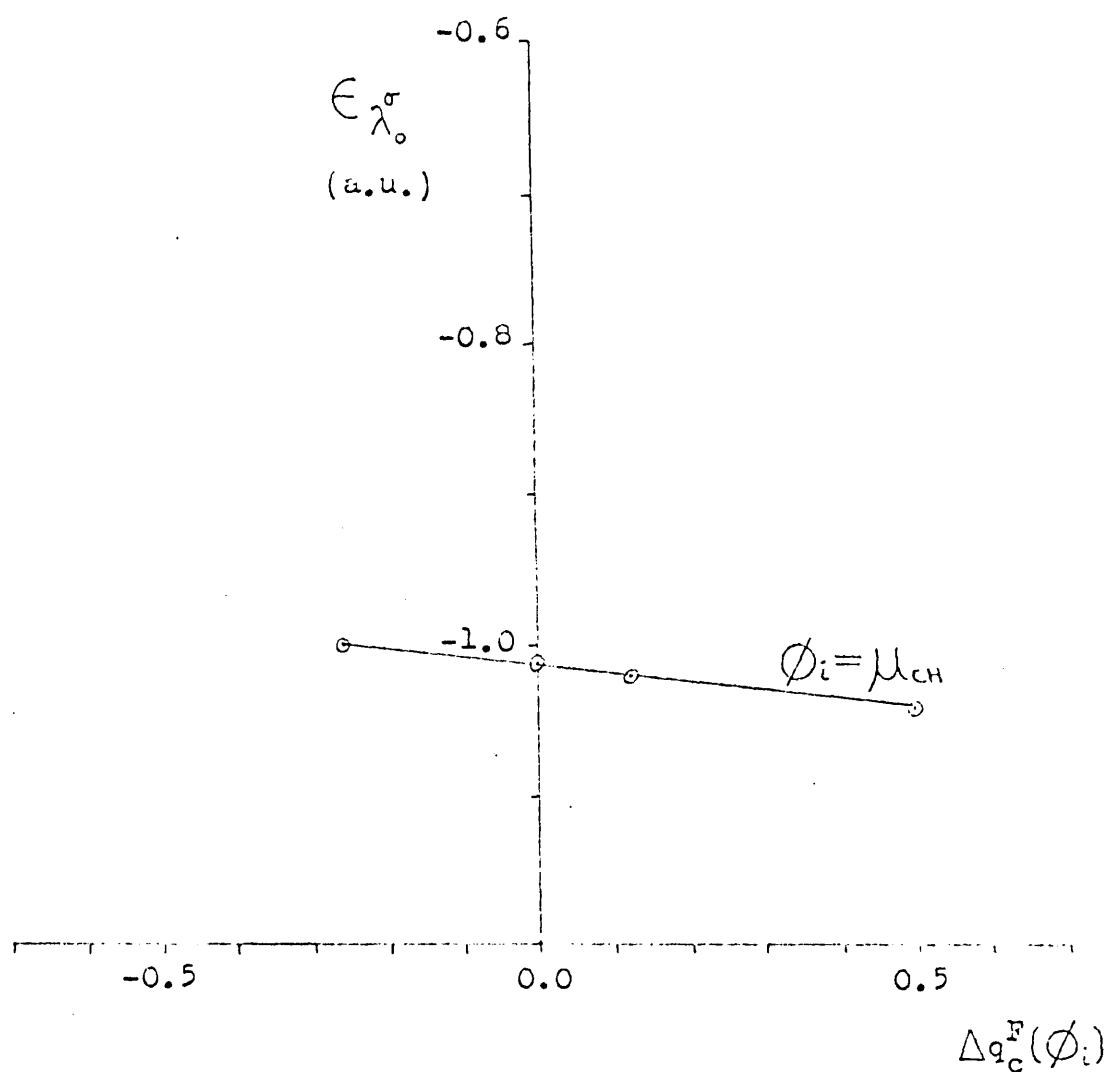


Figure 5.12 Variation of the  $\lambda_0^\sigma$  Eigenvalue with Changes in the Atomic Charge on the Carbon Atom.

Table 5.17 Gradients of Figures 5.9 to 5.12

Bond whose polarity is fixed, $\phi_i$	Gradients			
	$\epsilon_{\chi_c^\pi \text{ vs. } \Delta q_0^F(\phi_i)}$	$\epsilon_{\chi_c^\sigma \text{ vs. } \Delta q_0^F(\phi_i)}$	$\epsilon_{\chi_c^\pi \text{ vs. } \Delta q_c^F(\phi_i)}$	$\epsilon_{\chi_c^\sigma \text{ vs. } \Delta q_c^F(\phi_i)}$
$\mu_{\text{CH}}$	-	-	-0.078	-0.063
$\mu_{\text{CO}}$	-0.212	-0.214	-	-
$\pi_{\text{CO}}$	-0.399	-0.402	-	-

The effect of changes in the polarity of one bond,  $\phi_i$ , on the eigenvalues of other bonds,  $\phi_j$ , are shown in Figures 5.13, 5.14 and 5.15, and the gradients of these plots are given in Table 5.18. In each case the polarity of the fixed bond is measured by the atomic charge on the carbon atom. In general, the eigenvalues of the bonds fall when the charge on the carbon atom increases, as would be expected, and each eigenvalue is affected by the polarity of the neighbouring bonds to a similar extent. The two exceptions are the variation in the eigenvalue of  $\mu_{CO}$  when the polarity of  $\pi_{CO}$  is altered and conversely the variation in the eigenvalue of  $\pi_{CO}$  when the polarity of  $\mu_{CO}$  is altered. These two bonds share the same two atoms and are closely linked. In each case an increase in the charge on the carbon atom is equivalent to a decrease in the charge on the oxygen atom. The eigenvalue of each bond is decreased when the other bond is polarised towards the carbon atom. At SCF the sigma-bond is polarised towards the oxygen atom, so its eigenvalue would be expected from electrostatic considerations to decrease when the pi-bond is polarised further away from the oxygen atom and to rise when the pi-bond is polarised towards the oxygen atom. This is the behaviour which is found to occur. The effect is an order of magnitude larger than the effect of the CH bond on the eigenvalue of  $\mu_{CO}$ . The converse, however, does not occur. At SCF the pi-bond is polarised towards the carbon atom, so its eigenvalue would be expected to increase when the sigma-bond is polarised towards the carbon atom and to decrease when the sigma-bond is polarised away from the carbon atom. The reverse behaviour is observed. In both cases, however, the variation of the eigenvalue with the changes in atomic charges is linear.

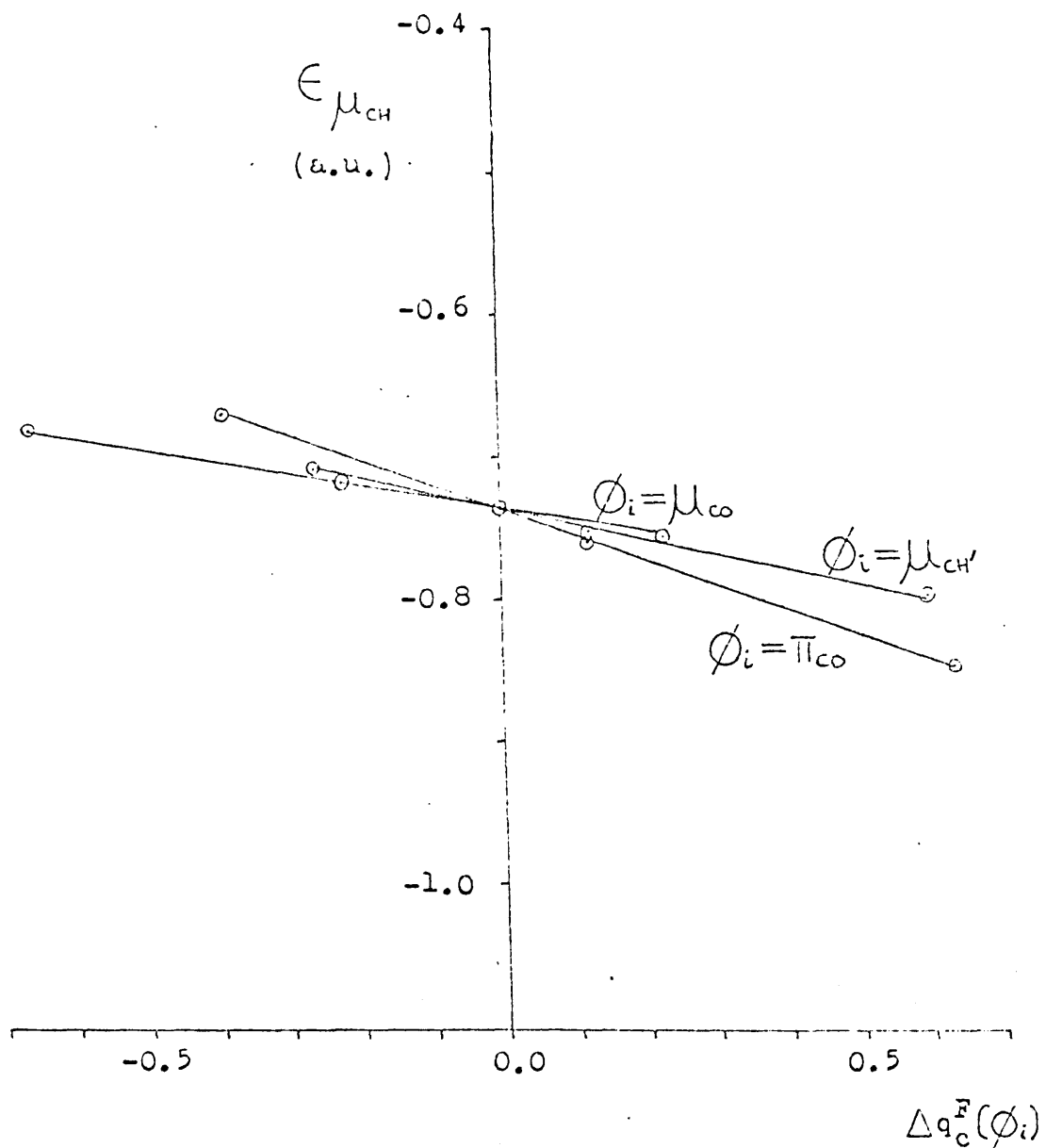


Figure 5.13 Variation of the  $\mu_{CH}$  Eigenvalue with Changes in the Atomic Charge on the Carbon Atom.



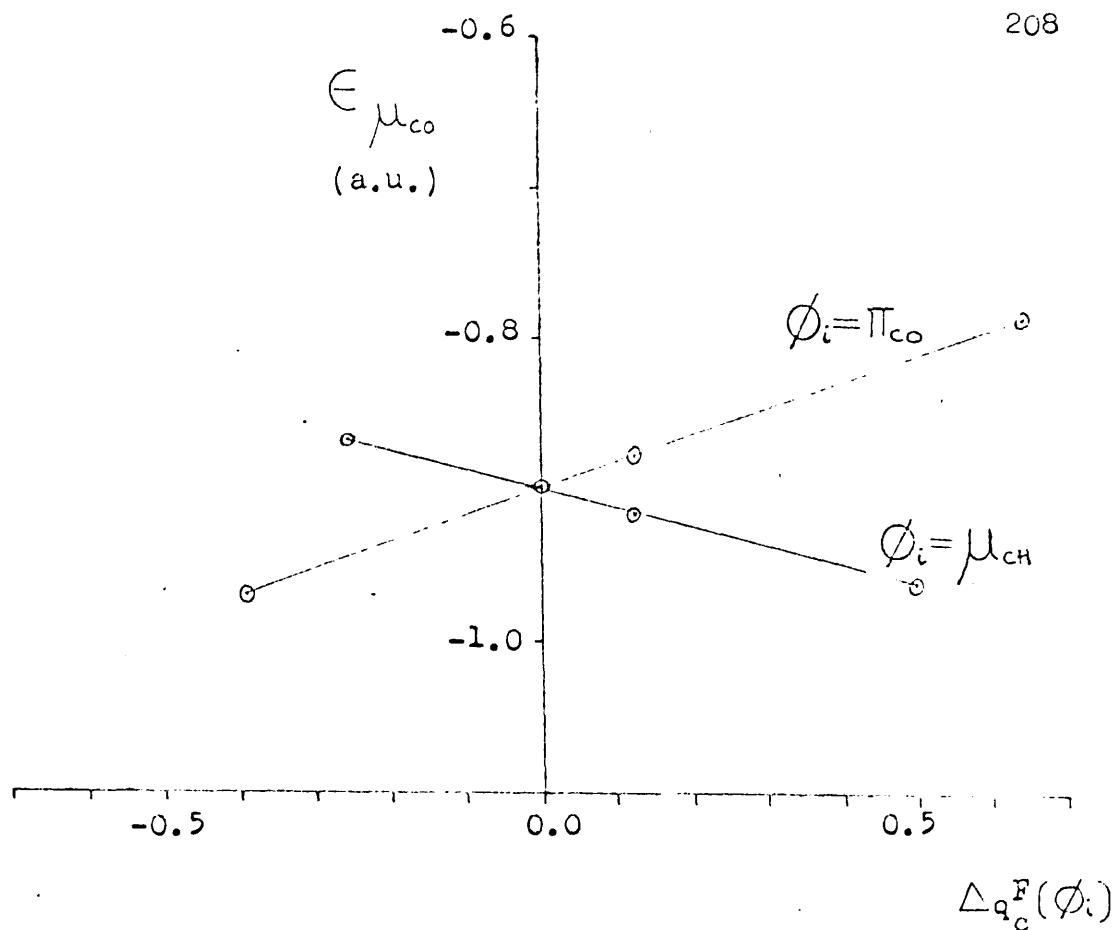


Figure 5.14 Variation of the  $\mu_{CO}$  Eigenvalue with Changes in the Atomic Charge on the Carbon Atom.

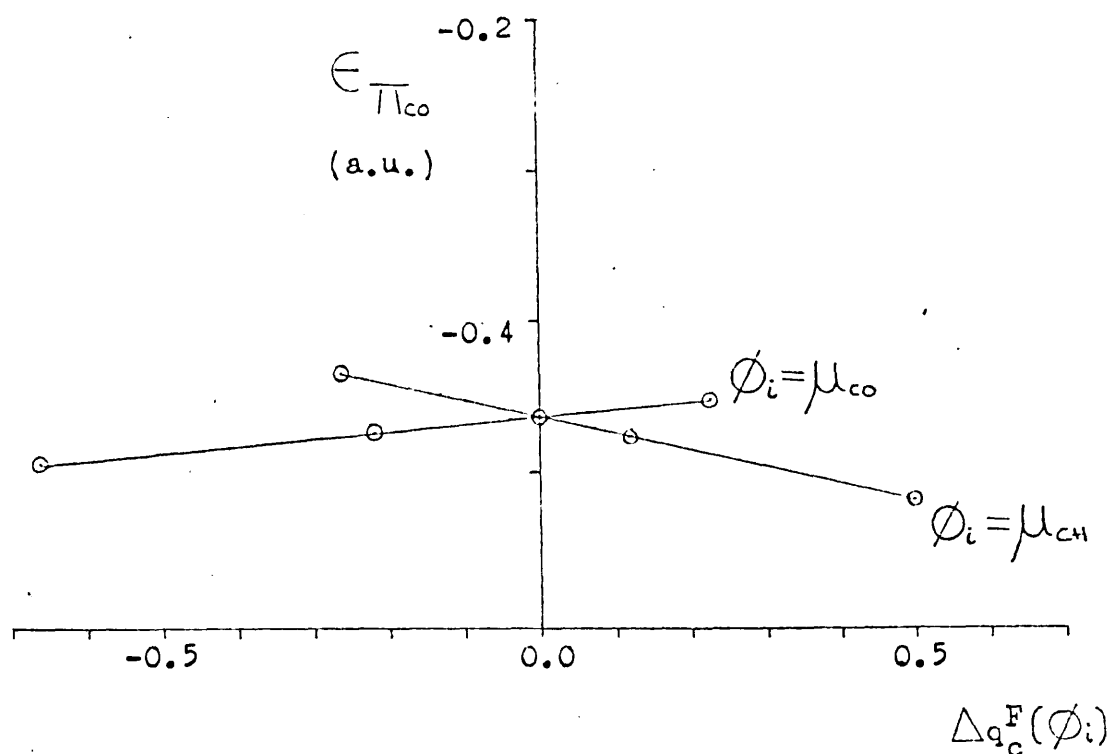


Figure 5.15 Variation of the  $\pi_{CO}$  Eigenvalue with Changes in the Atomic Charge on the Carbon Atom.

Table 5.18 Gradients of Figures 5.13 to 5.15

Bond whose polarity is fixed, $\phi_i$	Gradients		
	$\epsilon_{\mu_{\text{CH}}} \text{ vs. } \Delta q_{\text{C}}^{\text{F}}(\phi_i)$	$\epsilon_{\mu_{\text{CO}}} \text{ vs. } \Delta q_{\text{C}}^{\text{F}}(\phi_i)$	$\epsilon_{\pi_{\text{CO}}} \text{ vs. } \Delta q_{\text{C}}^{\text{F}}(\phi_i)$
$\mu_{\text{CH}}$	-0.118	-0.123	-0.110
$\mu_{\text{CO}}$	-0.087	-	+0.047
$\pi_{\text{CO}}$	-0.179	+1.206	-

The eigenvalues of the bonds  $\phi_j$  were also noted after an l.m.o. calculation had been performed on the bond. A calculation allows the form of  $\phi_j$  to change in response to the change made in the polarity of the fixed bond  $\phi_i$ . In this case a change in the eigenvalue of  $\phi_j$  occurs through a change in the form of  $\phi_j$ , as well as through the operator. The eigenvalues of  $\phi_j$  before and after a calculation were found to agree to well within 0.01 a.u., except when both  $\phi_i$  and  $\phi_j$  are the CO-sigma and pi-bonds. The eigenvalues therefore indicate that the form of  $\phi_j$  does not change significantly in response to the polarity of the other bond, except in these two cases. This confirms the earlier conclusion that there is little polarising of one bond by another.

## Section 6   Bond Energies

### (a) Introduction

One of the important objectives in calculating localised molecular orbitals is the direct computation of bond energies which may be compared with experimental values. The canonical molecular orbitals give only the atomisation energy, the sum of the bond energies.

To calculate the quantity usually termed the bond dissociation energy the bond is broken and the energy of the two fragments computed. The difference between the total energy of the molecule and that of the two fragments is the bond dissociation energy. Ideally the energy of the ground state of the fragment should be used. Where the fragment is a single atom this is easily done, but where this is not the case the calculation of the energy of the fragment poses problems. An accurate computation of the energy would require a separate SCF calculation of the fragment, in its ground state geometry, which would in general be an open-shell calculation.

The method used in the present work makes the assumption that there is no reorganisation of the geometry of the molecule or of the electrons on breaking the bond. The value for the bond dissociation energy of the CH bond in methane obtained using this method<sup>58</sup> was within 0.5 eV of the experimental value, a good result for a minimum basis set calculation.

Each fragment is formed by deleting from the l.m.o.s of the whole molecule all contributions from the atom or atoms in the other fragment, and re-normalising. For sets of perfectly localised functions only the l.m.o. whose bond dissociation energy is being calculated need be considered but for sets of slightly delocalised functions all the l.m.o.s in the molecule must be taken into account. The bond between two atoms is then replaced by two hybrid atomic orbitals, one on each atom, which

are each regarded as being occupied by a single electron. These hybrid atomic orbitals are not orthogonal to the other l.m.o.s and if a set of slightly delocalised l.m.o.s are used the doubly occupied orbitals are not orthogonal amongst themselves. There are three possible approaches to this problem. Firstly, the non-orthogonality may be neglected. Secondly, the orbitals in each fragment may be orthogonalised by for example Schmidt orthogonalising. Lastly, the energy of each fragment may be computed over a non-orthogonal set of functions. All three of these options was used to calculate the total energies of the fragments formed by breaking the CH bond and the CO double bond in formaldehyde. The bond dissociation energies of these bonds are then given by

$$\text{Bond Dissociation Energy} = E_M - (E_F + E'_F) \quad (5.26)$$

where  $E_M$  is the total energy of the formaldehyde molecule,  $-113.4026$  a.u., and  $E_F$  and  $E'_F$  are the total energies of the fragments. Defined in this way the bond dissociation energy is negative for a stable bond.

In addition to the difficulties already considered which are common to any calculation of a bond dissociation energy from a set of l.m.o.s, the present work has the extra complication that a unique set of l.m.o.s was not obtained from the l.m.o. calculations. Results for both bonds were obtained for the l.m.o.s given by calculation 12 and some results for the CO bond were also obtained for the l.m.o.s given by calculation 7.

(b) Calculation of the CH Bond Dissociation Energy

The two fragments formed by breaking the CH bond are the hydrogen atom and the formyl radical  $\cdot\text{CHO}$ .

The energy of the ground state of the hydrogen atom is given by using an exponent of  $-1.0$  for the hydrogen atomic orbitals in the expression

$$E_H = \langle 1s_H | -\frac{1}{2}\nabla^2 | 1s_H \rangle + \langle 1s_H | -1.0/r_H | 1s_H \rangle \quad (5.27)$$

This gives a value of  $-0.5000$  a.u. The experimental value is  $-0.4996$  a.u.<sup>105</sup>

The energy of the formyl radical is calculated by assuming that there is no electron reorganisation on breaking the CH bond. The geometry of the formyl radical is known to be similar to that of the formaldehyde molecule.<sup>106</sup> In the following work the seven doubly occupied orbitals are denoted by  $\phi_1, \dots, \phi_m$  and the singly occupied hybrid atomic orbital by  $\phi_{m+1}$ . If the functions  $\phi_1, \dots, \phi_{m+1}$  are assumed to be mutually orthogonal the energy of the fragment is given by

$$\begin{aligned} E_F = & 2 \sum_{i=1}^m \langle \phi_i | h | \phi_i \rangle + \langle \phi_{m+1} | h | \phi_{m+1} \rangle \\ & + \sum_{i=1}^m \sum_{k=1}^{m+1} \left\{ 2 \langle \phi_i \phi_i | \phi_k \phi_k \rangle - \langle \phi_i \phi_k | \phi_i \phi_k \rangle \right\} + R \end{aligned} \quad (5.28)$$

where  $R$  is the total nuclear repulsion in the fragment, and  $h$  is the one-electron operator, the sum being over the three atoms in the fragment.

$$h = -\frac{1}{2} \nabla^2 - \sum_{a=1}^3 \frac{Z_a}{r_a} \quad (5.29)$$

An estimate of the bond dissociation energy of the CH bond was first obtained by calculating the energy of the formyl radical using equation (5.28) and neglecting the non-orthogonality of the functions. More accurate values were then computed by Schmidt orthogonalising the functions. Two Schmidt orthogonalising sequences were used. Firstly, the singly occupied hybrid atomic orbital was placed at the beginning of the sequence so that it was unaltered by the orthogonalising but was mixed into the other functions. Secondly, the singly occupied hybrid atomic orbital was placed at the end of the sequence so that it was not mixed into the doubly occupied orbitals. The three values of the bond dissociation energy obtained are shown in Table 5.19.

The following expression for the energy of the formyl radical in terms of a set of non-orthogonal orbitals was derived using the method first formulated by Lowdin.<sup>107</sup>

$$\begin{aligned}
E_{\tilde{F}} = & \sum_{i=1}^m \sum_{j=1}^m \langle \phi_i | h | \phi_j \rangle P_{ji}^{-1} \\
& + \sum_{i=1}^{m-1} \sum_{j=1}^{m-1} \langle \phi_i | h | \phi_j \rangle Q_{ji}^{-1} \\
& + \sum_{i=1}^m \sum_{j=1}^m \sum_{k=1}^m \sum_{l=1}^m \left\{ \langle \phi_i \phi_k | \phi_j \phi_l \rangle - \langle \phi_i \phi_l | \phi_j \phi_k \rangle \right\} \\
& \quad (i < j) \quad (k < l) \quad \times \left[ P_{ki}^{-1} P_{lj}^{-1} - P_{li}^{-1} P_{kj}^{-1} \right] \\
& + \sum_{i=1}^{m+1} \sum_{j=1}^{m+1} \sum_{k=1}^{m+1} \sum_{l=1}^{m+1} \left\{ \langle \phi_i \phi_k | \phi_j \phi_l \rangle - \langle \phi_i \phi_l | \phi_j \phi_k \rangle \right\} \\
& \quad (i < j) \quad (k < l) \quad \times \left[ Q_{ki}^{-1} Q_{lj}^{-1} - Q_{li}^{-1} Q_{kj}^{-1} \right] \\
& + \sum_{i=1}^m \sum_{j=1}^{m+1} \sum_{k=1}^m \sum_{l=1}^{m+1} \left\{ \langle \phi_i \phi_k | \phi_j \phi_l \rangle \right\} \times P_{ki}^{-1} Q_{jl}^{-1} \\
& + R
\end{aligned} \tag{5.30}$$

where  $h$  is given by equation (5.29).

$\underline{P}$  is the  $m \times m$  overlap integral matrix of the functions  $\phi_1 \dots \phi_m$  and  $\underline{Q}$  is the  $(m+1) \times (m+1)$  overlap integral matrix of the functions  $\phi_1 \dots \phi_{m+1}$ , so that  $P_{ij}^{-1}$  and  $Q_{ij}^{-1}$  etc. are elements of the inverses of the matrices  $\underline{P}$  and  $\underline{Q}$ . Equation (5.30) was obtained using Jacobi's ratio theorem<sup>108, 109</sup> which states that

$$\tilde{P}_{ij} = P_{ji}^{-1} \det(\underline{P}) \tag{5.31}$$

where  $\tilde{P}_{ij}$  is the co-factor obtained by deleting row  $i$  and column  $j$  from the matrix  $\underline{P}$ , and multiplying by  $(-1)^{(i+j)}$

$$\text{and } \tilde{P}_{ij,kl} = [P_{ki}^{-1} P_{lj}^{-1} - P_{li}^{-1} P_{kj}^{-1}] \det(\underline{P}) \tag{5.32}$$

where  $\tilde{P}_{ij,kl}$  is the co-factor obtained by deleting rows  $i$  and  $j$  and columns  $k$  and  $l$  from the matrix  $\underline{P}$ , and multiplying by  $(-1)^{(i+j+k+l)}$ .

The bond dissociation energy of the CH bond calculated using equation (5.30) is given in Table 5.19. This value is very similar to the second value calculated by Schmidt orthogonalising the functions, which was obtained by the Schmidt orthogonalising sequence which does not allow the singly occupied hybrid atomic orbital to mix into the doubly occupied orbitals.

The experimental value of the bond dissociation energy of the first CH bond in formaldehyde has been determined as less than 78 kcal/mole by photolysis in the presence of iodine<sup>9</sup> and as  $75 \pm 2$  kcal/mole ( $3.25 \pm 0.1$  eV) by electron impact at  $400 - 500^\circ\text{K}$ .<sup>110</sup> The best calculated values shown in Table 5.18 differ from the experimental value by 1.2 to 1.4 eV (about 30 kcal/mole). The agreement is therefore not as good as that obtained for the methane molecule,<sup>58</sup> but is still good when compared to the usual calculation of Dissociation Energies.<sup>68a</sup> The question of whether a better result would be obtained with one of the other sets of l.m.o.s from the l.m.o. calculations remains to be answered.

### (c) Calculation of the CO Bond Dissociation Energy

The two fragments formed by breaking the CO double bond are the oxygen atom and the CH<sub>2</sub> radical. The breaking of the two bonds leaves two unpaired electrons on each fragment. Where no electron reorganisation is assumed the question therefore arises of whether the spins of these electrons are paired or parallel.

The energy of a fragment with  $m$  doubly occupied orbitals  $\phi_1, \dots, \phi_m$  and two singly occupied hybrid atomic orbitals  $\phi_{m+1}$  and  $\phi_{m+2}$  is given by



$$\begin{aligned}
E_F = & \sum_{i=1}^m \sum_{j=1}^m \langle \phi_i | h | \phi_j \rangle P_{ji}^{-1} \\
& + \sum_{i=1}^{m+2} \sum_{j=1}^{m+2} \langle \phi_i | h | \phi_j \rangle Q_{ji}^{-1} \\
& + \sum_{i=1}^m \sum_{j=1}^m \sum_{k=1}^m \sum_{l=1}^m \left\{ \langle \phi_i \phi_k | \phi_j \phi_l \rangle - \langle \phi_i \phi_l | \phi_j \phi_k \rangle \right\} \\
& \quad (i < j) \quad (k < l) \quad \times [P_{ki}^{-1} P_{lj}^{-1} - P_{li}^{-1} P_{kj}^{-1}] \\
& + \sum_{i=1}^{m+2} \sum_{j=1}^{m+2} \sum_{k=1}^{m+2} \sum_{l=1}^{m+2} \left\{ \langle \phi_i \phi_k | \phi_j \phi_l \rangle - \langle \phi_i \phi_l | \phi_j \phi_k \rangle \right\} \\
& \quad (i < j) \quad (k < l) \quad \times [Q_{ki}^{-1} Q_{lj}^{-1} - Q_{li}^{-1} Q_{kj}^{-1}] \\
& + \sum_{i=1}^m \sum_{j=1}^{m+2} \sum_{k=1}^m \sum_{l=1}^{m+2} \left\{ \langle \phi_i \phi_k | \phi_j \phi_l \rangle \right\} \times P_{ki}^{-1} Q_{jl}^{-1} \\
& + R
\end{aligned} \tag{5.36}$$

where  $h$  is given by equation (5.35).  $\underline{P}$  is the  $m \times m$  overlap integral matrix of  $\phi_1, \dots, \phi_m$  and  $\underline{Q}$  is the  $(m+2) \times (m+2)$  overlap integral matrix of  $\phi_1, \dots, \phi_{m+2}$ . The bond dissociation energy of the CO double bond calculated using equation (5.36) is given in Table 5.20. It can be seen that this value is the same as that obtained by Schmidt orthogonalising the functions so that the singly occupied orbitals do not mix into the doubly occupied orbitals, when the electrons in the singly occupied orbitals have the same spin ( $x = 1$ ).

The bond dissociation energy of the CO double bond was also evaluated for the l.m.o.s given by calculation 7, using equation (5.36) to compute the energy of the  $\text{CH}_2$  radical. A value of  $-0.0477$  a.u. ( $-1.30$  eV) was obtained, which agrees well with the result from the l.m.o.s given by calculation 12. However, values for all the various sets of l.m.o.s obtained at stage 4 are needed to reveal how sensitive the bond dissociation energy is to the details of the l.m.o.s.

Table 5.19 Bond Dissociation Energy of the CH Bond in Formaldehyde

		Bond Dissociation Energy of the CH bond.	
		(a.u.)	(eV)
Calculated values <sup>1</sup>			
Method of Calculating the Energy of the Formyl Radical	Total Energy of the Formyl Radical (a.u.)		
1. Neglecting non- orthogonality and using equation (5.28).	-112.8197	-0.0829	-2.26
2. Schmidt orthogonalising and using equation (5.28)			
(i) hybrid atomic orbital at beginning of sequence.	-112.6800	-0.2226	-6.06
(ii) hybrid atomic orbital at end of sequence.	-112.7395	-0.1631	-4.44
3. Calculation over non- orthogonal orbitals using equation (5.30).	-112.7318	-0.1708	-4.65
Experimental value <sup>2</sup>		-0.1194	-3.25

1. Using l.m.o.s from calculation 12.

2. Reference 110.

$$\begin{aligned}
E_{\text{F}} = & \left\langle \sum_{i=1}^M \langle \phi_i | h | \phi_i \rangle + \langle \phi_{M+1} | h | \phi_{M+1} \rangle + \langle \phi_{M+2} | h | \phi_{M+2} \rangle \right. \\
& + \sum_{i=1}^M \sum_{k=i}^{M+2} \left\{ 2 \langle \phi_i \phi_i | \phi_k \phi_k \rangle - \langle \phi_i \phi_k | \phi_i \phi_k \rangle \right\} \\
& + \langle \phi_{M+1} \phi_{M+1} | \phi_{M+2} \phi_{M+2} \rangle - x \langle \phi_{M+1} \phi_{M+2} | \phi_{M+1} \phi_{M+2} \rangle \\
& + R
\end{aligned} \tag{5.33}$$

where  $x$  is the exchange factor and  $h$  is the one-electron operator.

In the case of the oxygen atom  $R$  equals zero and  $h$  is given by

$$h = -\frac{1}{2} \nabla^2 - \frac{Z_0}{r_0} \tag{5.34}$$

The ground state of the oxygen atom is a triplet state, according to Hund's Rules, so that the energy of the ground state may be calculated using equation (5.33) by putting the three doubly occupied orbitals  $\phi_1$  to  $\phi_3$  as  $1s_0$ ,  $2s_0$  and  $2p_{z_0}$ ,  $\phi_4$  and  $\phi_5$  as  $2p_{x_0}$  and  $2p_{y_0}$ , and  $x$  equal to 1.0. This gives a value of  $-74.5330$  a.u. The experimental value is  $-75.109$  a.u.<sup>105</sup>

For comparison the energy of the oxygen atom was also calculated with the hybrid atomic orbitals as they appear in the formaldehyde molecule. The hybrid atomic orbitals were first Schmidt orthogonalised in a sequence which did not allow the singly occupied orbitals to mix into the doubly occupied orbitals and then equation (5.33) was used to calculate the total energy of the atom. Results of  $-74.4563$  a.u.,  $-74.4254$  a.u. and  $-74.3946$  a.u. were obtained using values of the exchange factor  $x$  of 1.0, 0.5 and 0.0 respectively. The value of the exchange factor therefore makes a difference of 0.06 a.u. in the resulting total energy, the lowest value being given when  $x$  is 1.0 and the spins of the two electrons in the singly occupied hybrid atomic orbitals are parallel. This value is 0.08 a.u. higher than the energy of the ground state of the atom, giving an indication of the order of magnitude of the error resulting from the assumption that there is no electron reorganisation.

The energy of the  $\text{CH}_2$  radical was calculated by assuming that there is no reorganisation of the geometry of the molecule, or of the electrons, when the CO bond is broken. In fact the most stable state of the  $\text{CH}_2$  radical is a triplet state which is linear.<sup>111</sup> From the l.m.o.s given by calculation 12 an estimate of the bond dissociation energy of the CO bond was first obtained by neglecting the non-orthogonality of the functions and by calculating the energy of the  $\text{CH}_2$  radical using equation (5.33). In this case

$$h = -\frac{1}{2}\nabla^2 - \sum_{a=1}^3 \frac{Z_a}{r_a} \quad (5.35)$$

the sum being over the three atoms in the fragment.

More accurate values of the energy of the fragment were then obtained by Schmidt orthogonalising the functions in a sequence so that the singly occupied orbitals were not mixed into the doubly occupied orbitals. In each case three results were obtained using values for  $x$  of 1.0, 0.5 and 0.0. The values of the bond dissociation energy, computed using the calculated ground state energy of the oxygen atom, are shown in Table 5.20.

The following expression for the energy of the  $\text{CH}_2$  radical in terms of a set of non-orthogonal orbitals was derived, assuming the electrons in the singly occupied hybrid atomic orbitals to have the same spin.

Table 5.20 Bond Dissociation Energy of the CO Bond in Formaldehyde

			Bond Dissociation Energy of the CO bond.	
			(a.u.)	(eV)
Calculated values <sup>1</sup>				
Method of Calculating the Energy of the CH <sub>2</sub> radical.	x	Total Energy of the CH <sub>2</sub> radical (a.u.) <sup>2</sup>		
1. Neglecting non- orthogonality and using equation (5.33)	0	-38.8435	-0.0249	-0.68
	$\frac{1}{2}$	-38.8734	-0.0050	-0.14
	1	-38.9032	+0.0348	+0.95
2. Schmidt orthogonal- ising and using equation (5.33)	0	-38.7597	-0.1087	-2.96
	$\frac{1}{2}$	-38.7896	-0.0824	-2.24
	1	-38.8195	-0.0489	-1.33
3. Calculation over non-orthogonal orbitals using equation (5.36)	-	-38.8195	-0.0489	-1.33
Experimental value <sup>2</sup>			-0.2014	-5.48

1. Using l.m.o.s from calculation 12.

2. Reference 9.

The bond dissociation energy of the CO double in formaldehyde cannot be measured directly experimentally. A value of the bond energy of 149 kcal/mole (5.48 eV) has been given<sup>9</sup> by assuming a value for the bond energy of the two CH bonds in formaldehyde of 90.5 kcal/mole, and subtracting these from the atomisation energy of the molecule. However, the calculated values differ from the experimental value by 4.15 eV, so the results of the calculated bond dissociation energy of the CO bond clearly underestimate the experimental value by several eV.

CHAPTER SIX

ELECTRON DENSITIES

IN

TWO-ELECTRON CHEMICAL

BONDS

### Section 1 Introduction

The work described in this Chapter is an attempt to understand the physical significance of l.m.o.s by an investigation of their electron density distributions. 33 l.m.o.s describing two-electron chemical bonds, both sigma and pi, occurring in 19 different molecules were studied. The forms of the l.m.o.s used are those given in references 44, 51 and 58. These l.m.o.s were truncated to give perfectly localised functions. For an l.m.o. describing a bond between atoms A and B,  $\phi_{AB}$ , the electron density is given by

$$\rho_{AB} = \phi_{AB}^2 \quad (6.1)$$

The change in electron density on bond formation is examined in order to ascertain whether the conclusion reached by Daudel and co-workers for the  $H_2$  molecule,<sup>72</sup> that the formation of a two-electron chemical bond is accompanied by an increase of electron density in the region between the two nuclei and a decrease of electron density outside this region, is a general conclusion for all l.m.o.s describing two-electron bonds. This is achieved by calculating the density difference function, first defined by Daudel as the difference between the actual electron density and that which would occur if the electron density of the "free atoms" were simply superimposed. The electron density in the l.m.o. is  $2\rho_{AB}$ , as there are two electrons, and if the electron density in the atomic orbitals on atoms A and B forming the bond is  $\rho_A$  and  $\rho_B$  respectively, the density difference function,  $\delta$ , is given by

$$\delta = 2\rho_{AB} - (\rho_A + \rho_B) \quad (6.2)$$



A positive value of  $\delta$  then indicates an increase of electron density on bond formation.

The question arises of the exact form of the atomic orbitals forming the bond. If the simple atomic orbitals of the free atom are used, difficulties arise in molecules with extensive hybridisation, such as the carbon compounds. A hybrid atomic orbital with the same hybridisation as in the l.m.o. was therefore used. As in equation (2.24) the l.m.o. may be written in terms of the atomic orbitals

$$\begin{aligned} \phi_{AB} = & c_{1s_A} 1s_A + c_{2s_A} 2s_A + c_{2p_A} 2p_A + c_{1s_B} 1s_B \\ & + c_{2s_B} 2s_B + c_{2p_B} 2p_B \end{aligned} \quad (6.3)$$

It may also be expressed in terms of two normalised hybrids  $\psi_A$  and  $\psi_B$  on atoms A and B

$$\phi_{AB} = c_A \psi_A + c_B \psi_B \quad (6.4)$$

where

$$\psi_A = (c_{1s_A} 1s_A + c_{2s_A} 2s_A + c_{2p_A} 2p_A) / c_A \quad (6.5)$$

and similarly for  $\psi_B$ . The density difference function is then given by

$$\delta = 2 \phi_{AB}^2 - (\psi_A^2 + \psi_B^2) \quad (6.6)$$

Profiles of  $\delta$  along the inter-nuclear axis, and contour diagrams of  $\delta$  were obtained for the 33 bonds studied. In all diagrams 1 inch represents 1 Bohr radius,  $a_0$  (0.529 Å).

A measure of the total build-up of electron density in the inter-nuclear region on molecule formation,  $D$ , is given by integrating  $\delta$  between two planes intersecting the inter-nuclear axis perpendicularly at  $a$  and  $b$ .

Using cylindrical polar coordinates,

$$D = \int_a^b dz \int_0^\infty dr \int_0^{2\pi} d\theta \delta(z, r, \theta) \quad (6.7)$$

The values of  $a$  and  $b$  used are discussed below.

## Section 2 Results

A typical result is shown by the l.m.o. describing the sigma-bond of the  $N_2$  molecule. Figure 6.1 shows the variation along the inter-nuclear axis of the electron density distribution of two electrons in the l.m.o., and Figure 6.2 gives the  $\delta$  value calculated using hybrid atomic orbitals on the two nitrogen atoms.  $\delta$  profiles were also obtained for the molecules  $N_2$ , HF and  $F_2$  using the pure 2p atomic orbitals to calculate  $\rho_A$  and  $\rho_B$  in equation (6.2). They differed from those obtained by using the hybrid atomic orbitals only around the two nuclei.

The contour diagram of  $\delta$  for the  $N_2$  sigma-bond is shown in Figure 6.3 and for the  $N_2$  pi-bond in Figure 6.4. Contour diagrams of  $\delta$  for all of the other bonds studied are given in Figures 6.6 to 6.32. Thirty of the thirty-three bonds show the same general behaviour as the bonds in  $N_2$ . There is an accumulation of electron density in the inter-nuclear region as compared with the valence atomic orbitals of the two atoms forming the bond, and also on accompanying decrease in electron density outside the region of the bond. This is the same result which occurs with the  $H_2$  molecule (Figure 6.5).

The three bonds studied which do not show the build-up of electron density in the inter-nuclear region are LiH and the sigma- and pi-bonds of CO. (Figures 6.12, 6.13 and 6.14). These are strongly polar bonds in the sense that  $C_A$  and  $C_B$  of equation (6.4) are very different. To investigate these three cases further artificially non-polar l.m.o.s, in which  $C_A$  and  $C_B$  are equal, were constructed. These non-polar bonds show the normal accumulation of electron density in the inter-nuclear region, and decrease of electron density outside that region. It was

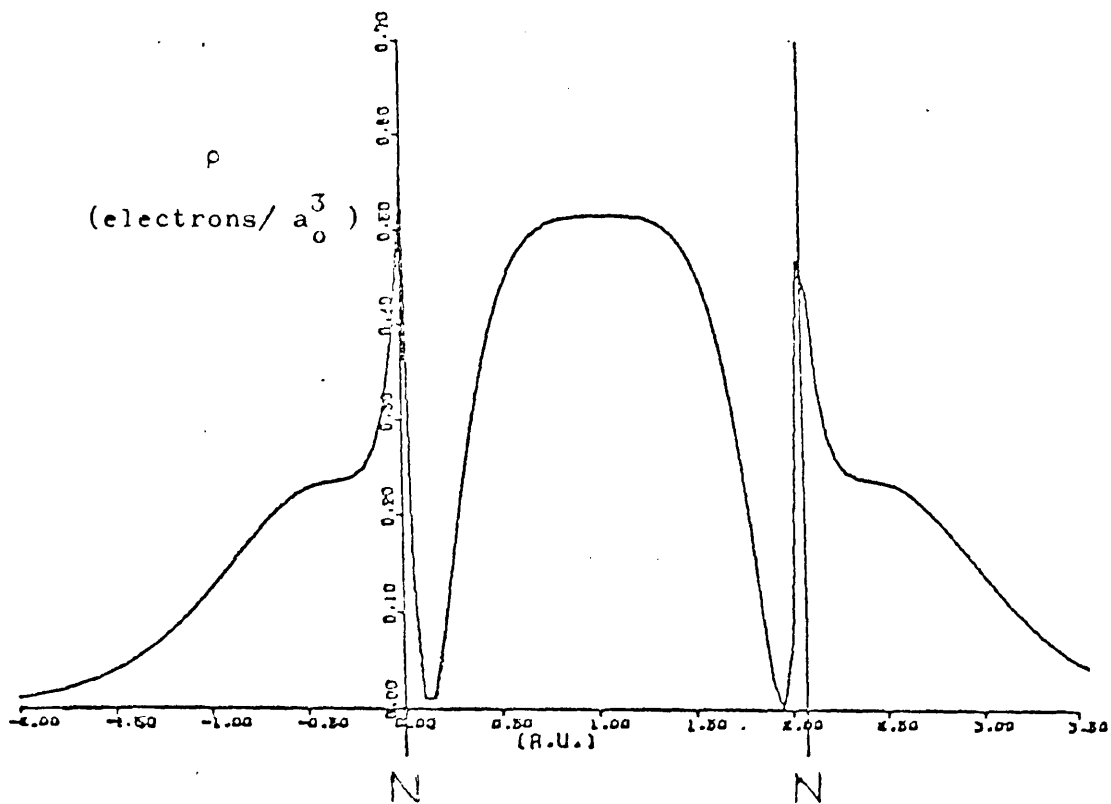


Figure 6.1 Electron Density Distribution along the Inter-nuclear Axis for the l.m.o. describing the  $\sigma$ -bond in  $N_2$ .

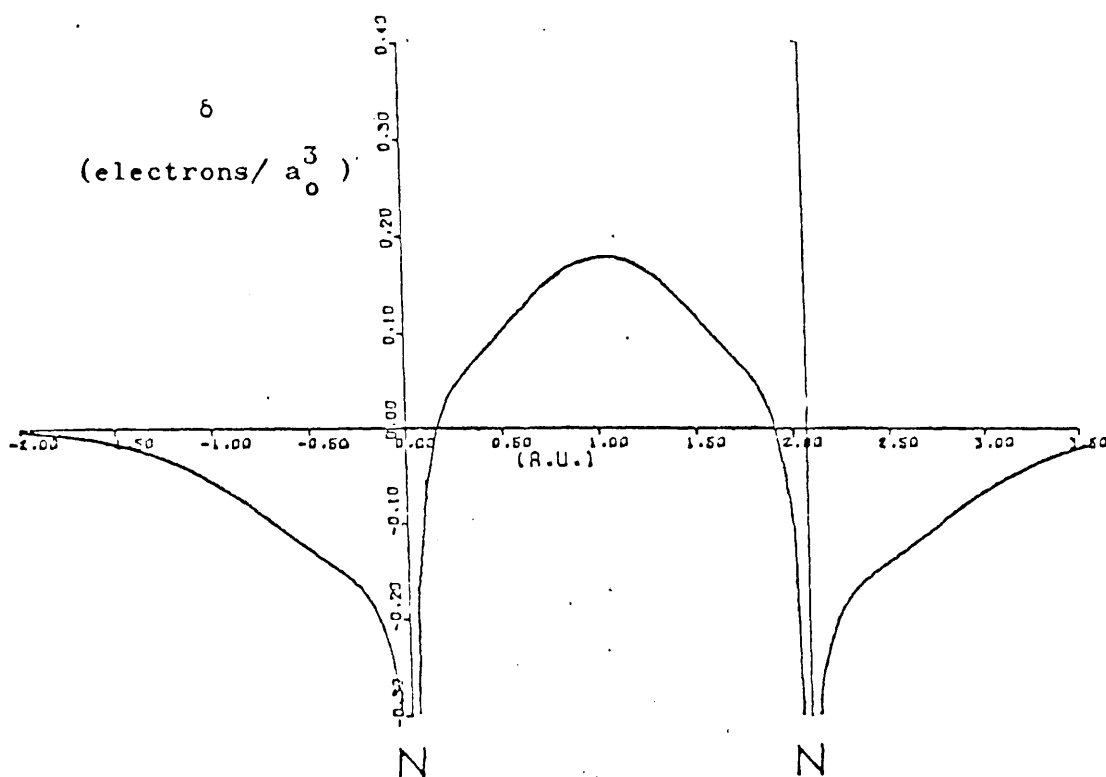


Figure 6.2 Density Difference,  $\delta$ , along the Inter-nuclear Axis for the l.m.o. describing the  $\sigma$ -bond in  $N_2$ .

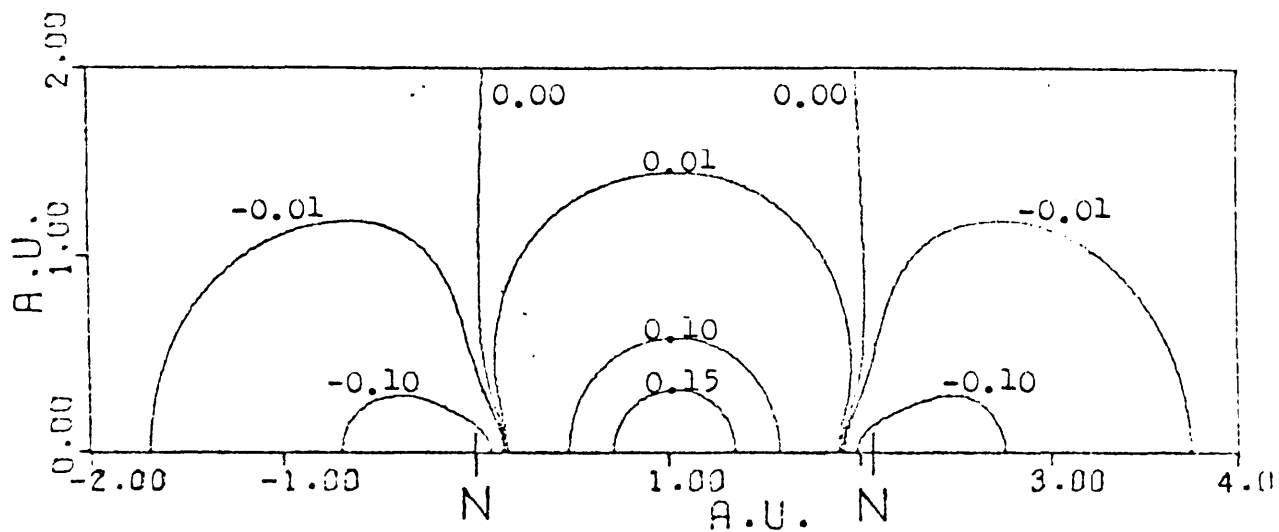


Figure 6.3 Contours of  $b$  (in electrons/ $a_0^3$ ) for the  $\sigma$ -bond in  $N_2$ .

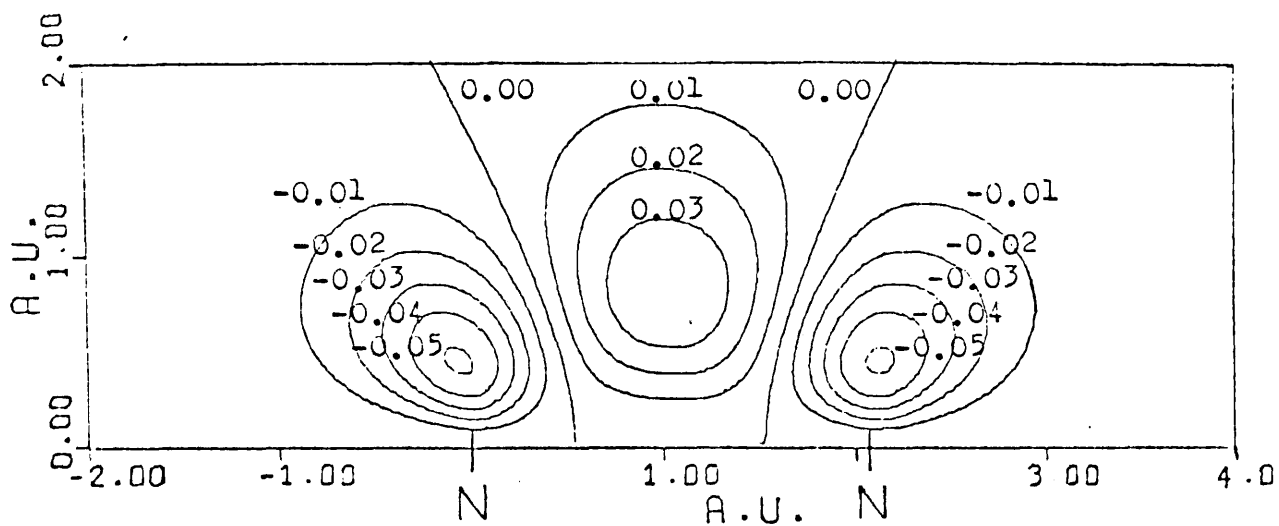


Figure 6.4 Contours of  $b$  (in electrons/ $a_0^3$ ) for the  $\pi$ -bond in  $N_2$ .

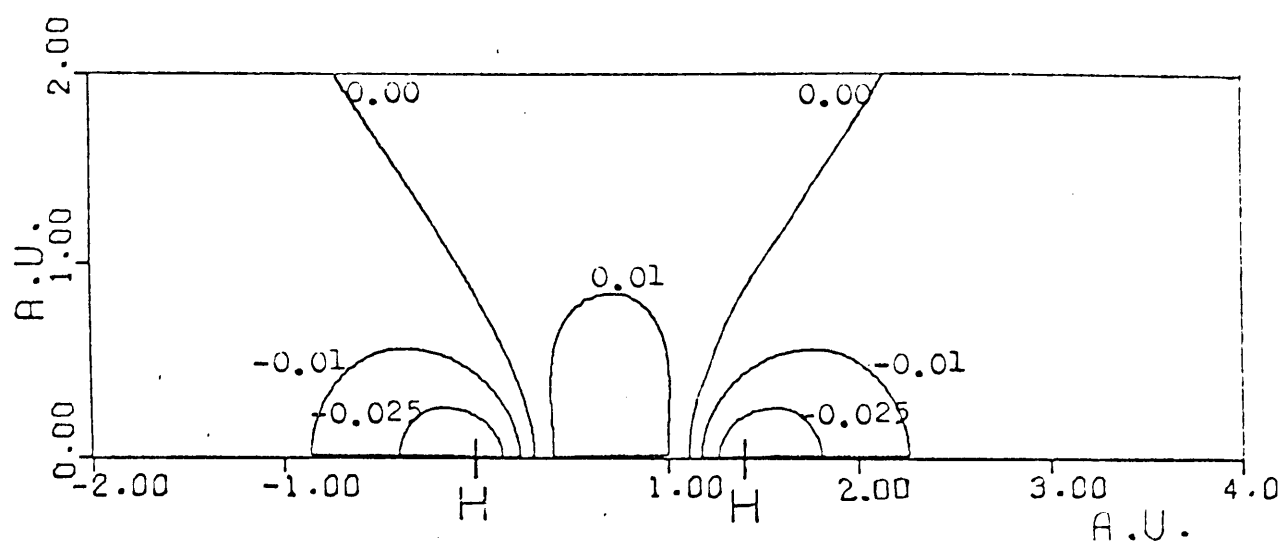


Figure 6.5 Contours of  $\rho$  (in electrons/ $a_0^3$ ) for the  $1\sigma_g$  Molecular Orbital in  $H_2$ .

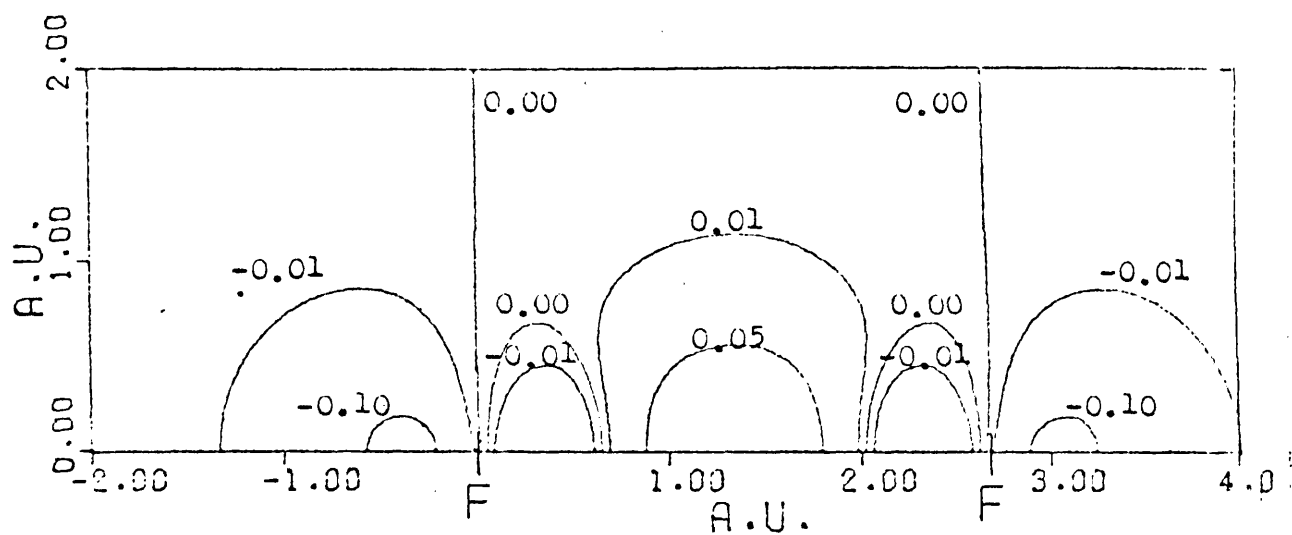


Figure 6.6 Contours of  $\delta$  (in electrons/ $a_0^3$ ) for the  $\sigma$ -bond in  $F_2$ .

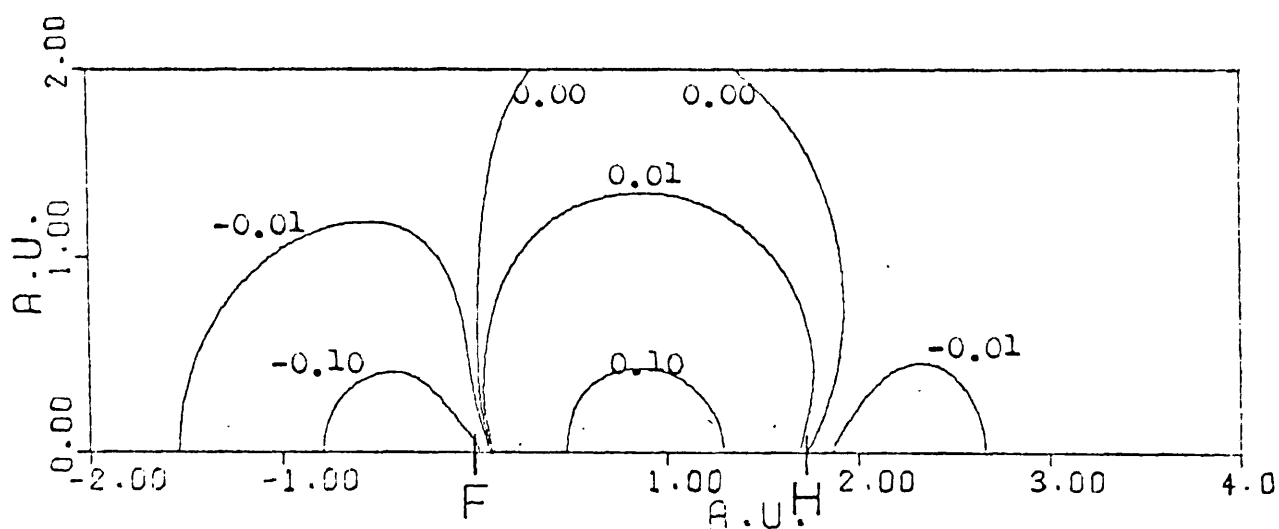


Figure 6.7 Contours of  $\delta$  (in electrons/ $a_0^3$ ) for the  $\sigma$ -bond in HF.

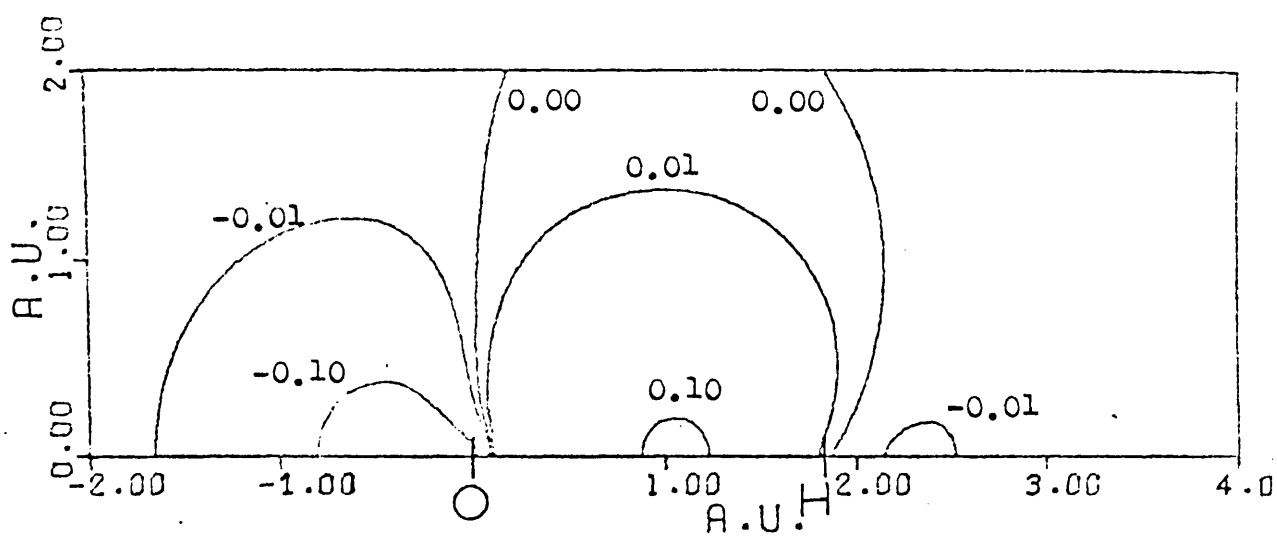


Figure 6.8 Contours of  $\delta$  (in electrons/ $a_0^3$ ) for the  $\sigma$ -bond in OH.

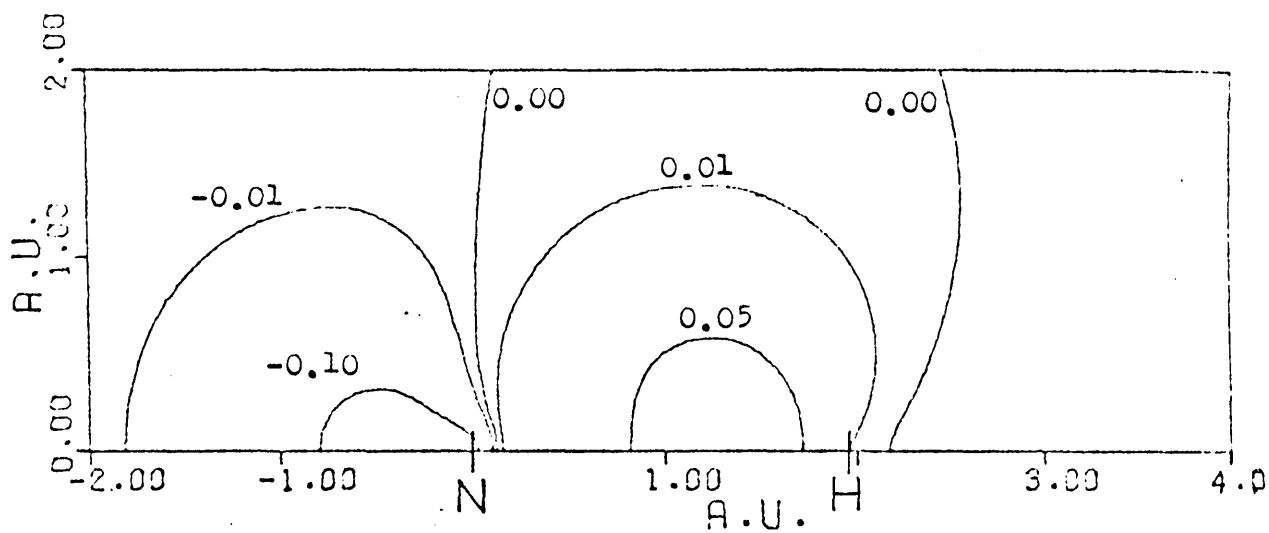


Figure 6.9 Contours of  $\delta$  (in electrons/ $a_0^3$ ) for the  $\sigma$ -bond in NH.

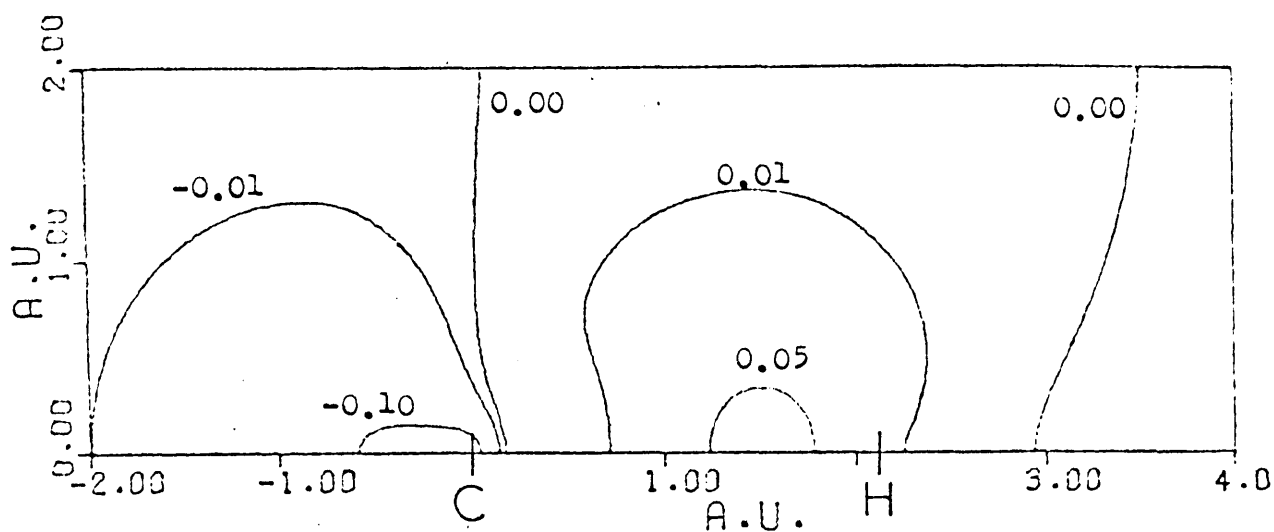


Figure 6.10 Contours of  $\delta$  (in electrons/ $a_0^3$ ) for the  $\sigma$ -bond in CH.

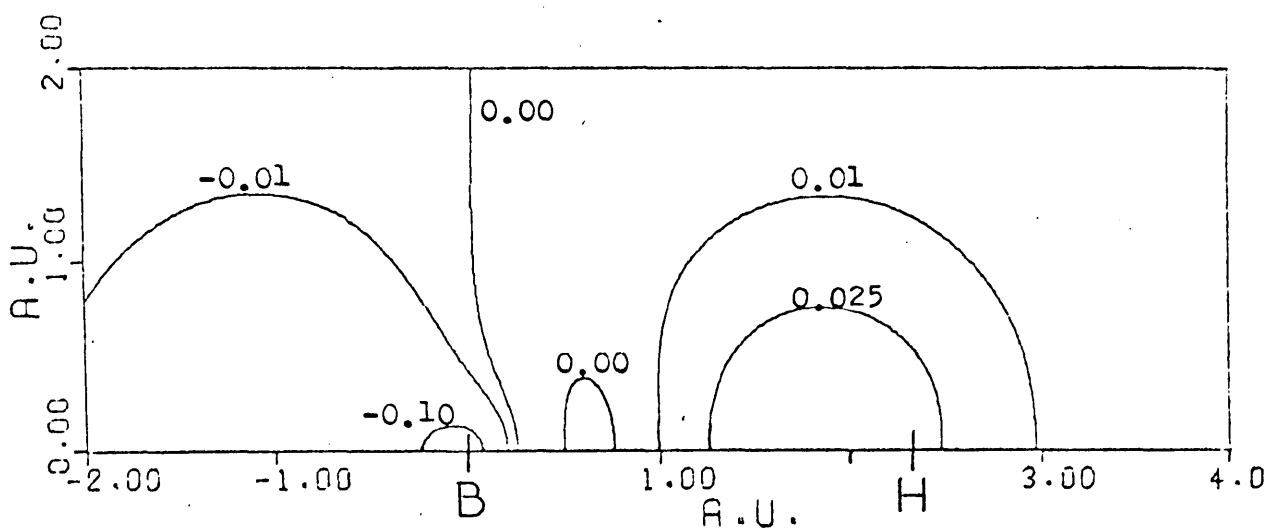


Figure 6.11 Contours of  $\delta$  (in electrons/ $a_0^3$ ) for the  $\sigma$ -bond in BH.

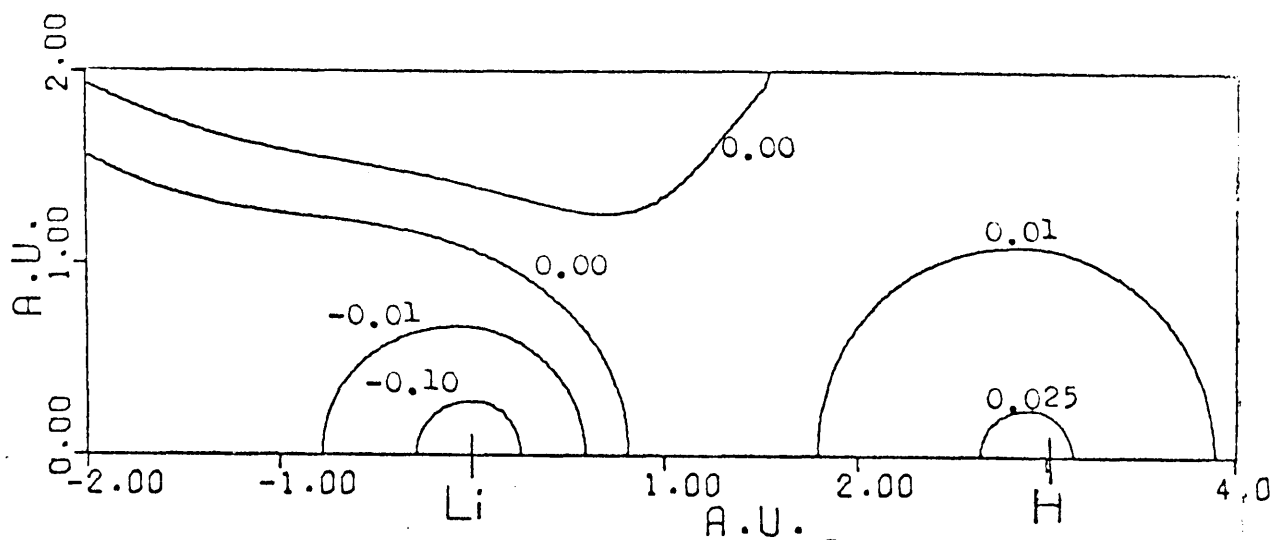


Figure 6.12 Contours of  $\delta$  (in electrons/ $a_0^3$ ) for the  $\sigma$ -bond in LiH.

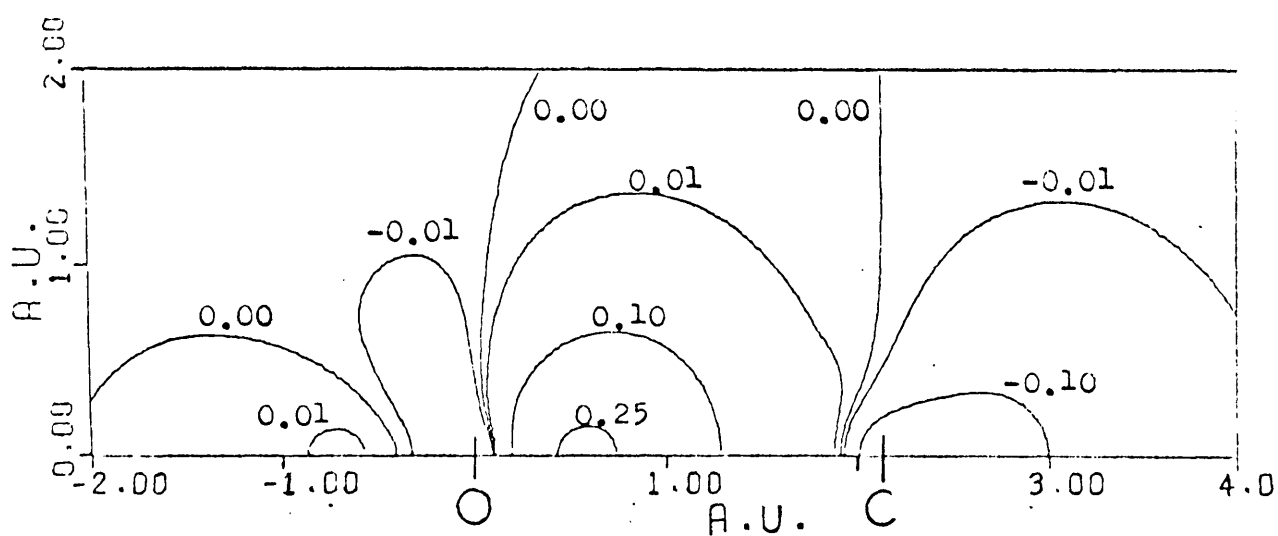


Figure 6.13 Contours of  $\delta$  (in electrons/ $a_0^3$ ) for the  $\sigma$ -bond in CO.

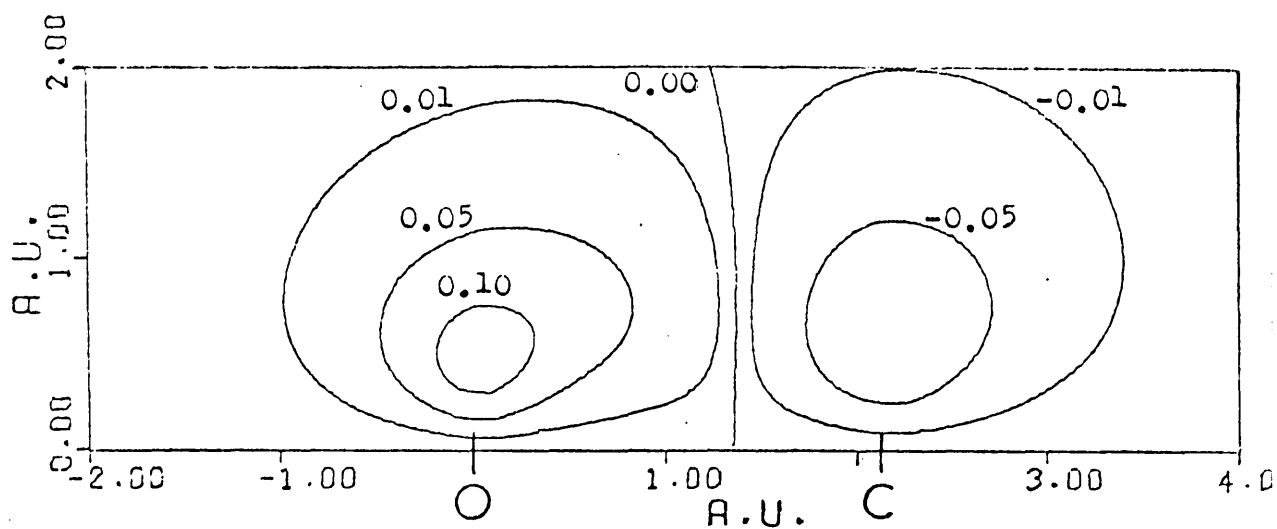


Figure 6.14 Contours of  $\delta$  (in electrons/ $a_0^3$ ) for the  $\pi$ -bond in CO.



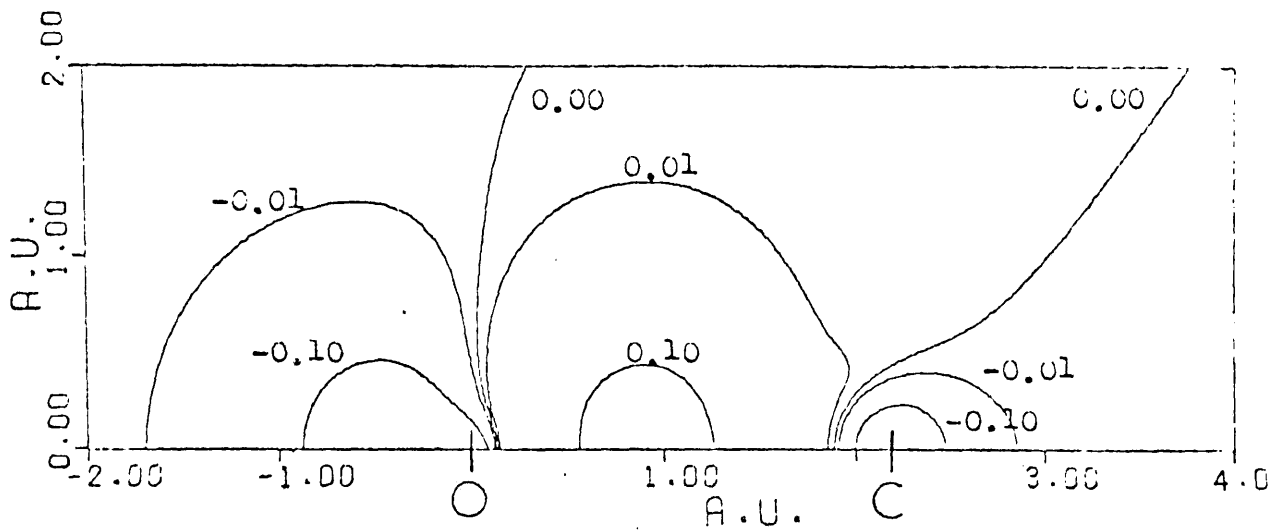


Figure 6.15 Contours of  $\delta$  (in electrons/ $a_0^3$ ) for the C-O  $\sigma$ -bond in  $\text{CO}_2$ .

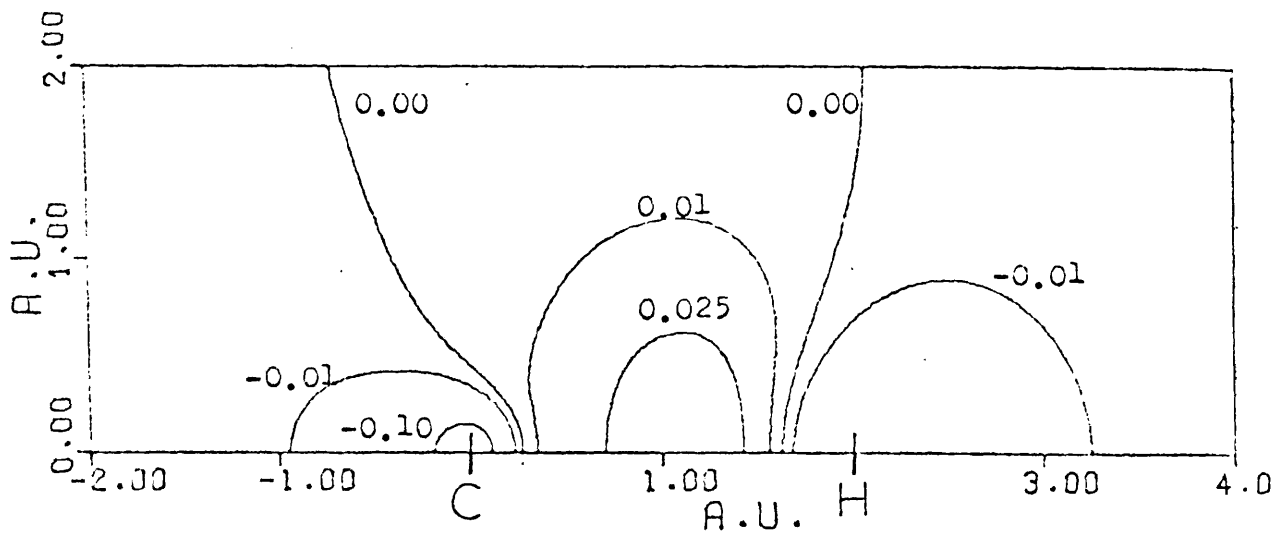


Figure 6.16 Contours of  $\delta$  (in electrons/ $a_0^3$ ) for the C-H  $\sigma$ -bond in HCN.

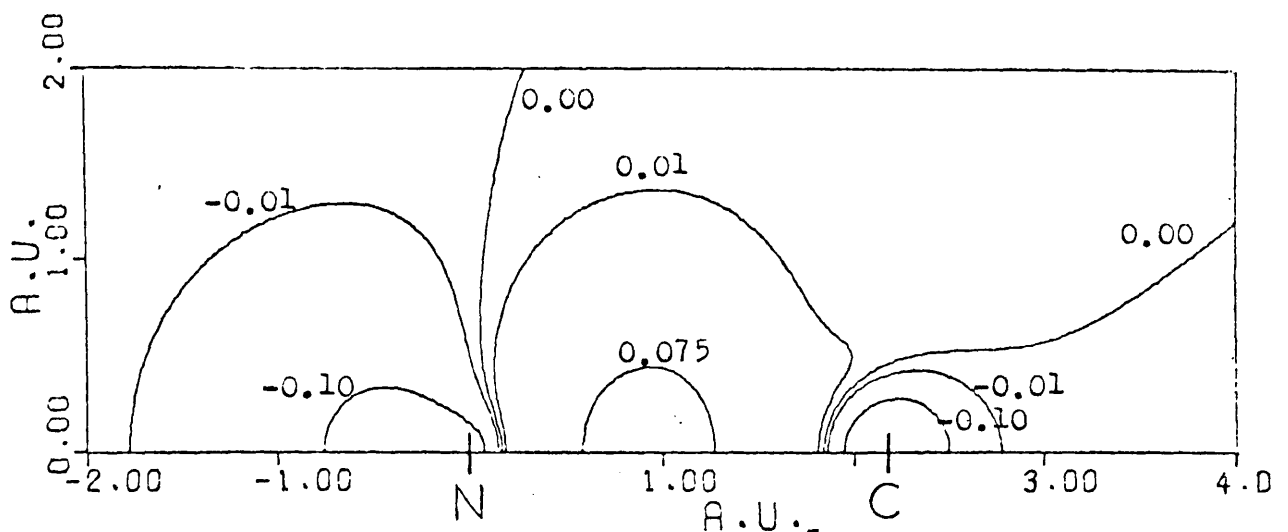


Figure 6.17 Contours of  $\delta$  (in electrons/ $a_0^3$ ) for the C-N  $\sigma$ -bond in HCN.

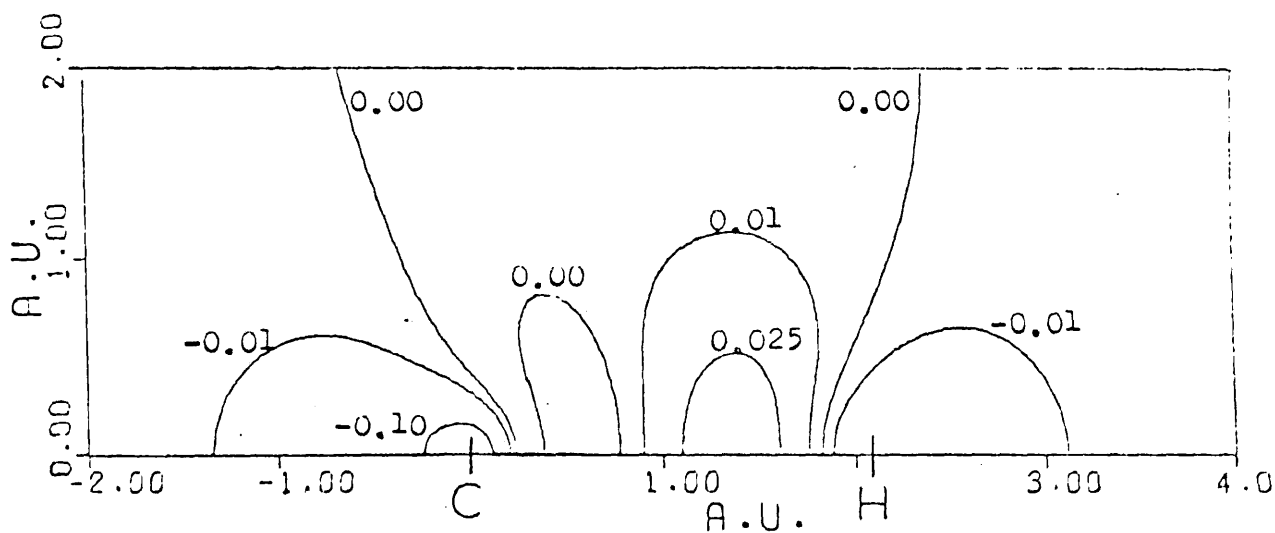


Figure 6.18 Contours of  $\delta$  (in electrons/ $a_0^3$ ) for the C-H  $\sigma$ -bond in  $\text{CH}_4$ .

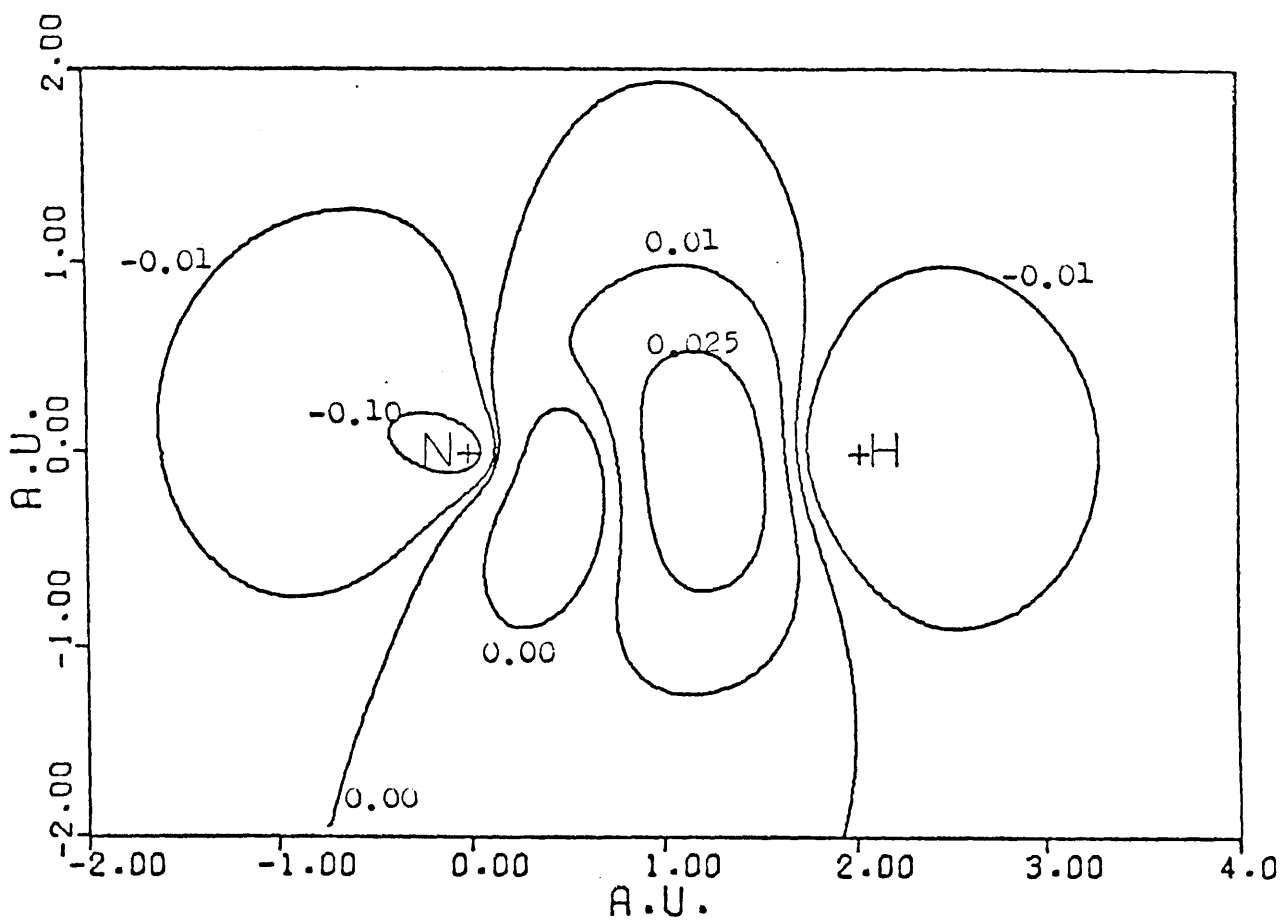


Figure 6.19 Contours of  $\delta$  (in electrons/ $a_0^3$ ) for the N-H  $\sigma$ -bond in  $\text{NH}_3$ . Contours are shown in the  $xz$  plane of the molecule, using the axis system given in reference 120.

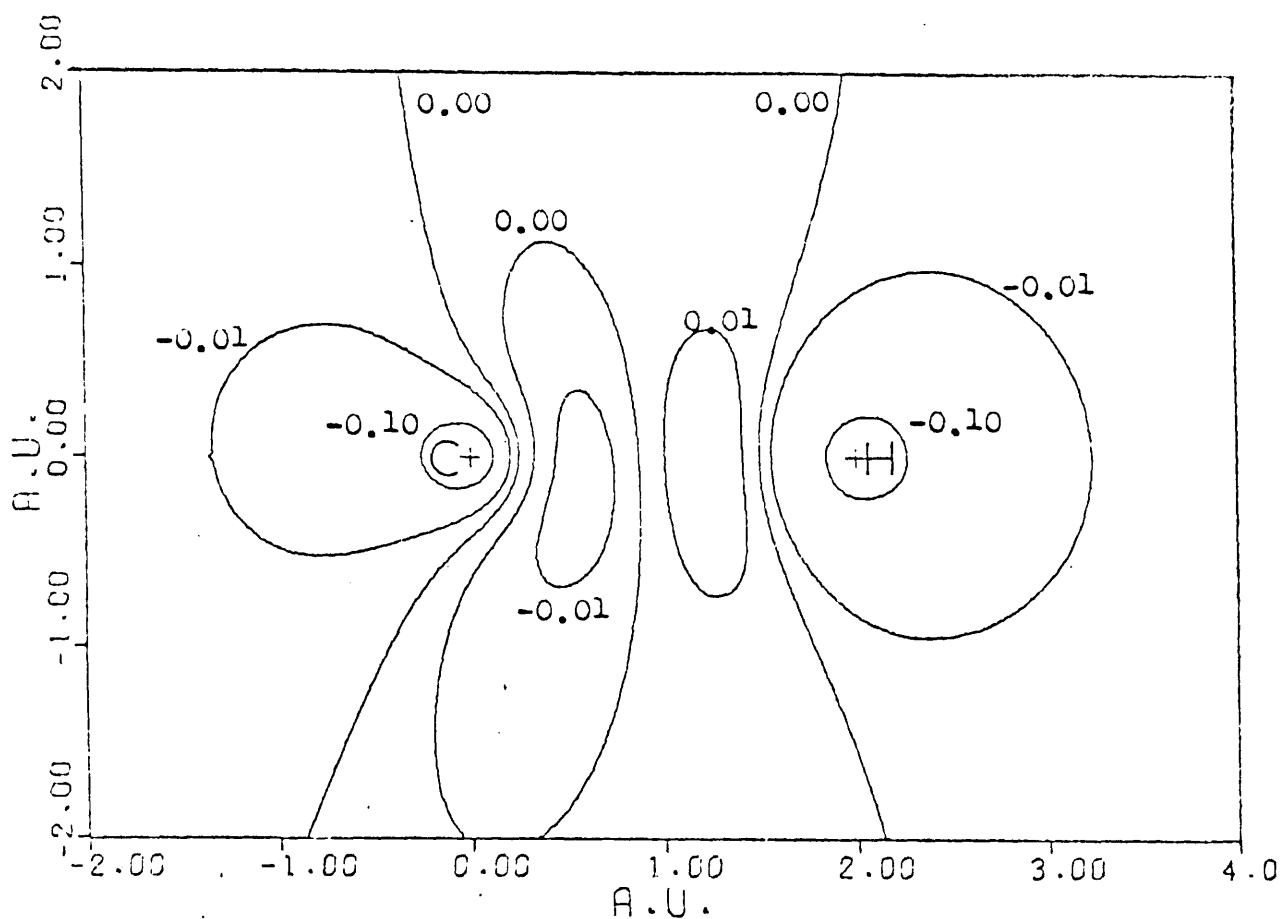


Figure 6.20 Contours of  $\delta$  (in electrons/ $a_0^3$ ) for the C-H  $\sigma$ -bond in  $\text{CH}_2\text{O}$ . Contours are shown in the  $yz$  plane of the molecule, using the axis system given in reference 63.

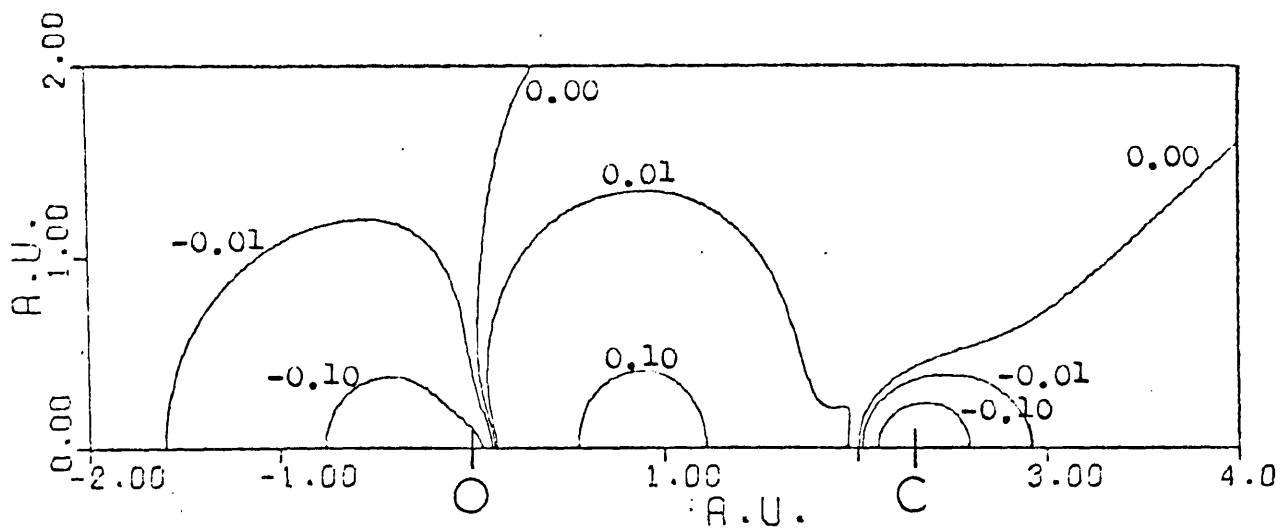


Figure 6.21 Contours of  $\delta$  (in electrons/ $a_0^3$ ) for the C-O  $\sigma$ -bond in  $\text{CH}_2\text{O}$ .

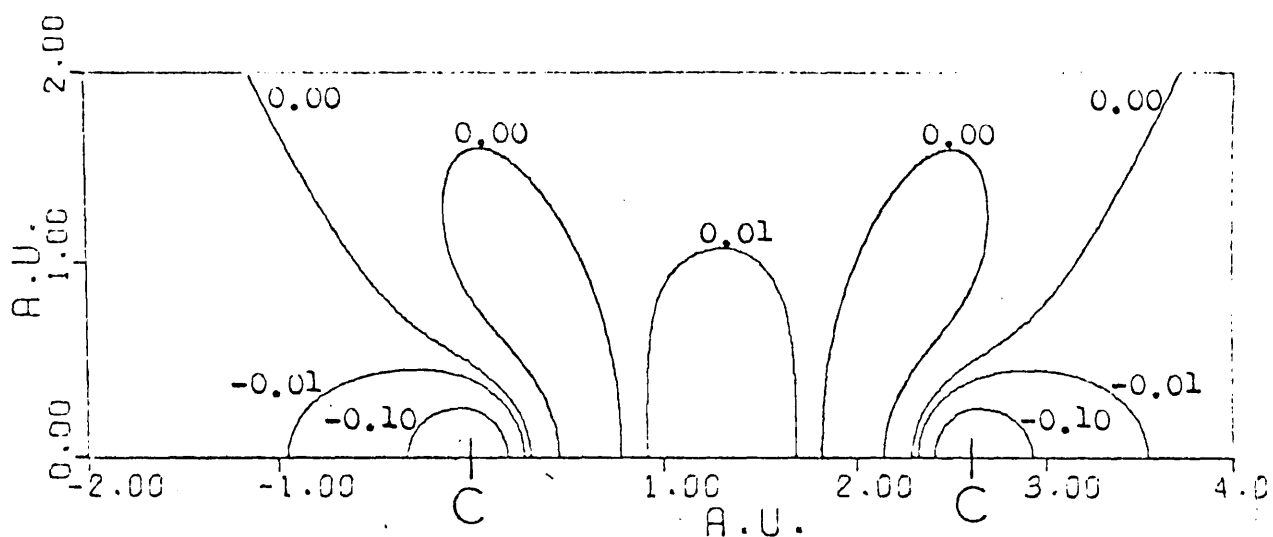


Figure 6.22 Contours of  $\delta$  (in electrons/ $a_0^3$ ) for the C-C  $\sigma$ -bond in  $C_2N_2$ .

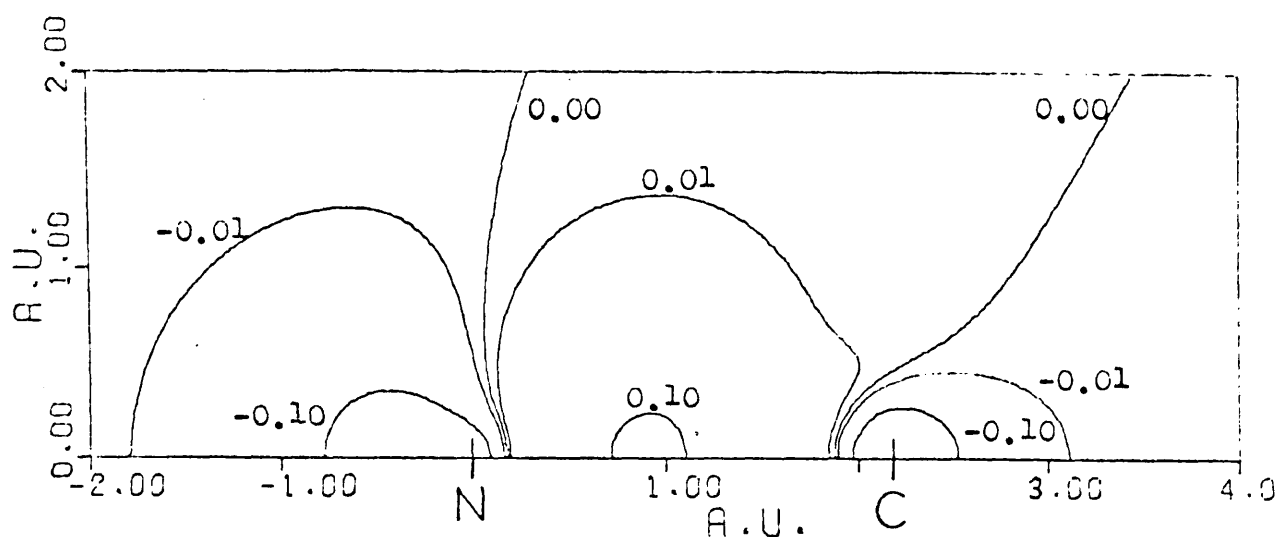


Figure 6.23 Contours of  $\delta$  (in electrons/ $a_0^3$ ) for the C-N  $\sigma$ -bond in  $C_2N_2$ .

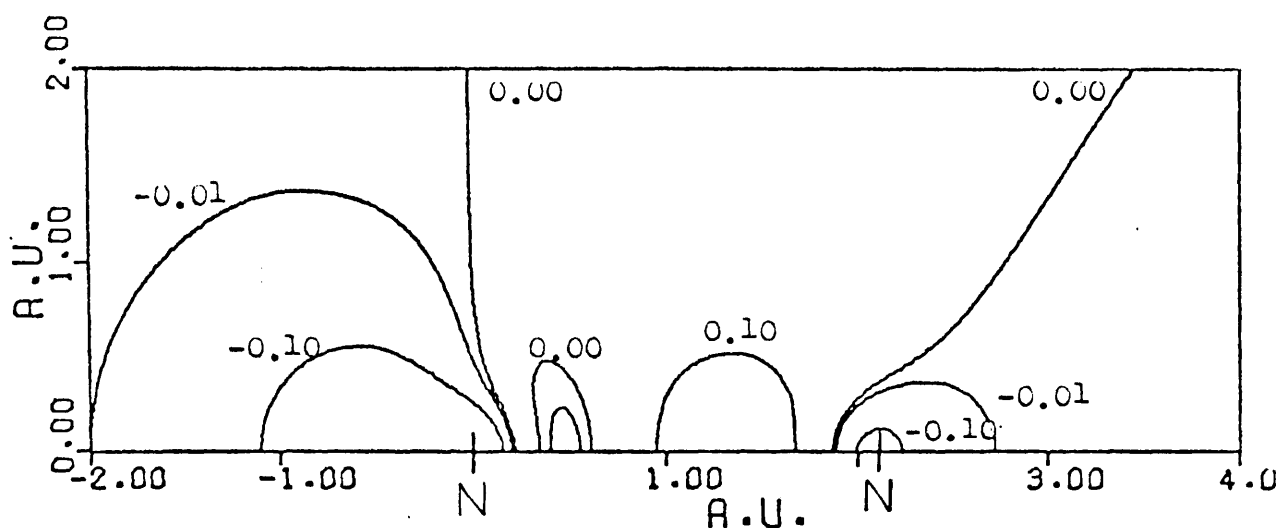


Figure 6.24 Contours of  $\delta$  (in electrons/ $a_0^3$ ) for the N-N  $\sigma$ -bond in  $N_3^-$ .

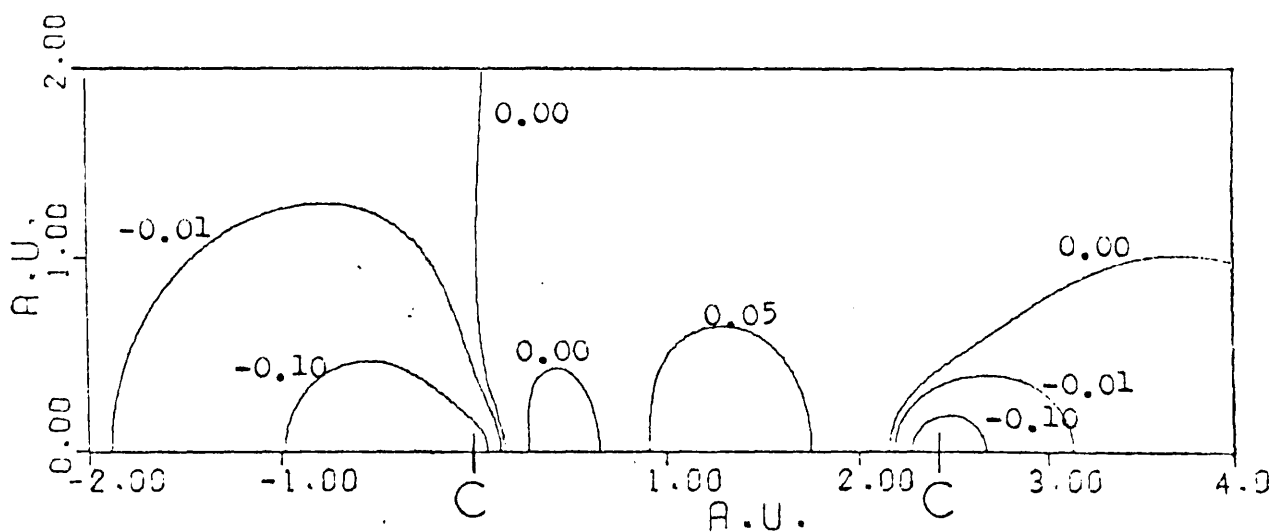


Figure 6.25 Contours of  $\delta$  (in electrons/ $a_0^3$ ) for the C-C  $\sigma$ -bond in  $C_3$ .

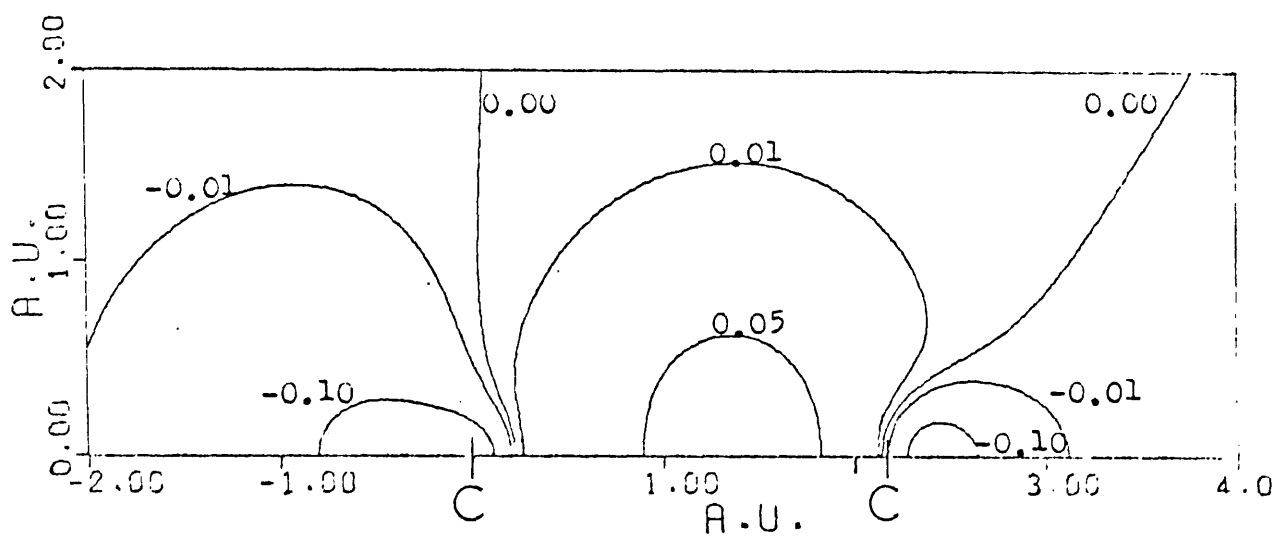


Figure 6.26 Contours of  $\delta$  (in electrons/ $a_0^3$ ) for the  $C_1$ - $C_2$   $\sigma$ -bond in  $C_4$ .

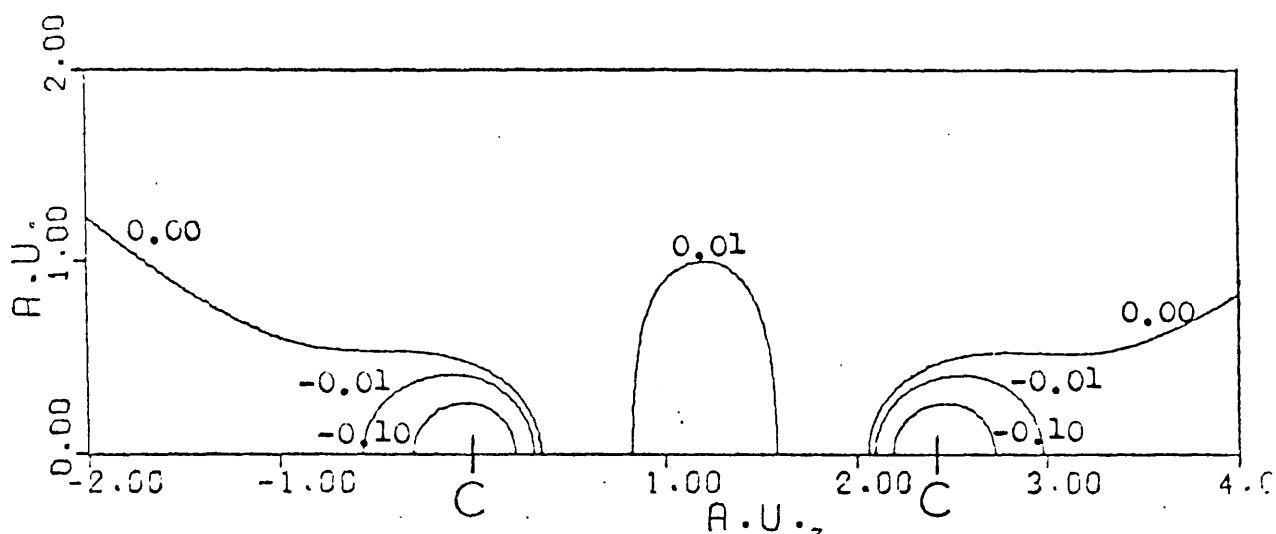


Figure 6.27 Contours of  $\delta$  (in electrons/ $a_0^3$ ) for the  $C_2$ - $C_3$   $\sigma$ -bond in  $C_4$ .

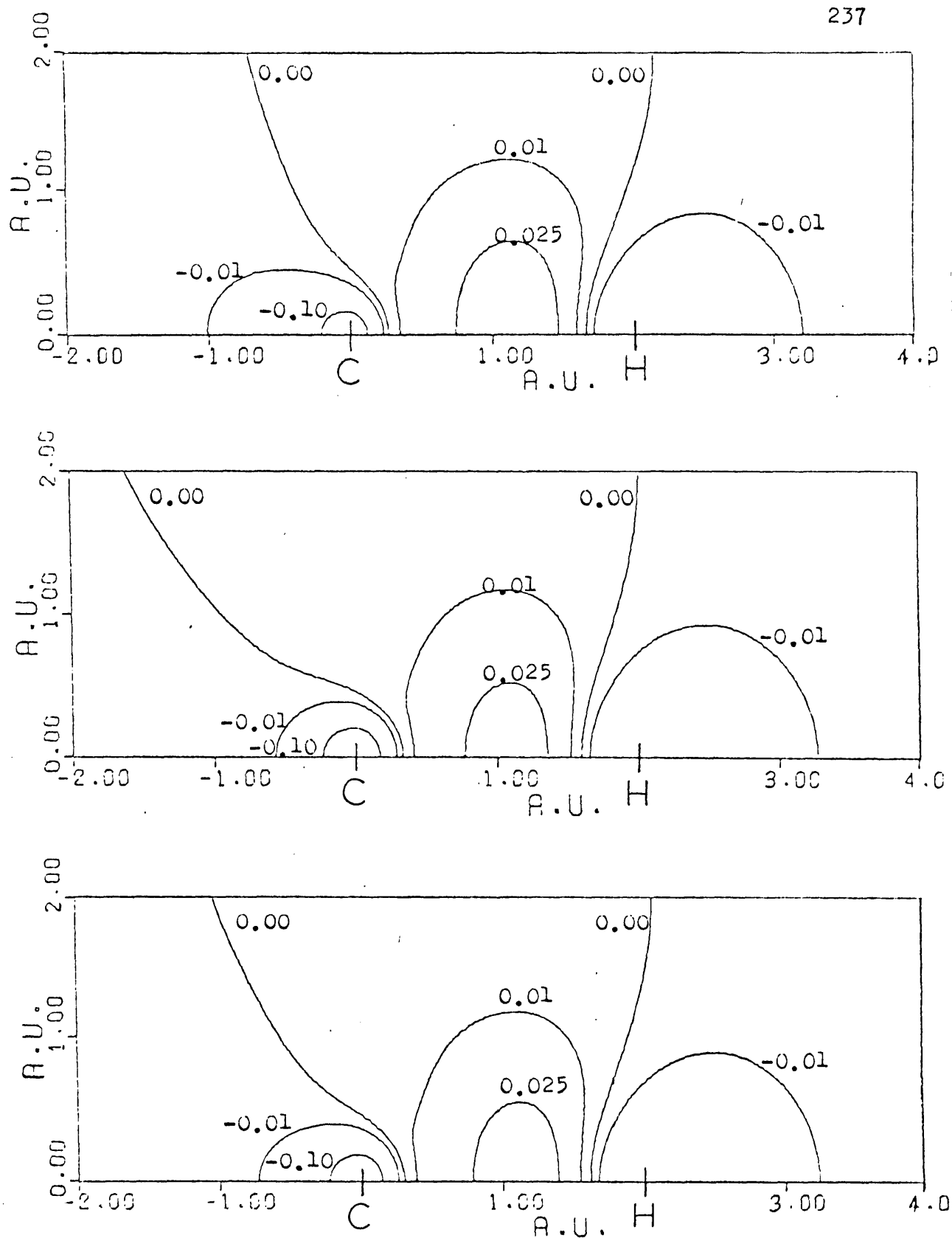


Figure 6.28 Contours of  $\delta$  (in electrons/ $a_0^3$ ) for the C-H  $\sigma$ -bond in  $C_2H_2$ . The three l.m.o.s shown are obtained by different localisation routes.<sup>44</sup>

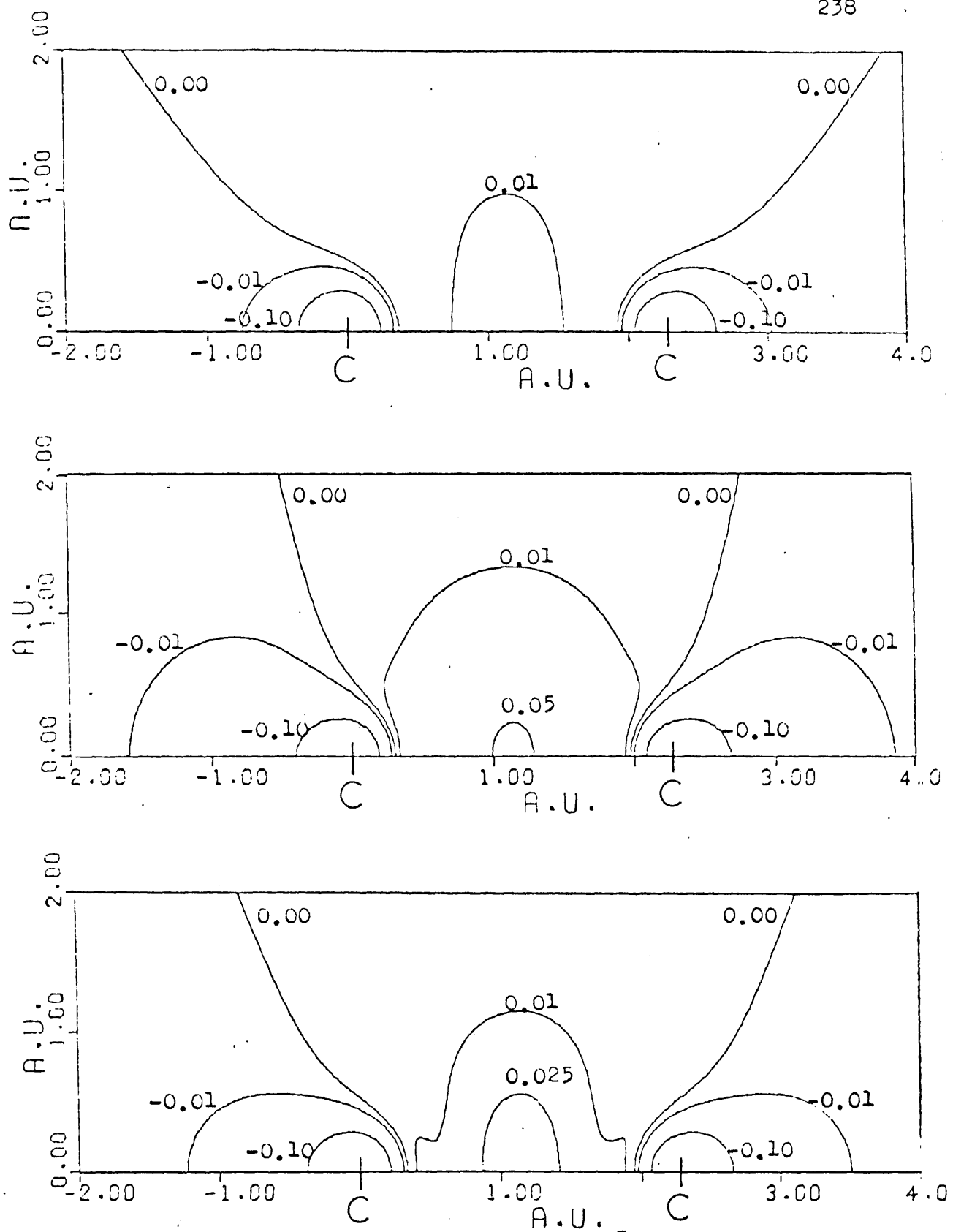


Figure 6.29 Contours of  $\delta$  (in electrons/ $a_0^3$ ) for the C-C  $\sigma$ -bond in  $C_2H_2$ . The three l.m.o.s shown are obtained by different localisation routes.<sup>44</sup>

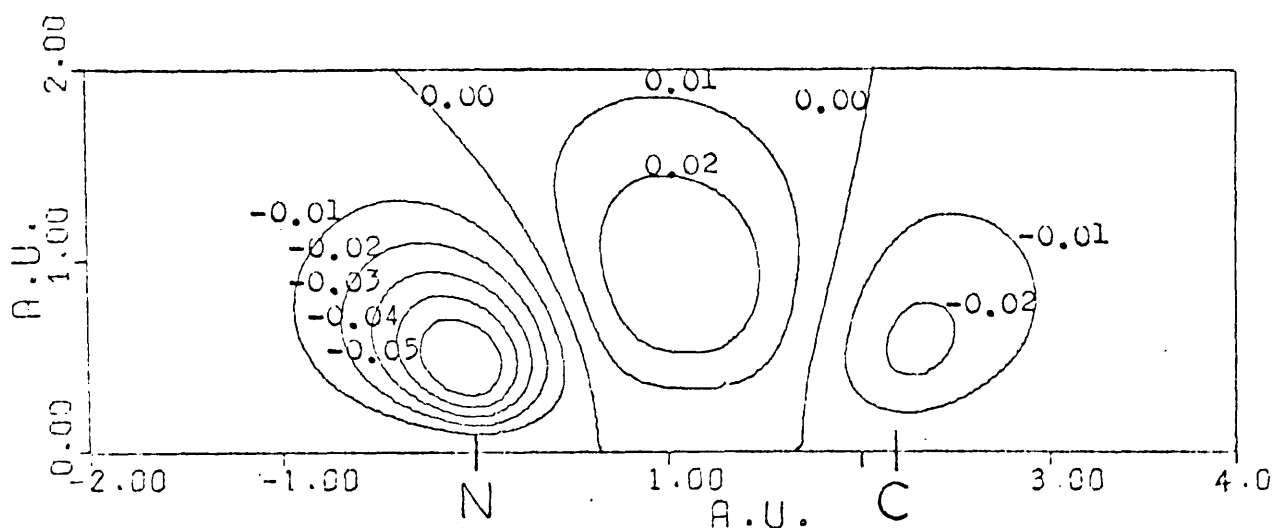


Figure 6.30 Contours of  $\delta$  (in electrons/ $a_0^3$ ) for the  $\pi$ -bond in HCN.

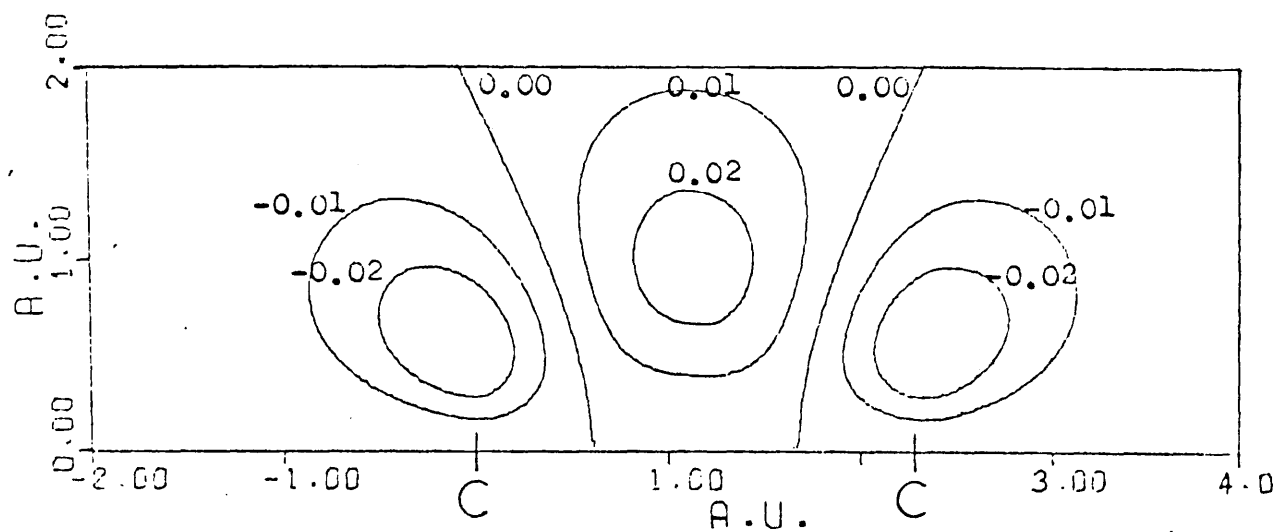


Figure 6.31 Contours of  $\delta$  (in electrons/ $a_0^3$ ) for the  $\pi$ -bond in  $C_2H_2$ .

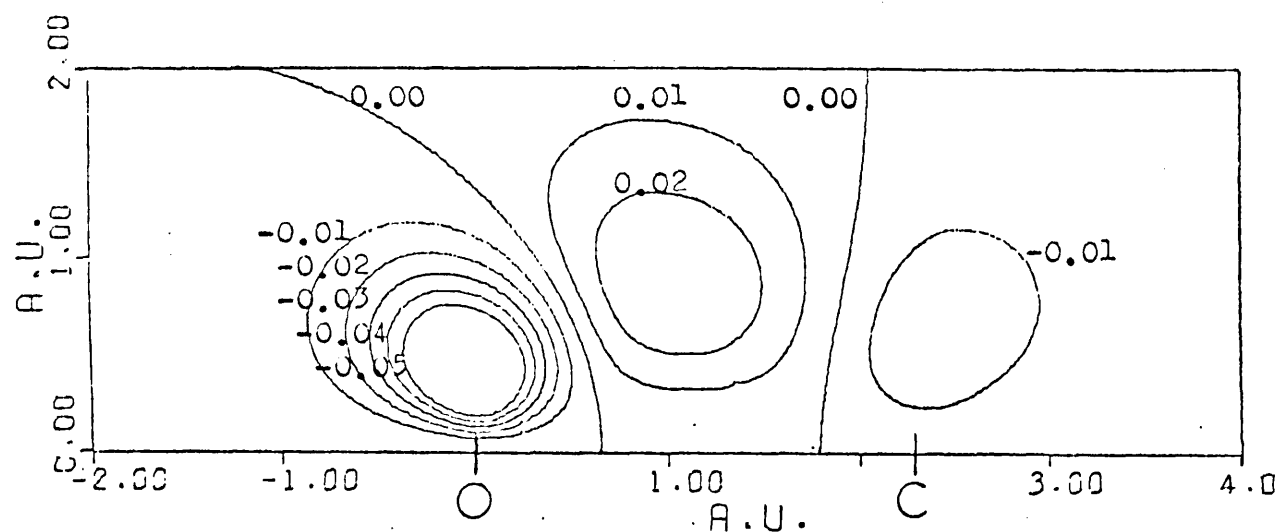


Figure 6.32 Contours of  $\delta$  (in electrons/ $a_0^3$ ) for the  $\pi$ -bond in  $CH_2O$ .



therefore concluded that the polarity effects in these molecules outweigh the build-up of electron density between the two nuclei. On the other hand, the HF sigma-bond, which is usually supposed to be highly polar, might also have been expected to show this effect, but its  $\delta$  contour diagram (Figure 6.7) follows the general conclusion, and a non-polar HF sigma-bond has a  $\delta$  contour diagram much the same as that in Figure 6.7.

To complete the argument, the case of the hypothetical He<sub>2</sub> "molecule" was then examined. A profile of  $\delta$  along the inter-nuclear axis, assuming an inter-nuclear distance of 2.0 a.u. (1.058 Å) is given in Figure 6.33. There is an increase in electron density between the nuclei for the two electrons in the bonding molecular orbital, but a larger decrease in electron density between the nuclei for the two electrons in the anti-bonding molecular orbital, giving an overall decrease in electron density in the inter-nuclear region, on "molecule" formation.

The total charge build-up between the nuclei for all the bonds studied was evaluated according to equation (6.7). A difficulty arises here in defining the inter-nuclear region. The simplest definition would be to take the integration limits a and b in equation (6.7) as the positions of the two nuclei. However,  $\delta$  generally becomes large and negative near the nuclei, a result which is sensitive to the choice of atomic orbitals in equation (6.3), and which may have no physical significance since the absolute value of the electron density is high near the nuclei. This region which is not thought to be primarily concerned with bond formation may be excluded by arbitrarily taking the integration limits at the points where the zero  $\delta$  contour crosses the inter-nuclear axis. The results of both choices of integration limits are given in Table 6.1. Although in some cases negative values of D are obtained when a and b are defined

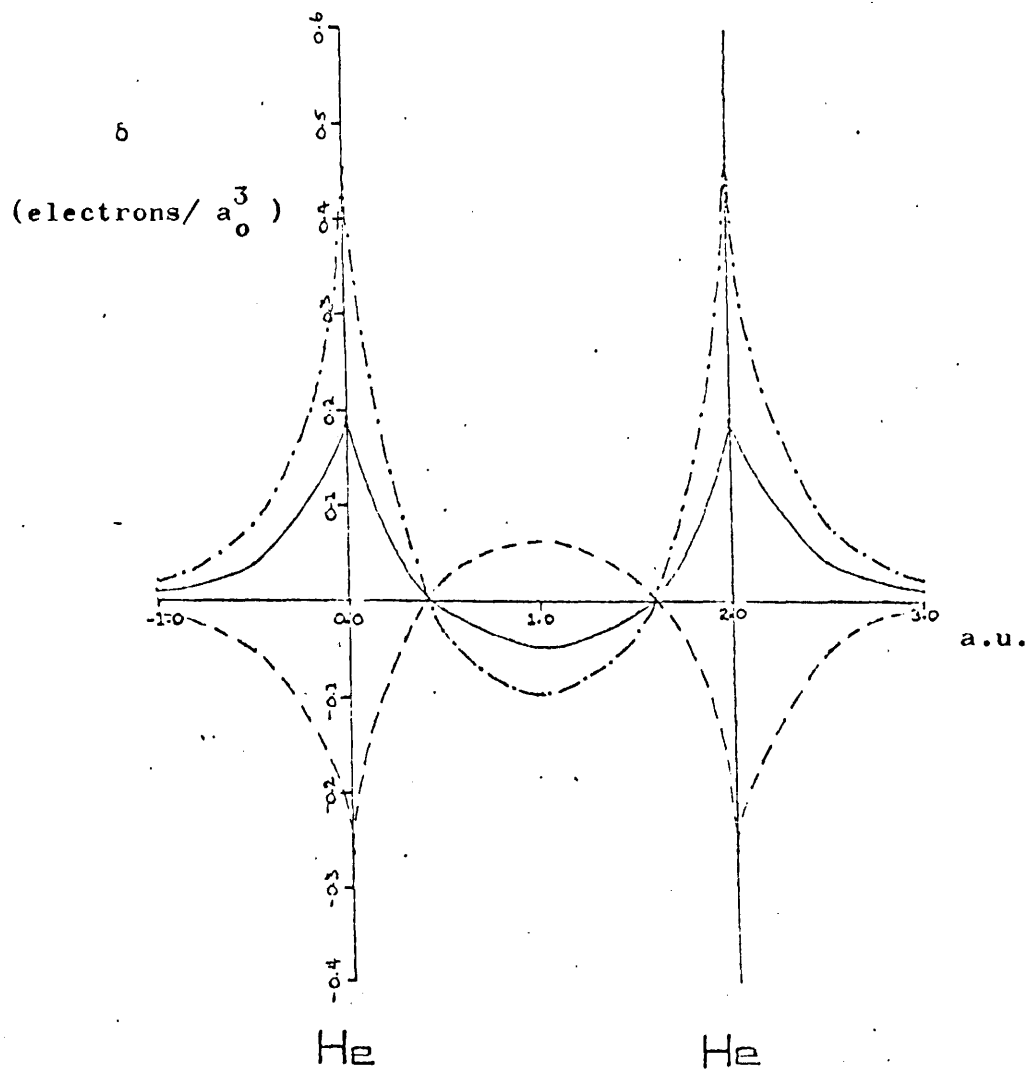


Figure 6.33 Density Difference,  $\delta$ , along the Inter-nuclear Axis for the  $\text{He}_2$  "Molecule".

KEY:

---	$1\sigma_g$
- · - · -	$1\sigma_u$
—	Total $\delta$ ( $1\sigma_g + 1\sigma_u$ )

Table 6.1 Total charge Accumulation, D, in the Internuclear Region.<sup>1</sup>

Molecule	Bond	D( $\xi = 0$ )	D (nuclei)
HF	-	0.67	0.67
OH	-	0.58	0.58
NH	-	-	0.47
CH	-	-	0.38
BH	-	-	0.31
LiH	-	-	0.05
N <sub>2</sub>	$\sigma$	0.92	0.90
	$\pi$	0.23	0.18
F <sub>2</sub>	$\sigma$	0.31	0.31
CO	$\sigma$	0.98	0.95
	$\pi$	-	0.29
CO <sub>2</sub>	$\sigma$	0.68	0.59
C <sub>3</sub>	$\sigma$	0.46	0.42
HCN	C-H	0.22	0.18
	C-N $\sigma$	0.52	0.36
	C-N $\pi$	0.21	0.16
C <sub>2</sub> N <sub>2</sub>	C-C $\sigma$	0.11	-0.08
	C-N $\sigma$	0.57	0.45
C <sub>4</sub>	C <sub>1</sub> -C <sub>2</sub> $\sigma$	0.55	0.51
	C <sub>2</sub> -C <sub>3</sub> $\sigma$	0.11	-0.16
N <sub>3</sub> <sup>-</sup>	N-N $\sigma$	0.71	0.66
CH <sub>4</sub>	C-H	0.16	0.13
CH <sub>2</sub> O	C-O $\sigma$	0.61	0.51
	C-O $\pi$	0.20	0.13
C <sub>2</sub> H <sub>2</sub>	C-H	0.22	0.19
		0.19	0.11
		0.19	0.14
	C-C $\sigma$	0.12	-0.20
		0.34	0.20
		0.20	-0.04
	C-C $\pi$	0.19	0.16

1. The definition of  $D$  is given in equation (6.7). The terms  $D(\xi = 0)$  and  $D(\text{nuclei})$  refer to the limits of integration  $a$  and  $b$  in equation (6.7). The results reported for  $D(\xi = 0)$  were obtained taking  $a$  and  $b$  as the points where the zero contour crosses the inter-nuclear axis, and those reported for  $D(\text{nuclei})$  were obtained taking  $a$  and  $b$  as the positions of the nuclei. The three values shown for the acetylene molecule refer to the three different localisation routes given in reference 44.

as the positions of the nuclei, in general the difference between the two sets of results is not great. The values show an accumulation of electrons between the nuclei of up to one electron out of the pair of electrons forming the bond.

Both the  $\delta$  contour diagrams and the D values were examined to see if there is any connection between them and such experimental and theoretical bond quantities as bond energies, electronegativity differences and overlap populations. Two relationships which may be of significance were found.

The first concerns electronegativity differences. Within certain restricted sets of similar bonds there does seem to be a tendency for  $\delta$  to accumulate progressively over towards the increasingly electronegative atom. This was measured by the distance from the mid-point of the bond of the maximum value of  $\delta$  reached along the inter-nuclear axis. The series FH, OH, NH, CH, BH, LiH (Figures 6.7 to 6.12) shows the progression well. LiH is then seen to be an extreme example of this effect, in which the accumulation of  $\delta$  towards the more electronegative atom has gone so far as to conceal the overlap build up. This may represent a transition away from a covalent bond to an ionic one.<sup>81,112</sup> A similar series is given by the CH bonds of methane, formaldehyde, acetylene and hydrogen cyanide. The polarisation towards the H atom in these two series is shown plotted against the difference in electronegativity of the two atoms forming the bond in Figure 6.34. The above result is interesting in that it connects the theoretical idea of polarity with the observable quantity electron density.

The second relationship found is between bond energies and the total build-up of charge density in the inter-nuclear region as measured by D. Figure 6.35 shows that the D values for the diatomic molecules do show a tendency to be proportional to the bond energy, although this seems to be less so for the polyatomic molecules studied.

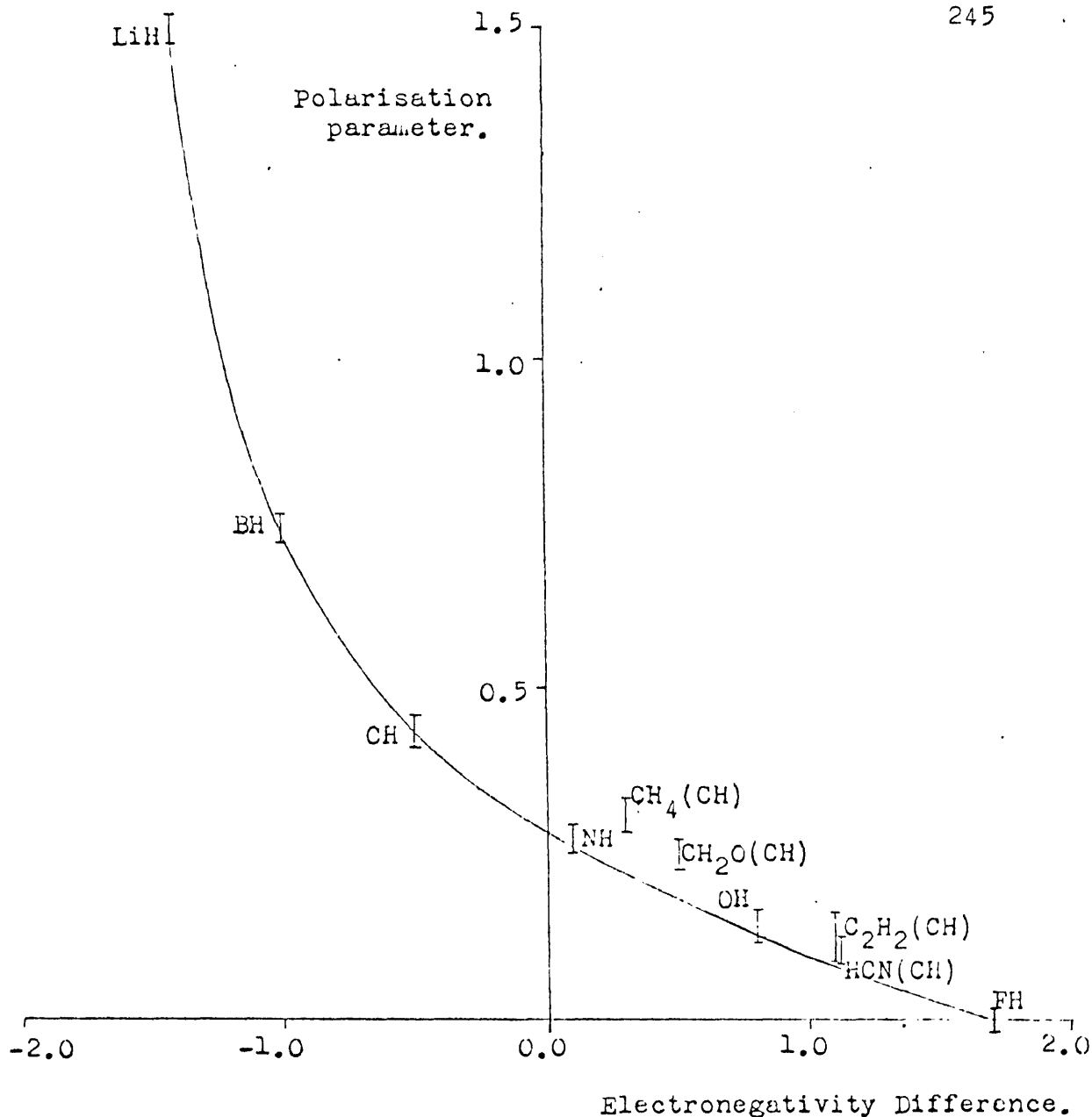


Figure 6.34 Variation of the Polarisation Parameter<sup>1</sup> with Electronegativity Differences.<sup>2</sup>

1. The polarisation parameter is defined as the distance (in a.u.) of the maximum  $\delta$  value from the mid-point of the bond in the direction of the H atom. For polyatomic molecules the bond to which the point refers is shown in brackets.

2. To obtain the electronegativity of atom A,  $X_A$ , the conventional hybridisation was assumed and Pauling's scale given in reference 121 used. The electronegativity difference is then  $(X_A - X_H)$

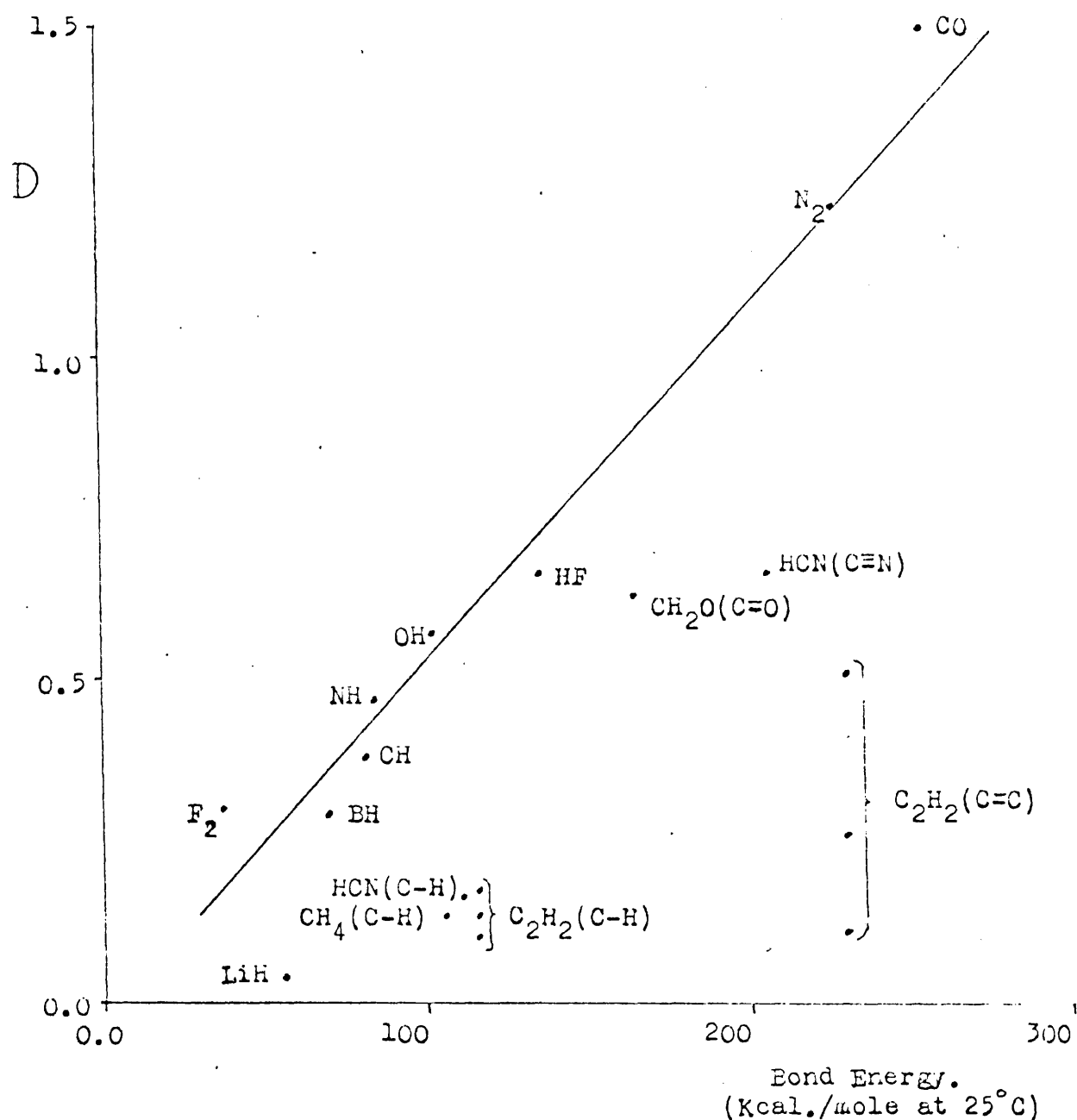


Figure 6.35 Variation of  $D^1$  with Bond Energy.<sup>2</sup>

1.  $D$  is given by equation(6.7), with the limits of integration as the points where the zero  $\delta$  contour crosses the inter-nuclear axis. Where necessary a total  $D$  for a multiple bond is obtained by adding together the  $\sigma$  and  $\pi$  contributions. For polyatomic molecules the bond to which a point refers is shown in brackets.
2. Bond Energies were obtained from references 9 and 110.

### Section 3    Discussion

The conclusion drawn from the  $\delta$  contour diagrams in Figures 6.3 to 6.32 is that the build-up of electron density in the inter-nuclear region and decrease of electron density outside that region on bond formation shown by the  $H_2$  molecule is, in general, shown by all l.m.o.s. Examination of the electron density distribution of individual l.m.o.s therefore gives a clearer physical picture of bond formation than the electron density distribution of the whole molecule which has been studied by many workers.<sup>74-82</sup>

The qualitative meaning of the term "inter-nuclear region" is clear, but it is difficult to define rigorously. The definition used in this work, in equation (6.7) is a simple and arbitrary one, used for the comparison of increases in electron density between the nuclei in different bonds. The "binding region", defined by Berlin<sup>113</sup> through the forces exerted on the nuclei, is often used for the examination of electron density distributions.<sup>76, 114</sup>

The explanation for accumulation of electron density in this region often given is that it is a region of low potential energy.<sup>115</sup> However, the role of the kinetic energy has been discussed by many workers.<sup>116-118</sup> Ruedenberg and co-workers have given a detailed analysis of the binding of the  $H_2^+$  molecule.<sup>118</sup> Their findings confirm that the actual process of the overlap of atomic orbitals to form a covalent bond is accompanied by a build-up of electron density between the nuclei, and they find that the accompanying decrease in total energy results from an increase in potential energy and a decrease in kinetic energy. Contraction of the wavefunction then lowers the potential energy and raises the kinetic energy.



The l.m.o.s used in the present work are obtained from molecular orbital wavefunctions which are not of as high a quality as those given by present day small molecule calculations. The question therefore arises of whether the results obtained are due to inaccuracies in the molecular orbitals. Comparisons of wavefunction quality and density functions have been given in the literature.<sup>74</sup> The accurate James-Coolidge wavefunction for the H<sub>2</sub> molecule<sup>119</sup> gives the same qualitative result as the simple molecular orbital wavefunction but gives larger numerical values for  $\delta$ .<sup>72</sup> It is therefore to be hoped that the present  $\delta$  contour diagrams are qualitatively the same as those which would be obtained with l.m.o.s from more accurate calculations.

The l.m.o.s examined in the present work are also not unique since no formal localisation criterion was used in their localisation.  $\delta$  contour diagrams for the CH and CC bonds in acetylene obtained by the three localisation routes given in reference 44 are shown in Figures 6.28 and 6.29. The three diagrams are very similar in both cases although they vary slightly in the numerical values of D and the maximum  $\delta$  value, indicating that  $\delta$  is not too sensitive to the localisation route. However, no examination was undertaken in this work of l.m.o.s obtained by other localising criteria.

CHAPTER SEVEN  
COMPUTATIONAL DETAILS

## Section 1 L.m.o. and c.m.o. Calculations

All computer programs employed in the work described in the previous chapters were written in FORTRAN IV and were used on the University of London CDC 6600 and CDC 7600 computers.

### (a) L.m.o. calculations

The program FORM was written to carry out l.m.o. calculations for the formaldehyde molecule according to the method described in Chapter Two. A general version of the program was stored on a disc file, with a copy on magnetic tape. Modifications to the general program were then made according to the method of orthogonalisation used and the stage of approximation as discussed in Chapter Three.

The main outline of the program is shown by the flow-diagram in Figure 7.1. The atomic orbital coefficients of the starting-point functions (equations (2.24) and (2.25)) were read in from punched cards. The various integrals over atomic orbitals needed for the evaluation of the  $\underline{F}$  matrix (equation (3.22)) were stored on a disc file, with a copy on magnetic tape. The overlap integrals and kinetic energy integrals were stored by the program in two 12 x 12 arrays and the nuclear attraction integrals in a 12 x 12 x 4 array. The electron repulsion and exchange attraction integrals were stored in a 1-dimensional array, the position of the integral

$$\langle \chi_i \chi_j | \chi_k \chi_l \rangle \quad (7.1)$$

being given by

$$1 + (i - 1 + 12(j - 1 + 12(k - 1 + 12(l - 1)))) \quad (7.2)$$

The total number of electron repulsion and exchange attraction integrals is  $12^4 = 20,736$ . However, for a given value of  $i, j, k$  and  $l$ , integrals which differ by exchanging the indices  $i$  and  $j$ , or  $k$  and  $l$ , or by

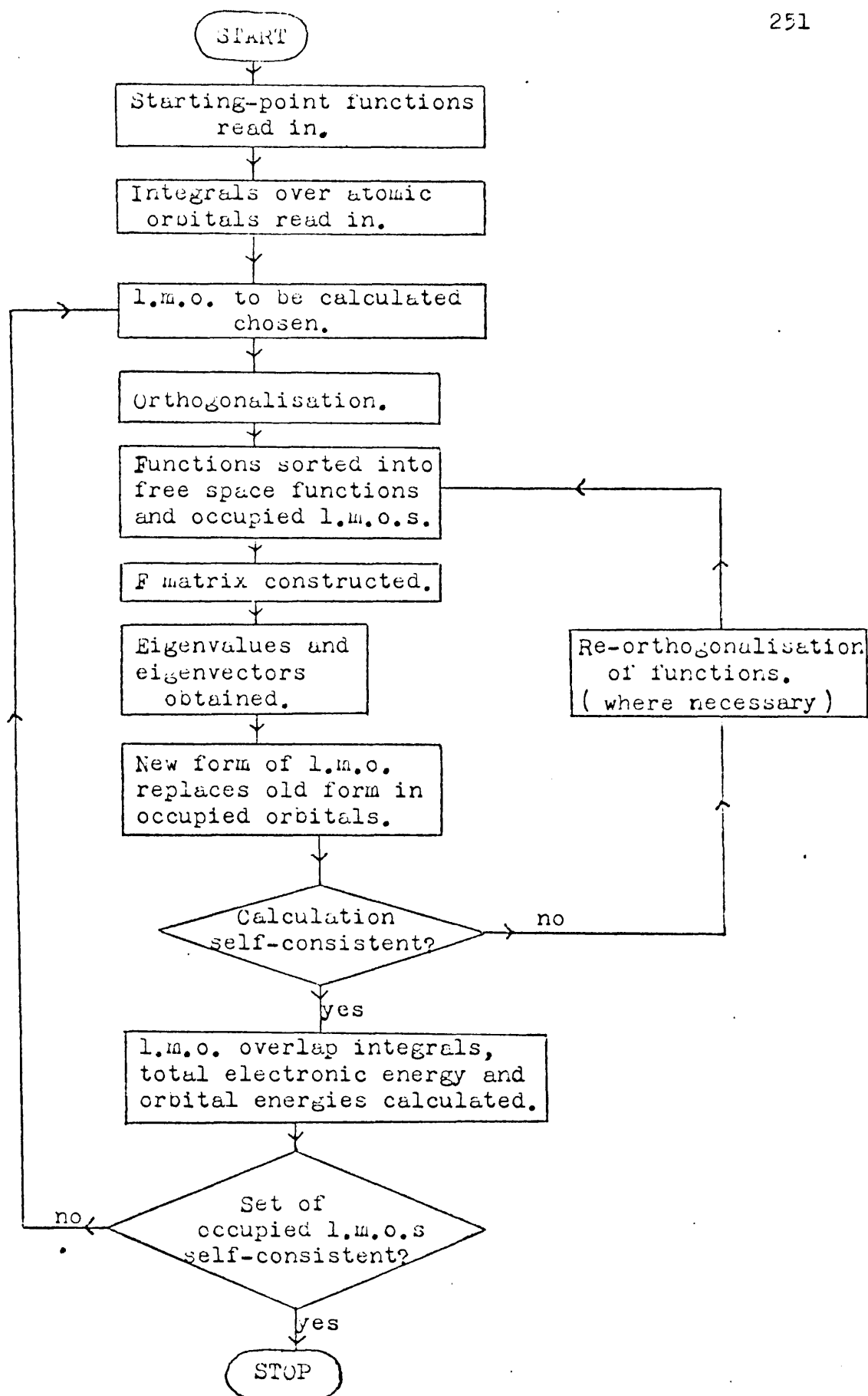


Figure 7.1 Flow-diagram for l.m.o. Calculations.

exchanging the pair  $i$  and  $j$  with the pair  $k$  and  $l$  have the same value. Only integrals with the indices in canonical order were therefore stored on the disc file. In this case the index with the larger value occurs first within the pairs  $i, j$  and  $k, l$  and the pair containing the index with the largest value occurs before the other pair. Of these integrals all except 1,499 are zero to 6 decimal places. Only non-zero integrals were stored on the disc file and their values were read into the program together with the corresponding values of  $i, j, k$  and  $l$ . At stages 1 and 2 only the one- and two-centre electron repulsion and exchange attraction integrals are used. These integrals were therefore sorted into various groups containing one-, two-, three- and four-centre integrals and stored on the disc file in these groups.

Having read in the necessary data, the program FORM carries out a calculation of an l.m.o. First the orthogonality conditions are satisfied, as described in Chapter Three, and then the  $\underline{\underline{F}}$  matrix is constructed, the size of the  $\underline{\underline{F}}$  matrix depending on the stage of approximation. As the free space basis functions are mutually orthogonal, the elements of the  $\underline{\underline{S}}$  matrix (equation (2.32)) are given by

$$S_{pq} = \delta_{pq} \quad (7.3)$$

so that the secular determinant (equation (2.33)) has elements

$$F_{pq} = \epsilon \delta_{pq} \quad (7.4)$$

The eigenvalues and eigenvectors of this matrix are calculated by the subroutine EIGEN in the University of London Computing Centre Scientific Subroutine Package. This subroutine uses the diagonalisation method originated by Jacobi and adapted by von Neumann for large computers.<sup>122</sup> For a rigorous final stage calculation of formaldehyde five eigenvalues are obtained and for earlier stages two eigenvalues are obtained. The lowest and only negative value is taken as that associated with the improved form of the l.m.o. being calculated,  $\epsilon_i$ .

The eigenvectors obtained,  $C_{qp}$ , refer to the free space basis functions and define a new set of functions  $U'_1 \dots U'_5$

$$u'_p = \sum_{q=1}^5 u_q C_{qp} \quad p = 1 \dots 5 \quad (7.5)$$

which may be expressed in terms of atomic orbitals by substitution of equation (2.25)

$$u'_p = \sum_{q=1}^5 \sum_{m=1}^{12} \chi_m k_{mq} C_{qp} \quad p = 1 \dots 5 \quad (7.6)$$

The function which is associated with the lowest eigenvalue,  $\epsilon_i$ , corresponds to the improved form of the l.m.o. being calculated,  $\phi_i$ . As in equation (2.27)

$$\phi_i = \sum_{q=1}^5 u_q C_{qi} \quad (2.27)$$

This form for  $\phi_i$  replaces the previous form in the occupied orbitals. The other four functions define new forms for the virtual orbitals.

In the majority of cases in the present work each l.m.o. is calculated separately. A new  $\underline{F}$  matrix is constructed from the new set of occupied and virtual orbitals, after re-orthogonalisation of the functions where this is necessary. New eigenvalues and eigenvectors are found and the process repeated until the value of the lowest eigenvalue agrees with that obtained from the previous cycle of the calculation to within 0.0001 a.u.

When self-consistency within the calculation of an l.m.o. is reached the program FORM calculates properties of the new set of occupied l.m.o.s. Firstly, the 8x8 overlap integral matrix of all the occupied orbitals is evaluated, as these orbitals are in general not mutually orthogonal. Secondly, the total electronic energy is computed. As this quantity is invariant to a linear transformation amongst the occupied orbitals,<sup>1</sup>

a set of non-orthogonal occupied l.m.o.s may be subjected to an orthogonalisation procedure and then used in the expression for the total electronic energy of an orthogonal set of orbitals.

$$E = 2 \sum_j \langle \phi_j | h | \phi_j \rangle + \sum_j \sum_k \left\{ 2 \langle \phi_j | \phi_j | \phi_k | \phi_k \rangle - \langle \phi_j | \phi_k | \phi_j | \phi_k \rangle \right\} \quad (7.7)$$

$$\text{where } h = -\frac{1}{2} \nabla^2 - \sum_{a=1}^4 \frac{Z_a}{r_a} \quad (7.8)$$

The program FORM uses Schmidt orthogonalisation in the sequence  $\phi_1 \dots \phi_8$ .

Thirdly, the orbital energies of all eight occupied l.m.o.s are re-calculated. The orbital energy of the  $j^{\text{th}}$  l.m.o. is given by

$$\epsilon_j = \langle \phi_j | F | \phi_j \rangle \quad (7.9)$$

The F operator, given by equation (2.4), is constructed from all the occupied orbitals which are assumed to be mutually orthogonal. The Hartree-Fock operator is invariant to a linear transformation of the occupied orbitals,<sup>1</sup> so to form the operator the non-orthogonal set of l.m.o.s may be subjected to an orthogonalisation procedure. However, the form of the l.m.o. whose orbital energy is calculated,  $\phi_j$ , must remain unchanged by the orthogonalisation, as it also appears explicitly in the expression for the orbital energy. This is achieved by Schmidt orthogonalising in such a way that  $\phi_j$  appears first in the orthogonalising sequence and is hence unaltered by the orthogonalisation. To calculate the orbital energies of all eight l.m.o.s, therefore, each l.m.o. is taken in turn, the set of occupied l.m.o.s Schmidt orthogonalised in the appropriate sequence and the orbital energy of the l.m.o. calculated according to equation (7.9).

Having computed these properties the calculation of another l.m.o. is performed, the free space consisting of the starting-point form of the orbital to be calculated and the virtual orbitals obtained from the previous calculation. The l.m.o.s are calculated in turn in this way until calculation of all eight l.m.o.s decreases the total electronic energy by less than 0.0005 a.u.

Modifications were also made to the program FORM to carry out l.m.o. calculations according to Wilhite and Whitten's method<sup>26</sup> using Lowdin orthogonalisation. In this case the procedure within each l.m.o. calculation is that described above, but the operations are performed in a different order so that all l.m.o.s are calculated together as described in Chapter Three. Each l.m.o. is not cycled to self-consistency, but a single calculation is made of each of the eight occupied orbitals. These are then re-orthogonalised and the process repeated until the total electronic energy varies by no more than 0.0005 a.u.

Having calculated a set of energy-minimised l.m.o.s, separate computer programs were used to calculate the various properties described in Chapter Five. In the evaluation of bond energies, the total energies of the fragments were computed by a subroutine ENOG. The inverses of the matrices  $\underline{P}$  and  $\underline{Q}$  occurring in the expressions for the total energy of the fragments in terms of a set of non-orthogonal orbitals (equations (5.30) and (5.36)) were found by the subroutine MINV in the University of London Computing Centre Scientific Subroutine Package.



(b) C.m.o. Calculations

The program DELOC was written to carry out a c.m.o. calculation for the formaldehyde molecule. The storing of the various integrals over atomic orbitals was the same as described for the l.m.o. calculations. An orthogonal basis set of functions was obtained by Schmidt orthogonalising the set of atomic orbitals. The orthogonal set,  $\chi_1^{\circ} \dots \chi_{12}^{\circ}$  may be expressed in terms of the non-orthogonal atomic orbitals,  $\chi_1 \dots \chi_{12}$ , as in equation (2.34)

$$\chi_j^{\circ} = \sum_{k=1}^{12} \chi_k A_{kj} \quad (7.10)$$

where  $A_{kj}$  are coefficients determined by the orthogonalising procedure.

The program DELOC constructs the  $\underline{F}$  matrix, with elements

$$F_{jk} = \langle \chi_j^{\circ} | F | \chi_k^{\circ} \rangle \quad (7.11)$$

as in equation (2.18). Solution of equation (2.20) using the subroutine EIGEN in the University of London Computing Centre Scientific Subroutine Package, as described for the l.m.o. calculations, gives 12 eigenvalues,  $\epsilon_i$ , and 12 eigenvectors,  $c_i$ . The lowest 8 eigenvalues correspond to the 8 occupied c.m.o.s.

The eigenvectors refer to the orthogonal basis set  $\chi_1^{\circ} \dots \chi_{12}^{\circ}$ . Each new c.m.o. may be expressed in terms of the atomic orbitals by

$$\theta_i = \sum_{j=1}^{12} \chi_j^{\circ} c_{ij} = \sum_{j=1}^{12} \sum_{k=1}^{12} \chi_k A_{kj} c_{ij} \quad (7.12)$$

The new forms for the occupied c.m.o.s. are then used to construct a new  $F$  operator, and hence a new  $\underline{F}$  matrix, and the process repeated until the total electronic energy varies by less than 0.0001 a.u.

Section 2    Solution of Simultaneous Non-Linear Equations

The satisfaction of the orthogonality conditions by an analytical method, as discussed in Chapter Three, requires the solution of a set of simultaneous non-linear equations. A program SIMEQN was written to attempt the solution of such a set of equations, using a package from the CERN Program Library, NEWTON, which carries out an M-dimensional generalisation of the Newton-Rapheson method (where M is the number of equations).

The solution,  $a$ , of a single non-linear equation

$$f(x) = 0 \quad (7.13)$$

may be obtained by Newton-Rapheson iteration in the following way.

If  $x_0$  is an approximation to the solution, a better approximation,  $x_1$ , is given by the general formula

$$x_n = x_{n-1} - f(x_{n-1})/f'(x_{n-1}) \quad (7.14)$$

where

$$f'(x_{n-1}) = \frac{d f(x_{n-1})}{d x_{n-1}} \quad (7.15)$$

$x_1$  is then used to obtain a further value,  $x_2$ , and the process repeated to give a series  $x_0, x_1, x_2, \dots$ . If equation (7.13) has a solution at  $x = a$  the series will converge to the value of  $a$  providing  $f(a) \neq 0$  and  $f''(x)$  is continuous at  $x = a$ .<sup>123</sup>

The CERN Library subroutine NEWTON searches for the solutions  $a_1, \dots, a_M$  of a set of M simultaneous non-linear equations

$$\begin{aligned} f_1(x_1, \dots, x_M) &= 0 \\ f_2(x_1, \dots, x_M) &= 0 \\ &\vdots \\ f_M(x_1, \dots, x_M) &= 0 \end{aligned} \quad (7.16)$$

Using vector notation,  $\underline{A}$  contains the solutions  $a_1, \dots, a_M$  and equation (7.16) is written

$$\underline{F}(\underline{X}) = 0 \quad (7.17)$$

If the vector  $\underline{X}^0$  contains  $x_1^0, x_2^0, \dots, x_M^0$ , approximations to the values of  $a_1, a_2, \dots, a_M$ , a series of sets of improved values  $\underline{X}^n$ , ( $n = 1, 2, \dots$ ) is given by

$$\underline{X}^n = \underline{X}^{n-1} - \underline{F}(\underline{X}^{n-1}) \cdot [\underline{G}(\underline{X}^{n-1})]^{-1} \quad (7.18)$$

or

$$\underline{X}^n = \underline{X}^{n-1} - \underline{H}^n \quad (7.19)$$

where  $\underline{G}(\underline{X})$  is the Jacobian

$$\underline{G}(\underline{X}) = \frac{\partial \underline{F}(\underline{X})}{\partial \underline{X}} \quad (7.20)$$

with elements

$$G_{ij} = \frac{\partial f_i(x_1, \dots, x_M)}{\partial x_j} \quad (7.21)$$

and

$$\underline{H}^n = \underline{F}(\underline{X}^{n-1}) \cdot [\underline{G}(\underline{X}^{n-1})]^{-1} \quad (7.22)$$

If equation (7.17) has a solution at  $\underline{X} = \underline{A}$  the series  $\underline{X}^n$  ( $n = 1, 2, \dots$ ) will converge to  $\underline{A}$  providing firstly the functions  $f_i$  ( $i = 1, \dots, M$ ) and their first and second partial derivatives are continuous and secondly the Jacobian matrix  $\underline{G}(\underline{X})$  has a non-vanishing determinant at  $\underline{X}$ .

The subroutine NEWTON only accepts a new vector  $\underline{X}^n$  if it satisfies the following two conditions.

1) That the method is converging. This is tested by comparing the sum of the squares of the functions  $f_1 \dots f_M$  evaluated with the new values of  $x_1 \dots x_M$ ,  $\underline{X}^n$ , with those evaluated with the previous values of  $x_1 \dots x_M$ ,  $\underline{X}^{n-1}$ . For convergence

$$\sum_{i=1}^M [f_i(\underline{X}^n)]^2 \ll \sum_{i=1}^M (f_i(\underline{X}^{n-1}))^2 \quad (7.23)$$

2) That  $\underline{X}^n$  lies within a domain defined by the user of the subroutine NEWTON. This provides the facility to put limits on the individual values of  $x_1 \dots x_M$ .

If one of these conditions is not satisfied  $\underline{H}^M$  is reduced by  $2^m$  ( $m = 1, 2, \dots$ ) until  $\underline{X}^n$  does obey the conditions.

$$\underline{X}_m^n = \underline{X}_{m-1}^n - \underline{H}^n / 2^m \quad (7.24)$$

The maximum number of reductions allowed must be specified by the main program and a value of 10 was used in the program SIMEQN.

$\underline{X}^n$  is accepted as a solution to the set of simultaneous equations if one of the conditions below is satisfied

$$|f_i(\underline{X}^n)| \ll 10^{-k} \quad (7.25)$$

or

$$\sqrt{\sum_{i=1}^M [f_i(\underline{X}^n)]^2} \ll 10^{-l} \quad (7.26)$$

$k$  and  $l$  are set by the main program and a value of 5 was used for both. If these conditions are not satisfied after a certain number of cycles the calculation is stopped. The number of cycles allowed is set by the main program and a value of 20 was specified in SIMEQN.

The CERN package consists of the function NEWTON, described above, together with a subroutine LINEQN and two functions SCAL and TEST. The

user of the package has to supply functions `SYSTEM` (defining  $f_1 \dots f_M$ ) and `LMITE` (setting bounds on the values of  $x_1 \dots x_M$ ) and the subroutine `DERIVE` (defining the Jacobian  $\underline{G}(\underline{X})$ ), handing them over to the function `NEWTON` by means of an `EXTERNAL` statement in the main program.

Section 3 Electron Density Calculations

The program CONTAN was written to evaluate  $\delta$  values according to equation (6.6) using the Calcomp graph plotting routine to draw  $\delta$  profiles and  $\delta$  contour diagrams. The axis system used for a bond between atoms A and B is that used in reference 44 and is shown in Figure 7.2.

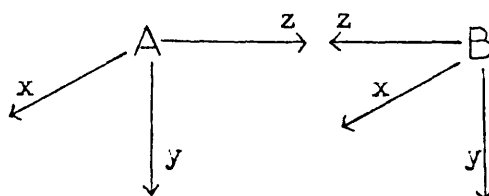


Figure 7.2 Axis system used in electron density calculations for a bond between atoms A and B

A sigma-bond is symmetrical about the inter-nuclear axis and it was chosen to draw contours of  $\delta$  in the x-z plane. For a pi-bond,  $\delta$  contours were drawn in the plane of the bond, so that for a  $2p_y$  pi-bond, for example, contours of  $\delta$  were drawn in the y-z plane.

The contours of  $\delta$  were obtained by a method based on that given by Wahl.<sup>124</sup> A contour line indicating a difference density value  $C$  in the x-z plane is defined by the equation

$$\delta(x, z) = C \quad (7.27)$$

and its path by the relation

$$d\delta = \frac{\partial \delta}{\partial x} \Delta x + \frac{\partial \delta}{\partial z} \Delta z = 0 \quad (7.28)$$

The direction of the tangent at any point on the contour is then given by

$$\frac{\Delta x}{\Delta z} = - \frac{\partial \delta / \partial z}{\partial \delta / \partial x} \quad (7.29)$$

Assuming the point  $(x_0, z_0)$  is on the contour, a second point on the contour may be found in the following way. A small step,  $\Delta s$ , is taken along the tangent to the contour at  $(x_0, z_0)$  to  $(x', z')$ , where

$$\begin{aligned} x' &= x_0 + \Delta x \\ z' &= z_0 + \Delta z \end{aligned} \quad (7.30)$$

$$\text{and } \Delta s = (\Delta x^2 + \Delta z^2)^{\frac{1}{2}} \quad (7.31)$$

In the program CONTAN a step of 0.02 a.u. was taken. The difference density,  $S'$ , at the point  $(x', z')$  is calculated, and the difference between this value and the required contour value found.

$$\Delta S = S'(x', z') - C \quad (7.32)$$

A correction is then applied perpendicular to the initial tangent, along the line

$$\frac{\Delta x'}{\Delta z'} = \frac{\partial S / \partial x}{\partial S / \partial z} \quad (7.33)$$

a distance given by

$$\Delta z' = \Delta S / \left[ \frac{\partial S'}{\partial x'} + \frac{\partial S'}{\partial z'} \times \frac{\partial S / \partial x}{\partial S / \partial z} \right] \quad (7.34)$$

to a point which it is hoped lies on the contour. The correction is continued until  $\Delta S$  falls below an acceptable value. This was taken as 0.0005 a.u. in the program CONTAN. This point is then joined to the previous point on the contour,  $(x_0, z_0)$ , by a straight line. The process is repeated to trace out the entire contour. The incremental step,  $\Delta s$ , was chosen small enough to give points sufficiently close together to present a smooth curve. The first point on the contour, needed to start tracing out the contour, was found from the profiles of  $S$  along the internuclear axis.

## REFERENCES

1. C.C.J. Roothaan, Rev. Mod. Phys., 1951, 23, 161.
2. J.E. Lennard-Jones, Proc. Roy. Soc. (London), 1949, A192, 1, 14.
3. V. Fock, Z. Physik, 1930, 61, 126.
4. G.N. Lewis, J. Am. Chem. Soc., 1916, 38, 762.
5. R.E. Christoffersen, Advances in Quantum Chemistry, 1972, 6, 333.
6. L. Pauling, "The Nature of the Chemical Bond" (Cornell University Press, New York, 1960).
7. J.D. Roberts and M.C. Caserio, "Basic Principles of Organic Chemistry" (W.A. Benjamin, New York, 1965).
8. W.E. Addison, "Structural Principles in Inorganic Compounds" (Longmans, London, 1961).
9. T.L. Cottrell, "The Strengths of Chemical Bonds" (Butterworths, London, 1958).
10. J.C.D. Brand and J.C. Speakman, "Molecular Structure" (Edward Arnold, London, 1960) p.246.
11. T.L. Allen and H. Schull, J. Chem. Phys., 1961, 35, 1644.
12. S.F. Boys, Rev. Mod. Phys., 1960, 32, 296.
13. S. Rothenberg, J. Chem. Phys., 1969, 51, 3389; J. Am. Chem. Soc., 1971, 93, 68.
14. D. Peters, J. Am. Chem. Soc., 1972, 94, 707.
15. M. Levy, W.J. Stevens, H. Schull and S. Hagstrom, J. Chem. Phys., 1970, 52, 5483.
16. W.H. Adams, J. Chem. Phys., 1961, 34, 89; *ibid*, 1962, 37, 2009; *ibid*, 1965, 42, 4030.
17. T.L. Gilbert, in "Molecular Orbitals in Chemistry, Physics and Biology", edited by P.O. Lowdin and B. Pullman (Academic Press, New York, 1964) p.405.
18. W. Von Neissen, J. Chem. Phys., 1971, 55, 1948.
19. M. Klessinger and R. McWeeny, J. Chem. Phys., 1965, 42, 3343.



20. J.R. Hoyland, *J. Am. Chem. Soc.*, 1968, 90, 2227; *J. Chem. Phys.*, 1969, 50, 473.
21. J.D. Petke and J.L. Whitten, *J. Chem. Phys.*, 1969, 51, 3166.
22. J.E. Lennard-Jones and J.A. Pople, *Proc. Roy. Soc. (London)*, 1951, A210, 190.
23. J.M. Foster and S.F. Boys, *Rev. Mod. Phys.*, 1960, 32, 300.
24. S. Diner, J.P. Malrieu and P. Claverie, *Theoret. Chim. Acta*, 1969, 13, 1, and subsequent papers in this series.
25. J.L. Whitten and M. Hackmeyer, *J. Chem. Phys.*, 1969, 51, 5584.
26. D.L. Wilhite and J.L. Whitten, *J. Chem. Phys.*, 1973, 58, 948.
27. E. Steiner, *J. Chem. Phys.*, 1971, 54, 1114.
28. L. Pauling, *Proc. Natl. Acad. Sci.*, 1928, 14, 359; *J. Am. Chem. Soc.*, 1931, 53, 1367, 3225.
29. R.S. Mulliken, *Phys. Rev.*, 1928, 32, 186, 388, 761; *ibid*, 1932, 41, 49.
30. For example: (a) B.J. Ransil, *Rev. Mod. Phys.*, 1960, 32, 245.  
(b) W.G. Richards, T.E.H. Walker and R.K. Hinkley, "A Bibliography of ab initio Molecular Wavefunctions" (Clarendon Press, Oxford 1971).  
(c) References given in reference 5.
31. (a) J.E. Lennard-Jones and G.G. Hall, *Proc. Roy. Soc. (London)*, 1950, A202, 155, 336.  
(b) J.E. Lennard-Jones and J.A. Pople, *Proc. Roy. Soc. (London)*, 1950, A202, 166.
32. J.A. Pople, *Quart. Rev.*, 1957, 11, 273.
33. W. England, L.S. Salmon and K. Ruedenberg, *Topics in Current Chemistry*, 1971, 23, 31.
34. W.A. Bennett, *J. Chem. Ed.*, 1969, 46, 746.
35. H. Weinstein, R. Pauncz and M. Cohen, *Advances in Atomic and Molecular Physics*, 1971, 7, 97.

36. C. Edmiston and K. Ruedenberg, *Rev. Mod. Phys.*, 1963, 35, 457;  
*J. Chem. Phys.*, 1965, 43, S97; "Quantum Theory of Atoms,  
Molecules and the Solid State", edited by P.O. Lowdin (Academic  
Press, New York, 1966) p.273.
37. R.M. Pitzer, *J. Chem. Phys.*, 1964, 41, 2216.
38. U. Kaldor, *J. Chem. Phys.*, 1967, 46, 1981.
39. (a) E. Switkes, R.M. Stevens, W.N. Lipscomb and M.D. Newton,  
*J. Chem. Phys.*, 1969, 51, 2085.  
(b) E. Switkes, W.N. Lipscomb and M.D. Newton, *J. Am. Chem. Soc.*,  
1970, 92, 3847.  
(c) M.D. Newton and E. Switkes, *J. Chem. Phys.*, 1971, 54, 3179.  
(d) M.D. Newton and J.M. Schulman, *J. Am. Chem. Soc.*, 1972, 94,  
767, 773.
40. W. Von Neissen, *J. Chem. Phys.*, 1972, 56, 4290.
41. S.F. Boys, in "Quantum Theory of Atoms, Molecules and the Solid  
State", edited by P.O. Lowdin (Academic Press, New York, 1966)  
p.253.
42. R. Bonaccorsi, E. Scrocco and J. Tomasi, *J. Chem. Phys.*, 1970,  
52, 5270.
43. K. Ruedenberg, in "Modern Quantum Chemistry", edited by  
O. Sinanoglu (Academic Press, New York, 1965) Part I, p.85.
44. D. Peters, *J. Chem. Soc.*, 1963, 2003.
45. D. Peters, *J. Chem. Soc.*, 1963, 2015.
46. D. Peters, *J. Chem. Soc.*, 1963, 4017.
47. D. Peters, *J. Chem. Soc.*, 1964, 2901.
48. D. Peters, *J. Chem. Soc.*, 1964, 2908.
49. D. Peters, *J. Chem. Soc.*, 1964, 2916.
50. D. Peters, *J. Chem. Soc.*, 1965, 3026.
51. D. Peters, *J. Chem. Soc. (A)*, 1966, 644.
52. D. Peters, *J. Chem. Soc. (A)*, 1966, 652.

53. D. Peters, *J. Chem. Soc. (A)*, 1966, 656.
54. V. Magnasco and A. Perico, *J. Chem. Phys.*, 1967, 47, 971;  
*ibid*, 1968, 48, 800.
55. R.S. Mulliken, *J. Chem. Phys.*, 1955, 23, 1833, 1841, 2338, 2343.
56. P.W. Anderson, *Phys. Rev. Letters*, 1968, 21, 13; *Phys. Rev.*,  
1969, 181, 215.
57. D. Peters, *J. Chem. Phys.*, 1969, 51, 1559.
58. D. Peters, *J. Chem. Phys.*, 1969, 51, 1566.
59. D. Peters, *J. Chem. Phys.*, 1972, 57, 4351.
60. W.J. Hunt, T.H. Dunning and W.A. Goddard, *Chem. Phys. Lett.*  
1969, 3, 606.
61. D. Peters, *Theoret. Chim. Acta*, 1972, 24, 16.
62. (a) T. Anno and A. Sado, *J. Chem. Phys.*, 1957, 26, 1759.  
(b) J.W. Sidman, *J. Chem. Phys.*, 1957, 27, 1270.  
(c) R.D. Brown and M.L. Heffernan, *Trans. Faraday Soc.*, 1958,  
54, 757.  
(d) F.L. Pilar, *J. Chem. Phys.*, 1967, 47, 884.  
(e) M.S. Gordon and J.A. Pople, *J. Chem. Phys.*, 1968, 49, 4643.
63. J.M. Foster and S.F. Boys, *Rev. Mod. Phys.*, 1960, 32, 303.
64. P.L. Goodfriend, F.W. Birss and A.B.F. Duncan, *Rev. Mod. Phys.*,  
1960, 32, 307.
65. M.D. Newton and W.E. Palke, *J. Chem. Phys.*, 1966, 45, 2329.
66. J.M. Parks and R.G. Parr, *J. Chem. Phys.*, 1960, 32, 1657.
67. E. Switkes, R.M. Stevens and W.N. Lipscomb, *J. Chem. Phys.*, 1969,  
51, 5229.
68. (a) D.B. Neumann and J.W. Moskowitz, *J. Chem. Phys.*, 1969, 50, 2216.  
(b) N.W. Winter, T.H. Dunning and J.H. Letcher, *J. Chem. Phys.*,  
1968, 49, 1871.  
(c) R. Ditchfield, W.J. Hehre and J.A. Pople, *J. Chem. Phys.*,  
1971, 54, 724.

69. B. Levy, Chem. Phys. Lett., 1969, 4, 17; Int. J. Quantum Chemistry, 1970, 4, 297.
70. M.D. Newton, E. Switkes and W.N. Lipscomb, J. Chem. Phys., 1970, 53, 2645.
71. (a) J.B. Moffat, J. Theor. Biol., 1970, 26, 437.  
(b) A. Pullman and M. Dreyfus, Theoret. Chim. Acta, 1970, 19, 20.  
(c) J.A. Ryan and J.L. Whitten, J. Am. Chem. Soc., 1972, 94, 2396.
72. M. Roux, S. Besnainou and R. Daudel, J. chim. phys., 1956, 53, 939.
73. O. Martensson and G. Sperber, Acta Chem. Scand., 1970, 24, 1749.
74. C.W. Kern and M. Karplus, J. Chem. Phys., 1964, 40, 1374.
75. J.L.J. Rosenfeld, Acta Chem. Scand., 1964, 18, 1719; J. Chem. Phys., 1964, 40, 384.
76. F.J. Ransil and J.J. Sinai, J. Chem. Phys., 1967, 46, 4050.
77. R.F.W. Bader, W.H. Henneker and P.E. Cade, J. Chem. Phys., 1967, 46, 3341.
78. M. Roux, S. Besnainou and R. Daudel, J. chim. phys., 1956, 53, 218.
79. (a) M. Roux, J. chim. phys., 1958, 55, 754.  
(b) M. Roux, J. chim. phys., 1960, 57, 53.  
(c) G. Bessis and S. Bratoz, J. chim. phys., 1960, 57, 769.  
(d) M. Roux, M. Cornille and G. Bessis, J. chim. phys., 1961, 58, 389.  
(e) M. Roux, M. Cornille and L. Burnelle, J. Chem. Phys., 1962, 37, 933.
80. P.R. Smith and J.W. Richardson, J. Phys.Chem., 1965, 69, 3346.
81. K.E. Banyard, M. Dixon and M.R. Hayns, J. Chem. Phys., 1971, 54, 5418.
82. J.D. Petke and J.L. Whitten, J. Chem. Phys., 1972, 56, 830.
83. For example, J.C. Slater, "Quantum Theory of Molecules and Solids" (McGraw-Hill Book Company, New York, 1963) Vol. 1, p.92.

84. P.O. Lowdin, *Advances in Quantum Chemistry*, 1970, 5, 185.
85. P.O. Lowdin, *J. Chem. Phys.*, 1950, 18, 365.
86. J.C. Slater, *Phys. Rev.*, 1930, 36, 57.
87. C.C.J. Roothaan, *J. Chem. Phys.*, 1951, 19, 1445.
88. E.A. Magnusson and C. Zauli, *Proc. Phys. Soc.*, 1961, 78, 53.
89. R.D. Nelson, D.R. Lide and A.A. Maryott, *Natl. Std. Ref. Data. Ser. Natl. Bur. Std.*, 1967, 10.
90. T. Koopmans, *Physica*, 1933, 1, 104.
91. D. Peters, *J. Chem. Phys.*, 1964, 41, 1046.
92. A.D. Baker, C. Baker, C.R. Brundle and D.W. Turner, *J. Mass Spectrometry and Ion Physics*, 1968, 1, 285.
93. U. Gelius, Private communication.
94. M.D. Newton, *J. Chem. Phys.*, 1968, 48, 2825.
95. D.S. Urch, "Orbitals and Symmetry" (Penguin Books Ltd., England, 1970), p.54.
96. U. Gelius, P.F. Heden, J. Hedman, B.J. Lindberg, R. Manne, R. Nordberg, C. Nordling and K. Siegbahn, *Physica Scripta*, 1970, 2, 70.
97. R.S. Mulliken, *J. Chem. Phys.*, 1935, 3, 564.
98. R.S. Mulliken, *J. Chem. Phys.*, 1955, 23, 1833, 1841, 2338, 2343.
99. K. Siegbahn, C. Nordling, A. Fahlman, R. Nordberg, K. Hamrin, J. Hedman, G. Johansson, T. Bergmark, S.-E. Karlsson, I. Lindgren and B. Lindberg, "ESCA - Atomic, Molecular and Solid State Structure Studied by Means of Electron Spectroscopy" (Almqvist and Wiksells, Uppsala, 1967).
100. K. Siegbahn, C. Nordling, G. Johansson, J. Hedman, P.F. Heden, K. Hamrin, U. Gelius, T. Bergmark, L.O. Werme, R. Manne and Y. Baer, "ESCA Applied to Free Molecules" (North-Holland, Amsterdam, 1969).
101. T.D. Thomas, *J. Am. Chem. Soc.*, 1970, 92, 4184.

102. R.S. Mulliken, *J. chim. phys.*, 1949, 46, 675.
103. M.E. Schwartz, J.D. Switalski and R.E. Stronski, *Electron Spectroscopy-Proc. Int. Conf.*, 1971, 605.
104. B.J. Cocksey, J.H.D. Eland and C.J. Danby, *J. Chem. Soc. (E)*, 1971, 790.
105. C.E. Moore, "Atomic Energy Levels", *Natl. Bur. Std. Circular* 467, 1949, Vol. I.
106. D.A. Ramsey, *Advances in Spectry.*, 1959, 1, 1.
107. P.O. Lowdin, *Phys. Rev.*, 1955, 97, 1474.
108. J.W. Archbold, "Algebra" (Pitman and Sons, London, 1961) p.338.
109. R. McWeeny and B.T. Sutcliffe, "Methods of Molecular Quantum Mechanics" (Academic Press, London, 1969) p.49.
110. V.I. Vedeneyev, L.V. Gurvich, V.N. Konrat'yev, V.A. Medvedev and Ye. I. Frankevich, "Bond Energies, Ionisation Potentials and Electron Affinities" (Edward Arnold, London, 1966).
111. G. Hertzberg, *Proc. Roy. Soc. (London)*, 1961, A262, 291.
112. R.F.W. Bader and W.H. Henneker, *J. Am. Chem. Soc.*, 1965, 87, 3063.
113. T. Berlin, *J. Chem. Phys.*, 1951, 19, 208.
114. R.F.W. Bader and G.A. Jones, *Can. J. Chem.*, 1961, 39, 1253.
115. (a) C.A. Coulson and J.T. Lewis, in "Quantum Theory", edited by D.R. Bates (Academic Press, New York, 1962) Vol. 10, Part 2, p.189.  
(b) H. Eyring, J. Walter and G. Kimball, "Quantum Chemistry" (John Wiley and Sons, New York, 1944) p.198.  
(c) J.C. Slater, *J. Chem. Phys.*, 1933, 1, 687.  
(d) J.C. Slater, "Quantum Theory of Molecules and Solids" (McGraw-Hill Book Company, New York, 1963), Vol.1, p.9.
116. K. Ruedenberg, *Rev. Mod. Phys.*, 1962, 34, 326.
117. R.F.W. Bader and H.J.T. Preston, *Int. J. Quantum Chemistry*, 1969, 3, 327.

118. M.J. Feinberg, K. Ruedenberg and E.L. Mehler, *Advances in Quantum Chemistry*, 1970, 5, 27.
119. H.M. James and A.S. Coolidge, *J. Chem. Phys.*, 1933, 1, 825.
120. U. Kaldor and I. Shavitt, *J. Chem. Phys.*, 1966, 45, 888.
121. J. Hinze and H.H. Jaffe, *J. Am. Chem. Soc.*, 1956, 84, 540.
122. J. Greinstadt, in "Mathematical Methods for Digital Computers", edited by A. Palston and H.S. Wilf (John Wiley and Sons, New York, 1962) Chapter 7.
123. D.G. Moursund and C.S. Duris, "Elementary Theory and Application of Numerical Analysis" (McGraw-Hill Book Company, Tokyo, 1967).
124. A.C. Wahl, in "Quantum Theory of Atoms, Molecules and the Solid State", edited by P.O. Lowdin (Academic Press, New York, 1966) p.243; *Science*, 1966, 151, 961.

THE DIRECT S.C.F. COMPUTATION OF THE LOCALISED  
MOLECULAR ORBITALS OF THE  
FORMALDEHYDE MOLECULE

{ J. M. Heider  
    née  
J. M. CARPENTER } and DAVID PETERS

*Royal Holloway College, Englefield Green, Surrey, England*

**Abstract.** The localised molecular orbitals (l.m.o.s) of the formaldehyde molecule are computed in a rigorous manner at the Hartree-Fock level of approximation using a minimum basis set of Slater atomic orbitals. The theoretical and chemical significance of the results is examined.

### 1. Introduction

This work is an application of the general theory put forward some years ago [1] for the computation of localised molecular orbitals (l.m.o.s) in molecules at the Hartree-Fock level of approximation. The motive for working with such orbitals is that they may be used in molecules of any size whereas the familiar canonical m.o.s can only be used at this level of approximation with molecules which are small by chemical standards.

The l.m.o.s also have the advantage of being conceptually and algebraically simple with the result that correlation problems are easily studied with them. The l.m.o.s are also closely related to chemical theory and also to valence bond theory. The l.m.o.s are ideal for describing bond breaking processes. They are not so useful as the canonical m.o.s for describing ionisation processes.

### 2. Theory

This is a brief outline of the general theory given earlier [1]. Full details and definitions may be found there.

The well established method of computing the m.o.s( $\phi'$ ) of a closed shell molecule is based on the Hartree-Fock equation

$$F\phi'_i = e'_i\phi'_i, \quad (1)$$

where  $F$  is the Hartree-Fock operator defined in the usual way for a closed shell system and  $e'_i$  is the eigenvalue which is approximately equal to the ionisation energy of the electron in the  $i$ th m.o.

The m.o.s given in (1) are the canonical m.o.s which are distinguished from the l.m.o.s by the prime. The canonical m.o.s are often thought of as 'the m.o.s' of the molecule and they are in general spread over the entire molecule. But the single determinant wave function constructed from these m.o.s is invariant under a linear transformation and this fact was widely used some ten years ago [2] to localise the m.o.s of



a number of small molecules into the l.m.o.s which are confined within small regions of the molecule and which resemble closely the chemical bonds and lone pairs of classical chemical valence theory.

This route to the l.m.o.s via a linear transformation of the canonical m.o.s is not useful for large molecules because their canonical m.o.s are not available. It is thus essential to find an equation which will give the l.m.o.s directly and this is just the generalised form of the Hartree-Fock equation

$$F\phi_i = \sum_{k=1}^n e_{ik}\phi_k. \quad (2)$$

When this equation is written in the form

$$F\phi_i - \sum_{k \neq i=1}^n e_{ik}\phi_k = e_{ii}\phi_i \quad (3)$$

it is clear that this will become a simple eigenvalue equation if the sum on the left is made to vanish. This is done by supposing that we are interested in the  $i$ th l.m.o. alone, as we often are, and that all other l.m.o.s are given and fixed. The fixed orbitals form a function space called the fixed space which is part of the Hartree-Fock space. The remaining part of the Hartree-Fock space is called the free space and it contains the required orbital  $\phi_i$  and the virtual orbitals.

The essential point now is to construct the two spaces to be mutually orthogonal so that any function in the one space is orthogonal to any function in the other space.

We then select a basis for the free space  $u_1 \dots u_s$  ( $s$  is the quantity called  $t-n+1$  earlier [1]) and then expand  $\phi_i$  over these functions

$$\phi_i = \sum_{q=1}^s c_{qi}u_q. \quad (4)$$

Putting (4) into (3) and using the orthogonality of the two spaces gives the secular equation for the  $i$ th l.m.o.

$$\sum_{q=1}^s c_{qi}(F_{pq} - e_{ii}S_{pq}) = 0 \quad (p = 1, \dots, s). \quad (5)$$

The required function  $\phi_i$  is the lowest and only negative eigenvalue of this equation. It is natural to select for the functions  $u_q$  an approximate form of the required answer in order to get the secular determinant into a near diagonal form from the start. This was done in the earlier work and in the present work and seems quite successful but other choices are possible.

This theory has been tested by us [1] and by others [3] with good results.

### 3. Example of the Formaldehyde Molecule

The basis set of Slater atomic orbitals for this molecule contains 12 functions so the complete Hartree-Fock space is 12 dimensional. There are 16 electrons in 8 doubly

occupied l.m.o.s so the fixed space is 7 dimensional and the free space is 5 dimensional.

To get a start, the 8 doubly filled l.m.o.s are chosen in the simplest possible way with the lone pairs represented by pure atomic orbitals and the chemical bonds as Pauling hybrids combined together into non-polar bonds. Suppose that we are computing the l.m.o. of one of the carbon-hydrogen bonds. Then the fixed space is the 7 functions given approximately by the inner shells  $1s_O$  and  $1s_C$ , the two other bonds  $\mu_{CH}$  and  $\mu_{CO}$  plus the  $\pi$  bond  $\pi_{CO}$  and the two lone pairs  $\lambda_0^\pi, \lambda_0^\sigma$ . The next step is to generate 5 functions which are orthogonal to these 7 functions. There are various possibilities here but we have so far used the Pauling hybrids to form non-polar antibonding l.m.o.s corresponding to the four bonds. The functions are then orthogonalised by the Schmidt procedure or otherwise and the secular determinant is set up and solved in a straightforward way.

This process may then be repeated for all the 8 occupied l.m.o. using in a calculation on a given bond the improved orbitals from the earlier computations. After this has been done, we have 8 improved functions. It is possible to recycle the entire theory through all 8 bonds again and we have done this but the results suggest that a second cycle is not important as compared with the first cycle.

The main complication with this method is the necessity of generating sets of mutually orthogonal functions. The severity of this problem varies from case to case. In some cases, there is no difficulty whatever, [1] but where there are lone pairs present, the orthogonalising requires care. This topic will be dealt with elsewhere in detail.

#### 4. Results on the Formaldehyde Molecule

The following general points have been established.

(i) the total energy calculated with this theory is identical with that computed using the canonical m.o.s so the many electron wave function is the same for both sets of m.o.s.

(ii) The total energy obtained and so the total wave function are independent of the starting point and it seems from the limited results available now that the individual l.m.o.s are also independent of the starting point.

(iii) The theory is stable to the choice of starting point and we have never encountered divergence difficulties when using the theory in a straightforward way.

The specific results are summarised in Table I and Figure 1. Figure 1 shows the eigenvalues for the canonical m.o.s the l.m.o.s and the symmetrised l.m.o.s which differ from the l.m.o.s only in the use of the sum and difference of the two C—H bonds. The set of 'symmetrised l.m.o.s' all transform in the conventional way as the rows of the character table. The l.m.o.s do not transform under an irreducible representation of the group but under a reducible one.

Inspection of Figure 1 suggests that the canonical m.o.s and not the l.m.o.s describe the ionisation process so in dealing with ionisation (and probably excitation) processes one should use canonical m.o.s as far as possible.

TABLE I<sup>a</sup>  
Localised molecular orbitals in formaldehyde

	1 <sub>sc</sub>	2 <sub>sc</sub>	2 <sub>pzc</sub>	2 <sub>pxc</sub>	2 <sub>pyc</sub>	1 <sub>so</sub>	2 <sub>so</sub>	2 <sub>pzo</sub>	2 <sub>pxo</sub>	2 <sub>pyo</sub>	1 <sub>sh</sub>	1 <sub>sh</sub>
<i>I<sub>c</sub></i>	0.9995	0.0046	0.0116	-	-	-0.0006	0.0054	0.0051	-	-	-0.0071	-0.0073
<i>I<sub>o</sub></i>	0.0007	-0.0062	0.0066	-	-	0.9993	0.0059	0.0059	-	-	0.0008	0.0008
<i>λ<sup>σ</sup></i>	0.0053	-0.0437	0.0612	-	-0.0001	-0.2270	0.9978	-0.3428	-	-	-0.0029	-0.0029
<i>λ<sup>π</sup></i>	-	-	-	-	0.1508	-	-	-	-	0.9699	-0.1212	+0.1212
<i>μ<sub>co</sub></i>	-0.1123	0.3469	-0.3806	-	-	0.0576	0.0778	0.6532	-	-	-0.0415	-0.0415
<i>π<sub>co</sub></i>	-	-	-	0.6694	-	-	-	-	0.6123	-	-	-
<i>μ<sub>CH</sub></i>	-0.1216	0.4415	0.2139	-	0.3926	0.0060	-0.0490	-0.0502	-	0.0079	0.4710	-0.0614
<i>μ<sub>CH'</sub></i>	-0.1202	0.4304	0.2173	-	-0.3909	0.0052	-0.0433	-0.0443	-	-0.0083	-0.0616	0.4776

<sup>a</sup> The eigenvalues are given on the figure. The virtual orbitals obtained in this computation are the delocalised or canonical ones. To get localised virtual orbitals the theory is modified slightly in a straightforward way.

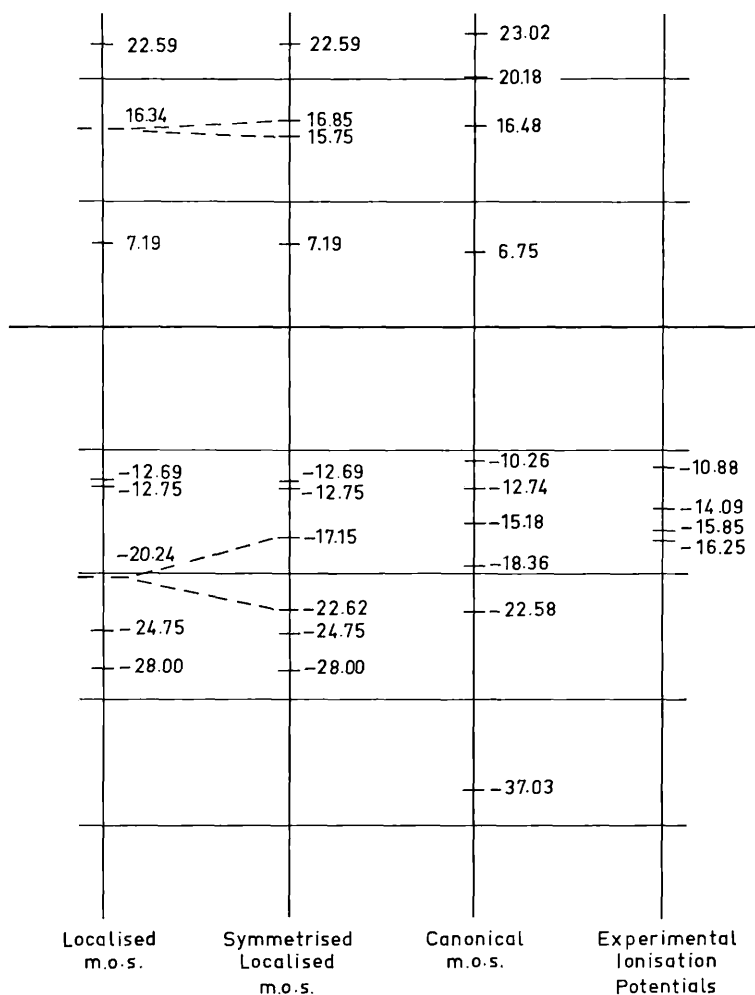


Fig. 1. Eigenvalues with various sets of molecular orbitals vs experimental ionisation potentials.

Table I gives the detailed form of the l.m.o.s and the significance of these is discussed in the following section. As a rough guide to these forms we write

$$\begin{aligned}\mu_{\text{CH}} &= 0.47 1s_{\text{H}} + 0.44 2s_{\text{C}} + 0.44 2p_{\text{C}} \\ \mu_{\text{CO}} &= 0.65 2p_{z_{\text{O}}} + 0.35 2s_{\text{C}} + 0.38 2p_{\text{C}} \\ \pi_{\text{CO}} &= 0.67 \pi_{\text{C}} + 0.61 \pi_{\text{O}}.\end{aligned}$$

We also define a truncated function  $\phi^T$  which is the original function with the contributions from other atomic orbitals crossed out, and then the function renormalised. The overlap integral between the two functions  $\phi$  and  $\phi^T$  gives a measure of how well localised are the l.m.o.s. The results are usually expressed in terms of the quantity  $d$  given by

$$d = 100(1 - \langle \phi | \phi^T \rangle)^{1/2}$$

and  $d$  is called the delocalisation parameter. If the overlap integral is 0.990 then  $d$  is about 10. Our impression from earlier work is that a  $d$  of less than 10 is required before the function may reasonably be called 'localised'. The highest  $d$  value of this sort of orbitals is 8.

The total energy using the functions given in Table I is  $-144.8532$  a.u. and that computed with all the functions in truncated form is  $-144.8066$  a.u. It is our impression that the third decimal place in these numbers is probably significant so we can conclude that the 'hyperconjugation energy' of the molecule is about 1.5 eV. We have done computations to break this down to show that the delocalisation of the  $\pi$  lone pair accounts for about 1 eV of the total and the delocalisation of the C-H bonds accounts for about  $\frac{1}{2}$  eV each. This result is similar to that obtained in the methane work [1].

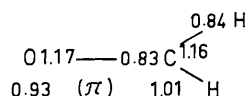
### 5. Chemical Information and Simple Electrostatics

The computation of wave functions and expectation values of observables is for some workers the end of the matter but for many the results only assume significance when translated into visualisable terms and familiar quantities such as hybridisations, bond polarities and a variety of electrostatic quantities such as ion-dipole, dipole-dipole interaction energies. The value of these ideas lies in their simplicity and ease of use by non-specialists in dealing with large molecules. In this section we interpret these results along these lines.

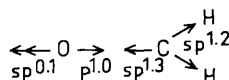
Thinking first of an isolated bond, then the l.m.o. given in Table I may be written as

$$\begin{aligned}\pi &= 0.67 \pi_C + 0.61 \pi_O \\ \mu_{CO} &= 0.51 h_{yC} + 0.65 h_{yO} \\ \mu_{CH} &= 0.47 1s_H + 0.61 h_{yC}.\end{aligned}$$

If one define atomic populations in the usual way one has the population diagram



and the corresponding hybridisation diagram is



These results may be compared and contrasted with conventional chemical dogma on these matters.

An interesting question is that of how much energy bonds gain by being polar rather than non-polar. It is true that much depends on the definitions of the terms 'polar' and 'non-polar' here but we found earlier that a carbon-hydrogen bond in methane is increased in energy by about 4 kcals/mole as a result of its polarity and perhaps much the same will be true for the formaldehyde bonds. We might call this quantity the 'ionic bond energy'.

A related idea is that one may usefully think of polar bonds as interacting by simple electrostatics as two dipoles do. We found some support for this idea in our earlier work [1] when the interaction energy of two polar C—H bonds in methane appeared to be about 1 kcal/mole for a pair of bonds. We have looked for evidence of bonds polarising each other but we have found none so far this work.

It is important to be cautious about these last two points because the values involved are very small and, strictly speaking, we cannot rely on the accuracy of the integrals to this extent. Nevertheless, these results do emerge in a consistent fashion from the computations.

#### Acknowledgements

One of us (J.M.C.) is indebted to the S.R.C. for a scholarship during which this work was done. We are also indebted to M. D. Newton [4] for the values of the integrals over the Slater basis.

#### References

1. Peters, D.: *J. Chem. Phys.* **51**, 1559 and 1566 (1969).
2. Peters, D.: *J. Chem. Soc.*, 1963, 2003: et seq., Edmiston, C. and Ruedenberg, K.: *J. Phys. Chem.* **69**, 2160 (1964); Weinstein, H., Pauncz, R., and Cohen, M.: in *Advances in Atomic and Molecular Physics* **7**, 97 (1971).
3. Wilhite, D. L. and Whitten, J. L.: *J. Chem. Phys.* **58**, 948 (1973).
4. Newton, M. D. and Palke, W. E.: *J. Chem. Phys.* **45**, 2329 (1966).